This is to certify that the
dissertation entitled

MECHANISM OF CANNABINOID-MEDIATED ELEVATION OF INTRACELLULAR CALCIUM IN T CELLS

presented by

Gautham Karkala Rao

has been accepted towards fulfillment
of the requirements for the

Ph.D. degree in Pharmacology and Toxicology

N. Kaminski

Major Professor's Signature

10/19/05

Date

MECHANISM OF CANNABINOID-MEDIATED ELEVATION OF INTRACELLULAR CALCIUM IN T CELLS

By

Gautham Karkala Rao

A DISSERTATION

Submitted to
Michigan State University
in partial fulfillment of the requirements
for the degree of

DOCTOR OF PHILOSOPHY

Department of Pharmacology and Toxicology

2005

ABSTRACT

MECHANISM OF CANNABINOID-MEDIATED ELEVATION OF INTRACELLULAR CALCIUM IN T CELLS

By

Gautham Karkala Rao

Cannabinoids are a class of over sixty structurally-related plant-derived compounds present in the marijuana plant, *Cannabis sativa*. Apart from their psychoactive and behavioral effects, cannabinoids are widely known to possess immunomodulatory properties. Generally, it is believed that cannabinoids exert their effects on physiology through the G protein-coupled cannabinoid receptors, CB1 and CB2, expressed primarily in the brain and immune system, respectively. In T cells, cannabinoid treatment has been demonstrated extensively to modulate T cell activation-related events, especially the expression of interleukin (IL)-2. The regulation of IL-2 transcription is critically dependent on intracellular calcium ($[Ca^{2+}]_i$), and the Ca^{2+}-dependent transcription factor, nuclear factor of activated T cells (NFAT). Prior results from this laboratory have found a strong correlation between the modulation of IL-2 expression by cannabinoids and the modulation of NFAT activation and nuclear translocation. However, little is known about the cellular mechanism by which cannabinoids exert their effects on T cells. The present dissertation project, therefore, first examined the hypothesis that the suppression of IL-2 expression in T cells by cannabinoids was dependent on the cannabinoid receptor-mediated elevation of $[Ca^{2+}]_i$. The first objective of the present studies was to examine the effect of cannabinoids, Δ^9-

THC and CP55,940, on IL-2 expression and $[Ca^{2+}]_i$ elevation in the human T cell lines, HPB-ALL and Jurkat E6-1. It was found that while both Δ^9-THC and CP inhibited the expression of IL-2, only Δ^9-THC treatment resulted in the elevation of $[Ca^{2+}]_i$. Therefore, it was concluded that the modulation of $[Ca^{2+}]_i$ and inhibition of IL-2 production by cannabinoids may be simultaneous, yet unrelated events. Regardless, the mechanism by which Δ^9-THC elevated $[Ca^{2+}]_i$ was characterized as the second objective of the present studies in the HPB-ALL cells, as $[Ca^{2+}]_i$ plays a critical role in many T cell processes including activation of enzymes, triggering of apoptotic pathways, and induction of T cell anergy. Results showed that Δ^9-THC elevated $[Ca^{2+}]_i$ in a cannabinoid receptor antagonist-sensitive and Ca^{2+} store-independent manner through the TRPC1 class of receptor-operated cation channels (ROCCs). In addition, it was established that the robust induction of $[Ca^{2+}]_i$ influx in resting T cells was a characteristic unique to the tricyclic classical cannabinoid compounds, which was not observed with either bicyclic congeners or the eicosinoid-derived endocannabinoids. A final objective of the current dissertation project was to determine unequivocally whether the CB1 and CB2 receptors were involved in the mechanism by which tricyclic cannabinoid compounds elevated $[Ca^{2+}]_i$. Measurements of $[Ca^{2+}]_i$ performed in the wildtype and $CB1^{-/-}/CB2^{-/-}$ murine splenocytes demonstrated that the tricyclic cannabinoids induced a rise in $[Ca^{2+}]_i$ independently of both CB1 and CB2 receptors. Altogether, the studies from the present dissertation project suggest that tricyclic cannabinoid compounds elevate $[Ca^{2+}]_i$ in a CB1 and CB2 receptor- and intracellular Ca^{2+} store-independent manner through ROCCs in T cells. The elevation of $[Ca^{2+}]_i$ mediated by a novel cannabinoid receptor may partly explain the mechanism by which tricyclic cannabinoids modulate T cell function.

.. AUM ..

DEDICATION

I dedicate this work to all my teachers, secular and spiritual, whose words of advice have been a constant source of inspiration throughout my dissertation process. In addition, I dedicate this dissertation to my parents and grandparents, who taught me the value of hard work, persistence and steadfastness.

ACKNOWLEDGEMENTS

First and foremost, I acknowledge my mentor, Dr. Norbert Kaminski, who has not only guided me along the arduous path toward the completion of my dissertation, but also provided me the freedom to carve my own niche within the framework of the project. His encouragement, positive reinforcement, and enthusiasm for science, in general, have been and will continue to be a constant source of inspiration for me.

Second, I would like to thank the members of my dissertation committee, Dr. Peter Cobbett, Dr. Patty Ganey and Dr. John LaPres, for providing me with deep insights and expert advice from their respective fields towards the interpretation and development of my dissertation project. The recommendations and thought-provoking questions from my committee members have been invaluable to my understanding of the field, and progress as a scientist.

Finally, I would like to thank the members of Dr. Kaminski's laboratory, Katie Boland, John Buchweitz, Bob Crawford, Kim Hambleton, Dr. Barb Kaplan, Colin North, Dina Shnaider, and Dr. Alison Springs. It has been my privilege to work with these great individuals on a day-to-day basis. Each of them has contributed to my project either by teaching me the techniques or providing insightful advice. I would especially like to thank Dr. Tong-Rong Jan and Dr. Cheryl Rockwell, former members of the lab, who convinced me to pursue my dissertation project in the field of cannabinoids.

TABLE OF CONTENTS

LIST OF TABLES

LIST OF FIGURES

LIST OF ABBREVIATIONS

AA	arachidonic acid
Abn-CBD	abnormal cannabidiol; (-)-4-(3-3,4-*trans*-*p*-menthadien-[1,8]-yl)-olivetol
AEA	*N*-arachionoylethanolamide (anandamide)
2-AG	2-arachidonoylglycerol
ANKTM1	ankyrin-like with transmembrane domains 1
2-APB	2-aminoethoxydiphenylborate
AP-1	activator protein-1
APC	antigen presenting cell
BCR	B cell receptor
8-Br-cADPR	8-bromo-cyclic-adenosine diphosphate ribose
$[Ca^{2+}]_i$	intracellular calcium
$[Ca^{2+}]_e$	extracellular calcium
cADPR	cyclic adenoside diphosphaste ribose
CaM	calmodulin
CaMKII	calmodulin-dependent kinase II
cAMP	cyclic adenosine monophosphate
CB1	cannabinoid receptor 1
$CB1^{-/-}$	cannabinoid receptor 1 null
$CB1^{-/-}/CB2^{-/-}$	cannabinoid receptor 1 and 2 null
CB2	cannabinoid receptor 2

$CB2^{-/-}$	cannabinoid receptor 2 null
CBD	cannabidiol; 2-[3-methyl-6-(1-methylethenyl)-2-cyclohexen-1-yl]-5-pentyl-1,3-benezenediol
CBN	cannabinol; 6,6,9-trimethyl-3-pentyl-6H-dibenzo [b,d]pyran-1-ol
CCE	capacitative calcium entry
CD	cluster of differentiation
$CD4^+$	helper T cells
$CD8^+$	cytotoxic T cells
CGRP	calcitonin-gene regulatory peptide
Con A	concanavalin A
CP	CP55,940; (-)-cis-3-[2-hydroxy-[3,5-3H]-4-(1,1-dimethylheptyl)phenyl]-*trans*-4-(3-hydroxypropyl) cyclohexanol
CP56,667	(+)-cis-3-[2-hydroxy-[3,5-3H]-4-(1,1-dimethyl heptyl)phenyl]-*trans*-4-(3-hydroxypropyl) cyclohexanol
CPC	capsaicin
CRAC	calcium release-activated calcium
CREB	cAMP response element-binding protein
DAG	diacylglycerol
DC	dendritic cell
DNP-ficoll	dinitrophenyl-ficoll

DSI	depolarization-induced suppression of inhibition
EBD	ERM (ezrin-radixin-moesin) binding domain
ELISA	enzyme-linked immunosorbant assay
ERK-MAP	extracellular signal-regulated mitogen-activated protein
Et-18-OCH_3	edelfosine; 1-O-octadecyl-2-O-methyl-*rac*-glycero-3-phosphorylcholine
FKBP	FK506 binding protein
Fura-2/AM	1-[2-(5-carboxyoxazol-2-yl)-6-aminobenzofuran-5-oxy]-2-(2-amino-5-methylphenoxy)-ethane-N,N,N,N-tetraacetic acid pentaacetoxymethyl ester
GABA	gamma-amino butyric acid
GM-CSF	granulocyte-macrophage cell stimulating factor
HPB-ALL	human peripheral blood acute lymphoid leukemia
HU-210	(6aR,10aR)-3-(1,1-dimethylbutyl)-6a,7,10,10a-tetrahydro-6,6-dimethyl-6*H*-dibenzo[b,d]pyran-9-methanol
IFN	interferon
IL	interleukin
INAD	inactivation-no-afterpotential D
iNOS	inducible nitric oxide synthase
Io	ionomycin
IP_3	inositoltrisphosphate

JWH-133	(6aR,10aR)-3-(1,1-dimethylbutyl)-6a,7,10,10a-tetrahydro-6,6,9-trimethyl-6*H*-dibenzo[b,d]pyran
KN92	2-[N-(4'-methoxybenzenesulfonyl)]amino-N-(4'-chlorophenyl)-2-propenyl-N-methylbenzylamine phosphate salt
KN93	N-[2-[N-(4-chlorocinnamyl)-N-methylamino methyl]phenyl]-N-(2-hydroxyethyl)-4-methoxy benzenesulfonamide phosphate salt
LPS	lipopolysaccharide
LY294002	2-(4-morpholinyl)-8-phenyl-1(4H)-benzopyran-4-one hydrochloride
Meth-AEA	methanandamide
MHC	major histocompatibility complex
MIP	macrophage inflammatory protein
NFκB	nuclear factor κB
NFAT	nuclear factor of activated T cells
NHERF	Na^+/H^+ exchange regulatory factor
NK cell	natural killer cell
NOMPC	no mechanoreceptor potential C
O-1918	(-)-4-(3-3,4-*trans*-*p*-menthadien-(1,8)-yl)-orcinol
OAG	1-oleoyl-2-acetyl-*sn*-glycerol
11-OH-Δ^9-THC	11-hydroxy-Δ^9-tetrahydrocannabinol
PDZ	PSD (postsynaptic density protein)-95, DLG

	(discs large), zone occludens-1
PHA	phytohemagglutinin
PIP_2	phosphotidylinositol-bisphosphate
PI3K	phosphotidylinositol-3-kinase
PKA	protein kinase A
PKC	protein kinase C
PMA	phorbol-12-myristate-13-acetate
PMCA	plasma membrane calcium-ATPase
PP2	AG 1879; 4-amino-5-(4-chlorophenyl)-7-(*t*-butyl)
	pyrazolo[3,4-d] pyrimidine
PTx	pertussis toxin
RANTES	regulated upon activation, normally t-expressed,
	and presumably secreted
ROCC	receptor-operated cation channel
RPMI	Roswell Park Memorial Institute
RT-PCR	reverse transcriptase polymerase chain reaction
RyR	ryanodine receptor
SCID	severe combined immunodeficiency
SERCA	smooth endoplasmic reticulum calcium-ATPase
siRNA	small interference RNA
SOC	store-operated calcium
SOCC	store-operated calcium channel
SOCE	store-operated calcium entry

SPLC	splenocytes
SKF	SK&F96365; 1-[_-[3-(4-methoxyphenyl)propoxy]-4-methoxyphenethyl]-1H-imidazole
SR1	SR141716A; N-(piperidin-1-yl)-5-(4-chlorophenyl) -1-(2,4-dichlorphenyl)-4-methyl-H-pyrazole-3 carboxyamidehydrochloride
SR2	SR144528; N-[(1S)-endo-1,3,3,-trimethyl-bicyclo [2,2,1] heptan-2-yl]-5-(4-chloro-3-methylphenyl)-1-(4-methylbenzyl)-pyrazole-3-carboxamide
sRBC	sheep red blood cells
TCR	T cell antigen receptor
Th1	T helper cell subtype 1
Th2	T helper cell subtype 2
TG	thapsigargin
TGF	transforming growth factor
Δ^9-THC	(-)-Δ^9-tetrahydrocannabinol; tetrahydro-6,6,9-trimethyl-3-pentyl-6H-dibenzo[b,d]pyran-1-ol
TNF	tumor necrosis factor
TRP	transient receptor potential
TRPA	transient receptor potential ANKTM1
TRPC	transient receptor potential canonical
TRPC2$^{-/-}$	transient receptor potential canonical 2 null
TRPC4$^{-/-}$	transient receptor potential canonical 4 null

$TRPC6^{-/-}$	transient receptor potential canonical 6 null
TRPM	transient receptor potential melastatin
TRPML	transient receptor potential mucolipin
TRPP	transient receptor potential polycystin
TRPV	transient receptor potential vanilloid
VOCC	voltage-operated calcium channel
VR-1	vanilloid receptor-1
WIN-2	WIN55,212-2; (*R*)-(+)-[2,3-dihydro-5-methyl-3[(4-morpholinyl)methyl]pyrrolo[1,2,3-de]-1,4-benzoxazinyl]-(1-naphthalenyl) methanone mesylate salt.
WIN55,212-3	(*S*)-(-)-[2,3-dihydro-5-methyl-3-[(morpholinyl) methyl]pyrrolo[1,2,3-de]-1,4-benzoxazin-6-yl]-(1-naphthalenyl) methanone mesylate salt
WT	wildtype

INTRODUCTION

I. Marijuana, cannabinoids and cannabinoid receptors

A. Marijuana

Marijuana is the common name for *Cannabis sativa*, the hemp plant that is native to temperate and tropical climates. The recorded use of cannabis in Asia, both recreational and medicinal, spans several millennia. From Asia and the Middle East, marijuana use spread into North Africa, Europe, and the Americas (Nahas, 1972). Western medicine was first introduced to marijuana by the Irish physician William O'Shaughnessy in the 1840s, as a treatment for rheumatism and appetite stimulation (Joy et al., 1999). Until the 1930s, cannabis preparations were routinely included in British and American pharmacopoeias for treatment of convulsive disorders and as analgesics. However, with the development of more effective synthetic drugs, cannabis preparations lost their medical attention (Berdyshev, 2000). As the medicinal use of cannabis declined, its use as a recreational drug increased, leading to successive laws in most industrialized nations prohibiting the possession and supply of cannabis. Although still illegal, marijuana is currently the third most common drug of abuse in the United States and most European countries, following nicotine and alcohol (Baker et al., 2003). Nearly 50% of all 18-year-olds in the US and most European countries admit to having tried cannabis at least once in their lifetime (Iversen, 2003). Despite the endemic recreational use, a growing body of scientific literature and anecdotal evidence has shed new light on the potential therapeutic benefits of cannabis.

B. **Physiological effects of cannabis**

Smoked cannabis has been shown to have a wide array of effects on human physiology. Acute effects of smoked cannabis include mild euphoria, relaxing intoxication, slight changes in psychomotor activity, altered cognitive function, amotivational syndrome, tachycardia, peripheral vasodilation, appetite stimulation, and dizziness (Baker et al., 2003). Furthermore, marijuana smoke also produces inflammation, edema, and cellular injury in tracheobronchial mucosa of smokers (Sarafian et al., 1999). Long-term use of cannabis has been associated with bronchitis and emphysema, and may lead to changes in attention, memory, and ability to process complex information (Ashton, 2001). Some regular cannabis users also develop tolerance and dependence to the drug. Upon cessation of chronic intake, cannabis users who have become dependent may experience somatic withdrawal syndrome characterized by restlessness, insomnia, anxiety, increased aggression, anorexia, muscle tremor, and other autonomic effects (Ashton, 2001). As with other drugs of abuse such as cocaine, the development of tolerance, dependence, and withdrawal syndrome is attributed to the effects of cannabis on the nucleus accumbens, and reduction of neuronal activity in the mesolimbic dopaminergic pathway in the brain (Diana et al., 1998; Iversen, 2003). Apart from exerting psychoactive and behavioral effects, cannabis also exhibits immunomodulatory properties. The first immune cells that come into contact with cannabis smoke are the resident phagocytic cells in the lungs known as the alveolar macrophages. In alveolar macrophages, marijuana smoke has been shown to suppress antimicrobial activity, cytokine production and responsiveness to cytokines (Klein et al., 2003). Long-term use of cannabis may also be associated with an increased incidence of

bacterial and viral infections due to suppression of alveolar macrophage and circulating lymphocyte function. Despite years of investigation into the physiological changes elicited by cannabis smoke, sufficient studies in chronic cannabis smokers have not yet been performed. In particular, a full assessment of the precise cellular mechanism by which cannabis may alter immune function in human subjects remains to be performed.

C. **Cannabinoid compounds**

The flowering tops and leaves of *Cannabis sativa* contain a family of structurally-related compounds known as cannabinoids. In the lay literature, cannabinoids are often described as the active constituents in cannabis smoke. The plant-derived cannabinoid family comprises over sixty dibenzopyran tricyclic ring structures consisting of a phenolic ring attached to a five carbon alkyl chain; a central pyran ring; and a monounsaturated cyclohexyl ring (Howlett et al., 2004). Although the presence and the biological effects of cannabinoids were long known, the structure of the primary psychoactive cannabinoid, Δ^9-tetrahydrocannabinol (Δ^9-THC), was not discovered until 1964 (Felder and Glass, 1998; Klein et al., 2000a). Together with Δ^9-THC, cannabinol (CBN) and cannabidiol (CBD), which exhibit little and no psychoactivity respectively, form a triad of the most-often experimentally utilized plant-derived cannabinoids (figure 1). Following the discovery of the chemical structure of Δ^9-THC, a variety of synthetic cannabimimetic compounds were developed as potential non-opioid analgesics (Howlett et al., 2004). The first generation of synthetic cannabinoids, such as CP55,940 (CP) and HU-210, were modeled after the chemical structure of Δ^9-THC (figure 1), the prototypical cannabinoid, with small changes to phenolic, cyclohexyl and alkyl

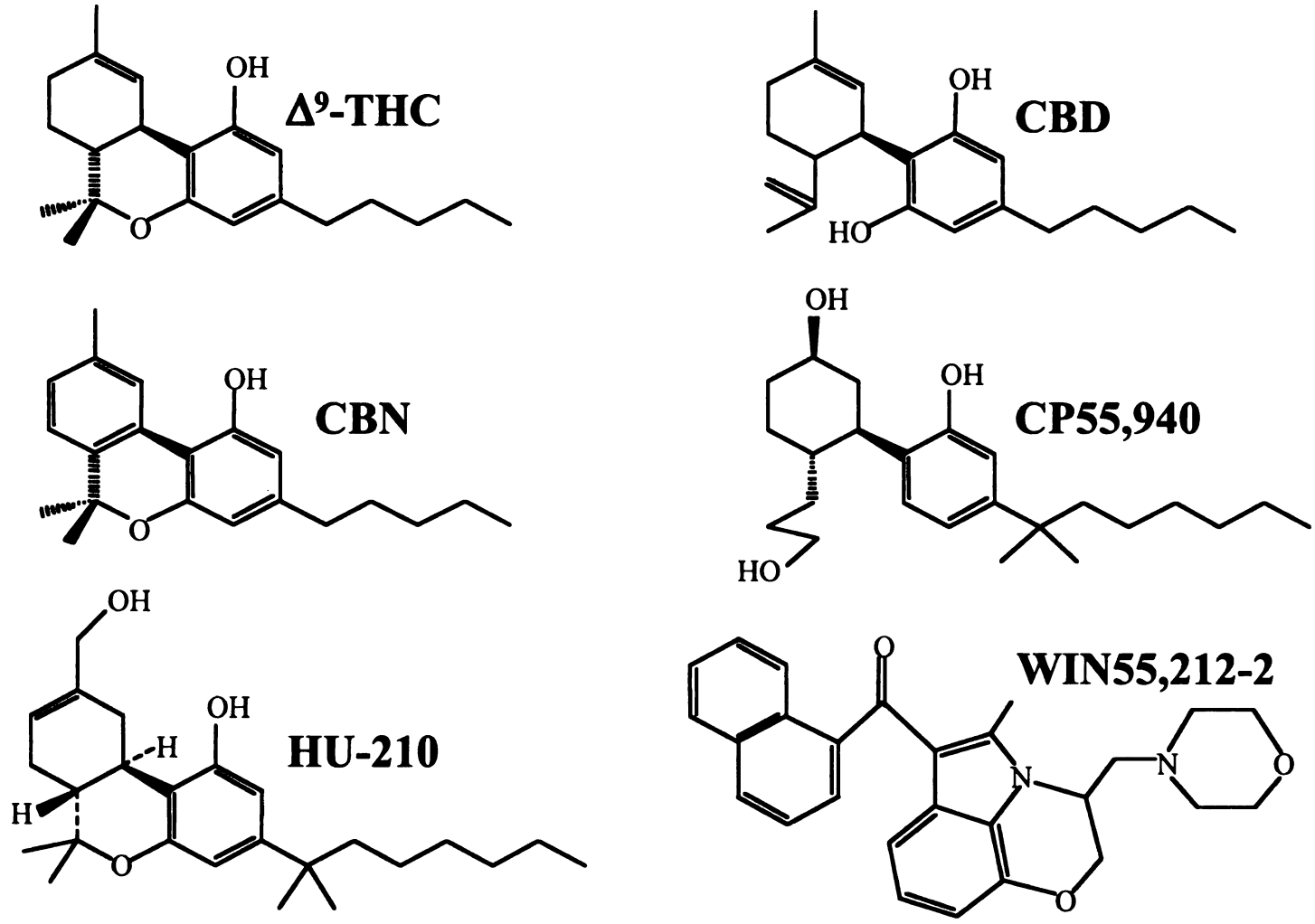

Figure 1. Structures of classical cannabinoid compounds. Δ^9-THC, CBN and CBD are plant-derived cannabinoids. CP55,940 (CP), HU-210 and WIN55,212-2 (WIN-2) are synthetic cannabinoid compounds.

functional groups. However, later classes of cannabinoids such as the aminoalkylindoles, typified by WIN55,212-2 (WIN-2; figure 1), represent a continuing evolution of cannabimimetic compounds that came into being as advances in cannabinoid biology were made.

D. Therapeutic potential of cannabinoids

The initial observation that marijuana exerts effects on different branches of human physiology fueled a search for potential therapeutic benefits of cannabinoid compounds. Over the past few decades, plant-derived as well as synthetic cannabinoids have been shown to possess therapeutic potential as treatments in many human diseases and conditions. Cannabinoids have been proposed as treatments for nausea associated with cancer chemotherapy, neuropathic pain, spasticity in multiple sclerosis, migraine headaches, epilepsy, glaucoma, hypertension, AIDS-induced wasting syndrome, bronchioalveolar constriction associated with asthma, and allergic airway diseases (Baker et al., 2003; Felder and Glass, 1998; Jan et al., 2003; Jan et al., 2002). Currently, the FDA-approved cannabinoid-based drug, Marinol®, an oral preparation of Δ^9-THC, is marketed in the United States for the treatment of cachexia observed in patients with AIDS or undergoing cancer chemotherapy (Felder and Glass, 1998). Additionally, Cesamet®, an oral preparation of a synthetic cannabinoid known as nabilone, is approved for treatment of cachexia in the United Kingdom (Pertwee, 2002). More recently, Sativex®, an oral spray of cannabis extract containing low amounts of psychoactive cannabinoids, has been approved in Canada for the treatment of neuropathic pain associated with multiple sclerosis, and is currently awaiting approval in the United

Kingdom. Moreover, since 1996 several states in the US including Alaska, Arizona, California, Colorado, Hawaii, Maine, Nevada, Maryland, Montana, Oregon and Washington have passed legislation that removes or softens state-level penalties for medicinal use of marijuana if prescribed by a physician. The legalization of medical marijuana in above-mentioned states has provided impetus for the fledgling medicinal marijuana movement in the US. The ever-growing body of scientific literature on the therapeutic potential of cannabinoids coupled with the medicinal marijuana movement among the lay public necessitates a comprehensive understanding of cannabinoid pharmacology and toxicology.

E. **Cannabinoid receptors**

The field of cannabinoid biology took a major leap forward upon the discovery of the cannabinoid receptors. To date, two cannabinoid receptors, CB1 and CB2, have been identified and cloned in mammalian tissues (Devane et al., 1988; Matsuda et al., 1990; Munro et al., 1993). Both CB1 and CB2 belong to the G protein-coupled hexahelical transmembrane receptor superfamily, and are believed to mediate many of the pharmacological effects produced by Δ^9-THC, as well as the synthetic cannabinoids. The CB1 receptor is expressed primarily in neurons of the central nervous system, and has been shown to mediate most of the psychoactive and behavioral effects of cannabinoids (Zimmer et al., 1999). The highest expression of CB1 receptors was found in the GABAergic interneurons in the cerebral cortex, basal ganglia, amygdala, and hippocampus (Iversen, 2003). Apart from the central nervous system, the CB1 receptor is also expressed in several peripheral tissues including the testes, uterus, vascular smooth

muscle, and spleen (Pertwee, 1999b). The CB2 receptor, on the other hand, is absent from CNS, but expressed in cells of the immune system including B cells, natural killer (NK) cells, monocytes, neutrophils, $CD8^+$ T cells and $CD4^+$ T cells (Berdyshev, 2000). The CB2 receptor is the predominant cannabinoid receptor expressed in the immune system, although most immune cells also express CB1 (Bouaboula et al., 1993; Munro et al., 1993; Schatz et al., 1997). Due to the higher levels of CB2 receptor expression in the immune system, it is generally believed that the majority of immunological effects of cannabinoids are mediated by the CB2 receptor. The CB1 and CB2 receptors bind to the plant-derived cannabinoids with moderately high affinity and pharmacological efficacy. However, the synthetic cannabinoid congeners have been subsequently shown to exhibit higher binding affinities and higher pharmacological efficacies than the plant-derived cannabinoids at both receptors (Klein et al., 2003; Pertwee, 1999b).

F. **Endogenous ligands**

Following the discovery of the cannabinoid receptors in mammalian cells, search for endogenous ligands for the cannabinoid receptors ensued. Soon after, the eicosinoid-derivatives, *N*-arachidonoylethanolamide (AEA or anandamide) (Devane et al., 1992), and 2-arachiodonoylglycerol (2-AG) (Lee et al., 1995; Mechoulam et al., 1995; Sugiura et al., 1995), were identified as endogenous ligands for the cannabinoid receptors, and labeled the endocannabinoids (figure 2). Both AEA and 2-AG exhibit moderately high affinities and pharmacological efficacies at the cannabinoid receptors, and are the most widely recognized endocannabinoids. In addition to these molecules, several other fatty acid and eicosinoid derivatives, including *N*-arachidonoyldopamine, *O*-

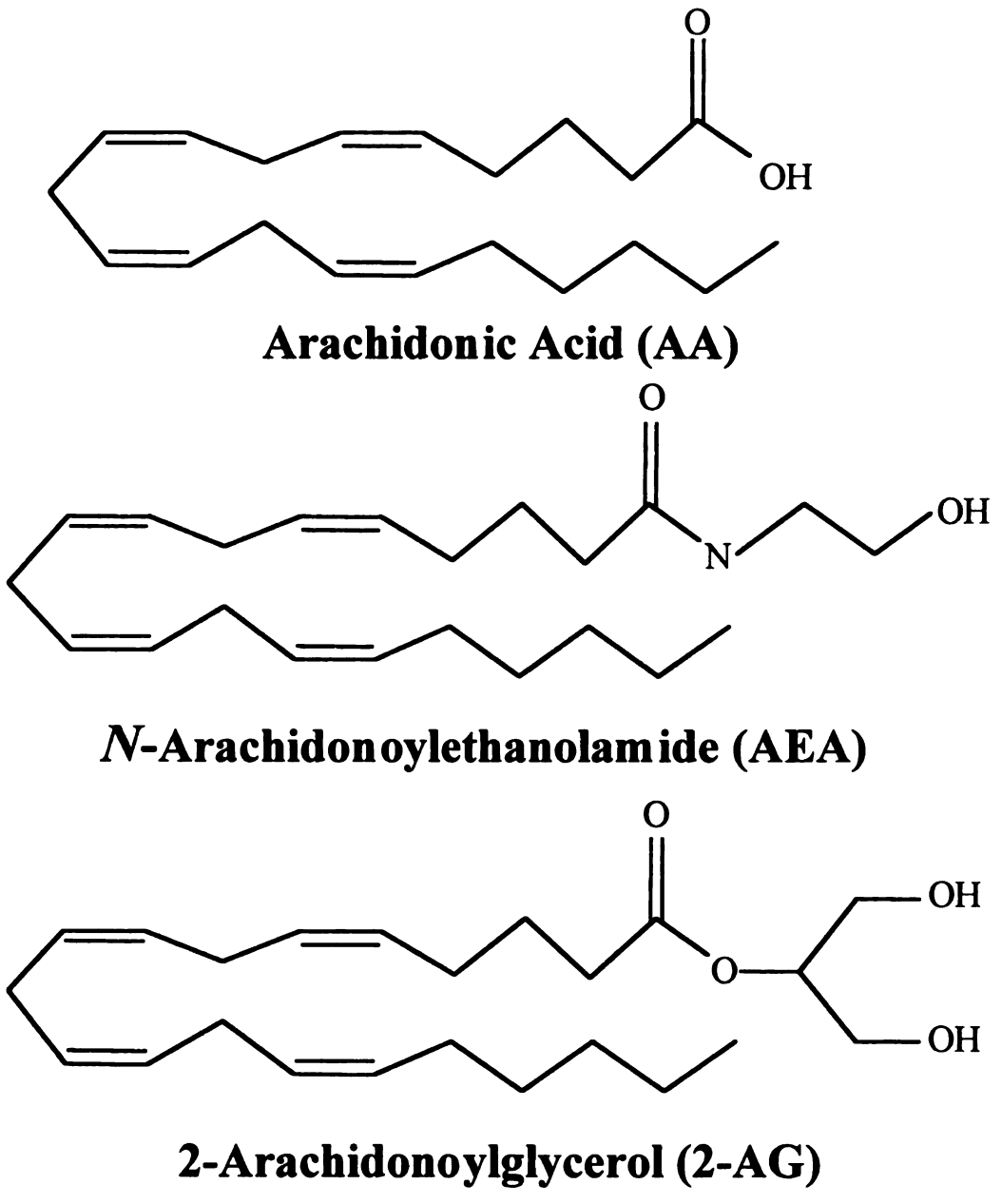

Figure 2. Structures of arachidonic acid and the endocannabinoids. *N*-arachidonoylethanolamide (AEA) and 2-archidonoylglycerol (2-AG) are endogenous cannabinoid compounds and arachidonic acid (AA) is the parent eicosinoid compound.

arachidonoylethanolamine (virodhamine), docosatetraenylethanolamine, and 2-arachidonoylglycerol-ether (nolandin ether) have been found to exhibit binding affinity to the cannabinoid receptors (Baker et al., 2003). However, the role of the newer putative endocannabinoids remains obscure. The production of endocannabinoids, in particular AEA and 2-AG, has also been reported to occur in tissues expressing higher densities of cannabinoid receptors, such as the brain and the spleen (Klein et al., 2003).

G. **Cannabinoid receptor antagonists**

At approximately the same time as the discovery of the endocannabinoids, search for antagonists for the cannabinoid receptors was also initiated. High-throughput screening techniques by Sanofi Recherche led to the discovery of the biarylpyrazole compounds, SR141716A (SR1) and SR144528 (SR2), the CB1 and CB2 receptor antagonists respectively (Rinaldi-Carmona et al., 1994; Rinaldi-Carmona et al., 1998). Both SR1 and SR2 (figure 3) are selective to their cognate receptors, but not specific; and exhibit binding affinities in the nanomolar concentration range. The discovery of the cannabinoid receptor antagonists revolutionized the field of cannabinoid biology, enabling the differentiation of cannabinoid receptor-dependent and -independent modes of action. It was soon discovered, however, that both SR1 and SR2 elicit inverse agonistic properties at both CB1 and CB2 (Bouaboula et al., 1999; Shire et al., 1999), confounding their use as exclusive neutral antagonists at either cannabinoid receptor. In addition, at higher concentrations, SR1 has been since shown to exhibit binding affinity at the CB2 receptor, and may exert antagonistic effects independent of both the CB1 and CB2 receptors (Pertwee, 2005). SR2 also may bind and antagonize the CB1 receptor at

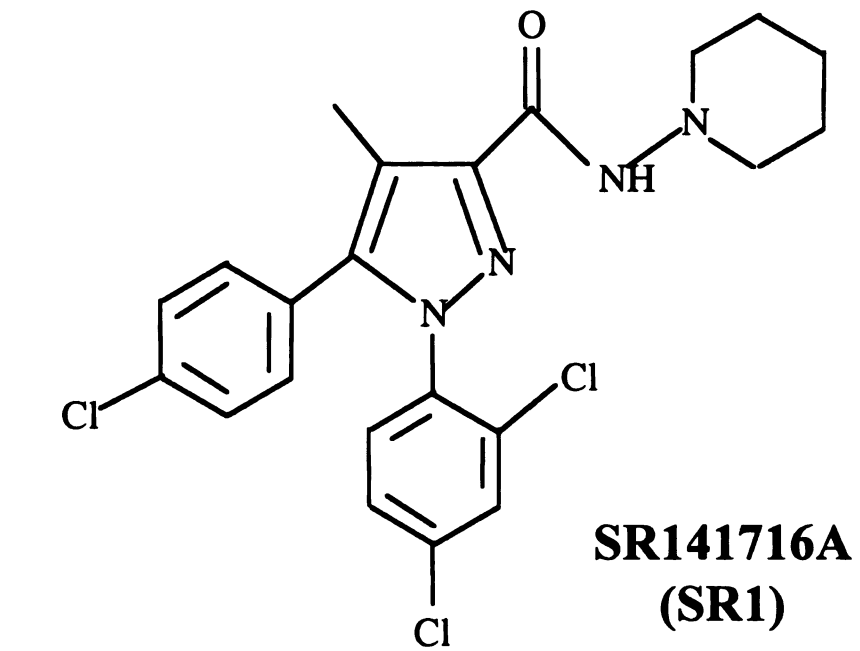

SR141716A (SR1)

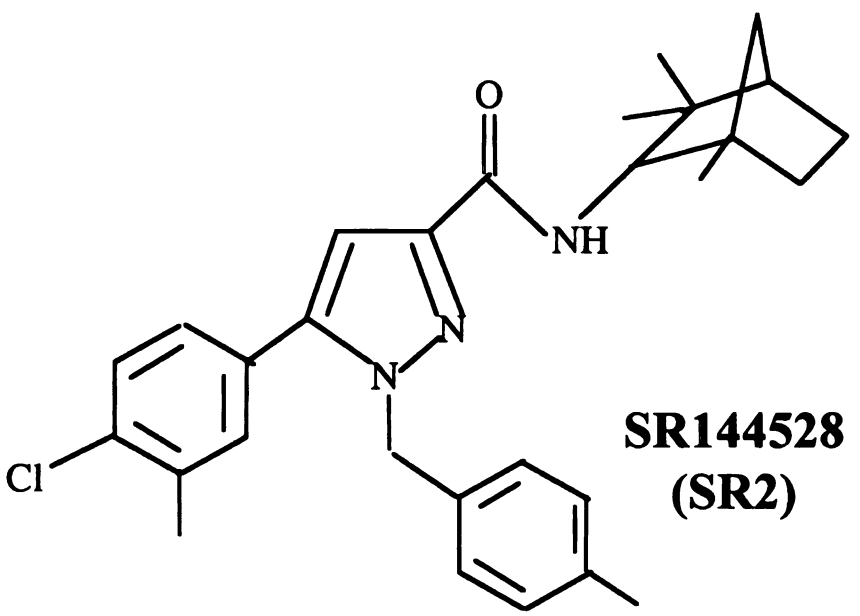

SR144528 (SR2)

Figure 3. Structures of the cannabinoid receptor antagonists. SR141716A (SR1) is a CB1 receptor-selective antagonist and SR144528 (SR2) is a CB2 receptor-selective antagonist.

higher concentrations (Pertwee, 1999b). Recently, novel classes of more selective cannabinoid receptor antagonists such as the CB2-selective antagonist, AM630, have been developed, but extensive characterization of the newer classes of antagonists has yet to take place.

II. Pharmacological and biochemical effects of cannabinoids

A. Effects of cannabinoids on the central nervous system

1. CNS neurons

Since the discovery of the cannabinoid receptors, the endogenous ligands, and the cannabinoid receptor antagonists, a multitude of cannabinoid effects on various cell types have been reported. Perhaps the most extensive studies of cannabinoid effects have been performed in the brain and central nervous system (CNS). Cannabinoids of all classes have been shown to modulate the secretion of most major vertebrate neurotransmitters including glutamate, GABA, glycine, norepinephrine, serotonin, dopamine, acetylcholine and neuropeptides (Baker et al., 2003). A vast majority of the inhibitory effects of cannabinoids on CNS neuronal function are mediated by CB1 receptors, which are expressed on axons and nerve terminals (Wilson and Nicoll, 2002). The GABAergic interneurons in the cerebral cortex, basal ganglia, amygdala and hippocampus express the highest density of CB1 receptors in the CNS (Iversen, 2003). The complex effects of cannabinoids on psychomotor behavior, learning, memory, and cognitive function are attributed to the inhibition of the GABAergic interneurons in the above-mentioned brain regions (Iversen, 2003). Under normal physiological conditions, it is hypothesized that upon depolarization of postsynaptic neurons rapid production of endocannabinoids

ensues. Endocannabinoids subsequently act as retrograde messengers to traverse the synaptic cleft and bind CB1 receptors on presynaptic nerve terminals. This phenomenon known as depolarization-induced suppression of inhibition (DSI) results in the inhibition of presynaptic neurons, thereby attenuating neurotransmitter release (Howlett et al., 2004). The major mechanism by which endogenous and exogenous cannabinoids inhibit the secretion of neurotransmitters involves the modulation of ion channels. Under experimental conditions, various classes of cannabinoids have been shown to inhibit the function of voltage-operated calcium (Ca^{2+}) channels (VOCCs), as well as to activate potassium (K^+) channels. In particular, activation of neuronal CB1 receptors leads to the inhibition of VOCCs type N, P and Q, as well as the activation of type A K^+ channels (Glass and Northup, 1999; Twitchell et al., 1997). Together, the inhibition of VOCCs and activation K^+ channels attenuate the presynaptic release of neurotransmitters. The changes in behavior and psychoactivity associated with cannabis use are physiological manifestations of the combined inhibitory effects of cannabinoids on the mammalian CNS.

2. **Astrocytes and microglial cells**

Apart from neurons in the CNS, cannabinoids have also been demonstrated to affect the function of astrocytes and other glial cells. Glial cells play an important role in the mammalian CNS by controlling the microenvironment of nerve cells, and modulating many neuronal functions. Astrocytes are a unique class of glial cells, which provide the support structure for neurons, and control proliferation and repair following nerve injury. Another class of glial cells are the microglia, which are involved in removal and

phagocytosis of debris in the CNS. In general, cannabinoids have inhibitory effects on the function of glial cells. Specifically, cannabinoids inhibit the production of cytotoxins and cytokines by astrocytes and microglia. Using Δ^9-THC as well as the synthetic cannabinoids, WIN-2 and CP, suppression of the production of several inflammatory cytokines, such as interleukin (IL)-1β, IL-1α, IL-6, and tumor necrosis factor (TNF)-α, has been shown in activated astrocytes (Berdyshev, 2000; Sheng et al., 2005). Furthermore, under conditions of neuroinflammation, endocannabinoid synthesis is induced in both microglia and astrocytes. The elevated levels of endocannabinoids are believed to act in an autocrine or paracrine manner to inhibit the activation of astrocytes and microglia, thus preventing the propagation of neuroinflammation and further cell damage due to the release of inflammatory mediators (Stella, 2004). The inhibition of astrocyte function has been demonstrated experimentally with methanandamide (meth-AEA), a non-hydrolysable analog of AEA, which inhibits astrocyte function by attenuating agonist-induced intracellular calcium ($[Ca^{2+}]_i$) rise (Venance et al., 1997).

Interestingly, whereas most inhibitory effects of cannabinoids on CNS neurons can be attributed to CB1-dependent mechanisms, several studies have shown cannabinoid-mediated inhibition of glial cell function to be independent of the CB1 receptor. For example, the inhibition of cyclic adenosine monophosphate (cAMP) formation in rat astrocytes by both WIN-2 and AEA was mediated by a G protein-coupled receptor distinct from CB1 (Sagan et al., 1999). Similarly, the suppression of pro-inflammatory cytokine production by CP in rat microglia could be replicated by an enantiomer of CP, CP56,667, which does not bind either CB1 or CB2, and was insensitive to either SR1 or SR2 (Berdyshev, 2000). Also, it is notable that microglial

cells, unlike CNS neurons, may express CB2 receptors. Immunofluorescent staining for CB1 and CB2 in cultured rat microglia revealed that whereas the CB1 receptor was localized to intracellular compartments, the CB2 receptor was expressed throughout the cell surface (Felder and Glass, 1998; Stella, 2004; Walter et al., 2003). However, the expression of CB2 in the mammalian CNS remains highly controversial.

B. **Effect of cannabinoids on the immune system**

Aside from the CNS, cannabinoid effects have also been widely characterized in immune cells. In general, cannabinoids differentially modulate the immune system depending on cell type used, mode of activation, and functional response being measured. Although cannabinoids have significant immunomodulatory effects when immune cells are exposed directly, acute intake of cannabinoids by means of smoked cannabis has negligible effects on systemic immunity (Klein et al., 2003). However, cannabinoids have significant suppressive effects on immune cells when directly exposed to cannabis smoke. Previous *in vivo* immunological studies performed in rodents have revealed that exposure to cannabinoids results in altered innate, humoral and cell-mediated immune responses (Yahya and Watson, 1987). Preliminary studies have also revealed that long-term exposure to cannabinoids in humans may result in an increased incidence of viral and bacterial infections, and modulation of cannabinoid receptor expression in immune cells (Klein et al., 2003). A caveat to the aforementioned observation is that only a few controlled studies on the immune effects of cannabinoids in humans have been conducted. No comprehensive study has been performed to date investigating the immune effects of heavy and chronic use of marijuana in human subjects.

1. **Innate immunity**

a. **Macrophages**

The innate immune response is critical in the first phase of infections until the adaptive immune response is mounted after a delay of 4-7 days. A majority of the studies of cannabinoid effects on innate immune responses have been limited to macrophages. Macrophages are resident phagocytic cells in many tissues and are available to combat a wide array of pathogens. Isolated alveolar macrophages from marijuana smokers show a suppressed ability to secrete pro-inflammatory cytokines, and to generate nitric oxide (NO) (Roth et al., 2002). Similarly, the suppression of pro-inflammatory cytokines has also been demonstrated in non-alveolar macrophages treated with cannabinoids. In cultured macrophage cell lines activated with lipopolysaccharide (LPS), Δ^9-THC and AEA inhibited the secretion of the pro-inflammatory cytokine, TNF-α (Berdyshev, 2000; Cabral and Fischer-Stenger, 1994). The suppression of TNF-α secretion was not a result of attenuation in TNF-α transcription, but represented an suppression of TNF-α maturation from its pre-secretory form (Cabral and Fischer-Stenger, 1994). Apart from acting as an inflammatory mediator, TNF-α has a secondary role in the tumoricidal activity of macrophages. Therefore, the suppression of TNF-α processing and secretion by cannabinoids may also result in the attenuation of the macrophage tumoricidal activity (McCoy et al., 1995).

Cannabinoids also affect the bactericidal function of macrophages by inhibiting the production of NO. CP and Δ^9-THC have both been demonstrated to inhibit the production of NO in macrophages stimulated with LPS (Jeon et al., 1996; Newton et al., 1998; Ponti et al., 2001). The inhibition of NO production by cannabinoids may involve

the cannabinoid receptors, as well as inducible nitric oxide synthase (iNOS). Macrophages activated with LPS upregulate the transcription of iNOS, which in turn is responsible for the generation of NO. Treatment of macrophages with Δ^9-THC prior to LPS activation resulted in an inhibition of iNOS upregulation (Jeon et al., 1996). In another study the cannabinoid-mediated inhibition of LPS-activated NO production was reversed upon pretreatment with either SR1 or SR2 (Ponti et al., 2001). The observation that effects of cannabinoids on macrophages may be dependent on the cannabinoid receptors is not surprising given that macrophages express both CB1 and CB2, and are also known to produce endocannabinoids (Klein et al., 2000a). It is currently postulated that the macrophage-derived endocannabinoids may modulate macrophage function as well as the complex interactions between macrophages and other immune cells.

Another important role fulfilled by macrophages is the activation of $CD4^+$ T cells, leading to the onset of adaptive immunity. Upon trapping, engulfment and destruction of pathogens, macrophages process antigens to be presented to T cells in the context of major histocompatibility complex molecules (MHCs). Together with B7 co-stimulatory molecules, processed antigens in the context of MHC molecules provide a robust activation signal to $CD4^+$ T cells. In this capacity, macrophages are known as antigen presenting cells (APCs). Numerous studies point to the macrophage-T cell interaction as a target for cannabinoid action. Early on, cannabinoids were determined to impair the function of macrophages to act as APCs. Studies by McCoy and coworkers demonstrated that the ability of a macrophage hybridoma to process antigens was attenuated in the presence of Δ^9-THC (McCoy et al., 1995). The aforementioned study suggested that Δ^9-THC mainly alters antigen processing, and not presentation of antigens to T cells.

Further studies demonstrated that the T cell response, as measured by IL-2 secretion, was diminished when macrophages were presented with unprocessed antigens, but not when presented with processed antigens in the presence of either Δ^9-THC or CP (McCoy et al., 1999). Furthermore, SR2, but not SR1, attenuated the Δ^9-THC-induced inhibition of antigen-dependent activation of $CD4^+$ T cells by macrophages. More recently, the involvement of the CB2 receptor in the co-stimulation of $CD4^+$ T cells was examined using macrophages from CB2 null ($CB2^{-/-}$) mice. Peritoneal macrophages isolated from wildtype (WT) mice exhibited a diminished ability to co-stimulate a T cell hybridoma in the presence of Δ^9-THC, whereas macrophages from $CB2^{-/-}$ mice did not (Buckley et al., 2000). Taken together, the above studies indicate that one manner in which cannabinoids disrupt innate immune responses is by interfering with macrophage function.

b. **Neutrophils, NK cells and dendritic cells**

Apart from macrophages, several other important cell types such as neutrophils, NK cells, and dendritic cells (DCs) also contribute to innate immunity. It has been established previously that all three cell types mentioned above express CB1 and CB2 receptors (Klein et al., 2003; Matias et al., 2002). However, studies of cannabinoid effects on innate immune cells, other than the macrophage, have been scant. The available few such studies suggest that cannabinoids negatively affect the function of all innate immune cells.

Neutrophils play an important role in primary defense against bacteria. In particular, the process known as respiratory burst, which generates reactive intermediates such as superoxide and NO, is critical for neutrophil bactericidal activity. In isolated

human neutrophils, CP inhibited the production of superoxide anions induced by the peptide fMLP (Kraft et al., 2004). Interestingly, in the same system, AEA did not inhibit superoxide production. Furthermore, the effect of CP on superoxide production could not be reversed by either SR1 or SR2 (Kraft et al., 2004).

Cannabinoids have similarly been shown to have deleterious effects on NK cells. NK cells belong to the lymphoid family of immune cells, and are involved in the recognition and killing of abnormal cells, especially cells that are tumorogenic or virally-transformed. Critical to the function of NK cells is the secretion of small soluble molecules known as chemokines and cytokines. In a human NK cell line, Δ^9-THC was shown to inhibit the constitutive secretion of the chemokines, macrophage inflammatory protein (MIP)-1α, MIP-1β, IL-8 and RANTES, as well as the secretion of cytokines, TNF-α, GM-CSF, and IFN-γ (Srivastava et al., 1998). Furthermore, *in vivo* administration of Δ^9-THC significantly inhibited NK cell cytolytic activity, which was partially reversed by SR1 and SR2 (Massi et al., 2000). A full characterization of the cannabinoid modulation of NK cell activity and the involvement of the cannabinoid receptors therein remains to be investigated.

Very little is known about the effects of cannabinoids on DCs. DCs are the most important type of APC, and have a central role in the initiation of adaptive immune responses by providing activation signals to T cells. Although the effect of cannabinoids on antigen presentation by DCs has not been accessed, *in vivo* treatment of mice with Δ^9-THC has been shown to deplete DCs in the spleen (Do et al., 2004). The depletion of DCs in the spleen is believed to be a result of cannabinoid receptor-dependent activation of the apoptotic pathway. Both Δ^9-THC and AEA were found to induce apoptosis in a

CB1 and CB2 receptor-dependent manner in murine bone marrow-derived DCs (Do et al., 2004). In addition, LPS activation of DCs was found to induce synthesis of endocannabinoids (Matias et al., 2002). However, the role of endocannabinoids in the complex DC dynamics is unknown.

2. Adaptive immunity

Adaptive immunity is a delayed, yet specific, immune response that oftentimes confers lifelong protection against re-infection by the very same pathogen. Adaptive immunity is generally divided into two parts: humoral immunity and cell-mediated immunity, mediated by B and T cells respectively. Whereas the cell-mediated immune response is important for combating intracellular pathogens, resistance to extracellular pathogens is conferred by the humoral immune response. Cannabinoid effects on the adaptive immune response have been widely documented over the past few decades. Early immunological experiments revealed that administration of Δ^9-THC in mice suppressed the adaptive immune response induced by pathogenic microorganisms or by the antigen, sheep red blood cells (sRBCs) (Morahan et al., 1979; Zimmerman et al., 1977). Although the mechanism of cannabinoid-mediated immune suppression was not yet known, it was soon discovered that Δ^9-THC treatment did not alter the total number of circulating B or T cells (Silverman et al., 1982). As efforts toward developing a more in-depth understanding of cannabinoid-mediated immune modulation continued, it was found that cannabinoids inhibited the proliferation of both B and T cells activated by mitogens in culture (Klein et al., 1985; Pross et al., 1987). A large body of literature has

since emerged examining the effects of cannabinoids on various endpoints associated with B and T cell activation.

a. B cells and humoral immunity

The secretion of antigen specific immunoglobulins (antibodies) by activated B cells characterizes the humoral immune response. Antibodies secreted by B cells bind specifically to pathogens or their toxic products thereby neutralizing them and enhancing their phagocytosis. Moreover, antibodies also enable complement factor-dependent opsinization of microbes by phagocytic cells. Normally, the production of antibodies is initiated when B cells come into contact with small peptide antigens, which they process and present on the cell surface in the context of MHC class II molecules. Subsequently, antigen-specific $CD4^+$ T cells recognize the MHC-antigen complex and interact with the B cells to deliver activation and co-stimulatory signals. In response to the T cell signals, B cells undergo clonal expansion and differentiate into antibody-forming cells (AFCs).

(i). Antibody production

Extensive work by Kaminski and coworkers examined the effect of various cannabinoids on the generation of AFCs in murine splenocytes (SPLC) stimulated by the T cell-dependent antigen, sRBCs. The mechanism by which sRBCs stimulate naïve B cells to clonally expand and differentiate into AFCs involves the accessory function of macrophages, as well as the helper function of $CD4^+$ T cells. In assays where sRBCs were used as a stimulus, both *in vivo* administration of Δ^9-THC in mice, as well as the *in vitro* treatment of murine SPLC with Δ^9-THC, CP, HU-210 or CBN resulted in a

selective and dose-dependent inhibition of AFC production (Herring et al., 1998; Kaminski et al., 1992; Schatz et al., 1993). However, due the ambiguity of the mechanism by which cannabinoids inhibited AFC production, further AFC response studies were performed using antigens that stimulate B cells independently of T cells. In particular, B cells were stimulated with dinitrophenyl-ficoll (DNP-ficoll), a synthetic antigen, which requires accessory function of macrophages; or LPS, a polyclonal B cell activator. Interestingly, AFC production induced by either DNP-ficoll or LPS was not inhibited by Δ^9-THC (Schatz et al., 1993). The observation that AFC production stimulated by T cell-independent antigens was not affected by Δ^9-THC suggested that cannabinoid-mediated alteration of AFC responses was not a direct effect on B cells. Therefore, the AFC studies indicated that both B cell effector function and macrophage accessory function for humoral responses were insensitive to cannabinoid treatment.

(ii). **B cell proliferation**

A few studies have demonstrated direct effects of cannabinoids on B cells. Initially, Klein et al. examined the effect of Δ^9-THC and 11-OH-Δ^9-THC, the primary metabolite of Δ^9-THC, on the LPS-stimulated proliferation of human B cells (Klein et al., 1985). Under these conditions, B cell proliferation was strongly inhibited by micromolar concentrations of both Δ^9-THC and 11-OH-Δ^9-THC. Similarly, 2-AG, but not AEA, inhibited the LPS-induced proliferation of murine splenic B cells (Lee et al., 1995). By contrast, in human tonsillar B cells stimulated by cross-linking of the B cell receptor or by ligation of the CD40 antigen, nanomolar concentrations of CP, WIN-2 and Δ^9-THC enhanced the proliferation of B cells (Derocq et al., 1995). Moreover, the cannabinoid-

mediated enhancement of B cell proliferation could be reversed by pertussis toxin (PTx), implicating the involvement of G protein-coupled receptors in the process. Subsequently, a second group confirmed the enhancement of proliferation induced by CD40 ligation in virgin tonsillar and germinal center B cells using CP (Carayon et al., 1998). The enhancement of B cell proliferation mediated by CP was antagonized by SR2. B cells are known to express one of the highest densities of CB2 and CB1 receptors among immune cells (Carayon et al., 1998; Klein et al., 2003). However, the significance of the high cannabinoid receptor density in B cell function remains largely unknown. Based on the above studies, Carayon et al. have hypothesized that CB2 receptors may act as co-receptors of CD40-induced proliferation in B cells (Carayon et al., 1998).

b. **T cells and cell-mediated immunity**

Cell-mediated immunity is the second branch of the adaptive immune system and involves responses mediated by T cells. Whereas the humoral immune response confers resistance against extracellular pathogens, the cell-mediated immune response is responsible for the elimination of intracellular pathogens, including viruses and some bacteria. The elimination of intracellular pathogens depends on a direct interaction between T cells and cells bearing the antigen that the T cell recognizes. Two major types of T cells participate in cell-mediated immune responses: $CD4^+$ (helper) T cells and the $CD8^+$ (cytotoxic) T cells. $CD4^+$ T cells recognize specific antigens in the context of MHC class II molecules that are presented by the APCs, i.e. macrophages, B cells and DCs. Upon recognition of antigens, $CD4^+$ T cells interact with the APCs and secrete cytokines. $CD4^+$ T cells play an important role in delayed-type responses, which involve

the activation of macrophages, and also participate in the activation of B cells leading to the production of antibodies. $CD8^+$ T cells, by contrast, recognize specific antigens in the context of MHC class I molecules, which can be presented by almost any cell in the body. Upon recognition of a specific antigen, $CD8^+$ T cells interact with the cells presenting antigen and secrete cytokines and cytotoxic factors to induce cell death in the infected cell. $CD8^+$ T cells are critical in the induction of cell death in tumorogenic and virus infected cells.

(i). T cell proliferation

A majority of cannabinoid studies in T cells have been focused on T cell activation-associated endpoints. Preliminary investigation by Klein and coworkers on cannabinoid-mediated modulation of T cell activation examined the proliferation of T cells upon stimulation by T cell-specific mitogens, phytohemagglutinin (PHA) and concanavalin A (Con A). In murine T cells activated with either PHA or Con A, both Δ^9-THC and 11-OH-Δ^9-THC inhibited cell proliferation in a dose-dependent manner (Klein et al., 1985). Furthermore, the effect of cannabinoids on T cell proliferation was dependent on the age of mice, as well as the lymphoid organ used. Splenic T cells from younger mice and immature thymic T cells from older mice appeared to be more susceptible to the effects of Δ^9-THC (Pross et al., 1987; Pross et al., 1990). Based on the aforementioned observations, it was proposed that cannabinoids suppress the normal development of mature effector T cells from less mature precursor cells. The inhibition of T cell function was also demonstrated with $CD8^+$ T cells. Both Δ^9-THC and 11-OH-Δ^9-THC inhibited the proliferation and cytolytic activity of $CD8^+$ T cells (Klein et al.,

1991; Pross et al., 1992). To date, the precise mechanism of cannabinoid inhibition of proliferative and functional T cells responses remains unclear. However, the modulation of the mobilization of $[Ca^{2+}]_i$ by Δ^9-THC may underlie many cannabinoid effects on T cell activation-associated endpoints (Yebra et al., 1992).

(ii). **IL-2 suppression**

Recent studies of cannabinoid effects on T cell activation have focused on cytokine production and secretion. Cannabinoids have been shown to modulate the expression of several cytokines including interferon (IFN)-γ, transforming growth factor (TGF)-β, TNF-α, IL-2, IL-4, IL-6, IL-10, IL-12, IL-13 and IL-15 in human and murine cell models (Berdyshev et al., 1997). However, the most extensive investigation of cannabinoid modulation of cytokine production has been conducted with IL-2. IL-2 is a critical T cell cytokine that is *de novo* synthesized and secreted upon the full activation of T cells. IL-2 acts as an autocrine or paracrine T cell growth factor and is responsible for the induction of T cell clonal expansion. A majority of studies of IL-2 regulation by cannabinoids have utilized robust activation stimuli that either bypass the T cell receptor using phorbol ester and ionomycin (PMA/Io), or polyclonally activate T cells using anti-CD3 antibodies, PHA or Con A. Under conditions of robust T cell stimulation, suppression of the production and secretion of IL-2 has been demonstrated with a wide array of cannabinoid compounds including Δ^9-THC, CP, WIN-2, CBN, CBD, AEA, and 2-AG in murine SPLC, thymocytes, and T cell lines (Condie et al., 1996; Faubert Kaplan et al., 2003; Herring and Kaminski, 1999; Klein et al., 2000b; Ouyang and Kaminski, 1999; Rockwell and Kaminski, 2004). The suppression of IL-2 has also been

demonstrated in Con A-stimulated SPLC cultures from mice which were acutely treated with Δ^9-THC (Massi et al., 1998).

More recent studies of IL-2 regulation have found that cannabinoids interfere with the expression of IL-2 at the level of gene transcription. The inhibition of the DNA-binding activity of several transcription factors regulating IL-2 by cannabinoids has been reported. Some of the transcription factors modulated by cannabinoids include activator protein-1 (AP-1), cAMP response element-binding protein (CREB), nuclear factor κB (NFκB), and nuclear factor of activated T cells (NFAT) (Condie et al., 1996; Faubert and Kaminski, 2001; Herring and Kaminski, 1999; Herring et al., 1998; Koh et al., 1997; Ouyang et al., 1998; Yea et al., 2000). The mechanism by which cannabinoids attenuate the binding of the above-mentioned transcription factors may involve an inhibition of upstream signaling mechanisms. For example, in murine SPLC and thymocytes, CBN, Δ^9-THC and AEA inhibited the production of cAMP by adenylate cyclase, as well as the concomitant activation of protein kinase A (PKA) (Condie et al., 1996; Koh et al., 1997). The cAMP-PKA pathway regulates the activation of NFκB and CREB, and may explain the attenuation of NFκB and CREB DNA binding by cannabinoids. Similarly, CBN treatment of PMA/Io-activated murine SPLC resulted in the inhibition of p42 and p44 ERK-MAP kinase activation, as well as the expression of AP-1 proteins, c-jun and c-fos (Faubert and Kaminski, 2001). The activation of ERK-MAP kinase pathway is necessary for the upregulation of the expression of AP-1 proteins, which in turn are involved in the upregulation of IL-2 transcription. Finally, alterations in NFAT activation and DNA binding to the IL-2 promoter have also been demonstrated with CBN and AEA in murine SPLC (Ouyang et al., 1998; Yea et al., 2000). NFAT is a critical transcription factor for

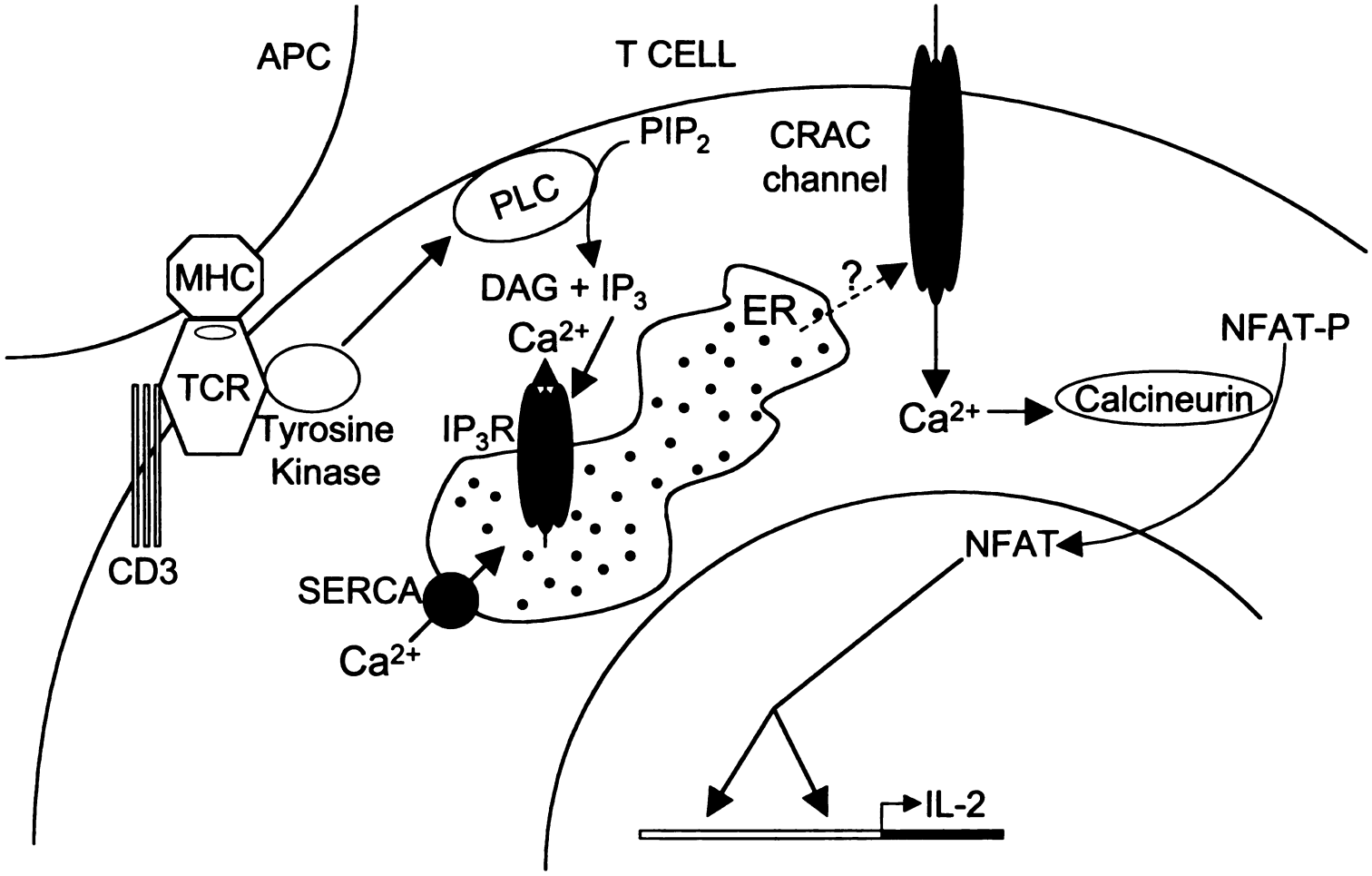

Figure 4. Ca^{2+} signaling in T cell activation and concomitant IL-2 gene expression. Figure adapted from: (Lewis, 2001)

IL-2 gene transcription, whose activity and nuclear translocation is dependent on $[Ca^{2+}]_i$, calmodulin (CaM) and the protein phosphatase, calcineurin (figure 4) (Rao et al., 1997). The inhibition of NFAT activation and DNA binding by cannabinoids is postulated to involve a dysregulation of $[Ca^{2+}]_i$, or alternatively an inhibition of calcineurin activity. In fact, the dysregulation of $[Ca^{2+}]_i$ by cannabinoids has been shown in T cells (Faubert Kaplan et al., 2003; Rao et al., 2004; Yebra et al., 1992), and may help partly explain the inhibition of NFAT activity.

Although it is widely established that human and murine T cells express both the CB1 and CB2 receptors (Klein et al., 2003; Schatz et al., 1997), the role of the cannabinoid receptors in IL-2 regulation remains unknown. In an initial study, the production of IL-2 by T cells activated by macrophages was found to be sensitive to SR2, but not SR1 (McCoy et al., 1999). More recent studies, however, have produced results to the contrary. In particular, in murine SPLC activated with PMA/Io, CBN and WIN-2 mediated suppression of IL-2 was insensitive to either SR1 or SR2 (Faubert Kaplan et al., 2003). In addition, WIN55,212-3, an enantiomer of WIN-2 with little affinity to either CB1 or CB2, also equally inhibited IL-2 secretion. Furthermore, Rockwell et al. demonstrated that the effect of AEA on IL-2 could be partially reversed by non-selective cyclooxygenase inhibitors as well as antagonists of peroxisome proliferator-activated receptor-γ (Rockwell and Kaminski, 2004). Therefore, it is quite likely that the suppression of IL-2 by cannabinoids may be mediated by mechanisms independent of CB1 and CB2 receptors.

(iii). **IL-2 enhancement**

Cannabinoids not only inhibit the expression of IL-2, but can also enhance it. In a preliminary study in murine SPLC and lymph node cells, Δ^9-THC was found not only to inhibit IL-2 secretion, but also to enhance it (Nakano et al., 1992). Whether Δ^9-THC enhanced or suppressed IL-2 secretion appeared to be dependent on the mode of cellular activation. It was only later discovered that the cannabinoid compounds have divergent effects on the production and secretion of IL-2, depending on the mode and level of T cell stimulation. When T cells were suboptimally stimulated using soluble anti-CD3 and anti-CD28 antibodies or low concentrations of PMA/Io, cannabinoids enhanced the secretion of IL-2 (Jan and Kaminski, 2001). However, when T cells were optimally stimulated using immobilized anti-CD3 and anti-CD28 antibodies or high concentrations of PMA/Io, cannabinoids suppressed IL-2 secretion (Jan and Kaminski, 2001). The mechanism by which cannabinoids, and CBN in particular, enhance IL-2 production may involve the activation of ERK-MAP kinases, protein kinase C (PKC), and CaM-dependent kinases (CaMK), and an increase in the DNA binding of NFAT to the IL-2 promoter (Jan and Kaminski, 2001; Jan et al., 2002). However, SR2 failed to antagonize the stimulatory effect of CBN, Δ^9-THC and CP on the IL-2 production, again bringing into question the involvement of the cannabinoid receptors in the modulation of IL-2 by cannabinoids.

(iv). ***In vivo* cytokine regulation**

The differential regulation of cytokine expression by cannabinoids has also been demonstrated using *in vivo* models. In most *in vivo* studies, the cannabinoid modulation of cytokine expression has been assessed in serum from mice infected with pathogens,

Corynebacterium parvum or *Legionella pneumophila.* The results suggest that while cannabinoids suppress the expression of some cytokines, expression of others is enhanced. In *L. pneumophila* infected mice, treatment with Δ^9-THC resulted in the suppression of IFN-γ, IL-15 and IL-12 p40, while the levels of IL-4 and IL-10 were elevated (Klein et al., 2000b; Newton et al., 1998). In this model, Δ^9-THC also decreased the expression of IL-12 receptor β2, a marker of Th1 subtype of T helper ($CD4^+$) cells, and increased the expression of GATA-3, a transcription factor that regulates cytokines of Th2 subtype cells (Klein et al., 2004). Similarly, in an endotoxemic mouse model primed with *C. parvum*, HU-210 and WIN-2 treatment resulted in decreased serum levels of TNF-α, IFN-γ and IL-12, but enhanced IL-10 levels (Smith et al., 2000, 2001b). At present, it is unclear how cannabinoids can differentially modulate the expression of cytokines, but it is hypothesized that cannabinoids may skew the phenotype of T helper cells toward Th2 subtype over Th1 subtype. However, the hypothesis that cannabinoid treatment may skew the phenotype of T helper cells remains highly controversial.

3. **Host-resistance studies**

In early experimental animal models, cannabinoids were reported to impair host resistance to viral, bacterial and protozoan infections. In mice infected with either *Listeria monocytogenes* or *Herpes simplex*, Δ^9-THC treatment suppressed resistance to both infections (Cabral et al., 1986; Morahan et al., 1979). In the case of *H. simplex* infection, the Δ^9-THC-induced decrease in resistance was shown to involve a delay in the onset of cell-mediated hypersensitivity responses (Mishkin and Cabral, 1985). Furthermore, injection of mice with Δ^9-THC and 11-OH-Δ^9-THC revealed that both

compounds suppressed the activity of NK cells in the spleen (Klein et al., 1987). In another study, Δ^9-THC inhibited the cytolytic activity of $CD8^+$ T cells in *H. simplex* infected murine SPLC (Fischer-Stenger et al., 1992). Since both $CD8^+$ T cells and NK cells are important in the defense against malignant cells and virus-infected cells, the inhibition of either cell type may, therefore, contribute partially to the modulation of host resistance by cannabinoids.

Over the last two decades, Klein and coworkers have extensively characterized the effects of cannabinoids, and Δ^9-THC in particular, on the host resistance to *L. pneumophila* in mice. *L. pneumophila* is a facultative intracellular bacterium that infects macrophages, and thus requires a Th1 subtype-mediated immune response for its elimination. In peritoneal macrophages recovered from *L. pneumophila* infected mice, Δ^9-THC treatment resulted in an increased intracellular replication of bacteria, and a decreased ability of macrophages to clear the infection upon activation with LPS (Arata et al., 1991). Moreover, Δ^9-THC treated mice were more prone to acute mortality due to *L. pneumophila* infection as compared to control mice. The increased acute mortality rate in Δ^9-THC treated mice was correlated with an increase in serum levels of acute-phase cytokines IL-6 and TNF-α (Klein et al., 1993). Subsequently it was found that Δ^9-THC modulates the production of several additional cytokines, and that the modulation of the cytokine network may result from the skewing of T helper cells toward the Th2 phenotype (Klein et al., 2000b; Newton et al., 1998). However, the skewing of T helper cell phenotype by cannabinoids is not widely accepted and remains controversial.

C. CB1 and CB2 receptor-independent effects

1. **Brain**

While cannabinoids are generally understood to mediate their effects on physiology via the cannabinoid receptors, CB1 and CB2, evidence to the contrary also exists. Recently, an ever increasing number of studies have concluded that additional unknown receptors may mediate some of the actions of cannabinoids, independently of CB1 or CB2 (Baker and Pryce, 2003). In the brain, for example, the anti-emetic effects elicited by cannabinoids have been reported to be independent of the CB1 receptor. It is believed that the cannabinoid-mediated inhibition of nausea and emesis involves an allosteric interaction of cannabinoids on the 5-hydroxytryptamine type 3 receptor in the brainstem, independently of CB1 or CB2 (Townsend et al., 2002).

Additional evidence for the involvement of CB1 independent actions of cannabinoids in the brain comes from studies in CB1 receptor null ($CB1^{-/-}$) mice. The administration of Δ^9-THC in $CB1^{-/-}$ mice confirmed that a majority of cannabinoid-mediated psychoactive and behavioral responses in the brain, such as Δ^9-THC-induced ring catalepsy, hypomotility, analgesia, and hypothermia were indeed mediated by the CB1 receptor (Zimmer et al., 1999). However, certain other effects of Δ^9-THC such as a delayed tail flick response, abdomen licking and diarrhea were preserved in the $CB1^{-/-}$ mice (Zimmer et al., 1999). Interestingly, while Δ^9-THC, CP and HU-210 elicited no changes in spontaneous activity, catalepsy and analgesia in $CB1^{-/-}$ mice, these effects could still be elicited by AEA and WIN-2 (Breivogel et al., 2001). Also, *in vitro* binding assays performed in $CB1^{-/-}$ brain tissue showed that treatment with AEA or WIN-2, but not other cannabinoids, stimulated the binding of [^{35}S]-guanosine trisphosphate in a concentration-responsive and saturable manner, which was not attenuated by SR1 (Wiley

and Martin, 2002). The specific binding demonstrated with AEA and WIN-2 in $CB1^{-/-}$ brain tissue has provided the strongest evidence yet that CB1-independent effects of cannabinoids in the brain are putatively mediated by novel cannabinoid G protein-coupled receptors.

2. **Peripheral vasculature**

CB1 and CB2 receptor-independent effects of cannabinoids have also been reported in the periphery. In the peripheral vasculature, classical and endocannabinoids are widely reported to cause hypotension by modulating autonomic outflow from neurons, and via direct vasodilatory effects on the vasculature (Randall and Kendall, 1998). However, the dependence of the cannabinoid receptors in the vasorelaxation induced by cannabinoids is unclear. The use of SR1 to study cannabinoid-induced vasorelaxation has generated conflicting and sometimes contradictory results. While some studies have reported that the vasorelaxant activity of cannabinoids was antagonized by SR1, others have provided data suggesting the contrary (Randall et al., 1996; White and Hiley, 1998). Furthermore, the use of SR1 to distinguish between cannabinoid receptor-dependent and -independent mechanisms has been problematic, as SR1 may also inhibit vasorelaxation in the absence of cannabinoids (Bukoski et al., 2002).

The strongest evidence for a novel G protein-coupled cannabinoid receptor in the vasculature has come from recent work by Kunos and coworkers. Much of the evidence for the novel cannabinoid receptor is pharmacological and was gathered using a cannabinoid known as abnormal cannabidiol (abn-CBD). Abn-CBD is an analog of

CBD, which does not exhibit binding affinity for either CB1 or CB2. In isolated segments of murine mesenteric arteries, abn-CBD caused endothelial cell-dependent vasorelaxation that was sensitive to PTx, but not to SR1 or SR2 (Begg et al., 2003; Offertaler et al., 2003). Further, it was shown that another CBD analog, O-1918, acted as an antagonist at the abn-CBD receptor, and attenuated the vasorelaxation induced by not only abn-CBD, but also AEA (Offertaler et al., 2003). Based on the aforementioned observations, it is possible that both AEA and abn-CBD may mediate their vasodilatory functions through a common receptor. The engagement of the abn-CBD receptor has since been shown to activate ERK-MAP kinases, protein kinase B and phosphotidylinositol-3-kinase (PI3K) (Mo et al., 2004; Offertaler et al., 2003). It is currently hypothesized that ligation of abn-CBD receptor on endothelial cells leads to the production of vasodilatory substances, which in turn cause relaxation of vascular smooth muscle. Conclusive proof for the non-involvement of CB1 and CB2 in the cannabinoid-mediated vasodilation came from studies with CB1/CB2 double knockout ($CB1^{-/-}/CB2^{-/-}$) mice. Treatment of isolated mesenteric arteries from the $CB1^{-/-}/CB2^{-/-}$ mice with AEA, meth-AEA or abn-CBD resulted in vasorelaxation, clearly indicating that the vasorelaxant effects of cannabinoids were independent of CB1 or CB2 (Jarai et al., 1999).

3. **Immune cells**

Evidence for CB1- and CB2-independent mechanisms of action for cannabinoids also exist in the immune system. While, the effects of cannabinoids on T cell cytokine expression *in vivo* have been shown to be reversed by SR1 and/or SR2 in certain studies, most *in vitro* studies have demonstrated that the modulation of cytokine expression by

cannabinoids is refractory to SR1 and SR2 (Kaplan et al., 2003; Klein et al., 2004; Rockwell and Kaminski, 2004; Smith et al., 2001a; Smith et al., 2000). Similarly, the *in vitro* inhibition of neutrophil superoxide production by CP was also insensitive to both SR1 and SR2 (Kraft et al., 2004). Nevertheless, it cannot be unequivocally stated that all *in vitro* effects of cannabinoids on immune cells are CB1 and CB2 receptor-independent. Whereas Δ^9-THC diminished the co-stimulatory function of peritoneal macrophages from WT mice in culture, Δ^9-THC had no effect on macrophages from $CB2^{-/-}$ mice (Buckley et al., 2000). Based on the studies performed in immune cells thus far, it is clear that not all effects of cannabinoids are mediated by CB1 and CB2, which may imply that additional cannabinoid receptors are expressed in the immune system as well.

4. **Implications**

Recent studies of cannabinoid effects independent of CB1 and CB2 receptors have raised several relevant issues related to cannabinoid biology. First, cannabinoid compounds may bind and activate receptors other than CB1 and CB2 in both brain and peripheral tissues. Given that cannabinoid compounds are highly lipophilic, it is possible that non-CB1 non-CB2 targets for cannabinoids may be intracellular. It was recently found that AEA is an agonist at vanilloid receptor (VR) 1, a ligand-gated ion channel, whose ligand binding domain is intracellular (Lutz, 2002). Similarly, classical cannabinoids may also bind intracellular target molecules. CBN and Δ^9-THC were both recently shown to regulate the release of calcitonin gene regulatory peptide (CGRP) in peripheral neurons in a CB1 and CB2-independent manner (Zygmunt et al., 2002). The induction of CGRP release by CBN and Δ^9-THC was sensitive to the VR1 antagonists,

but could not be replicated with VR1 agonists. It was proposed that CBN and Δ^9-THC may modulate CGRP release upon binding to a receptor within the transient receptor potential (TRP) ion channel family, of which VR1 is a member.

A second important issue stemming from cannabinoid antagonist studies is that antagonism of cannabinoid actions by either SR1 or SR2 does not consistently imply the involvement of either CB1 or CB2. At concentrations higher than 1 μM, SR1 can act as an antagonist at several receptors including the abn-CBD receptor, imidazoline receptor, VR1, and adenosine receptor (Pertwee, 2005). It is likely that SR2 also has similar non-specific antagonistic properties. It has now become necessary, given the novel insights into cannabinoid biology, to reconsider the assumption that CB1 and CB2 receptors mediate all the physiological and pharmacological effects of cannabinoids.

D. **Effects of cannabinoids on intracellular calcium**

Some of the earliest studies to report modulation of Ca^{2+} by cannabinoids were those investigating the mechanism of anticonvulsant actions of cannabinoids in the mammalian brain. In synaptosomes isolated from rodent brains, Δ^9-THC and CBD treatment inhibited the uptake of Ca^{2+}, enhanced Ca^{2+} efflux, and decreased the membrane potential (Harris et al., 1978). It was concluded from these studies that Δ^9-THC and CBD putatively inhibited Ca^{2+} channels, and the inhibition of Ca^{2+} channels may contribute to the anticonvulsant actions of cannabinoids. Similarly, early experiments investigating the effects of Δ^9-THC on testicular function also implicated the involvement of $[Ca^{2+}]_i$. Treatment of isolated mouse testes with Δ^9-THC significantly decreased or enhanced the hormone-induced production of testosterone depending on the

mode of stimulation (Dalterio et al., 1985). The inhibition and stimulation of testosterone production by Δ^9-THC was strongly correlated with the level of extracellular calcium ($[Ca^{2+}]_e$) present in the buffer, suggesting that the actions of Δ^9-THC on steroidogenesis involved modulation of $[Ca^{2+}]_i$ (Dalterio et al., 1985). Further mechanistic studies found that *in vivo* treatment of Δ^9-THC in mice led to the modulation of the activity of the plasma membrane Ca^{2+}-ATPase (PMCA) in both testicular cells as well as hypothalamic neurons (Dalterio et al., 1987a; Dalterio et al., 1987b). Since the demonstration of PMCA modulation by Δ^9-THC, cannabinoid effects on the dynamics of $[Ca^{2+}]_i$ regulation have been examined in many different tissues.

1. Inhibition of calcium elevation

Perhaps the most thorough investigation of the mechanism of $[Ca^{2+}]_i$ modulation by cannabinoids has been performed in neuronal cells. Using whole-cell voltage clamp technique, Mackie and coworkers demonstrated that WIN-2 reduced the amplitude Ca^{2+} currents mediated by VOCCs in the neuroblastoma-glioma cell line, NG108-15 (Mackie and Hille, 1992). The initial characterization described the inhibition of VOCC-mediated Ca^{2+} currents to be cannabinoid receptor-mediated, and sensitive to PTx (Mackie and Hille, 1992). Based on the characteristics of the Ca^{2+} current inhibited by WIN-2, it was postulated that the activity of N-type VOCCs was affected (Mackie and Hille, 1992). In addition, AEA was also shown to inhibit N-type VOCCs in a PTx-sensitive manner (Felder et al., 1993; Mackie et al., 1993). Another study in feline arterial smooth muscle cells corroborated that WIN-2 and AEA inhibit N-type VOCCs, and added that the effect was SR1-sensitive (Gebremedhin et al., 1999). A more thorough characterization WIN-2

and AEA-induced $[Ca^{2+}]_i$ modulation in the CB1-expressing AtT-20 murine tumor cell line revealed that in addition to N-type VOCCs, cannabinoid treatment also resulted in the activation of K^+ channels and inhibition of other VOCCs (Mackie et al., 1995). Using selective inhibitors of K^+ and Ca^{2+} channel subtypes, it was discovered that the aforementioned cannabinoids inhibited the P and Q-type VOCCs, and activated inwardly rectifying K^+ channels (K_{ir}) (Mackie et al., 1995; Shen and Thayer, 1998; Twitchell et al., 1997). It is now widely accepted that the action of cannabinoids on K_{ir}s and VOCCs in the brain is mediated by the CB1 receptor. Evidence for the involvement of CB1 comes from the observation that the cannabinoid inhibition of VOCCs was stereospecific, could be inhibited by SR1, and that AEA mimicked the actions of WIN-2 (Howlett, 1985). Furthermore, the PTx sensitivity of the cannabinoid-modulation of K_{ir} and VOCCs strongly implicated the involvement of the $G\alpha_i/G\alpha_o$, which are known to couple to the CB1 receptor (Howlett, 1985).

Apart from the brain, the inhibitory effects of cannabinoids on $[Ca^{2+}]_i$ elevation have also been documented in other tissues. In murine thymic T cells, Δ^9-THC has been shown to inhibit the rise in $[Ca^{2+}]_i$ elicited upon stimulation with Con A (Yebra et al., 1992). Generally, when mitogens such as Con A stimulate T cells, the rise in $[Ca^{2+}]_i$ involves both a release from intracellular Ca^{2+} stores as well as $[Ca^{2+}]_e$ influx. In the Con A-stimulated splenic T cells, Δ^9-THC inhibited both phases of $[Ca^{2+}]_i$ elevation (Yebra et al., 1992). The inhibition of $[Ca^{2+}]_i$ elevation by Δ^9-THC suggested that the CB2 receptor may also be coupled to modulation of ion channels. However, a preliminary experiment in AtT-20 cells found that heterologously expressed CB2 receptors could not modulate either VOCCs or K_{ir} channels (Felder et al., 1995). Nevertheless, the preliminary studies

did not eliminate the possibility that CB2 receptors may modulate the function of other types of ion channels.

2. Differential regulation of calcium elevation

Although the focus of most early investigations of cannabinoid effects on $[Ca^{2+}]_i$ has been the inhibition of the Ca^{2+} influx, more recent studies have demonstrated that cannabinoid compounds also stimulate $[Ca^{2+}]_i$ elevation. For example, in the NG108-15 cells, both 2-AG and WIN-2 were able to elevate $[Ca^{2+}]_i$ in a CB1-dependent manner (Sugiura et al., 1996). It is interesting to note that in NG108-15 cells the same cannabinoids were initially described to inhibit VOCCs. The dichotomous effect of cannabinoids on $[Ca^{2+}]_i$ may be explained by different experimental conditions used in different studies. Alternatively, it has been suggested that the elevation and inhibition of $[Ca^{2+}]_i$ by cannabinoids through the CB1 receptors may represent the coupling to different G proteins or signaling pathways (Mukhopadhyay et al., 2002). A similar mechanism may also be involved with the CB2 receptor. While Δ^9-THC was initially shown to attenuate the rise in $[Ca^{2+}]_i$ elicited by Con A in murine SPLC, a subsequent report showed that Δ^9-THC enhanced the rise in $[Ca^{2+}]_i$ elicited by anti-CD3 antibodies (Nakano et al., 1993; Yebra et al., 1992). Intriguingly, induction of $[Ca^{2+}]_i$ following stimulation with anti-CD3 was specific to Δ^9-THC, and could not be demonstrated with 11-OH-Δ^9-THC (Nakano et al., 1993). It has been suggested that only certain cannabinoid congeners elicit the coupling to the alternate signaling mechanisms involved in the induction of $[Ca^{2+}]_i$ (Sugiura et al., 1996). An emerging theme among studies of

cannabinoid-mediated modulation of $[Ca^{2+}]_i$ is that some cannabinoids can elicit a rise in $[Ca^{2+}]_i$, while others cannot.

3. Involvement of the CB1 and CB2 receptors

Another point of contention among studies of cannabinoid modulation of $[Ca^{2+}]_i$ is the involvement of identifiable cannabinoid receptors. A majority of the studies examining the effects of cannabinoids on the induction or attenuation of $[Ca^{2+}]_i$ in the CNS neurons and neuronal cell lines have reported that the effect was CB1-dependent, and blocked upon pretreatment with either SR1 or PTx (Netzeband et al., 1999). On the other hand, studies of $[Ca^{2+}]_i$ elevation induced by cannabinoids in the periphery have not consistently implicated the involvement of the cannabinoid receptors. The cannabinoid-mediated elevation of $[Ca^{2+}]_i$ in endothelial cells, smooth muscle cells and kidney epithelial cells was independent of CB1, CB2 and PTx-sensitive G proteins (Chou et al., 2001; Filipeanu et al., 1997; Mombouli et al., 1999). By contrast, in the HL60 promyelocytic cell line, the WIN-2 and 2-AG induced elevation in $[Ca^{2+}]_i$ was sensitive to both SR2 and PTx (Sugiura et al., 2000). Based on the above findings, it is feasible that in certain peripheral cells, the modulation of $[Ca^{2+}]_i$ may be mediated by non-CB1 non-CB2 receptors.

4. Non-CB1 non-CB2-dependent calcium regulation

Some recent investigations have indeed found that cannabinoids may elevate $[Ca^{2+}]_i$ via alternate receptors. Much of the work focused on novel mechanisms of $[Ca^{2+}]_i$ elevation by cannabinoids was performed with AEA acting as an agonist at VR1. VR1 is

a ligand-gated cation channel that belongs to the TRP channel superfamily, and responds to noxious hot stimuli (Cortright and Szallasi, 2004). In VR1 transfected HEK293 cells, AEA treatment led to an increase in VR1-mediated inward Ca^{2+} currents, as well as an increase in $[Ca^{2+}]_i$, similar to that induced by the VR1 agonist, capsaicin (CPC) (De Petrocellis et al., 2001; Smart and Jerman, 2000). Whereas the cannabinoid antagonists did not antagonize the actions of AEA, the VR1 antagonist, capsazepine did (Smart and Jerman, 2000). Interestingly, AEA is unique in its ability to activate VR1, and this property is not shared with other cannabinoids. In fact, classical cannabinoids such as HU-210 inhibit the activation of VR1 and concomitant $[Ca^{2+}]_i$ elevation in an SR1-sensitive manner (De Petrocellis et al., 2001; Hermann et al., 2003; Millns et al., 2001). However, it is possible that some classical cannabinoids may induce the production of AEA, thereby activating VR1 (Bisogno et al., 2001).

Although classical cannabinoids do not directly activate VR1, there is some evidence that classical cannabinoids may bind and exert an $[Ca^{2+}]_i$ elevation through ionophoric receptors distantly related to VR1. For example, in peripheral neurons Δ^9-THC and CBN-induced an increase in $[Ca^{2+}]_i$, which was independent of CB1, CB2 or VR1, but could be inhibited by VR1 antagonists (Zygmunt et al., 2002). It has been conjectured that the effects of the aforementioned cannabinoids were putatively mediated by a distant relative of VR1 in the TRP channel superfamily (Zygmunt et al., 2002). More recent data has provided evidence that Δ^9-THC directly activates a member of the TRP superfamily known as TRPA1, a ligand-gated cation channel that responds to noxious cold stimuli (Jordt et al., 2004). Together, the recent investigations on the

elevation of $[Ca^{2+}]_i$ by cannabinoids support the view that members of the TRP channel superfamily may act as ionophoric receptors for cannabinoid compounds.

III. Intracellular calcium and calcium channels

A. Calcium in T cells: CCE and CRAC channels

1. Calcium elevation in T cell activation

When a normal T cell receives an activation stimulus through the T cell antigen receptor (TCR) by an antigen in the context of an MHC molecule, several signaling events ensue. One of the first stages of T cell activation involves the phosphorylation of phospholipase C (PLC)-γ type 1 or 2 by soluble tyrosine kinases such as lyk and fyn, which are coupled to the TCR (Feske et al., 2001; Winslow et al., 2003). Active PLC-γ hydrolyzes phosphotidylinositol-bisphosphate (PIP_2) into inositoltrisphosphate (IP_3) and diacylglycerol (DAG). The PLC-γ-mediated generation of IP_3 initiates the process of $[Ca^{2+}]_i$ elevation by releasing stored Ca^{2+} from the endoplasmic reticulum (ER) (Lewis, 2001; Winslow et al., 2003). In addition, another second messenger, cyclic adenosine diphosphate ribose (cADPR), is also generated upon TCR engagement (Guse et al., 1995). IP_3 and cADPR are generated sequentially to enable a successive release of stored Ca^{2+} from the ER by binding to the IP_3 receptor (IP_3R) and the ryanodine receptor (RyR), respectively (Berg et al., 2000; Guse, 2002, 2004). The IP_3R and RyR are ligand-gated ion channels found on the ER membrane, and change their conformation upon ligand binding to allow for the release of stored Ca^{2+} (Nowycky and Thomas, 2002). Subsequent to the release of stored Ca^{2+}, a prolonged and significantly larger elevation of $[Ca^{2+}]_i$ occurs through cell surface Ca^{2+} channels known as calcium release-activated

calcium (CRAC) channels. The process of Ca^{2+} store release from the ER followed by $[Ca^{2+}]_e$ influx through cell surface Ca^{2+} channels is known as store-operated calcium entry (SOCE) or capacitative calcium entry (CCE). CCE is the primary mechanism of $[Ca^{2+}]_i$ mobilization in T cells and most electrically non-excitable cells (Putney et al., 2001).

In lymphocytes, CCE is critical for cell activation and function. In fact, failure to mobilize $[Ca^{2+}]_i$ by CCE is believed to result in the etiology of severe combined immunodeficiency (SCID) (Feske et al., 2001). The induction and repression of many cytokine genes in lymphocytes is mediated by an elevation of $[Ca^{2+}]_i$ through CCE. The functional link between the increase in $[Ca^{2+}]_i$ and change in gene expression is bridged by transcription factors that are either directly or indirectly activated by an elevation in $[Ca^{2+}]_i$. One T cell cytokine whose transcription is heavily dependent on $[Ca^{2+}]_i$ is IL-2. The transcriptional activation of the IL-2 requires a large sustained $[Ca^{2+}]_i$ elevation (200 nM to 1 μM) for 1-2 h, and the prolonged $[Ca^{2+}]_i$ requirement arises largely due to the need to keep NFAT in the nucleus and transcriptionally active (Lewis, 2001). In SCID lymphocytes, the $[Ca^{2+}]_i$-dependent dephosphorylation and nuclear translocation of NFAT is incomplete, and therefore, the expression of cytokine genes is inefficient. As a result, there is a profound lack of adaptive immunity in SCID patients (Kalman et al., 2004).

2. Properties of CRAC channels

a. Regulation

CRAC channels belong to a family of cation channels that are regulated downstream of Ca^{2+} store-depletion, and aptly named the store-operated calcium channels (SOCCs). Apart from their sensitivity to Ca^{2+} store-depletion, all SOCCs have in common that their molecular makeup and biochemical regulatory mechanisms remain elusive. CRAC channels are a very specialized branch of the SOCCs distinguished by very high Ca^{2+} selectivity and very low single-channel conductance (Prakriya and Lewis, 2003). Putative regulatory mechanisms for CRAC channels include: (a) conformational coupling between IP_3Rs or RyRs and CRAC channels; (b) a diffusible second messenger termed Ca^{2+}-induced factor released from Ca^{2+} stores; or (c) store-release induced fusion of endosomes containing CRAC channels into the plasma membranes (Prakriya and Lewis, 2003; Winslow et al., 2003). None of the above mechanisms, however, have yet been shown definitively to regulate CRAC channels.

b. **Conduction**

Although the molecular makeup of CRAC channels is not known, conduction properties of CRAC channels have been extensively studied. CRAC channels are described as non-voltage gated, inwardly rectifying, and highly selective for Ca^{2+} over other divalent and monovalent cations (Bakowski and Parekh, 2002). Under physiological conditions, the ratio of Ca^{2+} to Na^{+} ions conducted ($\rho Ca^{2+}/\rho Na^{+}$) through the CRAC channels is 1000:1 (Bakowski and Parekh, 2002). The high selectivity to Ca^{2+} is a unique feature of CRAC channels, and makes the CRAC channel the most Ca^{2+}-selective of any channel thus far described (Prakriya and Lewis, 2003). However, compared to the VOCCs, the single channel conductance through CRAC channels is very

low. Various laboratories studying the properties of CRAC channels in T cells have reported single channel conductance between 24 fs to 2 ps (Bakowski and Parekh, 2002).

c. **Inactivation**

CRAC channels are highly sensitive to inactivation by high $[Ca^{2+}]_i$ (Putney et al., 2001). The mechanism of CRAC channel inactivation is unknown, but putatively involves the intracellular domains of CRAC channels. It has been proposed that there may be binding sites for Ca^{2+} ions within the intracellular domains of CRAC channels, which act as regulatory switches to induce inactivation (Moreau et al., 2005). Interestingly, in lymphocytes the inactivation of CRAC channels is prevented even as high levels $[Ca^{2+}]_i$ are reached. It is postulated that the robust elevation of $[Ca^{2+}]_i$ in lymphocytes is maintained by the buffering capacity of mitochondria. When $[Ca^{2+}]_i$ levels reach 400 nM or higher in lymphocytes, the mitochondria rapidly begin to take up cytosolic $[Ca^{2+}]_i$ (Hoth et al., 1997). The rapid and relatively large capacity of mitochondria to sequester $[Ca^{2+}]_i$ aids in the maintenance of a prolonged $[Ca^{2+}]_i$ elevation in lymphocytes by preventing the inactivation of CRAC channels. Agents that uncouple mitochondrial transport of Ca^{2+} prevent the ability of T cells to maintain a high rate of CCE over prolonged periods (Hoth et al., 1997), further supporting a role for mitochondria in the prevention of CRAC channel inactivation.

d. **Inhibition**

Several inorganic and organic molecules have been described that inhibit the current and Ca^{2+} conduction through CRAC and other SOCCs. Primary among the

inorganic inhibitors of SOCCs are the lanthanide cations, gadolinium (Gd^{3+}) and lanthanum (La^{3+}). The lanthanide cations are potent inhibitors of CCE at concentrations in the low nanomolar range. The lanthanides have been shown to inhibit potently the elevation in $[Ca^{2+}]_i$ through SOCCs induced upon engagement of receptors, or induced by thapsigargin (TG), a compound that depletes Ca^{2+} stores by inhibiting the reuptake of Ca^{2+} by the smooth endoplasmic reticulum calcium ATPase (SERCA) (Trebak et al., 2002). The bulky trivalent lanthanide cations are proposed to inhibit SOCCs by blocking the pore region of the channel (Lewis, 2001). In many studies, lanthanides have been utilized to differentiate between SOC and non-SOC mediated $[Ca^{2+}]_i$ transients.

SOC and CRAC channels are also inhibited by nanomolar concentrations of 2-aminoethoxydiphenyl borate (2-APB), a molecule originally developed as an antagonist of the IP_3Rs (Ma et al., 2003). However, 2-APB was found to inhibit CCE even in the absence of IP_3Rs (Venkatachalam et al., 2002), indicating that 2-APB inhibits SOCCs either directly or by inhibiting coupling machinery. Interestingly, the effect of 2-APB on SOCCs is biphasic. At low concentrations, 2-APB is a weak activator of SOCCs, but at higher concentrations 2-APB is an effective blocker of SOCCs (Braun et al., 2003; Flemming et al., 2003; Ma et al., 2003; Prakriya and Lewis, 2003). The precise mechanism of 2-APB action on SOCCs is remains unknown. Finally, SK&F96365 (SKF) may also inhibit SOCCs. However, SKF is not as effective at inhibiting SOCCs as the lanthanides or 2-APB, and does not inhibit SOCCs in all models (Lewis, 2001; Merritt et al., 1990; Sydorenko et al., 2003).

B. **TRP channels: structure and function**

1. Discovery and cloning of TRP channels

The TRP channels are a superfamily of proteins originally discovered in *Drosophila melanogaster* retina, where they form Ca^{2+}-permeable cation channels involved in phototransduction mediated by the rhodopsin receptor (Vazquez et al., 2004; Vennekens et al., 2002). In drosophila, there are three members of the TRP family: TRP, TRPL and TRPγ, all gated via an unknown mechanism downstream of PLC activation (Hassock et al., 2002; Vennekens et al., 2002). Subsequent to the discovery of TRP proteins in drosophila, seven TRP homologs were discovered in mammals and labeled the canonical TRP (TRPC) channels. All seven members of the mammalian TRPC family exhibited more than 30% amino acid sequence identity with drosophila TRP and TRPL (Montell, 2001; Zhu et al., 1995). As the TRP channel field progressed, more and more members of the TRP superfamily were discovered in mammalian cells. Currently, there are twenty-eight members of the TRP channel superfamily in mammalians. All members of the TRP superfamily have high amino acid sequence similarity in the distal portion of the carboxy terminus, which contains a conserved domain known as the TRP box (Beech et al., 2004). The mammalian TRP superfamily proteins are classified under two broad groups based on their phylogenetic similarity, and further divided into seven subfamilies, each named after the first recognized family member (Montell, 2001). Group 1 contains five subfamilies: TRPC, TRPV (vanilloid), TRPM (melastatin), TRPA (ANKTM1) and TRPN (drosophila NOMPC). Group 2 contains two subfamilies: TRPML (mucolipin) and TRPP (polycystin) (Montell, 2005).

2. Structure of TRP channels

The TRP proteins are evolutionarily conserved throughout the animal kingdom from nematodes to homo sapiens, indicating the importance for TRP channels for the existence of life (Wes et al., 1995). Early characterization of the mammalian TRP channel amino acid sequences determined that TRP channels share considerable similarity with other mammalian ion channels. In particular, TRP channel structure was found to be similar to that of VOCCs, voltage-operated Na^+ channels, K^+ channels, and cyclic nucleotide-gated ion channels (Vennekens et al., 2002). Furthermore, hydropathy plot analyses determined that TRP proteins contained eight hydrophobic domains (Zhu et al., 1995). Upon detailed analysis, however, only six out of the eight hydrophobic domains were found to span the membrane. The currently accepted model states that TRP channels are hexahelical proteins, with the exception some TRPP subfamily members, and that all TRPs contain cytosolic amino and carboxy termini (figure 5) (Dohke et al., 2004; Moran et al., 2004). Based on the structure of the monomeric TRP channels, and their calculated homology with other mammalian ion channels, it is proposed that the functional TRP channel complexes assemble as tetramers (Hofmann et al., 2002). At present, the exact pattern of TRP channel oligomerization remains controversial. Nevertheless, protein models predict that the simplest conformations for functional TRP channels are homo- or heterotetramers (Zhu et al., 1996).

Additional information about the structure of TRP channels comes from study of the cytosolic amino and carboxy termini. It has been reported that TRP channels contain 3-4 ankyrin binding domains within the amino or carboxy termini (Montell, 2001; Vennekens et al., 2002). The ankyrin binding repeats allow TRP channels to form interactions with a variety of cellular proteins that putatively modulate their function. A

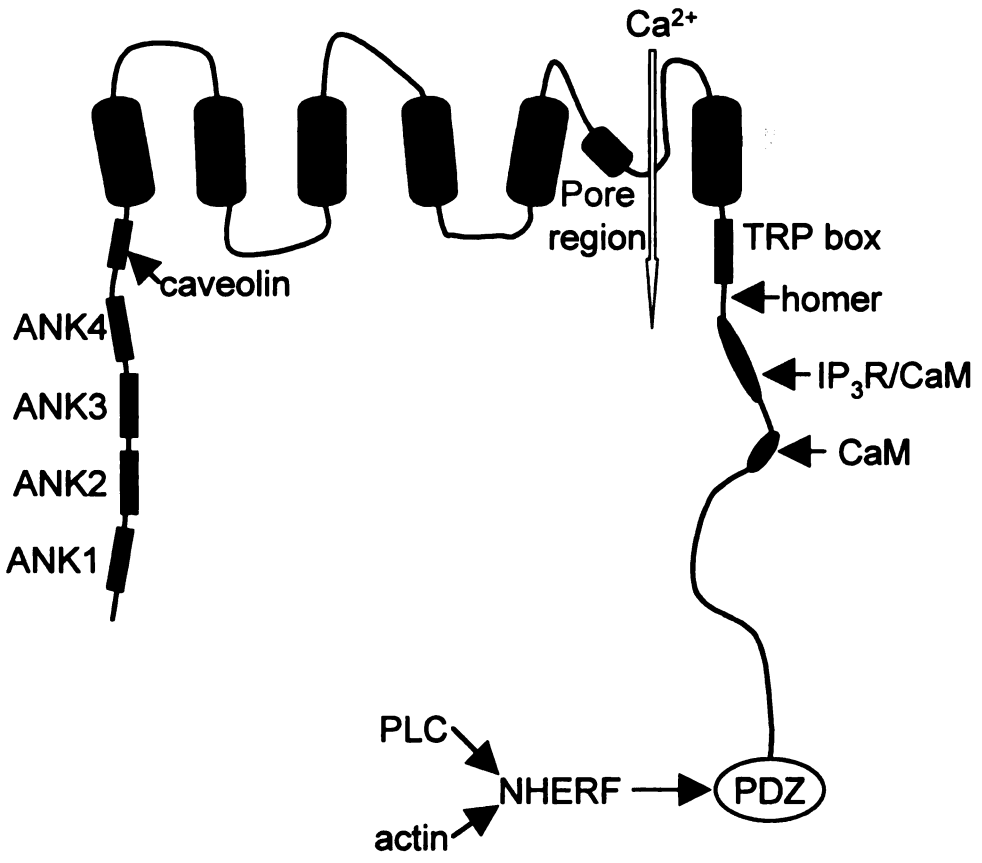

Figure 5. Proposed structure of TRPC channels showing the relative positions for channel modification by protein association. Also shown are the ankyrin (ANK) binding domains and the evolutionarily conserved TRP box. Figure adapted from: (Vazquez et al., 2004)

large number of proteins have been reported to interact with TRP channels. Some of the proteins that have been demonstrated to associate with TRP channels include PLC, IP_3R, RyR, PKC, G-protein α subunits, myosin III, CaM, f-actin, INAD (inactivation-no-afterpotential D), PDZ (PSD (postsynaptic density protein)-95, DLG, zone occludens-1), FKBP (FK506 binding protein), EBD (ERM binding domain), NHERF (Na^+/H^+ exchange regulatory factor), homer, and caveolin (figure 5) (Montell, 2001, 2005; Singh et al., 2000; Yuan et al., 2001). The proteins that associate with TRP channels form macromolecular assemblies, which orchestrate the signaling cascades that both facilitate TRP channel opening, and transduce external stimuli into a change in cellular function.

3. **Function of TRP channels**

In general terms, the TRP channels function as cellular switches that allow organisms to respond to the environment (Moran et al., 2004). More specifically, TRP channels have a wide array of functions, and the function of a given TRP channel depends on the subfamily and the cell in which it is expressed. Many TRP family members have been implicated to function in sensory physiology. TRP channels may play a role in the transduction of noxious heat, noxious cold, gustatory signals, auditory signals and mechanical stimuli. The common mechanism by which all TRP channels respond to stimuli is by carrying cationic currents (Beech et al., 2004). Although the TRP channels were initially imagined to be more important in non-excitable cells, recent work has demonstrated their importance also in electrically excitable cells. In the brain, for instance, the expression of almost every TRP channel has been documented (Moran et al., 2004).

a. TRPC, TRPV and TRPM

Like drosophila TRP and TRPL, the TRPC channels are gated downstream of store-depletion, or following ligation of agonists to metabotropic receptors (Boulay, 2002; Yuan et al., 2001). Therefore, TRPCs function primarily as receptor-operated cation channels (ROCCs) or SOCCs. An exception to this rule is TRPC2. TRPC2 is a human pseudogene, but is critical for pheromone sensing in rodents (Wes et al., 1995). TRPC2 null ($TRPC2^{-/-}$) mice have been shown to lose all ability for sex discrimination, displayed no male-male aggression, and both males as well as lactating females were docile (Freichel et al., 2001).

By contrast, most members of the TRPV and TRPM subfamily are involved in the transduction of sensory stimuli. TRPV channels are involved in the transduction of noxious heat, changes in pH and tonicity. Some members of the TRPV subfamily, i.e. TRPV1 (VR1) and TRPV4, may also be modulated by ligands such as CPC, endocannabinoids, and epoxyeicosatrieonic acids binding within the cytosolic domain (Tseng et al., 2004; Watanabe et al., 2003). The TRPM subfamily, by contrast, mediates cation fluxes in response to hypomagnesemia, oxidant stress, and gustatory signaling pathways (Moran et al., 2004). The TRPM subfamily is unique in its permeability to bulky Mg^{2+} ions. Also, TRPM channels contain atypical protein kinase domains on the carboxy termini (Montell, 2005), but the role the enzymatic domains in TRPM function is uncertain.

b. TRPN, TRPML, TRPP and TRPA

Little is known about TRPN, TRPML, TRPP and TRPA mainly because these subfamilies were discovered fairly recently. Initial studies on TRPN and TRPML channels have indicated that both may be involved in auditory signaling pathways (Montell, 2005). The role of TRPP channels is also not clear. However, a mutation in the TRPP2 gene may be responsible for the etiology of autosomal polycystic kidney disease (Montell, 2001). TRPA1, on the other hand, appears to be involved in the transduction of sensory stimuli, in particular noxious cold stimuli, and was found to be activated by mustard oil, cinnamon oil and cannabinoids such as Δ^9-THC (Jordt et al., 2004). In addition, TRPA1 may also account in the formation of mechanosensitive channels in vertebrate hair cells (Barritt and Rychkov, 2005). An interesting parallel between TRPA1 and TRPC1, despite their distant relationship, is that both may function as mechanosensitive non-selective cation channels in vertebrates (Morato et al., 2005).

4. Candidates for CRAC channels

Perhaps the most controversial role proposed for TRP proteins is in the formation of CRAC channels. Early studies of the drosophila TRP and TRPL channels showed that both could form Ca^{2+}-selective channels gated either by store-depletion or agonist-induced IP_3 generation (Vaca et al., 1994; Zhu et al., 1996). In the last decade, mammalian TRP channels have also been demonstrated to act as SOCCs under conditions of both heterologous and endogenous expression. Depending on the cell, expression conditions and activation stimuli, all members of the TRPC subfamily and TRPV6 have been demonstrated to function as SOCCs (Vanden Abeele et al., 2004).

Based on a preponderance of evidence, however, only TRPC1, TRPC4 and TRPV6 have emerged as viable CRAC channel candidates.

a. TRPC1 and TRPC4

Initial studies with overexpressed TRPC1 and TRPC4 showed that both enhance TG-induced $[Ca^{2+}]_i$ elevation suggesting a role for both proteins in SOCE (Philipp et al., 1996; Zhu et al., 1996; Zitt et al., 1996). The role for TRPC1 and TRPC4 in SOCE was further investigated by antisense, mutagenesis and knockdown techniques. Introduction of antisense oligonucleotides in various cell lines against TRPC1 or TRPC4 resulted in an attenuated SOC current amplitude and SOCC-mediated $[Ca^{2+}]_i$ elevation (Liu et al., 2003; Philipp et al., 2000). The strongest evidence for the involvement of TRPC1 in SOCE comes from mutagenesis and homologous recombination studies, which showed that mutations in the pore region of TRPC1 or disruption of TRPC1 gene results in the attenuation of SOCE (Liu et al., 2003; Mori et al., 2002; Singh et al., 2002). On the other hand, the strongest evidence for TRPC4 in SOCE comes from TRPC4 null ($TRPC4^{-/-}$) mice. The normal SOC current was substantially reduced in vascular endothelial cells isolated from $TRPC4^{-/-}$ mice, and the CRAC-like current that was retained exhibited striking dissimilarity to the CRAC current in WT endothelial cells (Freichel et al., 2001). Based on the fact that both TRPC1 and TRPC4 can modulate SOCE, both were suggested as putative CRAC channel candidates.

Primary among concerns over the interpretation that TRPC1 or TRPC4 may form CRAC channels is the fact that most investigations with TRPC1 and TRPC4 were performed in heterologous expression systems, and often involved an overexpression of

TRPC proteins. TRPC channels are well-known to act in divergent manners depending on the level of expression (Parekh, 2003; Parekh and Putney, 2005). In addition, expression of single TRPC isoforms may also hamper a true understanding of TRPCs in SOCE, as TRPCs are generally thought to form heteromultimers. Next, contradictory evidence exists to suggest that TRPC1 and TRPC4 may also act as ROCCs. Finally, neither TRPC1 nor TRPC4 exhibit strong Ca^{2+}-selectivity and the low single-channel conductance characteristic of CRAC channels (Prakriya and Lewis, 2003).

b. **TRPV6**

TRPV6, also known as CaT1 or ECaC2, is a member of the TRPV subfamily that serves as a conduit for apical Ca^{2+} entry in the intestines and the kidney (Parekh, 2003). The initial suggestion that TRPV6 may be involved in the formation of CRAC channels came from electrophysiological studies that showed that TRPV6 possessed a fairly high $\rho Ca^{2+}/\rho Na^{+}$ of 100:1 (Peng et al., 1999). Also, TRPV6 channels exhibited inactivation in response to high $[Ca^{2+}]_i$ elevation, similar to the CRAC channels (Yue et al., 2001). The involvement of TRPV6 in CRAC channel formation was investigated further by heterologous expression, overexpression and knockdown techniques. Results from biochemical manipulations confirmed that the biophysical properties of TRPV6 were similar to that of the endogenous CRAC channels, and knockdown of TRPV6 resulted in attenuated CCE (Cui et al., 2002; Kerschbaum and Cahalan, 1999; Vanden Abeele et al., 2003).

Despite the apparent similarity between TRPV6 and CRAC channels, it is highly unlikely that TRPV6 can alone account for all the CRAC channel permeation

characteristics. Compared with CRAC channels, TRPV6 channels exhibit a weaker inward rectification, higher Na^+ permeability, higher sensitivity to Mg^{2+}, higher single-channel conductance and lower Ca^{2+} selectivity (Prakriya and Lewis, 2003). However, Ca^{2+}-impermeable mutants of TRPV6 suppressed endogenous CRAC currents, and overexpression of TRPV6 was shown to enhance CRAC current amplitude (Cui et al., 2002; Schindl et al., 2002). Therefore, it is difficult to discount a modulatory or auxiliary role for TRPV6 in CCE.

C. TRPC subfamily: SOC and ROC channels

Regardless of whether they make up the CRAC channel or not, TRPC channels have been instrumental in the recognition of two distinct varieties of Ca^{2+} influxes in non-excitable cells: store-operated and receptor-operated. All members of the TRPC channel subfamily form Ca^{2+}-permeable non-selective cation channels, and each one has been implicated in the formation of either SOCCs or ROCCs in at least one investigation (Beech et al., 2003). The alternative regulation of TRPC channels as either SOCCs or ROCCs may depend on the expression level of TRPC proteins, presence of other TRP channels, oligomerization status, cell type in which they are expressed, mode of cellular stimulation, mechanism of channel activation, and presence of inhibitors. On the basis of sequence similarity, the mammalian TRPC channel subfamily is subdivided into four groups: group 1 – TRPC1, group 2 – TRPC2, group 3 – TRPC3/6/7 and group 4 – TRPC4/5. Homo sapien TRPC channels also follow the same grouping, except that TRPC2 is a pseudogene (Wes et al., 1995). For the purposes of summarizing the

extensive literature on TRPC regulation and function, the TRPC grouping scheme is used below.

1. Group 1 – TRPC1

TRPC1 is the archetypal TRPC channel and was the first to be discovered in mammalian cells. TRPC1 is highly expressed in brain, heart, testes, and ovaries, and at lower levels in the kidney, lungs, intestine, skeletal muscle, placenta, prostate, spleen, salivary glands, vascular smooth muscle, pancreatic β cells, and liver cell lines (Beech et al., 2003). TRPC1 interacts with a variety of proteins including IP_3R, RyR, caveolin-1, homer, CaM, PMCA, and TRPC4/5 (Montell, 2001; Singh et al., 2000; Singh et al., 2002; Yuan et al., 2001). A majority of investigations have reported that TRPC1 forms SOCCs regulated by PLC-dependent generation of IP_3. It is believed that the IP_3-bound IP_3R interacts with the IP_3R-binding domain in the carboxy terminus of TRPC1 (Beech et al., 2003). Evidence for TRPC1 in the formation of IP_3R-mediated SOCCs comes from inhibitor studies where TRPC1-mediated SOCE could be inhibited by Gd^{3+}, La^{3+}, 2-APB, or by the IP_3R antagonist, xestospongin C (Beech et al., 2003). The interaction of IP_3R and TRPC1 is modulated by several proteins, including homer, an adaptor protein, and CaM. While homer binding facilitates the interaction of TRPC1 with IP_3Rs, CaM binding inhibits it (Singh et al., 2002; Yuan et al., 2003). The binding site for CaM on the carboxy terminus of TRPC1 overlaps the IP_3R-binding site, and CaM is believed to act as a molecular sensor for Ca^{2+}-dependent feedback inhibition of TRPC1 (Singh et al., 2002). TRPC1 may also be modulated by protein phosphorylation. A recent study has

reported that PKCα is involved in the positive regulation of TRPC1-mediated SOCE induced by agonists or store-depletion (Ahmmed et al., 2004).

Although most studies have reported that TRPC1 channels function as SOCCs, evidence that TRPC1 may act as ROCCs also exists. The hallmark of ROCCs is their sensitivity to DAG analogs in the absence of store-depletion, ligand-receptor interactions or PKC activation. Generally, OAG (1-oleoyl-2-acetyl-*sn*-glycerol), a cell-permeant DAG analog, is used to characterize ROCCs. In at least one study, TRPC1 channels have been shown to function as ROCCs, which were gated by OAG, and were insensitive to store-depletion (Lintschinger et al., 2000). Similarly, in another study, co-expression of TRPC1 with TRPC3 resulted in ROCCs that were gated downstream of PLC activation, independently of IP_3 and store-depletion (Sydorenko et al., 2003). It has been proposed that co-expression of TRPC1 with other TRPC channels may transform TRPC1 into ROCCs (Beech et al., 2003; Lintschinger et al., 2000). However, there is no evidence to date to suggest TRPC1 homomultimers may form ROCCs.

2. Group 3 – TRPC3/6/7

The group 3 subset of TRPC channels are perhaps the best characterized of the TRPC subfamily. TRPC3, TRPC6 and TRPC7 share more than 75% primary sequence identity and are generally believed to be functionally redundant (Dietrich et al., 2003). The overwhelming majority of studies have reported that TRPC3 and TRPC6 form Ca^{2+}-permeable non-selective cation channels, that operate independently of store-depletion, and are activated by DAG, independent of PKC activation (Hofmann et al., 1999; Trebak et al., 2003b).

a. TRPC3

An initial characterization found that TRPC3 may be activated either by conformational coupling with IP_3R, or by exogenous addition of DAG analogs in the same cells (Putney, 1999). It was only later discovered that at low levels of expression TRPC3 formed SOCCs, whereas at higher levels TRPC3 formed ROCCs, which were gated independently of store-depletion or IP_3 (Vazquez et al., 2003). Since most studies with TRPC3 were conducted under conditions of overexpression, many insights have been gained into the regulation of TRPC3 as ROCCs. Receptor-mediated rise in $[Ca^{2+}]_i$ through TRPC3 channels occurs independently of IP_3Rs, store-depletion and PKC, but is dependent on PLC-mediated generation of DAG (Trebak et al., 2003a). While PKC does not play a role in the activation of TRPC3, it is potent inhibitor of TRPC3 channels. PKC activation has been shown to inhibit both receptor-mediated and OAG-induced opening of TRPC3 channels (Trebak et al., 2003a). Also involved in the activation of TRPC3 are src family soluble tyrosine kinases. Engagement of G protein-coupled receptors or receptor tyrosine kinases results in the activation of soluble tyrosine kinases, which activate TRPC3 indirectly, putatively by phosphorylation (Vazquez et al., 2004). Finally, consistent with the observation that in most studies TRPC3 is an ROCC, TRPC3 is generally insensitive to SOC inhibitors, the lanthanides and 2-APB (Trebak et al., 2002).

b. TRPC6

The function of TRPC6 and TRPC3 is highly redundant. Like TRPC3, TRPC6 also forms ROCCs gated by DAG in a membrane-delimited fashion independently of PKC, IP_3Rs, or store-depletion (Hofmann et al., 1999). Analogous to TRPC3, TRPC6

can also be regulated by src family tyrosine kinases, which interact with the amino terminus of TRPC6 to phosphorylate and enhance channel activity (Hisatsune et al., 2004). However, considerable differences exist between the regulatory mechanisms of the two channels. While TRPC3 exhibits considerable constitutive activity, TRPC6 is tightly regulated under basal conditions (Dietrich et al., 2003). The tight regulation of TRPC6 is attributed to the dual glycosylation of TRPC6, the second of which is absent in TRPC3. The elimination of the second glycosylation site has been shown to render TRPC6 into a constitutively active channel (Dietrich et al., 2003). A second major difference between TRPC3 and TRPC6 is that while TRPC3 channels are inhibited by PKC, TRPC6 channels may be insensitive to PKC inhibition (Hofmann et al., 1999). On the other hand, PKA may be involved in the inhibition of TRPC6 upon engagement of certain receptor tyrosine kinases (Hassock et al., 2002). Finally, unlike TRPC3, the physiological function of TRPC6 has been preliminarily investigated in the TRPC6 null ($TRPC6^{-/-}$) mice. In aortic and tracheal smooth muscle isolated from $TRPC6^{-/-}$ mice, it was shown that agonist-induced contraction was higher compared to WT mice (Freichel et al., 2004). It is now hypothesized that TRPC6 is critically important in the regulation of smooth muscle tone in the trachea and the vasculature. The above hypothesis is consistent with the prior observation that TRPC6 was involved in the formation of ROCCs in vascular smooth muscle (Plant and Schaefer, 2003).

c. **TRPC7**

TRPC7 was the last of the mammalian TRPC channels to be identified and cloned. The expression of TRPC7 is highest in the heart, lungs, eyes, kidney, brain,

spleen and testes (Hofmann et al., 2002). TRPC7 proteins has been reported to behave as ROCCs activated by OAG, as well as SOCCs gated upon store-depletion (Vennekens et al., 2002). Like TRPC3, the function of TRPC7, however, depends on the level and conditions of expression. At low expression conditions, TRPC7 is an ROCC sensitive to OAG, but at high expression conditions, TRPC7 is an SOCC sensitive to store-depletion or PLC activation (Lievremont et al., 2004). The parallel gating of TRPC7 by either store-depletion or PLC-activation under high expression conditions is the only demonstration to date suggesting that the same TRPC channel may mediate both SOCE and ROC entry.

3. **Group 4 – TRPC 4/5**

TRPC4 and TRPC5 are highly expressed in the brain, adrenal gland, placenta, uterus, ovaries, testes, prostate, kidneys, endothelial cells and vascular smooth muscle (Riccio et al., 2002). There is significant overlap of tissue expression between TRPC4, TRPC5 and TRPC1. The overlap between the expression of TRPC4, TRPC5 and TRPC1 is not surprising in light of the prior demonstration that the three TRPC isoforms can heteromultimerize via the PDZ domains (Montell, 2005; Plant and Schaefer, 2003). Available evidence suggests that upon heteromultimerization between TRPC4 or TRPC5 with TRPC1, the resultant channel is an SOCC that can be activated in a membrane-delimited fashion, but is insensitive to store-depletion (Beech et al., 2003; Vennekens et al., 2002). Evidence also exists to suggest that TRPC4 and TRPC5 may homomultimerize to form ROCC-like channels. At least one study has suggested that TRPC4 channels may be sensitive to OAG or its breakdown products (Wu et al., 2002).

The creation of TRPC4$^{-/-}$ mice has provided preliminary insights into the physiological role of TRPC4. TRPC4 appears to be involved in agonist-induced CCE in vascular endothelial cells (Tiruppathi et al., 2002a). In particular, the agonist-induced influx of $[Ca^{2+}]_e$ was significantly reduced in endothelial cells from TRPC4$^{-/-}$ mice. Furthermore, the endothelium-dependent vascular smooth muscle relaxation was drastically reduced in TRPC4$^{-/-}$ mice strongly suggesting that TRPC4, like TRPC6, was also involved in the regulation smooth muscle tone (Tiruppathi et al., 2002b).

D. TRPC channels and lymphocytes

Few studies have examined in detail the endogenous expression and function of TRPC channels in lymphocytes. A preliminary study performed by Gamberucci and coworkers found that in primary human peripheral blood T cells and Jurkat cells, OAG activated the influx of Ca^{2+}, Ba^{2+} and Sr^{2+} indicating the presence of non-specific cation channels (Gamberucci et al., 2002). The induction of $[Ca^{2+}]_i$ elevation by OAG was distinct from the $[Ca^{2+}]_i$ rise induced by TG or PHA, and was additive with the TG-induced $[Ca^{2+}]_i$ rise. Furthermore, the OAG-induced $[Ca^{2+}]_i$ rise was not blocked by the activation of PKC, inhibition of PLC, presence of lanthanides, SKF, or 2-APB (Gamberucci et al., 2002). On the other hand, all the above drugs inhibited TG and PHA-induced $[Ca^{2+}]_i$ elevation. RT-PCR analysis demonstrated that both Jurkat and peripheral blood T cells express transcripts for TRPC1, 3, 4, and 6. However, Western analysis revealed that only TRPC6 was expressed at the protein level. Based on the aforementioned observations, Gamberucci et al. concluded that T cells possess a unique

cation influx pathway activated by DAG, which is unrelated to CCE and mediated by TRPC6.

A subsequent study of TRPC channels also in Jurkat cells examined the role of TRPC3. It was found that TRPC3 is important in the elevation of $[Ca^{2+}]_i$ downstream of TCR activation induced by PHA or anti-CD3 antibodies (Philipp et al., 2003). In this particular study, Northern analysis demonstrated the mRNA expression of TRPC1, 3 and 4 in Jurkat cells, but not TRPC6. At the protein level, however, only TRPC3 was detected. Analogous to the previous study by Gamberucci et al., TRPC3 was found to be a non-specific cation channel gated downstream of PLC activation. Using Jurkat cells that expressed mutant versions of TRPC3, the authors determined that the activation of T cells through the TCR using either PHA or anti-CD3 antibodies resulted in an increase in $[Ca^{2+}]_i$ through TRPC3 in an IP_3-dependent manner. In contrast, store-depletion using TG did not result in $[Ca^{2+}]_e$ entry through TRPC3. The authors concluded that TRPC3 may be involved in the formation of independent cation channels important for Ca^{2+} entry in activated T cells.

A final investigation of TRPC channels in lymphocyte function was performed by in DT40 avian B cells. The authors, Mori et al., showed that both murine SPLC and DT40 cells express TRPC1 endogenously. TRPC1 was involved in the rise in $[Ca^{2+}]_i$ upon the stimulation of B cells using antibodies directed against the B cell receptor (BCR) (Mori et al., 2002). In addition, TRPC1-mediated elevation in $[Ca^{2+}]_i$ was activated in an IP_3-dependent manner. The authors also utilized homologous recombination to knockout TRPC1 in the DT40 cells, and showed that knockout of TRPC1 inhibited the BCR-induced $[Ca^{2+}]_i$ elevation. Moreover, reintroduction of

TRPC1 cDNA into TRPC1 knockout DT40 cells restored the BCR-induced $[Ca^{2+}]_i$ entry. Finally, the authors demonstrated that knockdown of TRPC1 in DT40 cells impaired, but did not eliminate SOCE induced by TG. The authors concluded that TRPC1 is important for both the induction of $[Ca^{2+}]_i$ rise downstream of BCR activation, and may have a role in CCE. It is clear from the preliminary studies in both B and T cells that TRPC channels are involved in normal lymphocyte function. In addition, cursory evidence suggests that in lymphocytes TRPC channels may be regulated differently than in other cell types.

IV. **Objective**

Cannabinoids exhibit broad immune modulating activity by targeting many cell types within the immune system. In T cells, cannabinoids alter cellular activation, proliferation, and cytokine expression. Due to the critical role for $[Ca^{2+}]_i$ in T cell activation and subsequent cellular function, the objective of the studies presented here was to perform a thorough investigation of the mechanism by which cannabinoids, and Δ^9-THC in particular, modulate $[Ca^{2+}]_i$ in T cells. The studies presented below examine using a variety of cell models, including murine SPLC, purified murine splenic T cells and human T cell lines, the effect of Δ^9-THC and other cannabinoid compounds on $[Ca^{2+}]_i$ elevation in unstimulated T cells. Many of the studies on IL-2 expression and $[Ca^{2+}]_i$ elevation were performed in HPB-ALL and/or Jurkat E6-1 human T cell lines because while both cell lines express CB2 transcripts, neither cell line expresses CB1 transcripts. Moreover, the CB2 receptor expressed by Jurkat E6-1 cells has previously been reported to be aberrant and dysfunctional (Schatz et al., 1997), allowing for putative discernment between CB2-mediated and -independent effects of cannabinoid compounds.

The preliminary goal of the assessment of $[Ca^{2+}]_i$ elevation by cannabinoids was to link functionally the modulation of $[Ca^{2+}]_i$ by cannabinoids and the alteration of Ca^{2+}-dependent production of IL-2 in T cells. However, in the course of the studies, it was determined that the modulation of $[Ca^{2+}]_i$ and alteration of IL-2 production by cannabinoids may be simultaneous and unrelated events occurring through divergent mechanisms. Nevertheless, the modulation of $[Ca^{2+}]_i$ by cannabinoid compounds was examined in detail, as $[Ca^{2+}]_i$ elevation plays a critical role in many cellular processes including activation of enzymes, triggering of apoptotic pathways, and induction of T cell anergy. The studies presented below examine the hypothesis that Δ^9-THC and structurally-related cannabinoid congeners induce a rise in $[Ca^{2+}]_i$ in a CB1 or CB2 receptor-dependent manner through the TRPC channels acting as ROCCs in T cells.

MATERIALS AND METHODS

I. Cannabinoid compounds

SR1, SR2, [^{3}H]-SR1, CP, CBN, CBD, 2-AG, AEA and Δ^9-THC were provided by the National Institute on Drug Abuse. WIN-2 was purchased from Sigma Chemical Company (St. Louis, MO). JWH-133 was from Tocris Cookson, Inc. (Ellisville, MO). HU-210 was a gift from Dr. Raphael Mechoulam (Hebrew University of Jerusalem, Israel). JWH-133, WIN-2, SR2 and SR1 were prepared as 10 mM stocks in DMSO, and stored in aliquots at –80°C. Δ^9-THC, CBN, CBD and CP were prepared as 20 mM stocks in EtOH and stored in aliquots at –80°C. 2-AG and AEA were prepared as 20 mM stocks in N_2-purged EtOH and stored aliquoted in cryovials at –80°C. All compounds were diluted 10-fold in appropriate buffer, and were added to cells at a 100-fold dilution.

II. Reagents

TG, PMA, Io, AA, OAG, 2-APB, PP2, LY294002, 8-Br-cADPR, PTx, and $LaCl_3$ were purchased from Sigma Chemical Company (St. Louis, MO). KN92, KN93, Et-18-OCH_3 were from Calbiochem (San Diego, CA). SKF was from Biomol (Plymouth Meeting, PA). All compounds were prepared as 1000X stocks in the diluent recommended by the manufacturer, aliquoted and stored in –80°C until use. All compounds, with the exception of OAG, were diluted 10-fold in appropriate buffer, and were added to cells at a 100-fold dilution. OAG was added directly to cells at a 1000-fold dilution.

III. **Animals**

Pathogen-free female B6C3F1 and C57BL/6J mice, 6 weeks, were purchased from Charles River Breeding. On arrival, mice were randomized, transferred to plastic cages containing sawdust bedding (5 animals per cage) and quarantined for one week. Mice were not used for experimentation until their body weight was 17-20 g.

Pathogen-free male and female C57BL/6J $CB1^{-/-}/CB2^{-/-}$ mice were generously provided by Dr. Andreas Zimmer (University of Bonn, Germany). Mice were bred by University Laboratory Animal Resources (Michigan State University). Upon weaning, the mice were housed in plastic cages containing sawdust bedding – 5 animals per cage for females or 1 animal per cage for males. Mice were not used for experimentation until their body weight was 17-20 g.

All mice were given food (Purina Certified Laboratory Chow) and water *ad libitum*. Animal holding rooms were maintained at 21–24°C and 40–60% relative humidity with a 12 h light/dark cycle. Animal breeding and experimentation was performed in compliance with the Michigan State University's AUCAUC committee.

IV. **Preparation of splenocytes**

A. **Whole splenocytes**

Mice were sacrificed and spleens (for B6C3F1, C57BL/6J WT and $CB1^{-/-}/CB2^{-/-}$ mice) were removed aseptically. Spleens from $TRPC1^{-/-}$ mice were generously provided by Dr. Lutz Birnbaumer (National Institute of Envirnomental Health Sciences, Research Triangle Park, NC). The spleens were mashed to yield a single cell suspension, washed with 1X RPMI 1640 solution and centrifuged at 270 x g for 5 min. For Ca^{2+}

determinations, erythrocytes were lysed using Gey's balanced salt solution (130 mM NH_4Cl, 5 mM KCl, 0.84 mM Na_2HPO_4, 5.6 mM D-glucose, 0.01% phenol red, 1 mM $MgCl_2$, 0.28 mM $MgSO_4$, 1.15 mM $CaCl_2$, 13.4 mM $NaHCO_3$) for 5 min on ice and washed copiously with 1X RPMI 1640 solution. For radioligand-binding studies, erythrocytes were lysed using ACK lysing buffer (10 μM EDTA-Na_2, 10 mM $KHCO_3$, 150 mM NH_4Cl) for 5 min at RT, and washed copiously with 1X Ca^{2+}/Mg^{2+}-free HBSS solution.

B. T cell isolations

SPLC from naïve B6C3F1 mice were depleted of red blood cells by lysis using Gey's balanced salt solution. The recovered cells were resuspended in 1X column wash buffer at a concentration of $1.5x10^8$ cells/ml and transferred in 2 ml aliquots onto T cell enrichment columns (R&D Systems, Minneapolis, MN) and incubated for 10 min at RT. Purification of T cells by T cell enrichment columns was through negative selection. The collected cells were then resuspended in Ca^{2+}-KREB buffer for calcium determinations. This method routinely yields > 95% pure T cells as established by flow cytometry.

V. Cultured cell lines

The HPB-ALL cell line was generously provided by Dr. J. A. Ledbetter (Pacific Northwest Research Institute). The human T cell leukemia line, Jurkat E6-1 clone, was obtained from the American Type Culture Collection (ATCC TIB 152). Both cell lines were cultured in RPMI 1640 medium supplemented with 100 units of penicillin/ml, 100

units of streptomycin/ml, 10% BCS (Hyclone, Logan, UT), 100 mM non-essential amino acids (Gibco, Grand Island, NY) and 1 mM sodium pyruvate (Gibco, Grand Island, NY).

VI. IL-2 ELISAs and mRNA quantification

A. Cell treatments

For IL-2 ELISA treatments, HPB-ALL or Jurkat E6-1 ($5x10^5$ cells/ml) were cultured in triplicate in 48-well plates at 0.8 ml/well in a 2% BCS in RPMI medium (100 units of penicillin/ml, 100 units of streptomycin/ml, 2% BCS, 100 mM non-essential amino acids, 1 mM sodium pyruvate). Antagonists or vehicle (VH; 0.1% DMSO) were added 60 min prior to cell stimulation and cannabinoids or VH (0.1% EtOH) were added 30 min prior to cell stimulation. Cells were stimulated using phorbol ester and ionomycin (PMA/Io; 80 nM and 1 μM respectively). Following a 24 h cell incubation at 37°C, plates were centrifuged at 270 x g for 10 min. Supernatants were collected, aliquoted and stored at -80°C until the day of the assay.

For IL-2 mRNA treatments, HPB-ALL cells ($5x10^5$ cells/ml) were cultured in triplicate in 6-well plates at 5 ml/well in a 2% BCS in RPMI medium. Δ^9-THC or VH (0.1% EtOH) were added 30 min prior to cell stimulation. Subsequently, cells were stimulated with PMA/Io (80 nM/1 μM) for 8 h. Following an 8 h incubation, total RNA was isolated from the cells using SV Total RNA Isolation System (Promega, Madison, WI), quantified and stored at -80°C until the day of the assay.

B. **IL-2 protein quantification**

IL-2 was quantified using a sandwich ELISA method. Immulon IV strip plates (Dynatech Laboratories, Chantilly, VA) were coated with 1 μg/ml of purified mouse anti-human IL-2 antibody (BD Pharmingen, San Diego, CA) overnight at 4°C. Immulon strip plates were washed with PBST (1.9 mM NaH_2PO_4, 8.1 mM Na_2HPO_4, 154 mM NaCl, 0.02% tween-20) and ddH_2O between each incubation step. Wells were blocked for 30 min at 37°C with 3% BSA in PBST. To generate a standard curve, a recombinant human IL-2 (0-8000 pg/ml) standard (BD Pharmingen, San Diego, CA) was included in each assay. Where needed, samples were diluted in 2% BCS in RPMI medium. Each sample and standard was placed into Immulon strip plates and incubated at 37°C for 2 h. Sample wells were incubated for 1 h at 37°C with 1 μg/ml of biotinylated anti-human IL-2 antibody (BD Pharmingen, San Diego, CA), followed by a 1 h incubation at 37°C with 1.5 μg/ml streptavidin peroxidase (Sigma Chemical Company, St. Louis, MO). IL-2 was detected colorometrically using tetramethylbenzidine to begin the reaction, and 6N H_2SO_4 to terminate the reaction. ELISA plates were read at 450 nm with a Bio-Tek Instruments EL-808 plate reader.

C. **IL-2 mRNA quantification**

Real time PCR was performed on a PE Applied Biosystems PRISM 7000 Sequence Detection System (Applied Biosystems, Foster City, CA). The PCR reaction was performed using 10 ng of reverse transcribed cDNA template and TaqMan predeveloped primers and probes (Applied Biosystems, Foster City, CA) for IL-2 and

18S ribosomal RNA, as a loading control, as recommended by the manufacturer. The amplication of each sample was plotted as the change in fluorescence dye (6-FAM) versus amplification cycle number. The cycle number at which the amplified product of each sample reaches a set threshold was termed the C_t value. The C_t value for the target gene (IL-2) was subtracted from the C_t value of the loading control gene (18S ribosomal RNA) to yield the ΔC_t value. The relative mRNA levels for the gene of interest were determined through subtraction of the ΔC_t value of the control sample (NA) form the ΔC_t values of each treated sample. The resultant difference $\Delta\Delta C_t$ was used to calculate the relative mRNA levels using the formula: $2^{\Delta\Delta C_t}$, and graphed as a fold increase over NA.

VII. **Intracellular calcium determination**

Whole SPLC, isolated splenic T cells or human T cell lines were washed twice in Ca^{2+}-KREB buffer (129 mM NaCl, 5 mM KCl, 1.2 mM KH_2PO_4, 1.2 mM $MgSO_4$, 1 mM $CaCl_2$, 5 mM $NaHCO_3$, 10 mM HEPES, 2.8 mM glucose, 0.2% BSA, pH 7.4). All experiments, except for those with $LaCl_3$, were performed in the Ca^{2+}-KREB buffer. The experiments with $LaCl_3$ were performed in modified HPSS buffer (120 mM NaCl, 5.3 mM KCl, 0.8 mM $MgSO_4$, 1.8 mM $CaCl_2$, 20 mM HEPES, 11.1 mM glucose, 0.2% BSA, pH 7.4), which contained a lower concentration of anions (Zhu et al., 1996). For studies with PTx, cells were pretreated with 100 ng/ml PTx for 18 h at 37°C and washed twice in Ca^{2+}-KREB buffer. Cells were incubated with cell-permeant fura-2 AM dye (1 μM, Molecular Research Products, Eugene, OR) for 30 min at 37°C in the dark. Cells were harvested, washed three times with Ca^{2+}-KREB buffer to remove extracellular fura-2 dye, and readjusted to $5x10^6$ cells/ml (for murine splenic cells) or $5x10^5$ cells/ml (for

human T cell lines) in Ca^{2+}-KREB buffer. Cells were placed in a 3 ml quartz cuvette with constant stirring. $[Ca^{2+}]_i$ determinations were performed at room temperature with a Beckman Spex 1681 0.22m Spectrometer with dual excitation at 340 and 380 nm and emission at 510 nm (all slit widths were 1 mm). $[Ca^{2+}]_i$ calculations were based on maximum and minimum calcium values, as assessed with use of 0.1% Triton-X and 500 mM EGTA, respectively. The dissociation constant for the fura-2-calcium complex was 1.45 X 10^{-7} M. For studies conducted in the absence of $[Ca^{2+}]_e$, the Ca^{2+}-KREB buffer was prepared as above without $CaCl_2$ and supplemented with 1 mM $MgCl_2$ and 20 μM EGTA. All compounds used in $[Ca^{2+}]_i$ determination were screened for autofluorescence using fura-2 sodium salt containing Ca^{2+}-KREB buffer. None of the compounds, with the exception of WIN-2, exhibited autofluorescence, nor did they interfere with fura-2 fluorescence.

VIII. **Kinase assays**

A. **Sample preparation**

HPB-ALL cells were cultured in 60 mm^2 tissue culture plates at a density of $5x10^5$ cells/ml (10 ml/plate) and incubated at 37°C for 2 h. Cells were left untreated (NA) or treated with VH (0.1% EtOH), various concentrations of Δ^9-THC (1-20 μM), or PMA (for PKC assays) for varying periods of time (0.5-60 min) at 37°C. Cells were harvested and centrifuged at 300 x g for 5 min, then rinsed with 1x ice-cold PBS (1.9 mM NaH_2PO_4, 8.1 mM Na_2HPO_4, 154 mM NaCl) and centrifuged again. For CaMKII assays, cells were resuspended in assay dilution buffer (20 mM MOPS, 25 mM β-glycerol phosphate, 1 mM $CaCl_2$, pH 7.2; supplemented with 1 mM dithiothreitol, 1 mM $NaVO_3$,

2 mM NaF and 1x EDTA-free solution of protease-inhibitor cocktail tablets). For PKC assays, cells were resuspended in triton-X lysis buffer (25 mM Tris-HCl, 20 mM $MgCl_2$, 140 mM NaCl, 1% triton-X 100, 1x EDTA-free solution of protease-inhibitor cocktail tablets, pH 7.2). The cells were lysed by briefly sonicating twice for 10 s on ice. For CaMKII assays, the cell lysate was further centrifuged at 6700 x g to remove membrane fractions, and the supernatants were stored at –80°C. The samples were assayed for protein using a BCA protein assay kit (Sigma Chemical Company, St. Louis, MO) per manufacturer's instructions.

B. **Substrate activity determination**

The phosphotransferase activity of CaMKII or PKC was determined in the cell lysates using a CaM Kinase II Assay Kit (Upstate Biotech, Lake Placid, NY) or a PKC Assay Kit (Upstate Biotech, Lake Placid, NY). The assay reactions were performed per manufacturer's instructions with 10 μCi [γ-^{32}P] ATP (specific activity 3000 Ci/mmol; PerkinElmer, Boston, MA) using buffers, inhibitors and substrates provided by the manufacturer for 10 min at 30°C. Each assay reaction was then spotted onto individual P81 phosphocellulose paper filters (Whatman International, Maidstone, England), allowed to dry, and washed three times in 0.75% H_3PO_4. The sample filters were assayed for ^{32}P using a Beckman LS1801 scintillation counter in polyethylene vials containing 10 ml scintillation cocktail.

IX. Western analysis

A. Sample preparation

HPB-ALL cells were cultured in 60 mm^2 tissue culture plates at a density of $5x10^5$ cells/ml (10 ml/plate) and incubated at 37°C for 2 h. Cells were left untreated (NA) or treated with VH (0.1% EtOH), or various concentrations of Δ^9-THC (1-20 μM) for varying periods of time (1-60 min) at 37°C. Cells were harvested and centrifuged at 300 x g for 5 min, then rinsed with 1x ice-cold PBS and centrifuged again. Cells were resuspended in HEDG buffer (20 mM HEPES, 1 mM EDTA, 0.5 mM dithiothreitol, 10% glycerol, pH 7.4; supplemented with a 1x solution of protease-inhibitor cocktail tablets). The cells were lysed by briefly sonicating twice for 10 s on ice. The cell lysate was centrifuged at 6700 x g, and the supernatants were stored at –80°C. The samples were assayed for protein using a BCA protein assay kit per manufacturer's instructions.

B. Electrophoresis and blotting

SDS polyacrylamide gel electrophoresis was performed using a glass plate assembly with 1.5 mm spacers. A separating gel solution (375 mM Tris-HCl, 10% acrylamide, 0.1% SDS, 0.03% ammonium persulfate, 0.001% TEMED) was poured between the glass plate assembly and allowed to polymerize for 2 h at RT with a layer of butanol-saturated ddH_2O. The separating gel was stacked with a stacking gel solution (125 mM Tris-HCl, 4% acrylamide, 0.1% SDS, 0.03% ammonium persulfate, 0.001% TEMED), fitted with a 1.5 mm comb, and allowed to polymerize for at least 1 h at RT.

Cell lysates were prepared in HEDG buffer to a protein concentration of 50 μg and incubated at 70°C for 10 min with loading buffer (62.5 mM tris-HCl, 2% SDS, 10%

glycerol, 0.01% bromophenol blue and 1% β-mercaptoethanol). Samples were loaded into the wells on the prepared gel assembly and electrophoresed at 100 V for 2 h at RT. Proteins were transferred onto nitrocellulose at 20 V overnight at 4°C. The nitrocellulose membranes were blocked with a 4% milk, 1% BSA in TBST solution (10 mM tris-HCl, 150 mM NaCl, 0.1% tween-20) for 2 h at RT with shaking. Membranes were then incubated with a 1:500 dilution of rabbit anti-active pT^{286} CaMKII polyclonal antibody (Promega, Madison, WI) in a 5% BSA in TBST solution for 2 h at RT with shaking. Next, blots were incubated for 30 min at RT with a donkey anti-rabbit antibody conjugated with horseradish peroxidase (Amersham, Arlington Heights, IL). Antibody binding was detected by exposing the blot to Supersignal West Femto Maximum Sensitivity Substrate (Pierce Scientific, Rockford, IL).

X. RT-PCR

A. CB1 and CB2

Total RNA from HPB-ALL or Jurkat E6-1 cells was isolated using Tri Reagent (Sigma Chemical Company, St. Louis, MO). Isolated RNA samples were confirmed to be free of DNA contamination by the absence of product after PCR amplification in the absence of reverse transcriptase. RT-PCR was performed using 100 ng of total RNA from HPB-ALL and Jurkat E6-1 cells. The PCR master mixture consisted of PCR buffer, 2.5 mM $MgCl_2$, 1.25 units of *Taq* DNA polymerase and 6 pmol of forward and reverse primers for either CB1 or CB2. Samples were heated to 94°C for 4 min and cycled 40 times at 94°C for 30 s, 57°C for 30 s, and 72°C for 1 min, after which an additional extension step of 72°C for 5 min was included. The forward and reverse primer

sequences, amplicon sizes and accession numbers for CB1 and CB2 are given in table 1. PCR products were resolved in a 3% NuSieve 3:1 agarose gel (FMC Bioproducts, Rockland, ME) and visualized with ethidium bromide staining.

B. TRPC1-7

Total RNA from HPB-ALL cells, Jurkat E6-1 cells, C57BL/6J WT and C57BL/6J TRPC1$^{-/-}$ SPLC was isolated using Tri Reagent. Isolated RNA samples were confirmed to be free of DNA contamination by the absence of product after PCR amplification in the absence of reverse transcriptase. The PCR master mixture consisted of Mg^{2+}-free PCR buffer, 2.5 mM $MgCl_2$, 1.25 units of *Taq* DNA polymerase, 6 pmol of forward and reverse primers, and 400 ng of cDNA reverse transcribed from isolated total RNA. Samples were heated to 94°C for 4 min and cycled 40 times at 94°C for 30 s, 56°C for 30 s, and 72°C for 1 min, after which an additional extension step of 72°C for 5 min was included. The forward and reverse primer sequences, amplicon sizes and accession numbers for human and murine TRPC1-7 are given in table 1. PCR products were resolved in a 2% NuSieve 3:1 agarose gel and visualized with ethidium bromide staining.

XI. DNA Sequencing

A. CB2 receptor sequencing

Total RNA from HPB-ALL or Jurkat E6-1 cells was isolated using Tri Reagent. CB2 cDNA was obtained by reverse transcription with 5 μg of isolated total RNA using PowerScript™ reverse transcriptase (BD Biosciences, Palo Alto, CA) and amplified by PCR using Advantage-HF 2 PCR Kit (BD Biosciences, Palo Alto, CA) as per

Table 1. Sequences of primers used for RT-PCR reactions.

Gene	Accession Number	Direction	Primer Sequence (5' to 3')	Size (bp)
hCB1	XM004350	Forward	GGCTGGAACTGCGAGAAACT	301
		Reverse	TGATCAACACCACCAGGATCA	
hCB2	XM086356	Forward	TCCCAGGCACCTAGACACG	203
		Reverse	TGGTCTCTGGAGGATGCAGG	
hTRPC1	NM003304	Forward	GGAGGTGAAGGAGGAGAATACGCTG	686
		Reverse	ATAATCCCCGTTTGTCAAGAGGCTCG	
hTRPC3	NM003305	Forward	TTCTACGCTTACGACGAGGACG	786
		Reverse	GAACCTGTCTGAGGCATTGAACAC	
hTRPC4	NM016179	Forward	AACAGATGTGGGATGGCGGAC	587
		Reverse	GTTGAGTAGAACAACCAGAGAGATGAC	
hTRPC5	NM012471	Forward	TAGTTCAGAGGTAGACAGCCTGCG	1195
		Reverse	GCCAAATACAGACCAGAAGAGTGAC	
hTRPC6	NM004621	Forward	ATGGTAACATCCCAGTGGTGCG	925
		Reverse	CCAATGGCAACAGCAAGGAC	
hTRPC7	NM023089	Forward	GCAAGGATTTTGTAGTGGGCG	1025
		Reverse	TGGGTTGTATTTGGCACCTCG	
mTRPC1	NM011643	Forward	GCCTCAGACATTCCAGGTTTCG	1129
		Reverse	TCATTGCTTTGCTGTTCGCAG	
mTRPC2	NM011644	Forward	ATCCCGAATCAACACCTACCG	601
		Reverse	AGACTCTCCCAGCAAGAAGATAAG	
mTRPC3	NM019510	Forward	GAGCAGACCATCGCTATCAAGTG	703
		Reverse	TGTCCTTCACAGTCCTTCCAAGAG	
mTRPC4	NM016984	Forward	GAACTCAGCAAGGTGGAGAACG	1108
		Reverse	CCCCAACAAACTCAGTGAACTCG	
mTRPC5	NM009428	Forward	GGTTCAACAACACCTTCTGTCCC	837
		Reverse	CCTCTCCCCAAGTTTCAAATACG	
mTRPC6	NM013838	Forward	GCTGAAGGCAAAAGGTTAGCG	799
		Reverse	AAATGGTGAAGGAGGCTGCGTG	
mTRPC7	NM012035	Forward	CACCCTAACTGTCAGCAGCA	647
		Reverse	GAGATGATCTGGGGGTCTGA	

manufacturer's instructions. Briefly, samples were heated to 94°C for 5 min and cycled 40 times at 94°C for 30 s, 60°C for 30 s, and 72°C for 90 s, after which an additional extension step of 72°C for 5 min was included. The PCR primers contained cleavage sites for restriction endonucleases, BamHI and HindIII, within the forward and reverse primers, respectively. The sequences for PCR primers from 5' to 3' were: CTGAAGGATCCACCCCATGGAGGAATGCTGGGTGAC (forward) and CCTCTCAAGCTTCCAGGGAGTGAACTGATTTCTGACTTGAG (reverse). The PCR products were then cloned into pCMV-Tag-1 (Stratagene, La Jolla, CA) and sequenced with T3 and T7 primers using an ABI PRISM® 3100 Genetic Analyzer at the Michigan State University Macromolecular Structure, Sequencing and Synthesis Facility (East Lansing, MI). The sequences for the T3 and T7 primers, respectively, from 5' to 3' were as follows: AATTAACCCTCACTAAAGGG and GTAATACGACTCACTATAGGGC.

B. TRPC1 alternative splice

PCR products were resolved in a 1.2% NuSieve 3:1 agarose gel (FMC Bioproducts, Rockland, ME) and visualized with ethidium bromide staining. The bands for TRPC1 were excised from the agarose gel and purified using Wizard® PCR preps DNA purification system (Promega, Madison, WI). Sequencing of TRPC1 bands was performed with either TRPC1 forward or reverse primers (see Table 1) using an ABI PRISM® 3100 Genetic Analyzer at the Michigan State University Macromolecular Structure, Sequencing and Synthesis Facility (East Lansing, MI).

XII. siRNA knockdown of TRPC1

A. Transfection of TRPC1 siRNA

Chemically synthesized and pre-annealed siRNA for TRPC1 and a non-silencing control sequence were custom synthesized from Ambion Inc. (Austin, TX). HPB-ALL cells ($2.5x10^5$ cells/ml) were transiently transfected with 20 nM siRNA specific for TRPC1 or a non-silencing control sequence for 48 h. CodeBreaker™ siRNA Transfection Reagent (Promega, Madison, WI) was diluted in Opti-MEM® medium (Gibco, Grand Island, NY) according to manufacturer's instructions. The mixture was incubated at RT for 20 min. siRNA specific for TRPC1 or non-silencing control sequence was diluted in the prepared mixture and allowed to incubate at RT for a further 20 min. Transfection complexes were then dropped onto the cells, swirled to mix, and allowed to incubate at 37°C for 48 h. After 48 h, cells were harvested, washed and used for RNA isolation or $[Ca^{2+}]_i$ determination. Sequences for siRNA oligonucleotides for TRPC1 and non-silencing control are listed in table 2A.

B. Detection of TRPC1 knockdown

Real time PCR was performed on a PE Applied Biosystems PRISM 7000 Sequence Detection System (Applied Biosystems, Foster City, CA). Briefly, total RNA was isolated from siRNA transfected HPB-ALL cells using SV Total RNA Isolation System (Promega, Madison, WI), and reverse transcribed. The PCR reaction contained 100 ng of cDNA template, 133 nM of forward and reverse primers, and the following components of the SYBR® Green PCR Core Reagents (Applied Biosystems, Foster City, CA): 0.025 units AmpliTaq™ Gold DNA polymerase, 1 mM dNTP mix, 3 mM $MgCl_2$

and 1x SYBR Green PCR buffer. Each plate contained duplicate standards of purified PCR products of known template concentration that covered at least seven orders of magnitude to interpolate relative template concentrations of the experimental samples from the standard curves of log copy number versus threshold cycle (C_t). In addition, no template controls were also included on each plate. The relative level of TRPC1 mRNA was standardized to the housekeeping gene, β-actin, to control for differences in RNA loading, quality, and cDNA synthesis. Comparisons between vehicle (transfection reagent), non-silencing control and TRPC1 siRNA treated groups were analyzed using a two-way analysis of variance followed by Dunnett's post test. The forward and reverse primer sequences for TRPC1 and β-actin are given in table 2B.

XIII. **Radioligand-binding analysis**

Spleens from WT C57BL/6J or $CB1^{-/-}/CB2^{-/-}$ C57BL/6J mice were isolated, made into a single cell suspension and erythrocytes lysed. The cells were washed using Ca^{2+}/Mg^{2+}-free Hanks balanced salt solution (GIBCO, Grand Island, NY), and adjusted to a cell density of $1x10^8$ cells/ml in binding buffer (38.45 mM Tris-HCl; 1 mM EDTA-Na_2; 5 g/L BSA in Ca^{2+}/Mg^{2+}-free Hanks balanced salt solution; pH 7.4). The binding assay was performed in triplicate in 13 x 100 mm glass culture tubes pre-siliconized using a 1% Aquasil siliconizing solution (Pierce Scientific, Rockford, IL). Binding reactions were performed in a total of 1 ml volume of binding buffer, [^{3}H]-SR1 (0.5 nM-80 nM), 10 μM unlabeled SR1 (in half the samples for non-specific determination), and 100 μl of cells ($1x10^7$ cells). The reaction mixture was incubated at 37°C for 60 min. After the incubation, the reaction was stopped by adding 2 ml ice-cold washing buffer

Table 2A. Real-time PCR primer sequences for TRPC1 and β-actin

Gene	Orientation	Oligonucleotide Sequence (5' to 3')	Amplicon Size (bp)
TRPC1	Forward	GCCTTCCTCTCCATCCTCTT	83
	Reverse	TCAGCGTATTCTCCTCCTTCA	
β-actin	Forward	TCATGAAGTGTGACGTGGACATC	156
	Reverse	CAGGAGGAGCAATGATCTTGATCT	

Table 2B. Oligonucleotide sequences for siRNA

Gene	Orientation	Oligonucleotide Sequence (5' to 3')	Corresponding Nucleotides
TRPC1	Sense	UGAACUUAGUGCUGAUUUA	612-630
	Antisense	AAAAUCAGCACUAAGUUCA	
Control	Sense	ACUUGUGACUGAAUAGUUU	---
	Antisense	UAACUAUUCAGUCACAAGU	

(38.45 mM Tris-HCl, 1 g/L BSA in ddH_2O, pH 7.4). The reaction mixture was then passed through 2.4 cm GF/C glass microfiber filters (Whatman International, Maidstone, England), which were presoaked overnight in 0.1% polyethylenimine (Sigma Chemical Company, St. Louis, MO), and washed four times with 4 ml washing buffer each time. The filters were transferred into 20 ml polyethylene scintillation vials containing 15 ml scintillation cocktail, and vortexed vigorously. The samples were assayed for ^3H using a Beckman LS1801 scintillation counter. Specific binding of [^3H]-SR1 was determined by subtracting non-specific binding from total binding. Saturation binding isotherms were plotted to demonstrate the relationship between total, non-specific and specific binding of [^3H]-SR1 to WT C57BL/6J or $CB1^{-/-}/CB2^{-/-}$ SPLC. Scatchard analysis was also performed to determine the K_d (binding affinity) and B_{max} (number of binding sites per cell). Scatchard analysis and binding isotherms were plotted using Graphpad Prism®.

XIV. **Statistical analysis**

The mean ± standard error was determined for each treatment group performed in triplicate (for Ca^{2+} determinations) or individual (for all others) experiments by parametric analysis of variance. When significant differences were detected, treatment groups were compared with appropriate controls with the Dunnett's two-tailed *t* test.

EXPERIMENTAL RESULTS

I. Effects of Δ^9-THC and CP on IL-2 expression in HPB-ALL and Jurkat E6-1 cells

A. Differential effects of Δ^9-THC and CP on IL-2 secretion

Cannabinoids have been shown to modulate the expression of several T cell cytokines (Berdyshev, 2000; Klein et al., 2000a). IL-2 is of particular interest because it is a critical cytokine in the immune response and a hallmark of T cell activation. Previous research on IL-2 secretion has determined that synthetic, endogenous as well as plant-derived cannabinoids alter the secretion of IL-2 from activated murine T cells (Condie et al., 1996; Jan et al., 2002; Ouyang et al., 1998). Presently, the effect of Δ^9-THC and CP on IL-2 secretion was investigated in the human T cell lines, HPB-ALL cells and Jurkat E6-1. The objective of the parallel studies in the HPB-ALL and Jurkat E6-1 cells was to elucidate the putative role of the CB2 receptor in the modulation of IL-2 by cannabinoids. The CB2 receptor expressed by Jurkat E6-1 cells has previously been reported to be aberrant, and also to be dysfunctional (Schatz et al., 1997). Therefore, the present studies were performed with the hypothesis that cannabinoids would differentially modulate IL-2 secretion in the HPB-ALL vs. Jurkat E6-1 cells. HPB-ALL and Jurkat E6-1 cells were pretreated with various concentrations of Δ^9-THC or CP (0.1-20 μM) followed by cell stimulation with PMA/Io. After a 24 h incubation, IL-2 was assayed from each culture supernatant. The results showed that while Δ^9-THC inhibited IL-2 secretion from HPB-ALL cells in a concentration-responsive manner (figure 6), Δ^9-THC did not significantly inhibit the secretion of IL-2 in Jurkat E6-1 cells (figure 7). In

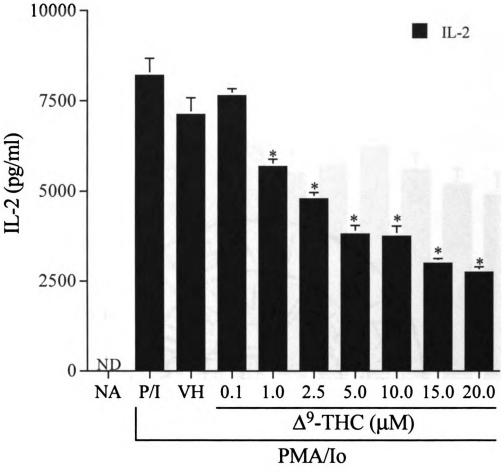

Figure 6. Δ^9-THC suppresses the secretion of IL-2 from PMA/Io-stimulated HPB-ALL cells. HPB-ALL cells were treated with various concentrations of Δ^9-THC or VH (0.1% EtOH) for 30 min followed by activation with PMA/Io (80 nM/1 μM) for 24 h. The supernatants were harvested and assayed for IL-2 by ELISA. * $p < 0.05$ as compared to VH group. Results represent four separate experiments with three replicates per treatment group. ND indicates no IL-2 detected.

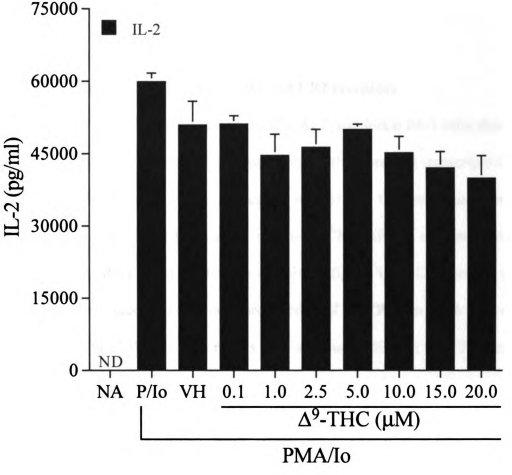

Figure 7. Δ^9-THC does not suppress the secretion of IL-2 from PMA/Io-stimulated Jurkat E6-1 cells. Jurkat E6-1 cells were treated with various concentrations of Δ^9-THC or VH (0.1% EtOH) for 30 min followed by activation with PMA/Io (80 nM/1 μM) for 24 h. The supernatants were harvested and assayed for IL-2 by ELISA. Results represent four separate experiments with three replicates per treatment group. ND indicates no IL-2 detected.

contrast to the differential effects of Δ^9-THC on IL-2 secretion, CP, the higher affinity CB1/CB2 non-selective ligand was equally efficacious at inhibiting the secretion of IL-2 in both cell lines (figure 8, 9).

B. **Characterization of the CB1 and CB2 receptors**

Previous Northern analysis results in HPB-ALL and Jurkat E6-1 cells showed that while neither cell line expressed CB1 transcripts, both expressed transcripts for CB2 (Schatz et al., 1997). Presently, the expression of CB1 and CB2 was characterized by RT-PCR, a significantly more sensitive method. CB1 mRNA expression was not detected by RT-PCR in either of the two cell lines (figure 10). Conversely, a single predicted 203 bp amplicon for CB2 was produced by RT-PCR from RNA derived from both cell lines (figure 10). Previous results have also suggested that the CB2 receptor in the Jurkat E6-1 cells was dysfunctional (Schatz et al., 1997). In order to elucidate whether the dysfunctionality of the CB2 receptor in the Jurkat E6-1 cells was due to putative mutations in the CB2 gene, CB2 cDNA was sequenced from both HPB-ALL and Jurkat E6-1 cells. Results showed that the CB2 coding sequence was 100% homologous between the two cells lines and 99.4% homologous as compared to the reported coding sequence for human CB2 (GenBank accession no. XM_086356; data not shown). In spite of the CB2 sequence homology between HPB-ALL cells and Jurkat E6-1 cells, CB2 does not negatively couple to adenylate cyclase in Jurkat E6-1 cells, which is in contrast to HPB-ALL cells and virtually all other cells known to express functional CB2 (Schatz et al., 1997).

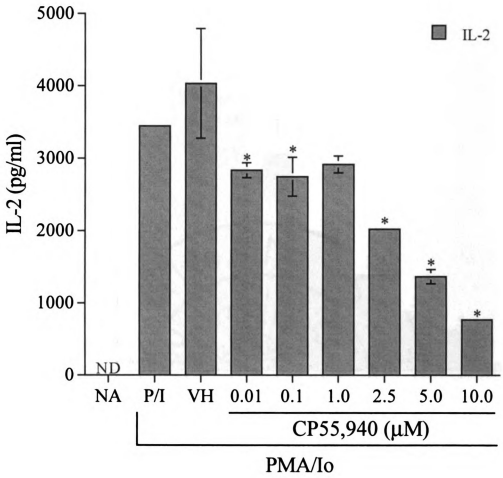

Figure 8. CP suppresses the secretion of IL-2 from PMA/Io-stimulated HPB-ALL cells. HPB-ALL cells were treated with various concentrations of CP or VH (0.1% EtOH) for 30 min followed by activation with PMA/Io (80 nM/1 μM) for 24 h. The supernatants were harvested and assayed for IL-2 by ELISA. * $p < 0.05$ as compared to VH group. Results represent three separate experiments with three replicates per treatment group. ND indicates no IL-2 detected.

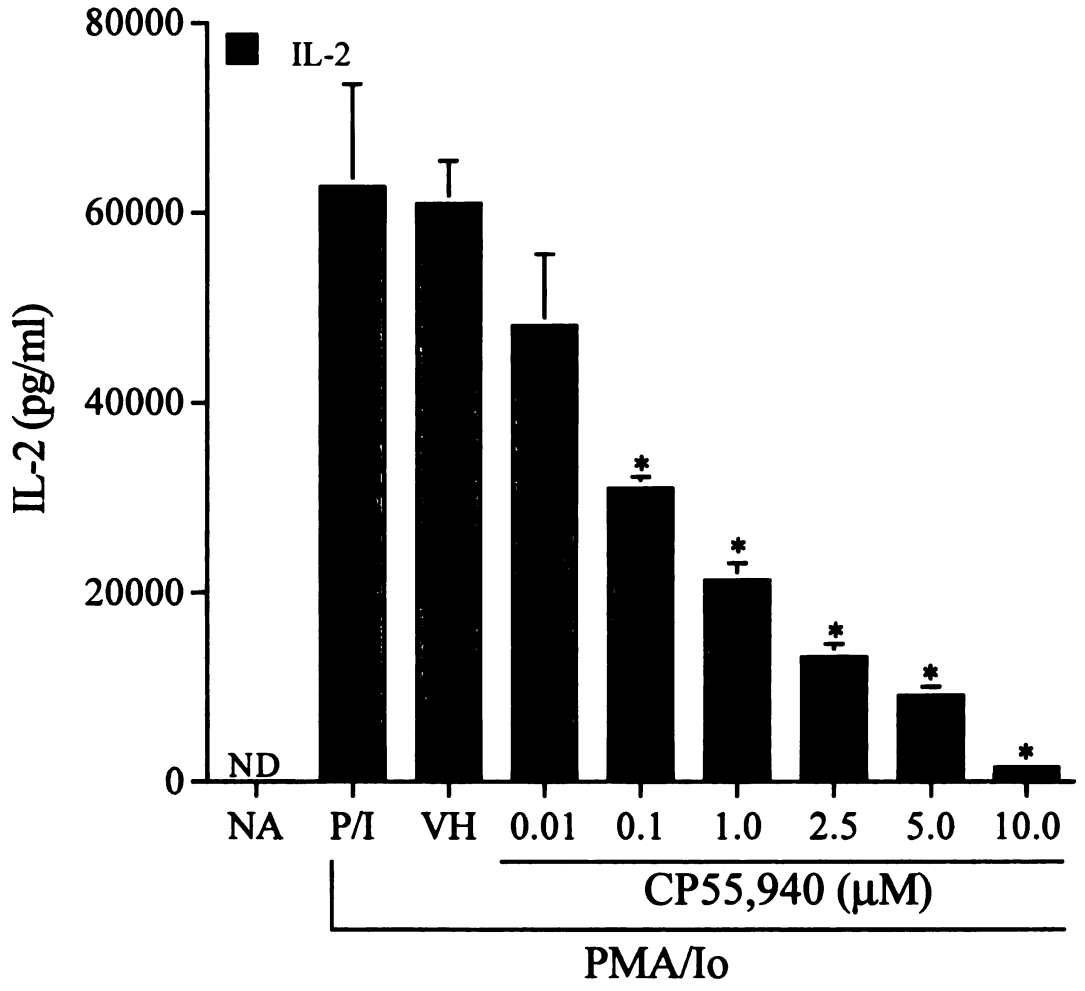

Figure 9. CP suppresses the secretion of IL-2 from PMA/Io-stimulated Jurkat E6-1 cells. Jurkat E6-1 cells were treated with various concentrations of CP or VH (0.1% EtOH) for 30 min followed by activation with PMA/Io (80 nM/1 μM) for 24 h. The supernatants were harvested and assayed for IL-2 by ELISA. * $p < 0.05$ as compared to VH group. Results represent three separate experiments with three replicates per treatment group. ND indicates no IL-2 detected.

Figure 10. RT-PCR for CB1 and CB2 in the HPB-ALL and Jurkat E6-1 cells. Total RNA was isolated from HPB-ALL and Jurkat E6-1 cells. Three separate RNA isolates were assayed for expression of CB1 and CB2 mRNA transcripts by RT-PCR. The RNA samples were confirmed to be free of DNA contamination by the absence of product after PCR amplification in the absence of reverse transcriptase (-RT). The results are representative of three independent experiments.

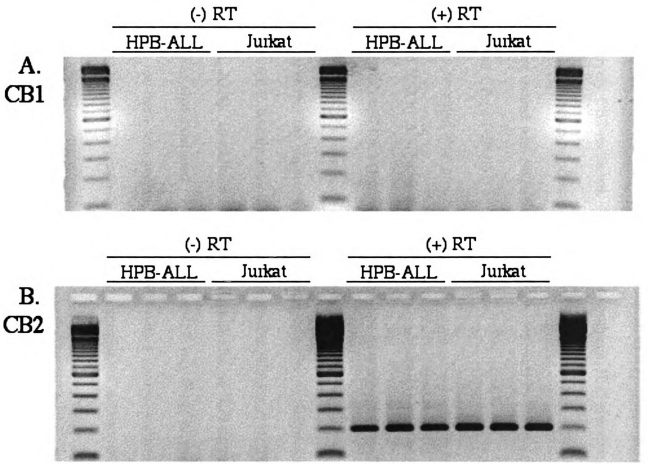

Figure 10. RT-PCR for CB1 and CB2 in the HPB-ALL and Jurkat E6-1 cells.

C. Cannabinoid receptor antagonists fail to antagonize the suppression of IL-2 by Δ^9-THC and CP

The above observation that both HPB-ALL and Jurkat E6-1 cells express only the CB2 receptor suggested that the differential modulation of IL-2 secretion by Δ^9-THC and CP was putatively CB2-mediated. To test this hypothesis, IL-2 secretion studies were performed in the absence or presence of SR2 with Δ^9-THC or CP. HPB-ALL or Jurkat E6-1 cells were treated with SR2 (1 μM) for 30 min, followed by varying concentrations of Δ^9-THC and CP (0.1-20 μM) and then stimulated with PMA/Io. The resulting IL-2 measurements revealed that pretreatment of cells with SR2 failed to antagonize the suppression of IL-2 by Δ^9-THC in the HPB-ALL cells (figure 11), and the suppression of IL-2 by CP in both cell lines (figure 12, 13). The lack of antagonism by SR2 of the Δ^9-THC- and CP-mediated suppression of IL-2, however, was not surprising considering the prior observation that the suppression of IL-2 expression by cannabinoids in murine T cells was reported to be cannabinoid receptor-independent (Kaplan et al., 2003; Rockwell and Kaminski, 2004). In addition to SR2, the effect of SR1 on IL-2 suppression by Δ^9-THC or CP was also examined. Although neither cell was found to express the CB1 receptor, SR1 has been demonstrated to cross react with a variety of other receptors and hence antagonize non-CB1 non-CB2 mediated cannabinoid actions (Pertwee, 2001, 2005). In the current experiments, SR1 (1 μM) pretreatment also failed to antagonize the suppression of IL-2 by Δ^9-THC in the HPB-ALL cells (figure 14), and the suppression of IL-2 by CP in both HPB-ALL and Jurkat E6-1 cells (figure 15, 16).

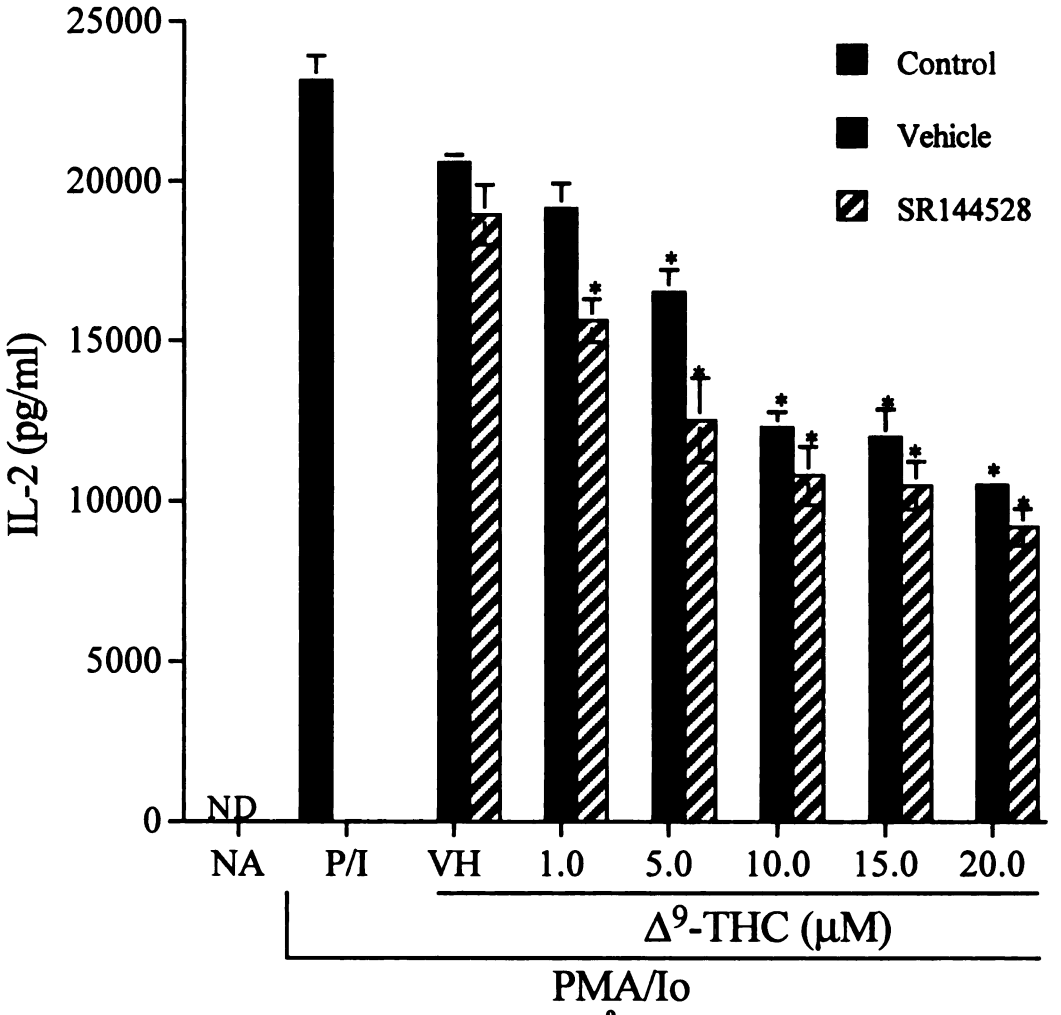

Figure 11. SR2 does not antagonize the Δ^9-THC-induced suppression of IL-2 secretion in HPB-ALL cells. HPB-ALL cells were pretreated with SR2 (1 μM) or VH (0.1% DMSO) for 30 min followed by various concentrations of Δ^9-THC or VH (0.1% EtOH) for 30 min. The cells were then activated with PMA/Io (80 nM/1 μM) for 24 h. The supernatants were harvested and assayed for IL-2 by ELISA. * $p < 0.05$ as compared to VH/VH group. Results represent three separate experiments with three replicates per treatment group. ND indicates no IL-2 detected.

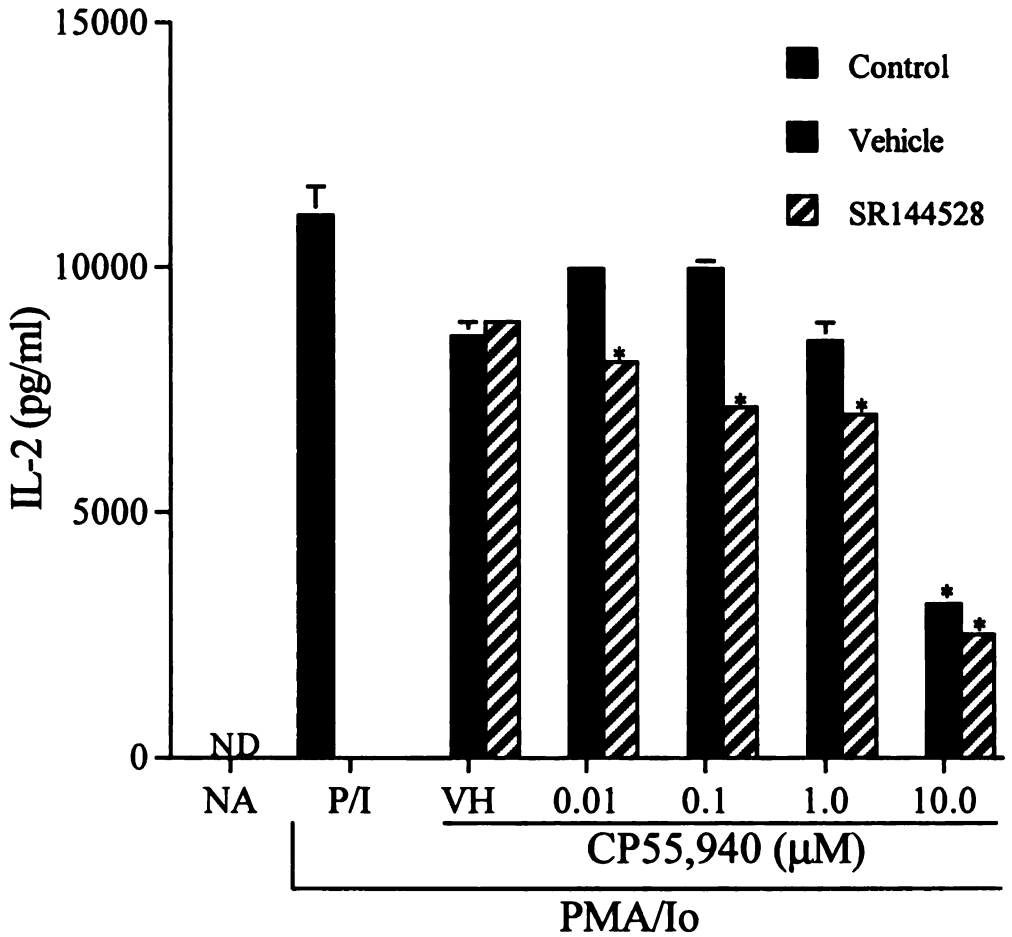

Figure 12. SR2 does not antagonize the CP-induced suppression of IL-2 secretion in HPB-ALL cells. HPB-ALL cells were pretreated with SR2 (1 μM) or VH (0.1% DMSO) for 30 min followed by various concentrations of CP or VH (0.1% EtOH) for 30 min. The cells were then activated with PMA/Io (80 nM/1 μM) for 24 h. The supernatants were harvested and assayed for IL-2 by ELISA. * $p < 0.05$ as compared to VH/VH group. Results represent three separate experiments with three replicates per treatment group. ND indicates no IL-2 detected.

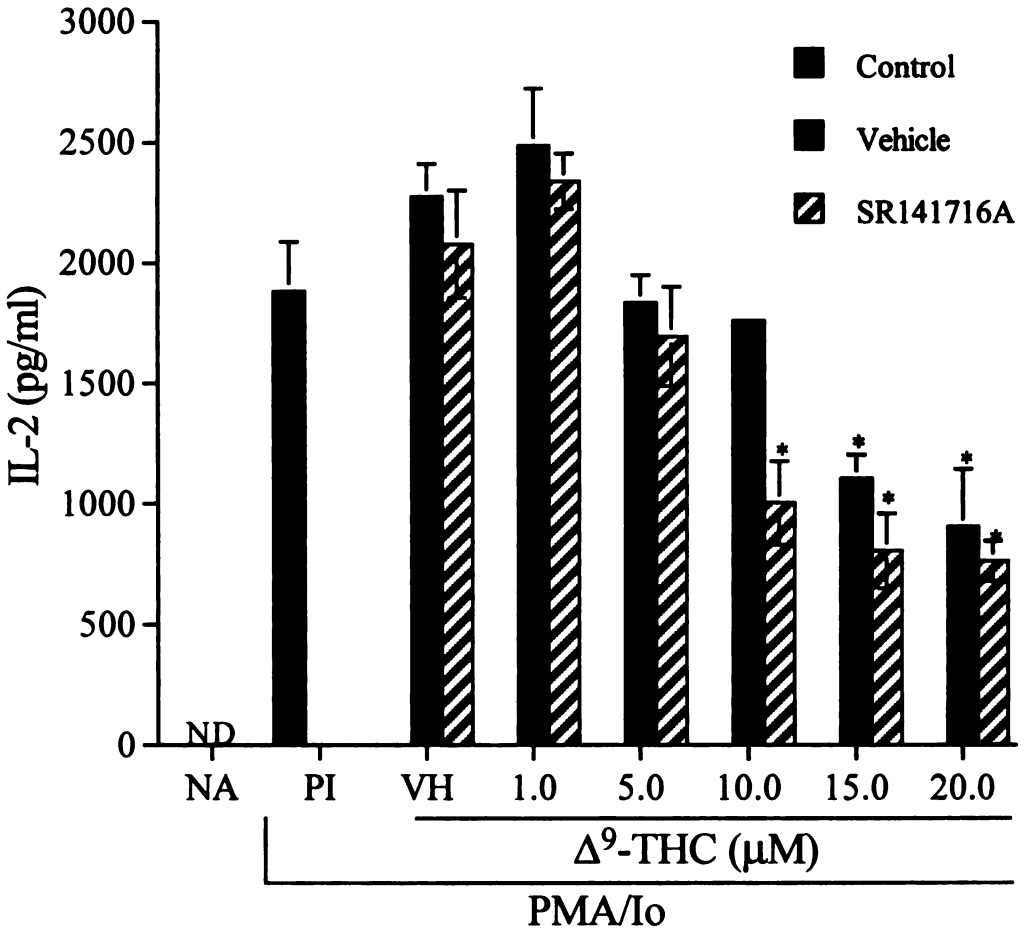

Figure 13. SR2 does not antagonize the CP-induced suppression of IL-2 secretion in Jurkat E6-1 cells. Jurkat E6-1 cells were pretreated with VH (0.1% DMSO) or SR2 (1 μM) for 30 min followed by various concentrations of CP or VH (0.1% EtOH) for 30 min. The cells were then activated with PMA/Io (80 nM/1 μM) for 24 h. The supernatants were harvested and assayed for IL-2 by ELISA. * $p < 0.05$ as compared to VH/VH group. Results represent three separate experiments with three replicates per treatment group. ND indicates no IL-2 detected.

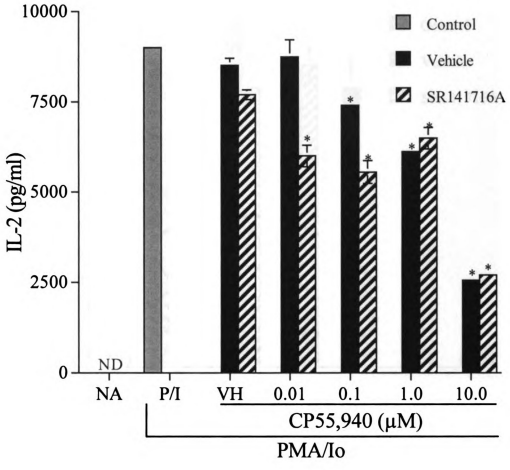

Figure 14. SR1 does not antagonize the Δ^9-THC-induced suppression of IL-2 secretion in HPB-ALL cells. HPB-ALL cells were pretreated with SR1 (1 μM) or VH (0.1% DMSO) for 30 min followed by various concentrations of Δ^9-THC or VH (0.1% EtOH) for 30 min. The cells were then activated with PMA/Io (80 nM/1 μM) for 24 h. The supernatants were harvested and assayed for IL-2 by ELISA. * $p < 0.05$ as compared to VH/VH group. Results represent three separate experiments with three replicates per treatment group. ND indicates no IL-2 detected.

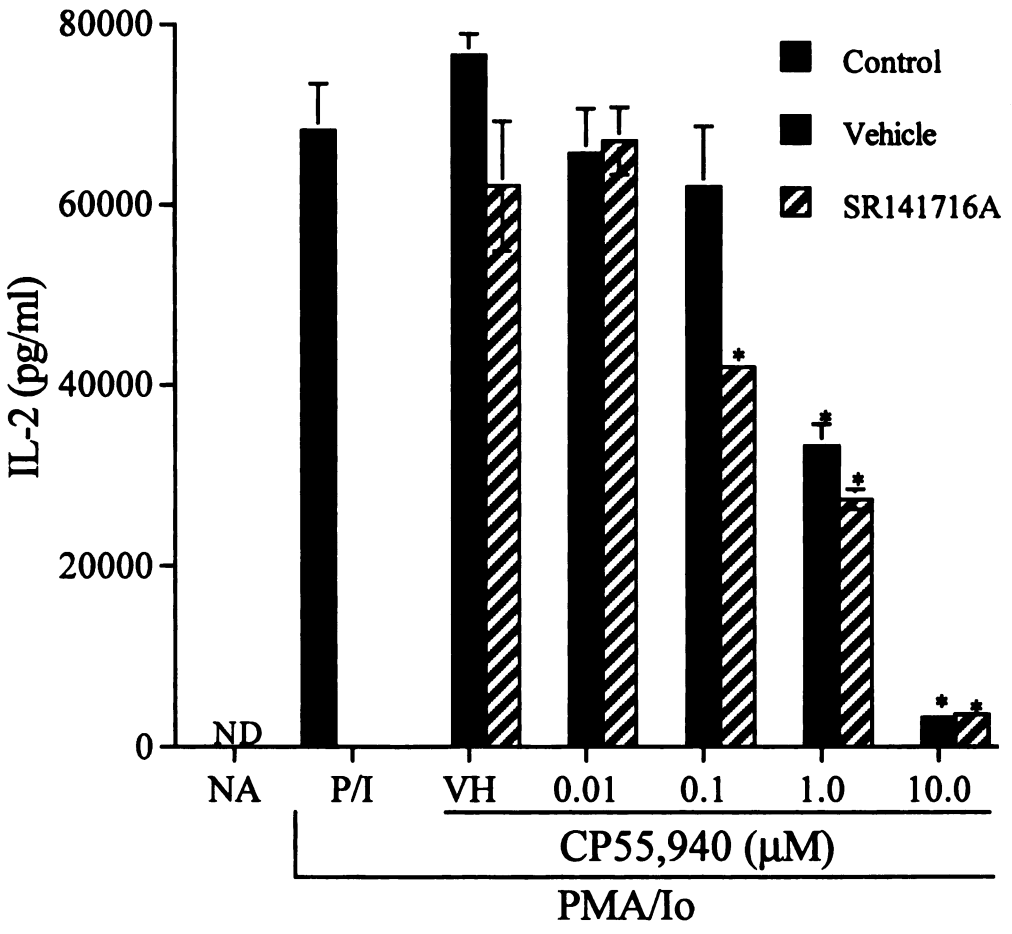

Figure 15. SR1 does not antagonize the CP-induced suppression of IL-2 secretion in HPB-ALL cells. HPB-ALL cells were pretreated with SR2 (1 μM) or VH (0.1% DMSO) for 30 min followed by various concentrations of CP or VH (0.1% EtOH) for 30 min. The cells were then activated with PMA/Io (80 nM/1 μM) for 24 h. The supernatants were harvested and assayed for IL-2 by ELISA. * $p < 0.05$ as compared to VH/VH group. Results represent three separate experiments with three replicates per treatment group. ND indicates no IL-2 detected.

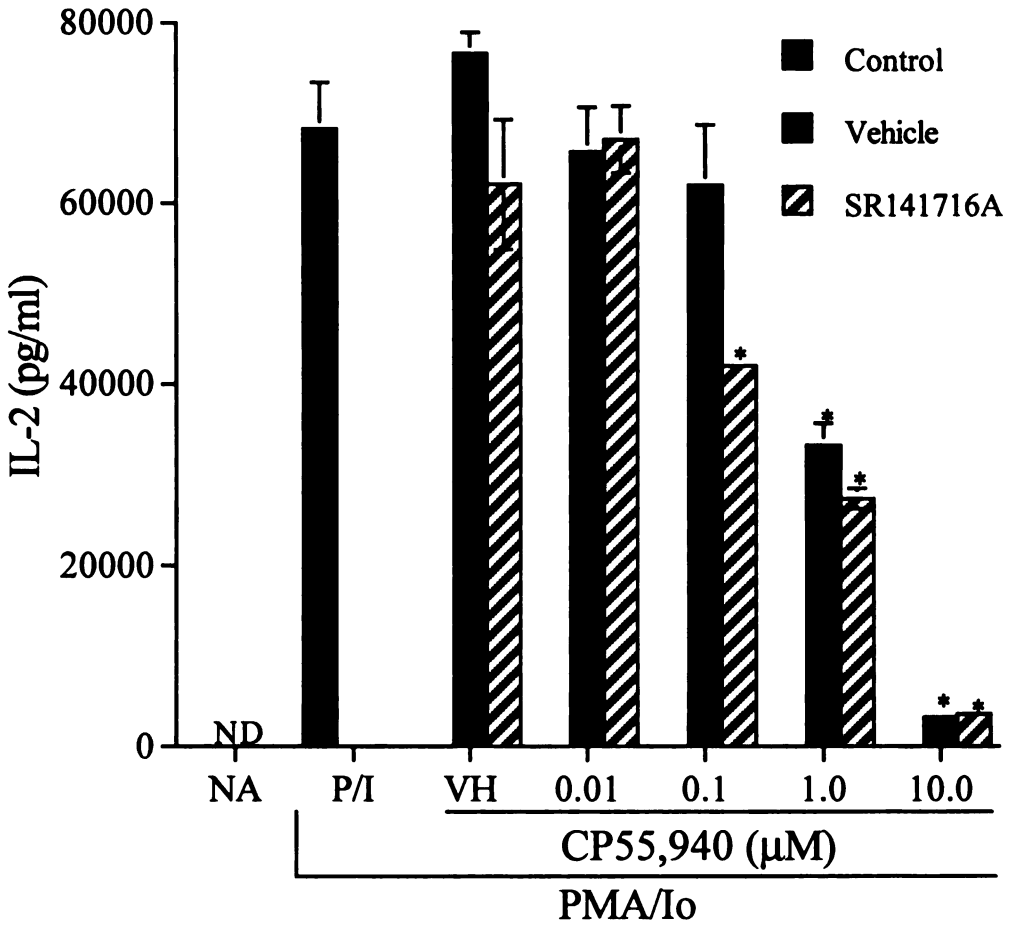

Figure 16. SR1 does not antagonize the CP-induced suppression of IL-2 secretion in Jurkat E6-1 cells. Jurkat E6-1 cells were pretreated with VH (0.1% DMSO) or SR1 (1 μM) for 30 min followed by various concentrations of CP or VH (0.1% EtOH) for 30 min. The cells were then activated with PMA/Io (80 nM/1 μM) for 24 h. The supernatants were harvested and assayed for IL-2 by ELISA. * $p < 0.05$ as compared to VH/VH group. Results represent three separate experiments with three replicates per treatment group. ND indicates no IL-2 detected.

D. PTx pretreatment does not attenuate the Δ^9-THC-induced suppression of IL-2 secretion

Given the prior reports that both CB1 and CB2 are G-protein coupled receptors, the involvement of G proteins in the Δ^9-THC-induced IL-2 suppression was examined. HPB-ALL cells were preincubated with PTx (100 ng/ml) or VH for 18 h for full ADP-ribosylation of $G\alpha_i/G\alpha_o$, and then used for IL-2 studies. PTx-loaded cells were treated with varying concentrations of Δ^9-THC (1-20 μM) followed by PMA/Io stimulation. As seen in figure 17, PTx treatment did not reverse the suppression of IL-2 secretion elicited by Δ^9-THC, suggesting that Δ^9-THC mediates the suppression of IL-2 secretion in a manner independent of $G\alpha_i/G\alpha_o$.

E. Δ^9-THC suppresses IL-2 mRNA production in HPB-ALL cells

In T cells, the production and secretion of IL-2 occurs *de novo* upon cellular stimulation. Previous investigations in murine T cells have revealed that the cannabinoid-mediated decrease of IL-2 expression occurred at the level of IL-2 gene transcription (Condie et al., 1996; Jan et al., 2002; Ouyang et al., 1998). To examine whether the suppression of IL-2 expression by cannabinoids was also due to the decrease of IL-2 transcription in human T cells, HPB-ALL cells were treated with Δ^9-THC followed by PMA/Io stimulation for 8 h. Total mRNA from treated cells was isolated and assayed for IL-2 by real-time PCR. Treatment of the HPB-ALL cells with varying concentrations of Δ^9-THC showed a concentration-dependent suppression of PMA/Io-stimulated IL-2 mRNA production (figure 18), consistent with prior observations made in murine T cells.

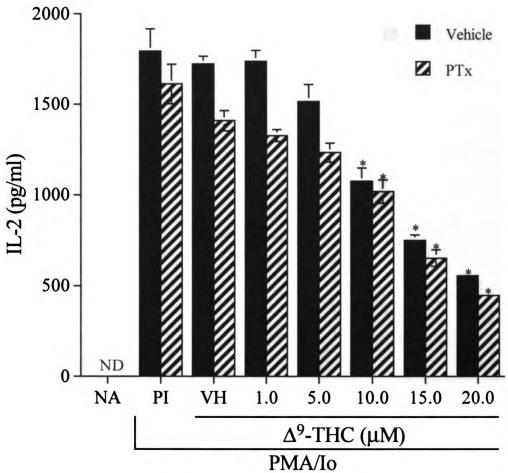

Figure 17. PTx does not reverse the Δ^9-THC-induced suppression of IL-2 secretion in HPB-ALL cells. HPB-ALL cells were preincubated with PTx (100 ng/ml) or VH (PBS) for 18 h. The cells were then pretreated with various concentrations of Δ^9-THC or VH (0.1% EtOH) for 30 min, followed by activation with PMA/Io (80 nM/1 μM) for 24 h. The supernatants were harvested and assayed for IL-2 by ELISA. * $p < 0.05$ as compared to VH/VH group. Results represent two separate experiments with three replicates per treatment group. ND indicates no IL-2 detected.

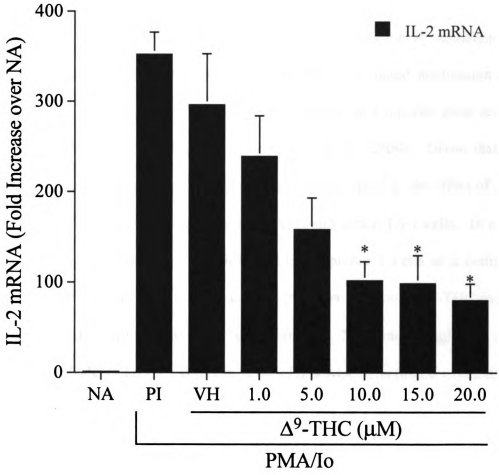

Figure 18. Δ^9-THC suppresses IL-2 mRNA production in HPB-ALL cells. HPB-ALL cells were pretreated with various concentrations of Δ^9-THC or VH (0.1% EtOH) for 30 min, followed by activation with PMA/Io (80 nM/1 μM) for 8 h. The supernatants were harvested and assayed for IL-2 by real time PCR for 40 cycles. Results are shown as percentage of mean IL-2 ± standard error of triplicate samples. * $p < 0.05$ as compared to VH group. Results are representative of three independent experiments.

II. Effects of cannabinoids on $[Ca^{2+}]_i$ in T cells

A. Δ^9-THC elevates $[Ca^{2+}]_i$ in T cells, but CP does not

Recent investigation of the modulation of IL-2 expression by cannabinoids has demonstrated a strong correlation between cannabinoid-mediated modulation of IL-2 gene expression and reciprocal changes in DNA binding and reporter gene activity of NFAT (Jan et al., 2002; Ouyang et al., 1998; Yea et al., 2000). Given that NFAT activation and nuclear translocation is tightly controlled by $[Ca^{2+}]_i$, the effect of Δ^9-THC and CP on $[Ca^{2+}]_i$ was examined in the HPB-ALL and Jurkat E6-1 cells. In addition, parallel studies were performed in primary murine splenic T cells as a comparative control. In both the HPB-ALL cells and murine splenic T cells, Δ^9-THC induced a concentration-responsive elevation in $[Ca^{2+}]_i$ (figure 19, 20). Interestingly, the increase in $[Ca^{2+}]_i$ by Δ^9-THC (10 μM) was robust in both HPB-ALL cells (883.0 ± 56.2 nM, n=3) and splenic T cells (1652.0 ± 216.8 nM, n=3), but at concentrations of Δ^9-THC concentrations below 10 μM, the elevation in $[Ca^{2+}]_i$ was small (HPB-ALL cells; figure 19) or negligible (splenic T cells; figure 20). Also in the splenic T cells the rise in $[Ca^{2+}]_i$ induced by Δ^9-THC (10 μM) did not reach a plateau during the entire period of $[Ca^{2+}]_i$ measurement. By contrast, treatment of the Jurkat E6-1 cells with Δ^9-THC (10 μM) led to a modest rise in $[Ca^{2+}]_i$ (101.7 ± 12.1 nM, n=3; figure 21), which was small in comparison to the effect of Δ^9-THC (10 μM) on $[Ca^{2+}]_i$ in the murine splenic T cells and HPB-ALL cells. In the Jurkat E6-1 cells, the Δ^9-THC-mediated rise in $[Ca^{2+}]_i$ was also comparatively slow and more concentration responsive. Remarkably, while Δ^9-THC elevated $[Ca^{2+}]_i$ in all three models, albeit modestly in the Jurkat E6-1 cells, the higher

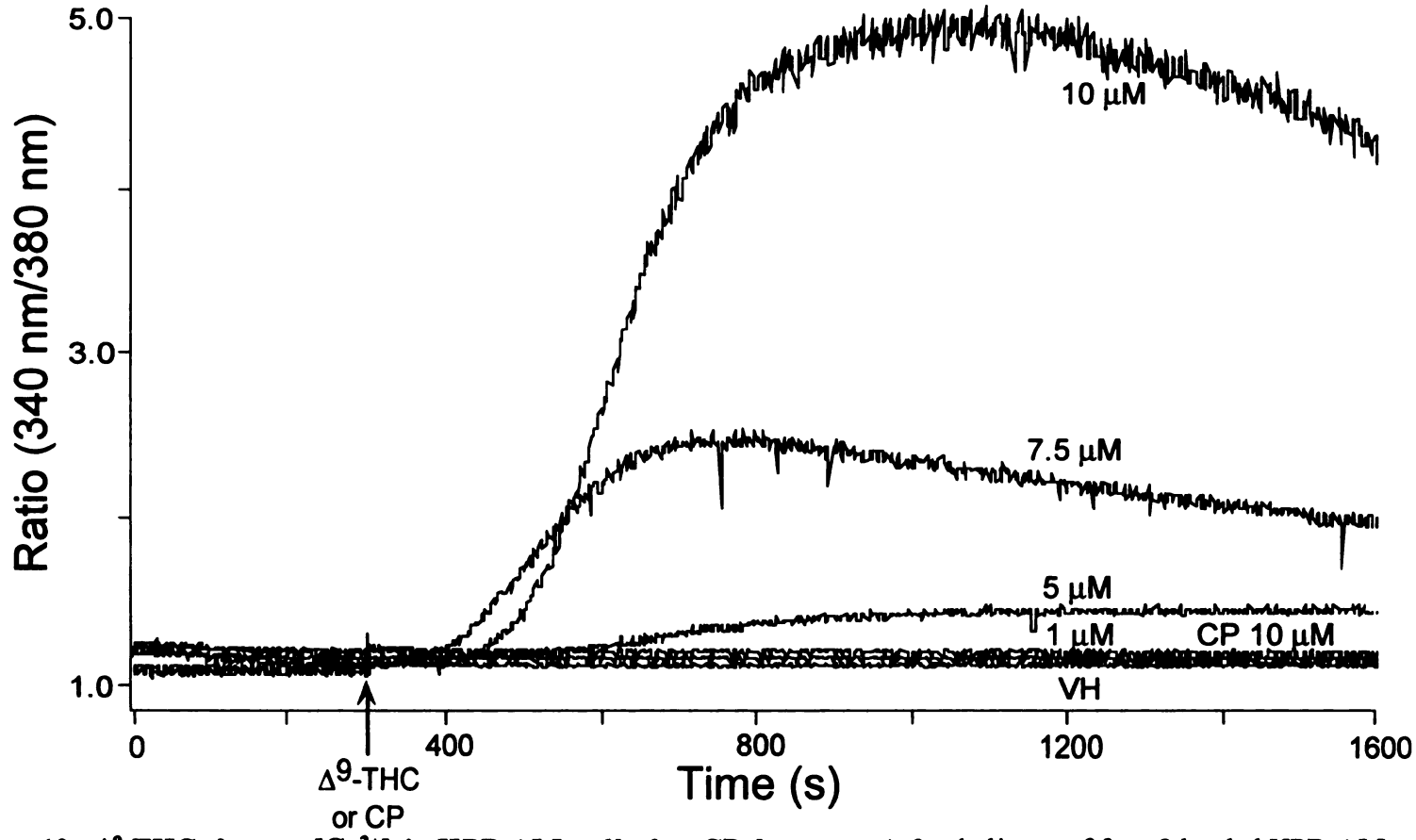

Figure 19. Δ^9-THC elevates $[Ca^{2+}]_i$ in HPB-ALL cells, but CP does not. A 3 ml aliquot of fura-2 loaded HPB-ALL cells was placed into a cuvette with constant stirring. At 300 s, various concentrations of Δ^9-THC, CP (10 μM), or VH (0.1% EtOH) was injected into the cuvette and the increase in $[Ca^{2+}]_i$ was measured for a total of 1600 s. $[Ca^{2+}]_i$ changes are presented as changes in the ratio of bound to free Ca^{2+} (340 nm/380 nm). The Ca^{2+} traces represent four independent experiments.

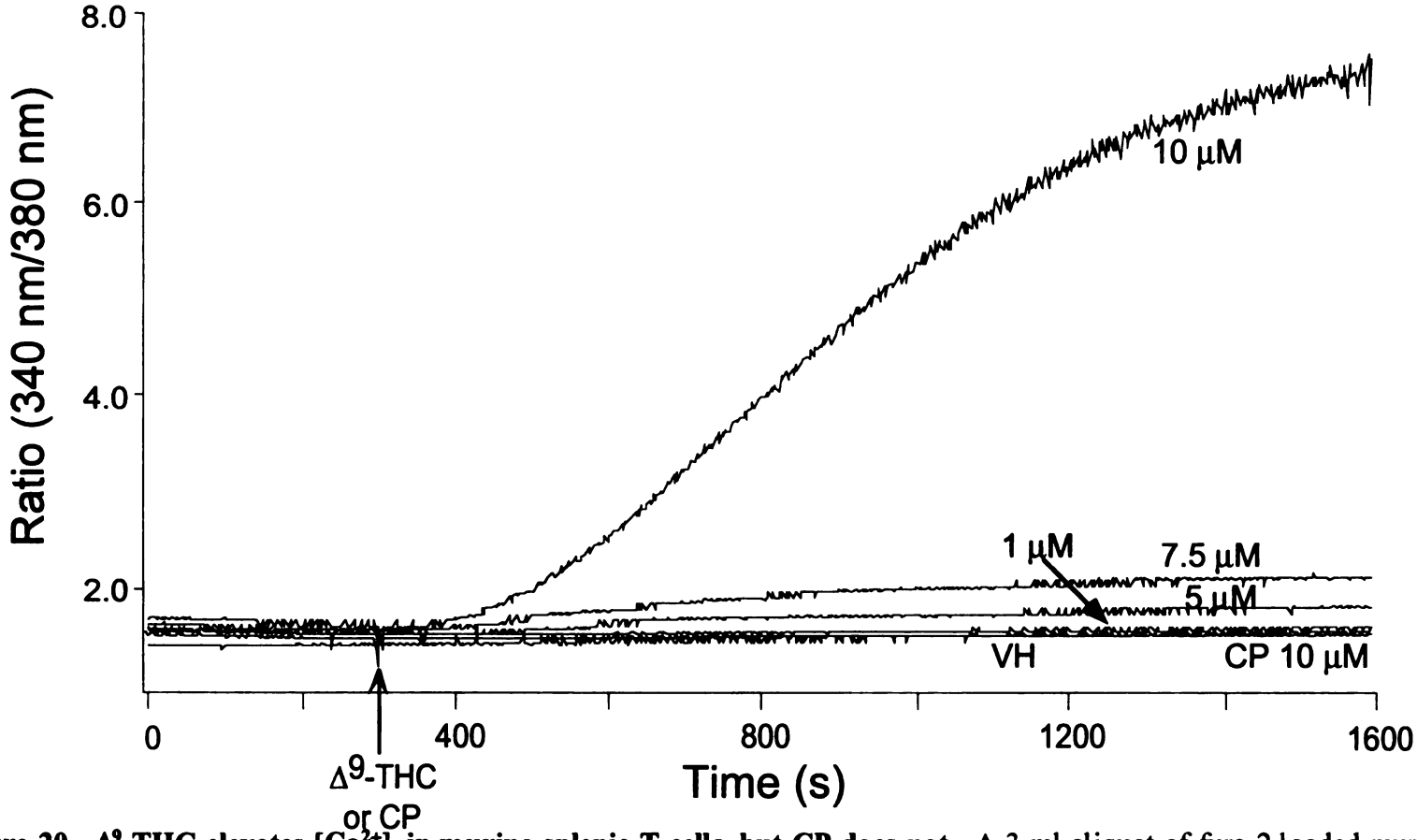

Figure 20. Δ^9-THC elevates $[Ca^{2+}]_i$ in murine splenic T cells, but CP does not. A 3 ml aliquot of fura-2 loaded murine splenic T cells was placed into a cuvette with constant stirring. At 300 s, various concentrations of Δ^9-THC, CP (10 μM), or VH (0.1% EtOH) was injected into the cuvette and the increase in $[Ca^{2+}]_i$ was measured for a total of 1600 s. $[Ca^{2+}]_i$ changes are presented as changes in the ratio of bound to free Ca^{2+} (340 nm/380 nm). The Ca^{2+} traces represent three independent experiments.

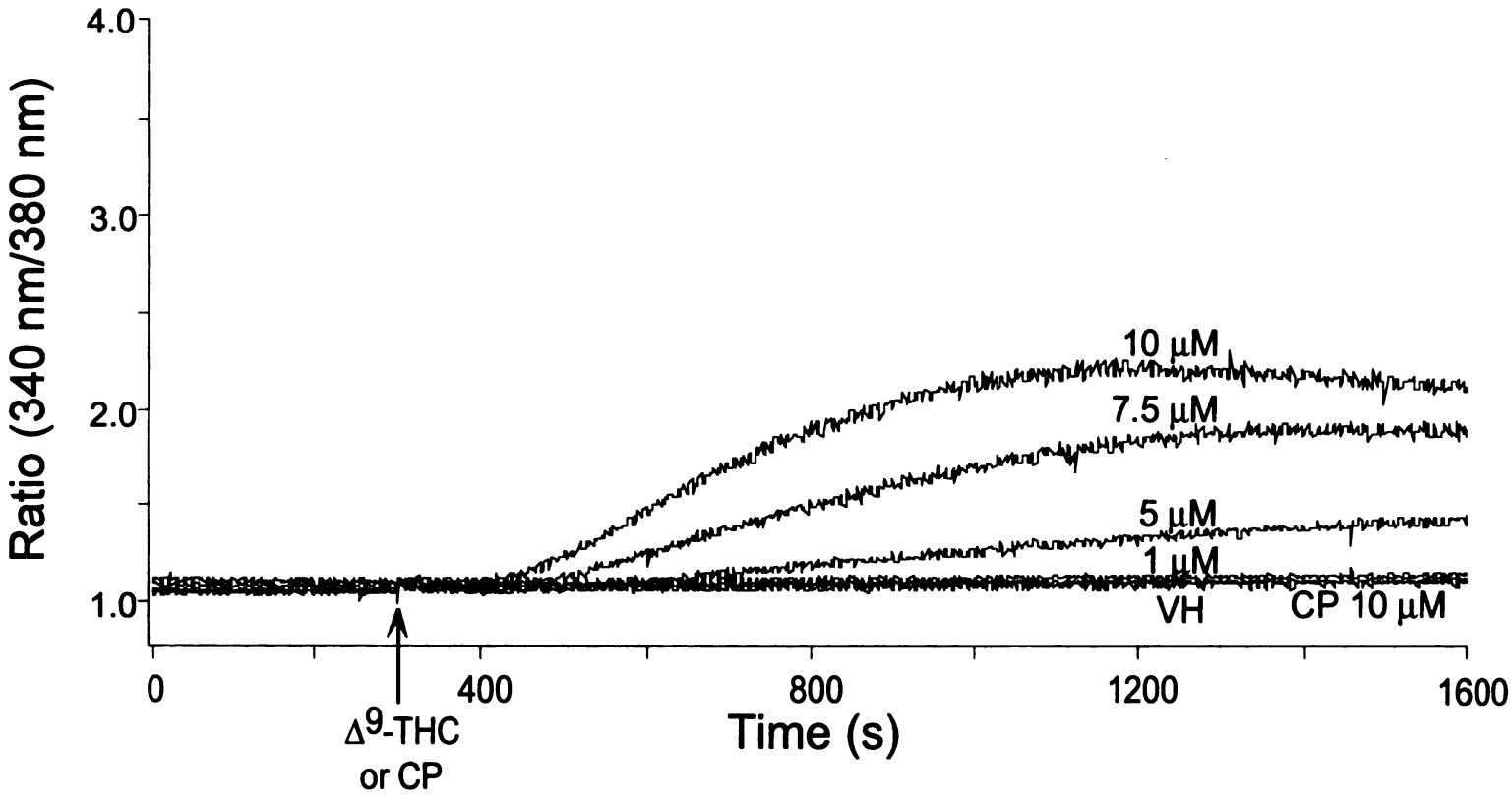

Figure 21. Δ^9-THC modestly elevates $[Ca^{2+}]_i$ in Jurkat E6-1 cells, but CP does not. A 3 ml aliquot of fura-2 loaded Jurkat E6-1 cells was placed into a cuvette with constant stirring. At 300 s, various concentrations of Δ^9-THC, CP (10 μM), or VH (0.1% EtOH) was injected into the cuvette and the increase in $[Ca^{2+}]_i$ was measured for a total of 1600 s. $[Ca^{2+}]_i$ changes are presented as changes in the ratio of bound to free Ca^{2+} (340 nm/380 nm). The Ca^{2+} traces represent three independent experiments.

affinity cannabinoid receptor agonist, CP, failed to induce a rise in $[Ca^{2+}]_i$ in all the models studied (figure 19, 20, 21).

In light of the observation that CP did not induce an elevation of $[Ca^{2+}]_i$, an additional series of experiments were performed in HPB-ALL cells to determine whether CP can block the effect of Δ^9-THC on $[Ca^{2+}]_i$ by acting as a neutral antagonist. HPB-ALL cells were pretreated with CP (1 μM) for 300 s followed by Δ^9-THC (10 μM). Interestingly, pretreatment of HPB-ALL cells with CP did not attenuate the increase in $[Ca^{2+}]_i$ elicited by Δ^9-THC (figure 22).

B. Removal of $[Ca^{2+}]_e$ and pretreatment with BAPTA-AM attenuate the rise in $[Ca^{2+}]_i$ elicited by Δ^9-THC

In order to determine whether the Δ^9-THC-mediated rise in $[Ca^{2+}]_i$ involved an influx of $[Ca^{2+}]_e$, $[Ca^{2+}]_i$ measurements were performed either in the presence or absence of $[Ca^{2+}]_e$ both in splenic T cells as well as in HPB-ALL cells. The results showed that absence of $[Ca^{2+}]_e$ severely attenuated (>90%; n=3) the Δ^9-THC-mediated $[Ca^{2+}]_i$ elevation, as compared to control conditions in the presence of $[Ca^{2+}]_e$ in both splenic T cells (figure 23) and HPB-ALL cells (figure 24). In the absence of $[Ca^{2+}]_e$, Δ^9-THC induced only a small and delayed rise in $[Ca^{2+}]_i$. To ascertain that stored Ca^{2+} from intracellular pools was not involved in the Δ^9-THC-mediated rise in $[Ca^{2+}]_i$, HPB-ALL cells were preloaded with BAPTA-AM (10 μM) to chelate all $[Ca^{2+}]_i$ for 30 min alongside fura-2. Pretreatment with BAPTA-AM failed to abrogate completely the rise in $[Ca^{2+}]_i$ elicited by Δ^9-THC, and induced a significantly smaller elevation in $[Ca^{2+}]_i$

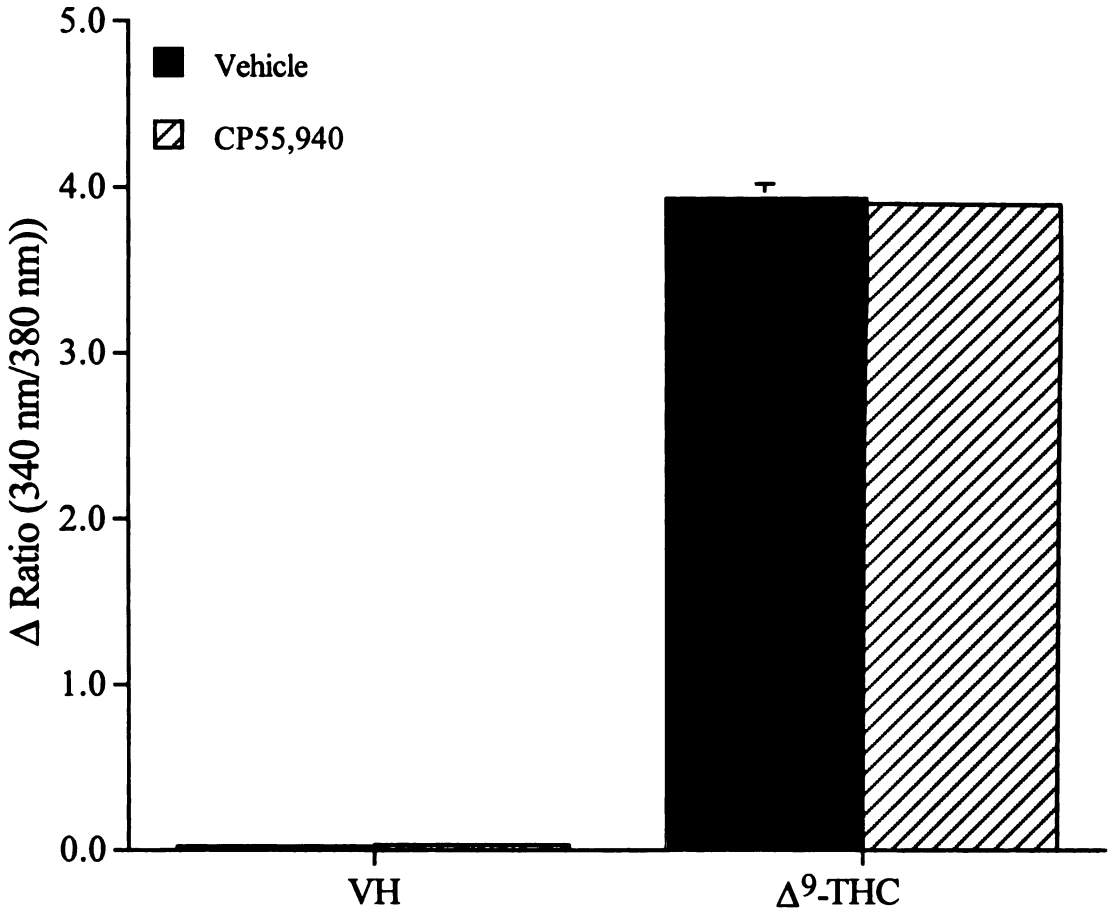

Figure 22. CP does not antagonize the elevation of $[Ca^{2+}]_i$ elicited by Δ^9-THC in HPB-ALL cells. A 3 ml aliquot of fura-2 loaded HPB-ALL cells was placed into a cuvette with constant stirring. CP (1 μM) or VH (0.1% EtOH) was added directly to the cuvette just prior to beginning $[Ca^{2+}]_i$ measurements. At 300 s, Δ^9-THC (10 μM) or VH (0.1% EtOH) was injected into the cuvette and the increase in $[Ca^{2+}]_i$ was measured for a total of 1600 s. $[Ca^{2+}]_i$ changes are presented as the mean ± SEM of the change in base to peak ratio of bound to free Ca^{2+} (340 nm/380 nm) of three independent experiments.

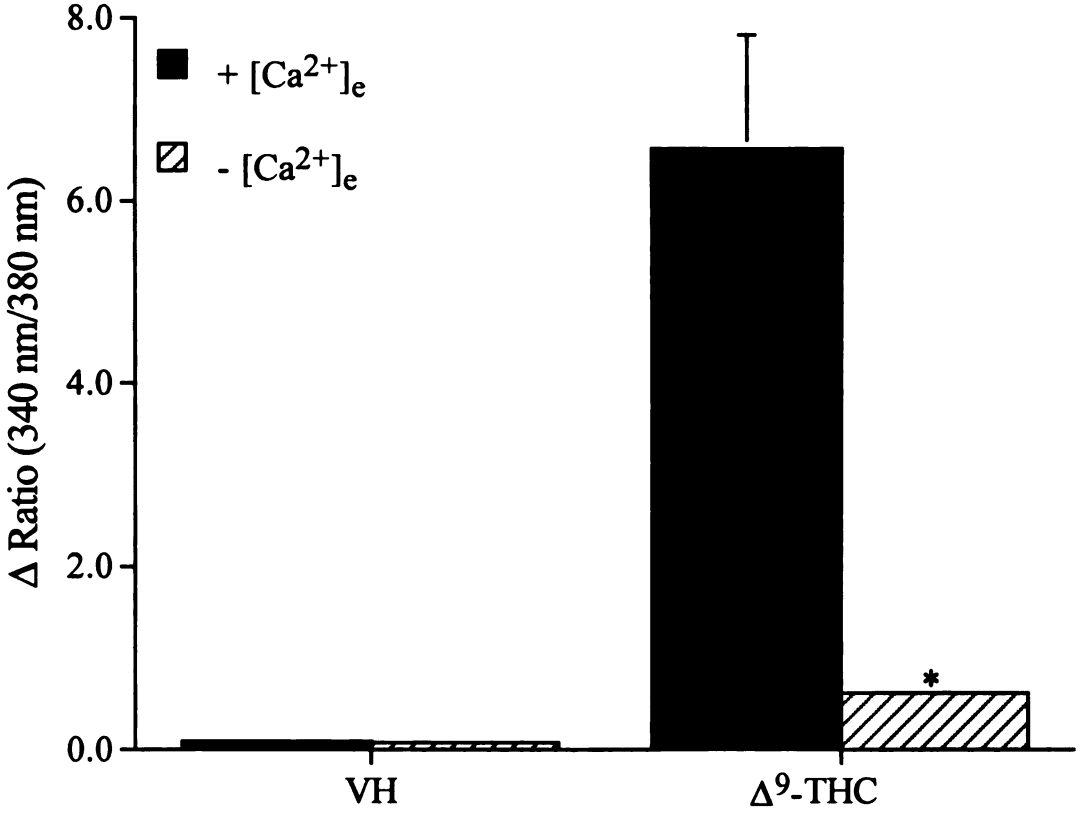

Figure 23. Removal of $[Ca^{2+}]_e$ severely abrogates the elevation of $[Ca^{2+}]_i$ elicited by Δ^9-THC in murine splenic T cells. A 3 ml aliquot of fura-2 loaded murine splenic T cells was resuspended in either Ca^{2+}-KREB or Ca^{2+}-free KREB buffer just prior to beginning $[Ca^{2+}]_i$ measurements. At 300 s, Δ^9-THC (10 μM) or VH (0.1% EtOH) was injected into the cuvette and the increase in $[Ca^{2+}]_i$ was measured for a total of 1600 s. Results are presented as mean change ± SEM in the 340 nm/380 nm fluorescence ratio of $[Ca^{2+}]_i$ from base to peak of three independent experiments. * $p < 0.05$ as compared to Δ^9-THC (+$[Ca^{2+}]_e$) group.

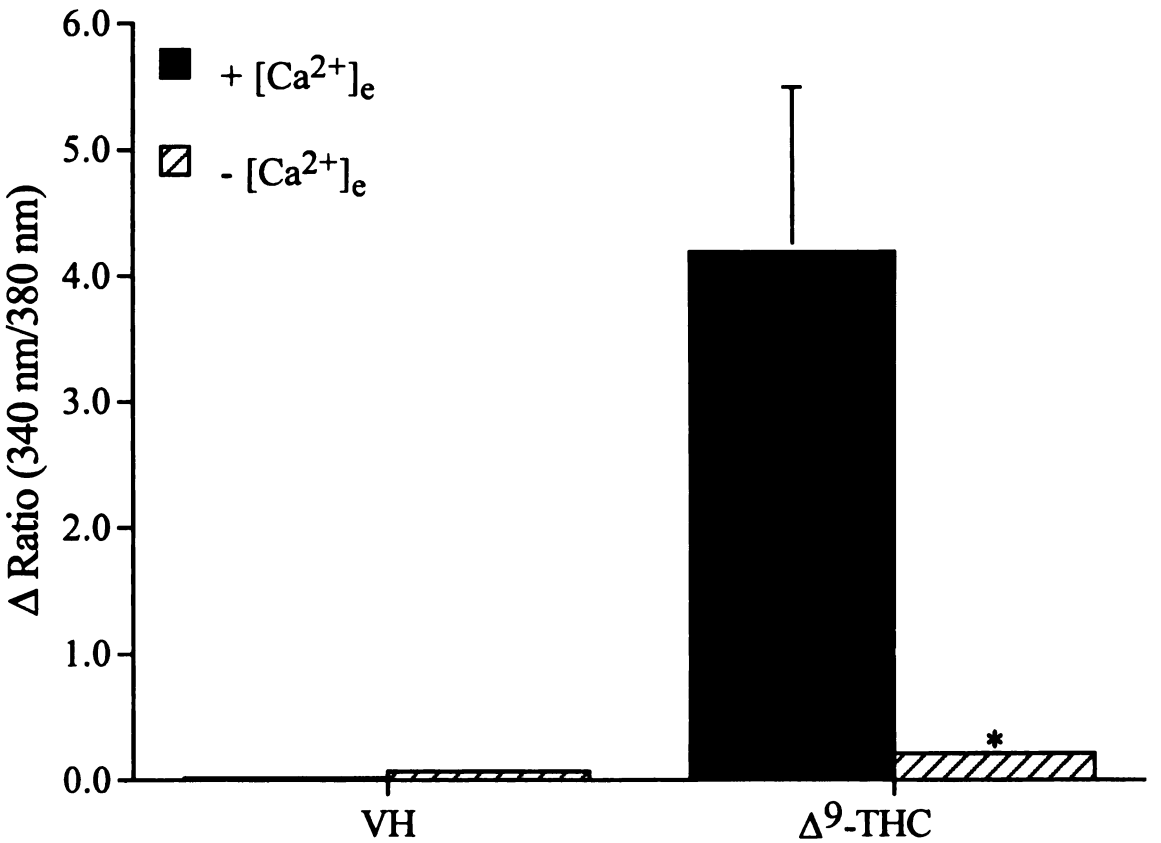

Figure 24. Removal of $[Ca^{2+}]_e$ severely abrogates the elevation of $[Ca^{2+}]_i$ elicited by Δ^9-THC in HPB-ALL cells. A 3 ml aliquot of fura-2 loaded HPB-ALL cells was resuspended in either Ca^{2+}-KREB or Ca^{2+}-free KREB buffer just prior to beginning $[Ca^{2+}]_i$ measurements. At 300 s, Δ^9-THC (10 μM) or VH (0.1% EtOH) was injected into the cuvette and the increase in $[Ca^{2+}]_i$ was measured for a total of 1600 s. Results are presented as mean change ± SEM in the 340 nm/380 nm fluorescence ratio of $[Ca^{2+}]_i$ from base to peak of three independent experiments. * $p < 0.05$ as compared to Δ^9-THC ($+[Ca^{2+}]_e$) group.

(figure 25). The significantly smaller elevation in $[Ca^{2+}]_i$ is attributed to the partial buffering of the influx of $[Ca^{2+}]_e$ by BAPTA-AM present in the cytosol.

C. Cannabinoid receptor antagonists attenuate the Δ^9-THC-mediated rise in $[Ca^{2+}]_i$

The role of the cannabinoid receptors in the Δ^9-THC-mediated elevation in $[Ca^{2+}]_i$ was examined with the use of SR1 and SR2. In light of previous findings showing that both CB1 and CB2 receptor transcripts are expressed in murine splenocytes (Jan et al., 2002; Schatz et al., 1997), SR1 and SR2 were used either individually or in combination in studies with splenic T cells. The antagonists by themselves had no effect on $[Ca^{2+}]_i$. However, pretreatment of splenic T cells with SR1 and SR2 (1.0 or 5.0 μM of each), either individually or in combination, for 300 s, followed by Δ^9-THC (10 μM) treatment showed a marked attenuation of Δ^9-THC-mediated rise in $[Ca^{2+}]_i$ (figure 26). Interestingly, the magnitude of the attenuation in the Δ^9-THC-mediated $[Ca^{2+}]_i$ rise by SR1 and SR2, individually, was almost as great as when used in combination. Similarly, pretreatment of HPB-ALL cells with SR1 or SR2 (0.1-5.0 μM) also caused a marked inhibition of the rise in $[Ca^{2+}]_i$ by Δ^9-THC (figure 27). The effect of both antagonists was concentration responsive, but SR2 was slightly more efficacious at inhibiting the Δ^9-THC-mediated rise in $[Ca^{2+}]_i$ than was SR1. By contrast, the modest rise in $[Ca^{2+}]_i$ elicited by Δ^9-THC in the Jurkat E6-1 cells was not significantly inhibited by either SR1 or SR2 (1.0 – 5.0 μM; figure 28).

To ensure that the cannabinoid receptor antagonists did not attenuate $[Ca^{2+}]_i$

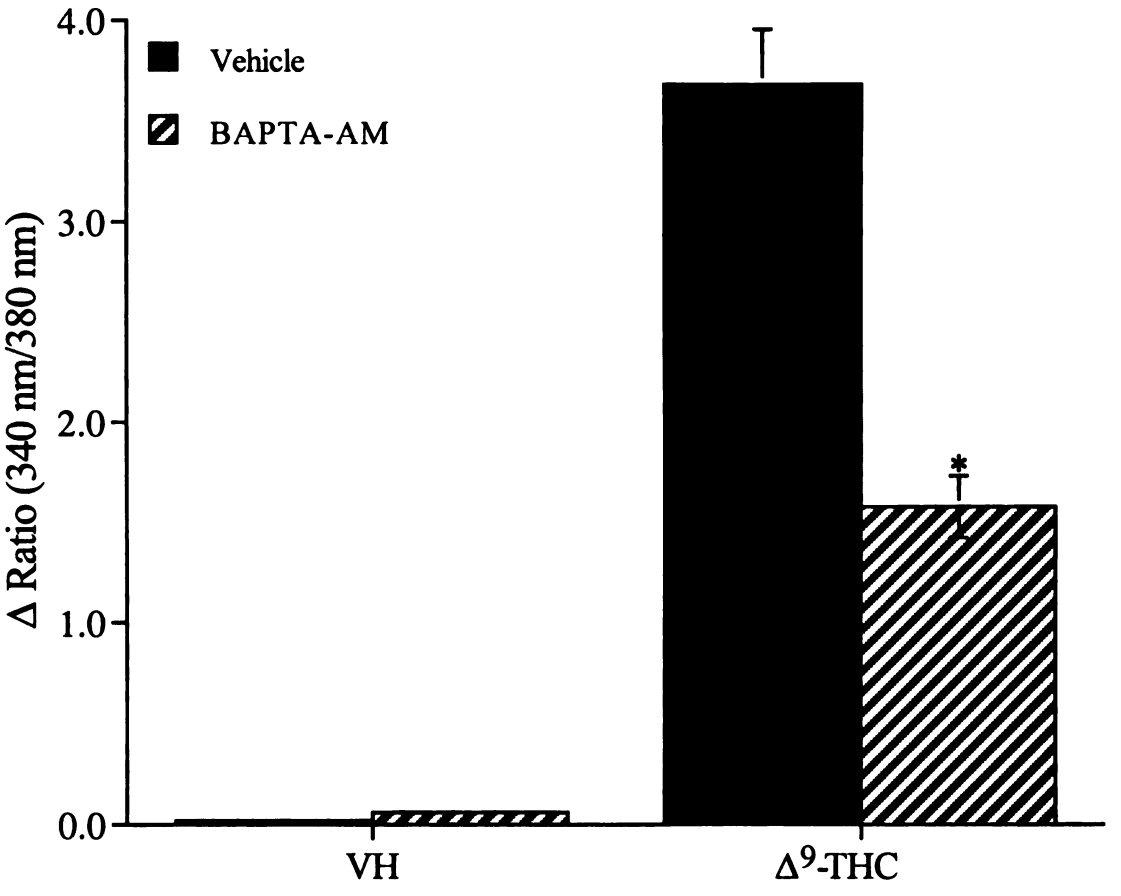

Figure 25. Pretreatment with BAPTA-AM attenuates the elevation of $[Ca^{2+}]_i$ elicited by Δ^9-THC in HPB-ALL cells. HPB-ALL cells were coloaded with fura-2 only, or a combination of fura-2 and BAPTA-AM (10 μM). A 3 ml aliquot of fura-2 and/or BAPTA-AM loaded HPB-ALL cells was resuspended in Ca^{2+}-KREB and treated with Δ^9-THC (10 μM) or VH (0.1% EtOH) at 300 s, and the increase in $[Ca^{2+}]_i$ was measured for a total of 1600 s. Results are presented as mean change ± SEM in the 340 nm/380 nm fluorescence ratio of $[Ca^{2+}]_i$ from base to peak of three independent experiments. * $p <$ 0.05 as compared to VH/Δ^9-THC group.

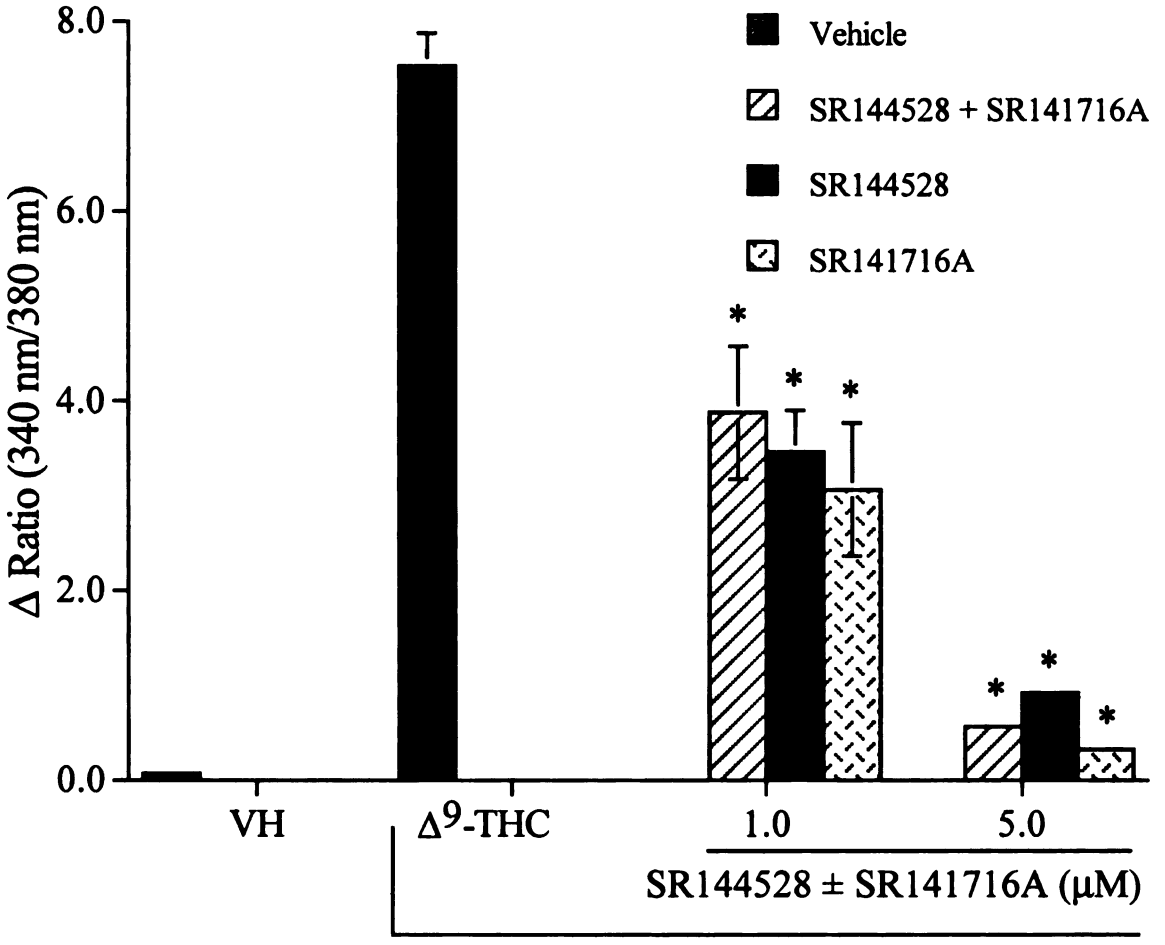

Figure 26. SR1 and SR2 antagonize the Δ^9-THC-mediated elevation in $[Ca^{2+}]_i$ in murine splenic T cells. A 3 ml aliquot of fura-2 loaded murine splenic T cells was placed into a cuvette with constant stirring. SR2 (1-5 μM), SR1 (1-5 μM) and/or VH (0.1% DMSO) were added directly to the cuvette just prior to beginning $[Ca^{2+}]_i$ measurements. At 300 s, Δ^9-THC (10 μM) or VH (0.1% EtOH) was injected into the cuvette and the increase in $[Ca^{2+}]_i$ was measured for a total of 1600 s. $[Ca^{2+}]_i$ changes are presented as the mean ± SEM of the change in base to peak ratio of bound to free Ca^{2+} (340 nm/380 nm) of three independent experiments. * $p < 0.05$ as compared to VH/Δ^9-THC group.

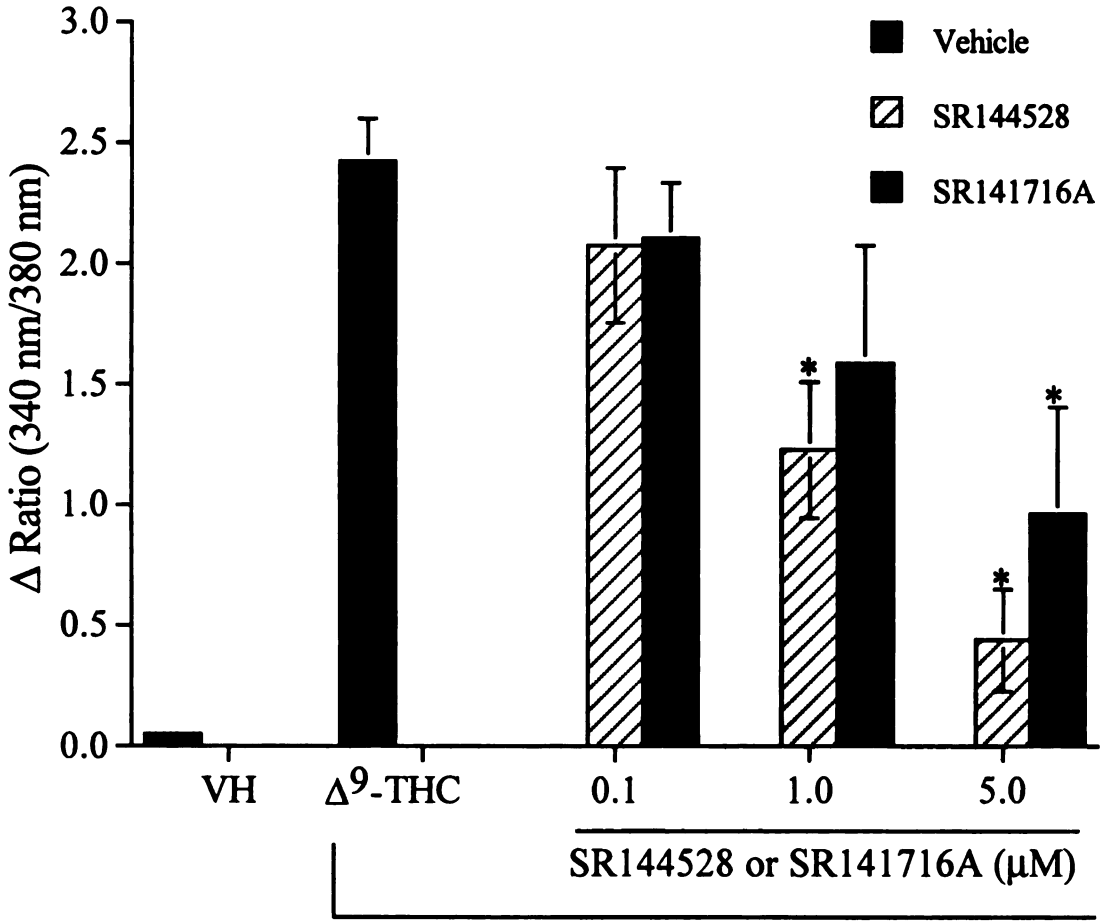

Figure 27. SR1 and SR2 antagonize the Δ^9-THC-mediated elevation in $[Ca^{2+}]_i$ in HPB-ALL cells. A 3 ml aliquot of fura-2 loaded HPB-ALL cells was placed into a cuvette with constant stirring. SR2 (0.1-5.0 μM), SR1 (0.1-5.0 μM) and/or VH (0.1% DMSO) was added directly to the cuvette just prior to beginning $[Ca^{2+}]_i$ measurements. At 300 s, Δ^9-THC (10 μM) or VH (0.1% EtOH) was injected into the cuvette and the increase in $[Ca^{2+}]_i$ was measured for a total of 1600 s. $[Ca^{2+}]_i$ changes are presented as the mean ± SEM of the change in base to peak ratio of bound to free Ca^{2+} (340 nm/380 nm) of three independent experiments. * $p < 0.05$ as compared to VH/Δ^9-THC group.

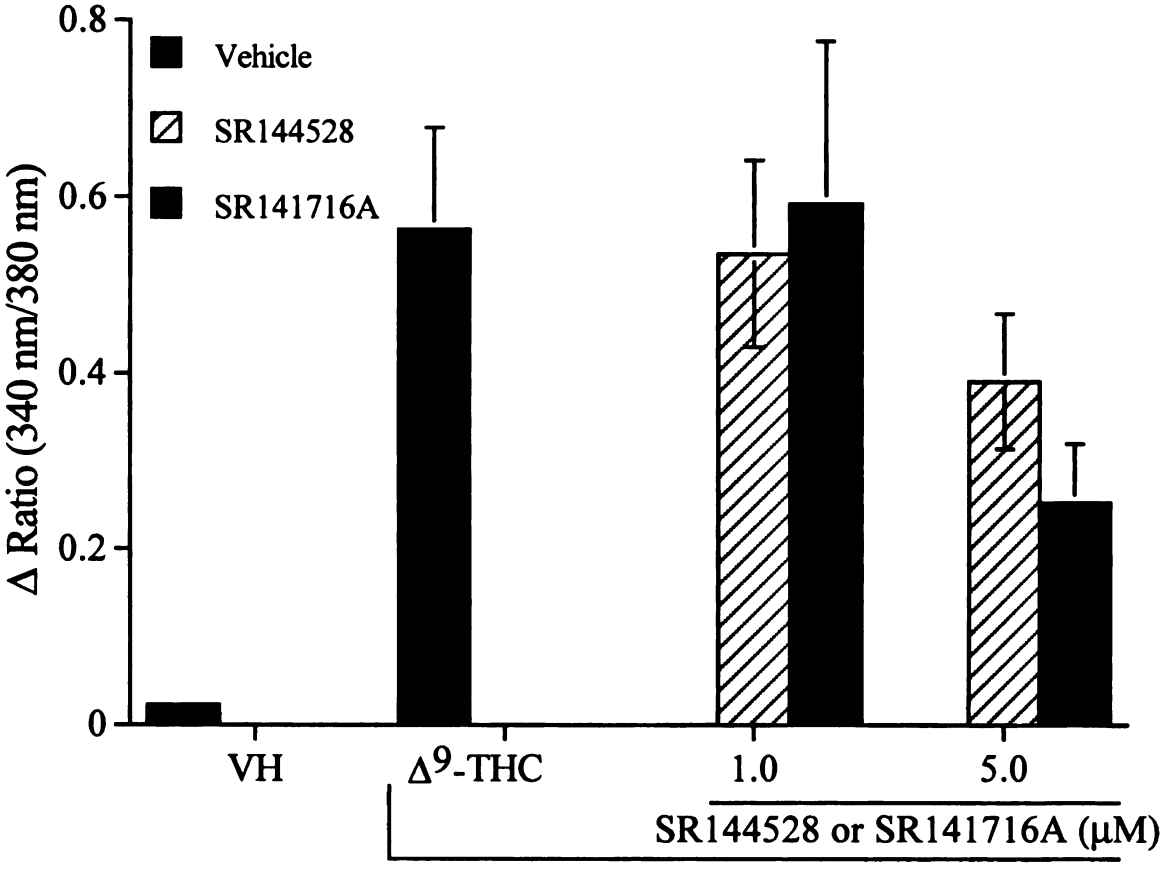

Figure 28. SR1 and SR2 do not antagonize the Δ^9-THC-mediated elevation in $[Ca^{2+}]_i$ in Jurkat E6-1 cells. A 3 ml aliquot of fura-2 loaded Jurkat E6-1 cells was placed into a cuvette with constant stirring. SR2 (1.0-5.0 μM), SR1 (1.0-5.0 μM) and/or VH (0.1% DMSO) was added directly to the cuvette just prior to beginning $[Ca^{2+}]_i$ measurements. At 300 s, Δ^9-THC (10 μM) or VH (0.1% EtOH) was injected into the cuvette and the increase in $[Ca^{2+}]_i$ was measured for a total of 1600 s. $[Ca^{2+}]_i$ changes are presented as the mean ± SEM of the change in base to peak ratio of bound to free Ca^{2+} (340 nm/380 nm) of three independent experiments.

responses by acting as Ca^{2+} channel blockers, $[Ca^{2+}]_i$ measurements were performed in HPB-ALL cells treated with SR1 or SR2 (1.0-5.0 μM) for 300 s followed by treatment with TG (1 μM). Under control conditions, TG induced a rapid elevation in $[Ca^{2+}]_i$ (348 ± 53 nM, n=3), which was significantly reduced in magnitude in the absence of $[Ca^{2+}]_e$, demonstrating that the elevation of $[Ca^{2+}]_i$ by TG was largely due to the influx of $[Ca^{2+}]_e$ (data not shown). Pretreatment of cells with either SR1 or SR2 did not attenuate the TG-induced elevation of $[Ca^{2+}]_i$ indicating that the cannabinoid receptor antagonists do not non-specifically block $[Ca^{2+}]_e$ influx through Ca^{2+} channels (data not shown).

Finally, $[Ca^{2+}]_i$ measurements were also performed in HPB-ALL cells with SR2 in the absence of $[Ca^{2+}]_e$ to investigate whether the small and modest rise in $[Ca^{2+}]_i$ elicited by Δ^9-THC was attributable to a CB2 receptor-dependent mechanism. HPB-ALL cells were pretreated with SR2 (5 μM) for 300 s followed by Δ^9-THC (10 μM) in the absence of $[Ca^{2+}]_e$. Interestingly, pretreatment with SR2 completely and significantly attenuated the small rise in $[Ca^{2+}]_i$ elicited by Δ^9-THC in the absence of $[Ca^{2+}]_e$ (figure 29).

D. PTx does not attenuate the Δ^9-THC-mediated rise in $[Ca^{2+}]_i$

Both CB1 and CB2 receptors belong to the G protein-coupled receptor superfamily and have been demonstrated to couple to the PTx-sensitive G proteins, $G\alpha_i/G\alpha_o$ (Bouaboula et al., 1999; Glass and Northup, 1999). To investigate whether the Δ^9-THC-mediated increase in $[Ca^{2+}]_i$ occurred in a $G\alpha_i/G\alpha_o$-dependent manner, HPB-ALL cells were preincubated with PTx (100 ng/ml) or VH for 18 h to allow for a full ADP-ribosylation. Subsequently, cells were used for $[Ca^{2+}]_i$ measurements with Δ^9-THC

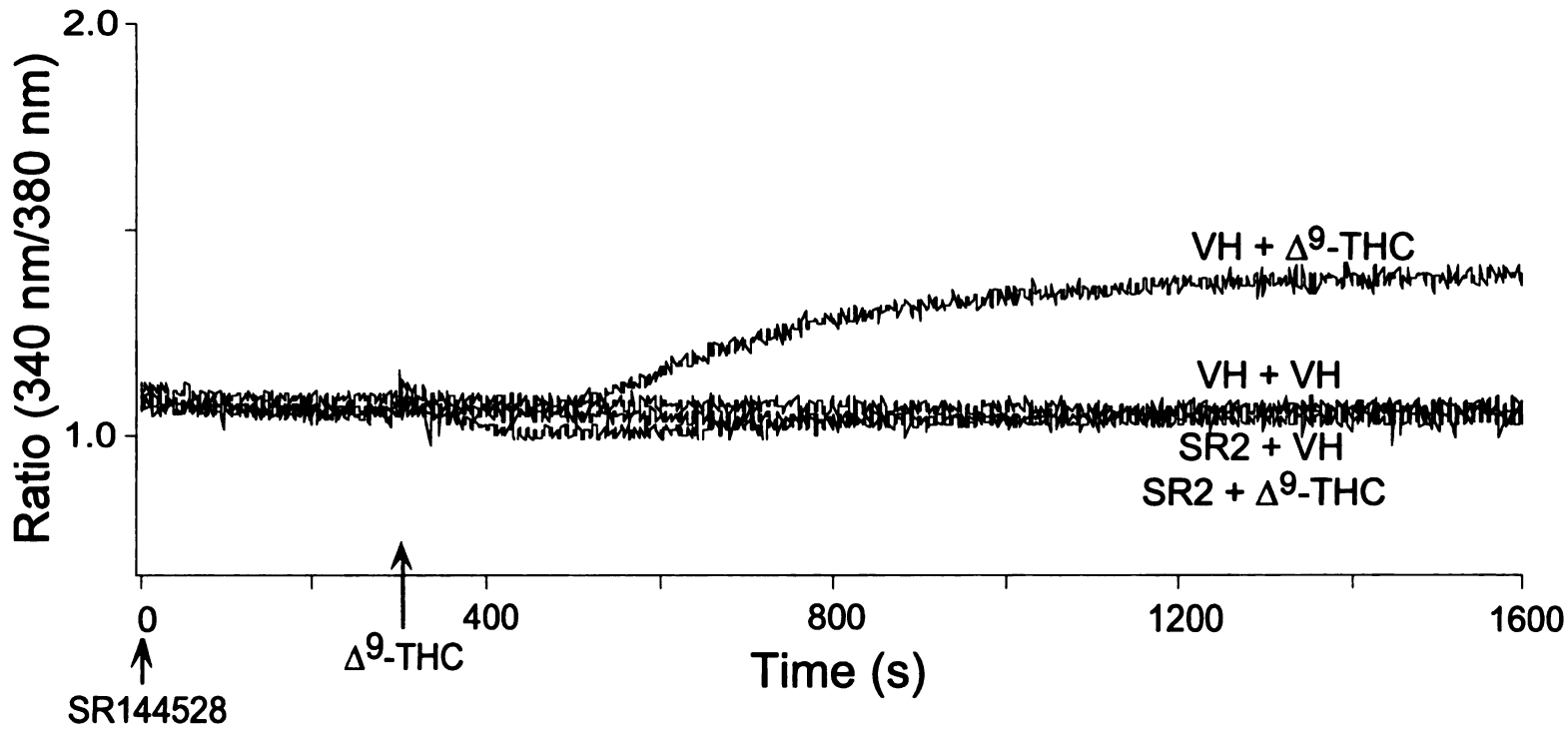

Figure 29. SR2 antagonizes the modest elevation in $[Ca^{2+}]_i$ elicited by Δ^9-THC in the absence of $[Ca^{2+}]_e$ in HPB-ALL cells. A 3 ml aliquot of fura-2 loaded HPB-ALL cells was resuspended in Ca^{2+}-free KREB buffer just prior to beginning $[Ca^{2+}]_i$ measurements and treated with either SR2 (5 μM) or VH (0.1% DMSO). At 300 s, Δ^9-THC (10 μM) or VH (0.1% EtOH) was injected into the cuvette and the increase in $[Ca^{2+}]_i$ was measured for a total of 1600 s. $[Ca^{2+}]_i$ changes are presented as changes in the ratio of bound to free Ca^{2+} (340 nm/380 nm). The Ca^{2+} traces represent two independent experiments.

(10 μM). Preincubation with PTx, however, did not attenuate the Δ^9-THC-mediated increase in $[Ca^{2+}]_i$ (figure 30).

E. HU-210 and CBN elevate $[Ca^{2+}]_i$

Given the observation that the tricyclic classical cannabinoid, Δ^9-THC, robustly elevated $[Ca^{2+}]_i$ in T cells, but the bicyclic cannabinoid CP did not, the effect of classical tricyclic cannabinoids, HU-210 and CBN, were also investigated on $[Ca^{2+}]_i$ in the HPB-ALL cells. Both HU-210 and CBN elicited a robust and concentration-responsive elevation of $[Ca^{2+}]_i$ in the HPB-ALL cells, with substantial elevation of $[Ca^{2+}]_i$ at concentrations greater than 10 μM (figure 31, 32). However, compared to Δ^9-THC, the magnitude of $[Ca^{2+}]_i$ elevation by both HU-210 and CBN at all concentrations (1-20 μM) was modest (figure 31, 32). At a concentration of 20 μM, HU210 elicited a $[Ca^{2+}]_i$ rise of 200.3 ± 13.9 nM (n=3), and CBN elicited a $[Ca^{2+}]_i$ rise of 185.5 ± 50.4 nM (n=4). Interestingly, the $[Ca^{2+}]_i$ rise elicited by all three classical tricyclic cannabinoid compounds followed a significant time delay after injection of the cannabinoid into the cuvette. The time delay to onset of $[Ca^{2+}]_i$ elevation varied depending on concentration and the cannabinoid employed. At a concentration of 20 μM, the time to onset of $[Ca^{2+}]_i$ elevation by CBN was 195.2 ± 8.0 s (n=5), whereas the time to onset of $[Ca^{2+}]_i$ elevation by HU-210 was at 342.1 ± 7.6 s (n=5). By contrast, at a lower concentration, Δ^9-THC (12.5 μM) time to onset of $[Ca^{2+}]_i$ elevation was only 123.7 ± 4.0 s (n=8). It is intriguing to note that the time delay to onset of $[Ca^{2+}]_i$ elevation by CBN (20 μM) and Δ^9-THC (12.5 μM) were similar, while HU-210 (20 μM) took significantly longer to induce an $[Ca^{2+}]_i$ rise.

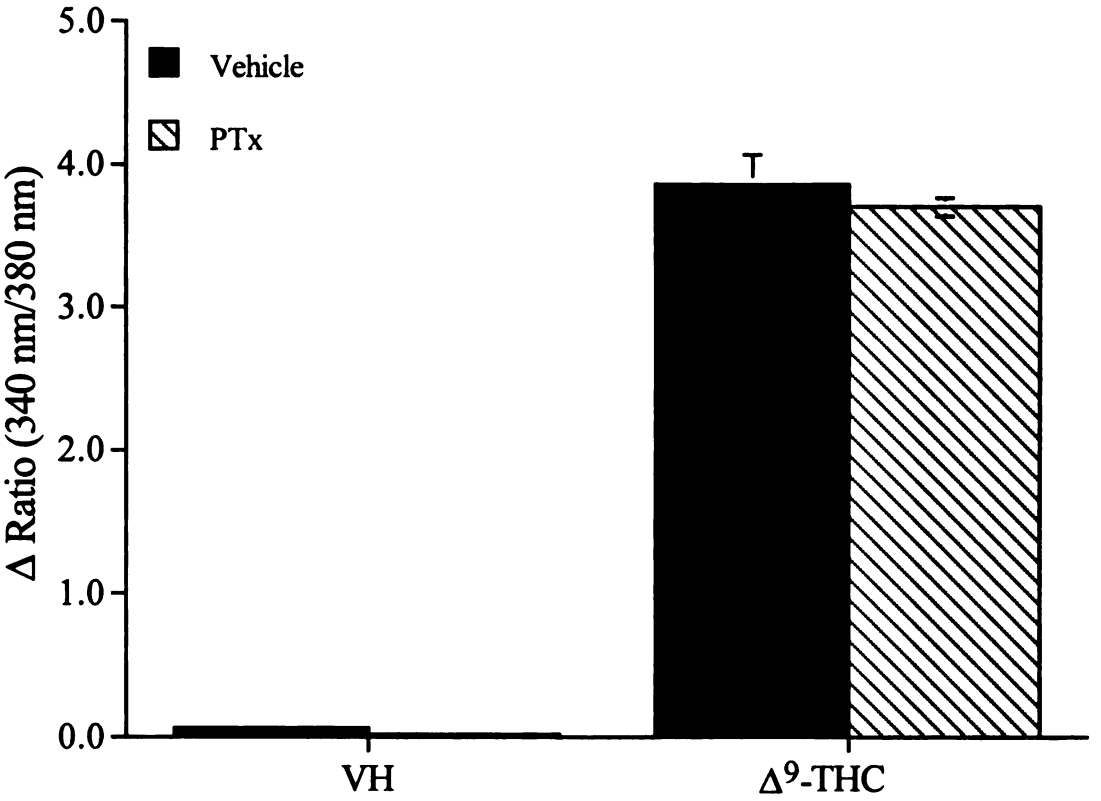

Figure 30. PTx does not attenuate the elevation in $[Ca^{2+}]_i$ elicited by Δ^9-THC in HPB-ALL cells. HPB-ALL cells were preincubated with PTx (100 ng/ml) or VH (PBS) for 18 h, then washed and loaded with fura-2. A 3 ml aliquot of fura-2 loaded HPB-ALL cells was resuspended in Ca^{2+}-KREB and treated with Δ^9-THC (10 μM) or VH (0.1% EtOH) at 300 s, and the increase in $[Ca^{2+}]_i$ was measured for a total of 1600 s. Results are presented as mean change ± SEM in the 340 nm/380 nm fluorescence ratio of $[Ca^{2+}]_i$ from base to peak of two independent experiments.

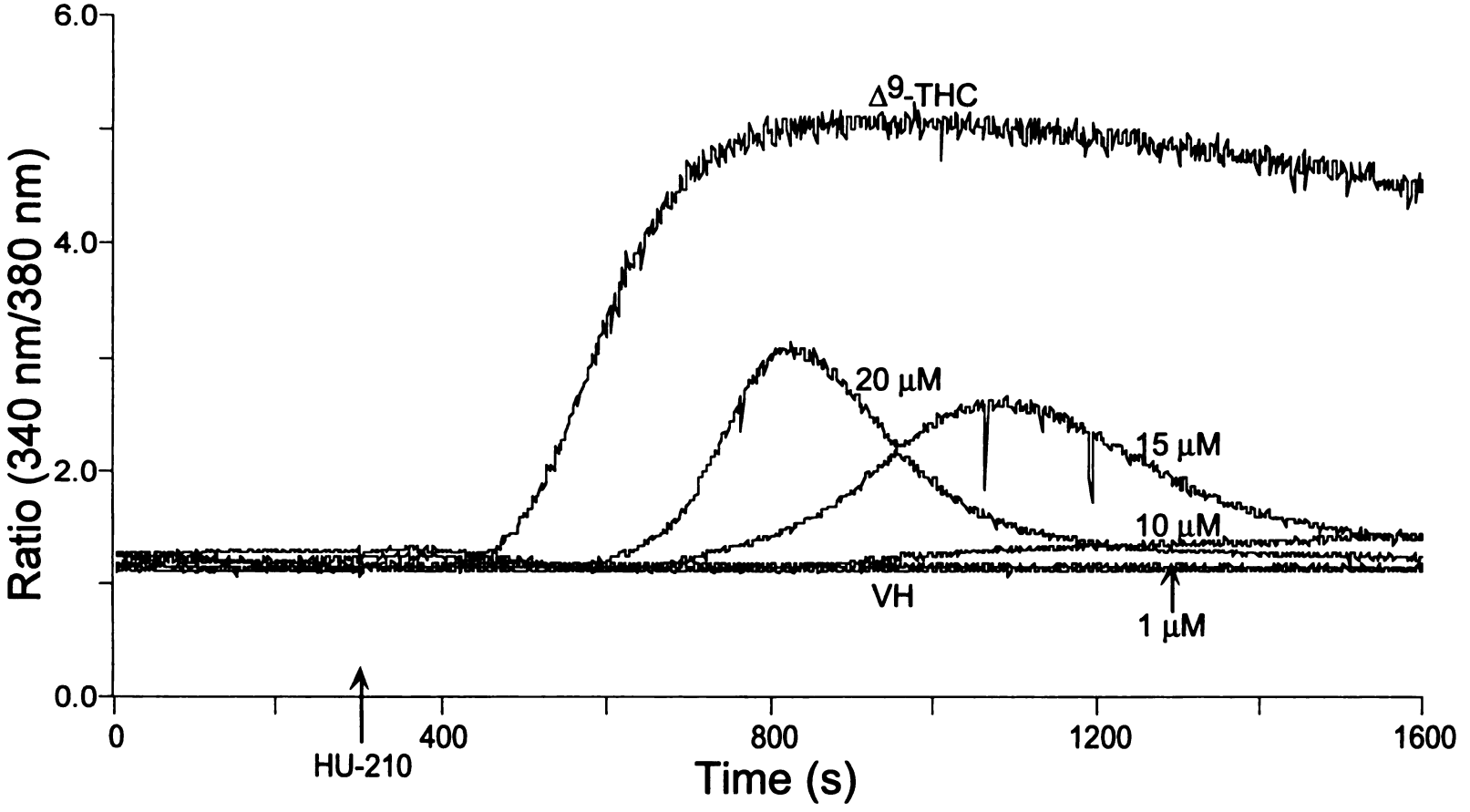

Figure 31. HU-210 elevates $[Ca^{2+}]_i$ in HPB-ALL cells. A 3 ml aliquot of fura-2 loaded HPB-ALL cells was placed into a cuvette with constant stirring. At 300 s, various concentrations of HU-210 (1-20 μM), Δ^9-THC (12.5 μM), or VH (0.1% EtOH) was injected into the cuvette and the increase in $[Ca^{2+}]_i$ was measured for a total of 1600 s. $[Ca^{2+}]_i$ changes are presented as changes in the ratio of bound to free Ca^{2+} (340 nm/380 nm). The Ca^{2+} traces represent four independent experiments.

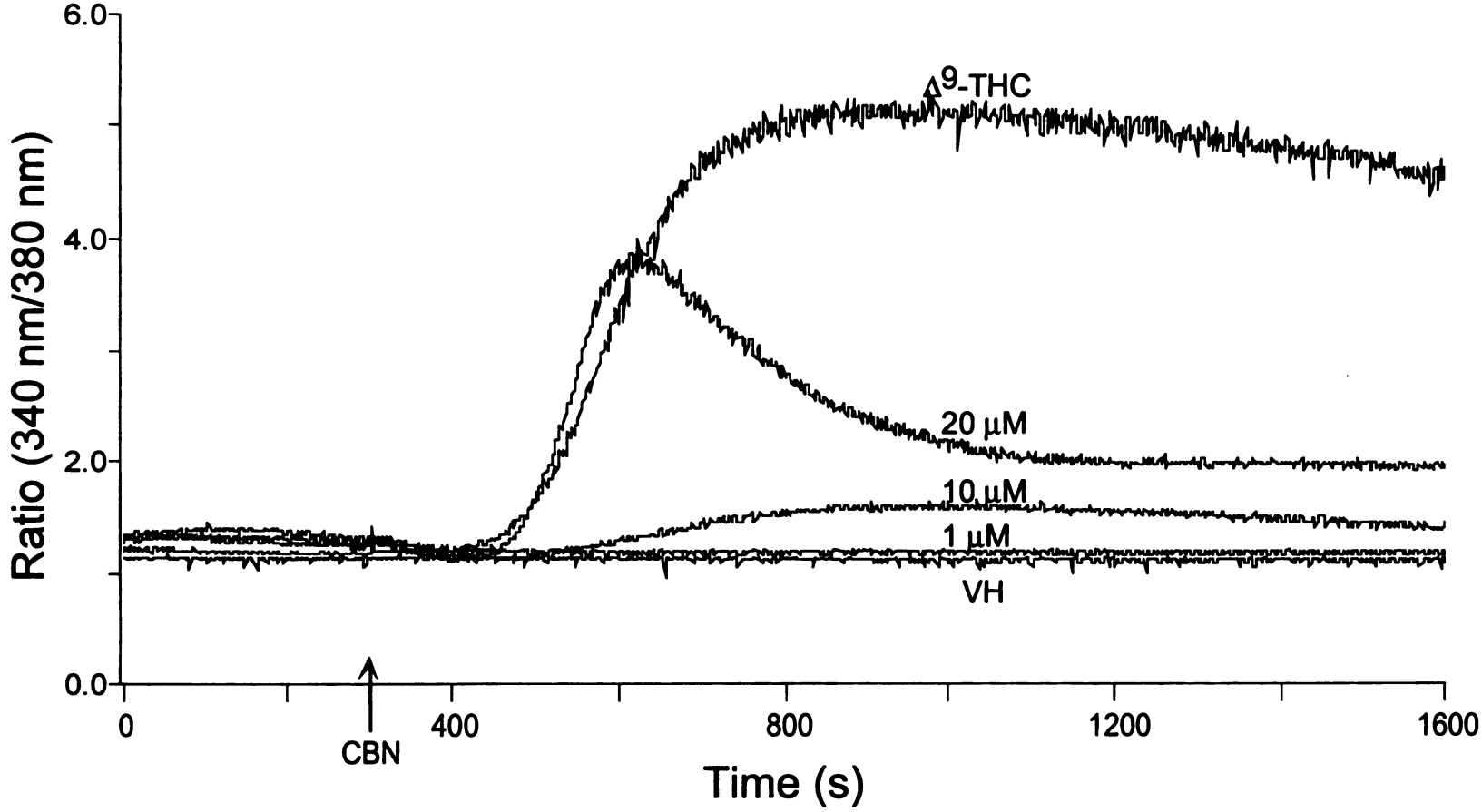

Figure 32. CBN elevates $[Ca^{2+}]_i$ in HPB-ALL cells. A 3 ml aliquot of fura-2 loaded HPB-ALL cells was placed into a cuvette with constant stirring. At 300 s, various concentrations of CBN (1-20 μM), Δ^9-THC (12.5 μM), or VH (0.1% EtOH) was injected into the cuvette and the increase in $[Ca^{2+}]_i$ was measured for a total of 1600 s. $[Ca^{2+}]_i$ changes are presented as changes in the ratio of bound to free Ca^{2+} (340 nm/380 nm). The Ca^{2+} traces represent three independent experiments.

F. Removal of $[Ca^{2+}]_e$ attenuates the rise in $[Ca^{2+}]_i$ elicited by HU-210 and CBN

The effect of both HU-210 and CBN on $[Ca^{2+}]_i$ elevation was further characterized by performing $[Ca^{2+}]_i$ measurements either in the presence or absence of $[Ca^{2+}]_e$. Analogous to the above observation for Δ^9-THC, the absence of $[Ca^{2+}]_e$ severely attenuated the elevation of $[Ca^{2+}]_i$ by both CBN and HU-210 (figure 33). Compared to the control experiment in the presence of $[Ca^{2+}]_e$, removal of $[Ca^{2+}]_e$ attenuated the magnitude of the rise in $[Ca^{2+}]_i$ elicited by CBN and HU-210 by 85–88 % (n=3). Also in the absence of $[Ca^{2+}]_e$, both compounds elicited a very small and slow increase in $[Ca^{2+}]_i$.

G. Cannabinoid receptor antagonists attenuate the HU-210- and CBN-mediated rise in $[Ca^{2+}]_i$

To address further the mechanism by which HU-210 and CBN elicited the rise in $[Ca^{2+}]_i$, HPB-ALL cells were pretreated with the SR1 or SR2 (1-5 μM), for 300 seconds prior to addition of cannabinoids. Pretreatment with either SR1 or SR2 produced a concentration-responsive attenuation of both the HU-210- as well as the CBN-mediated rise in $[Ca^{2+}]_i$ (figure 34). It was interesting to note that both antagonists were differentially sensitive at attenuating the elevation in $[Ca^{2+}]_i$ elicited by HU-210 and CBN. Compared to VH control, SR2 (5 μM) attenuated the $[Ca^{2+}]_i$ rise elicited by CBN by 71.9 ± 2.3% (n=3), whereas at the same concentration, SR2 attenuated the HU-210-mediated $[Ca^{2+}]_i$ rise by only 29.1 ± 6.9% (n=4). Similarly, compared to VH control, SR1 (5 μM) attenuated the $[Ca^{2+}]_i$ rise elicited by CBN by 70.9 ± 3.4 % (n=3), whereas at

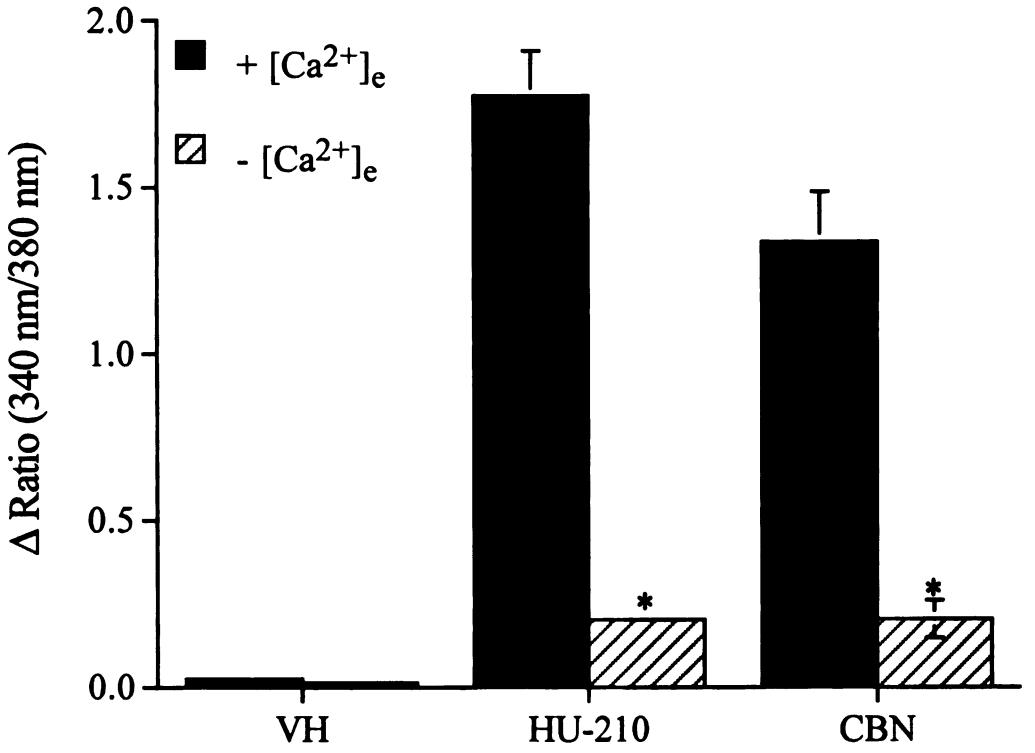

Figure 33. Removal of $[Ca^{2+}]_e$ severely abrogates the elevation of $[Ca^{2+}]_i$ elicited by HU-210 and CBN in HPB-ALL cells. A 3 ml aliquot of fura-2 loaded HPB-ALL cells was resuspended in either Ca^{2+}-KREB or Ca^{2+}-free KREB buffer just prior to beginning $[Ca^{2+}]_i$ measurements. At 300 s, HU-210 (20 μM), CBN (20 μM) or VH (0.1% EtOH) was injected into the cuvette and the increase in $[Ca^{2+}]_i$ was measured for a total of 1600 s. Results are presented as mean change ± SEM in the 340 nm/380 nm fluorescence ratio of $[Ca^{2+}]_i$ from base to peak of three independent experiments. * $p < 0.05$ as compared to either HU-210 (+$[Ca^{2+}]_e$) or CBN (+$[Ca^{2+}]_e$) group.

Figure 34. SR1 and SR2 antagonize the HU-210- and CBN-mediated elevation in $[Ca^{2+}]_i$ in HPB-ALL cells. A 3 ml aliquot of fura-2 loaded HPB-ALL cells was placed into a cuvette with constant stirring. SR2 (1.0-5.0 μM), SR1 (1.0-5.0 μM) or VH (0.1% DMSO) was added directly to the cuvette just prior to beginning $[Ca^{2+}]_i$ measurements. At 300 s, HU-210 (20 μM; **A**), CBN (20 μM; **B**) or VH (0.1% EtOH) was injected into the cuvette and the increase in $[Ca^{2+}]_i$ was measured for a total of 1600 s. $[Ca^{2+}]_i$ changes are presented as the mean ± SEM of the change in base to peak ratio of bound to free Ca^{2+} (340 nm/380 nm) of three (**B**) or four (**A**) independent experiments. * $p < 0.05$ as compared to either VH/HU-210 (**A**) or VH/CBN (**B**) group.

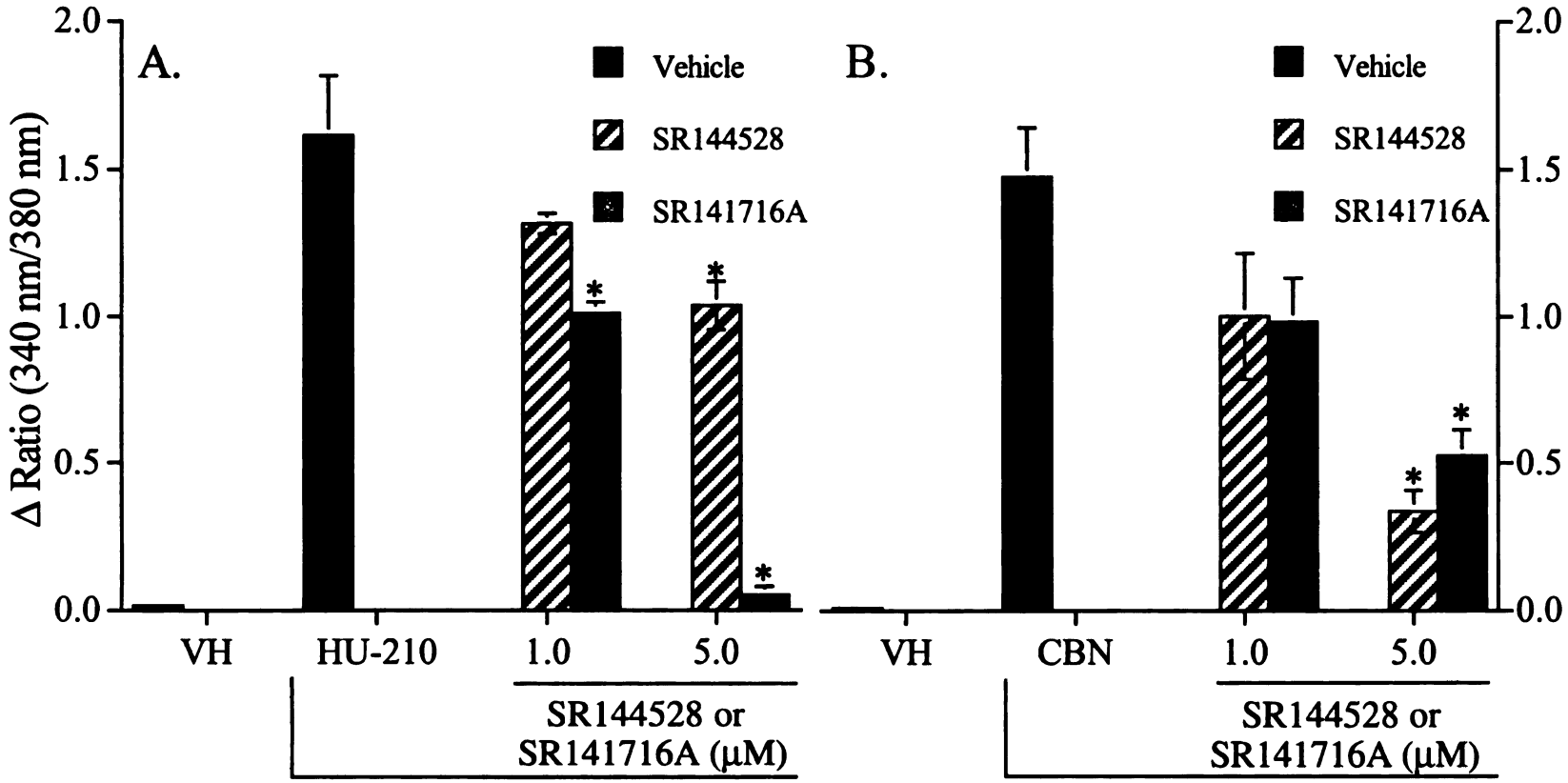

Figure 34. SR1 and SR2 antagonize the HU-210- and CBN-mediated elevation in $[Ca^{2+}]_i$ in HPB-ALL cells.

the same concentration, SR1 potently attenuated the HU-210-mediated $[Ca^{2+}]_i$ rise by 97.6 ± 1.1 % (n=3).

H. CBD elevates $[Ca^{2+}]_i$

In addition to CBN and HU-210, the effect of the non-classical bicyclic cannabinoid, CBD, on $[Ca^{2+}]_i$ was also assessed in the HPB-ALL cells. Unlike HU-210, CBN and Δ^9-THC, CBD is considered not to be an agonist at either the CB1 or CB2 receptors (Pertwee, 1999a). Nonetheless, treatment of HPB-ALL cells with CBD (1-20 μM) did lead to a small increase in $[Ca^{2+}]_i$ (figure 35). However, compared to the $[Ca^{2+}]_i$ elevation profiles of HU-210, CBN or Δ^9-THC, the $[Ca^{2+}]_i$ rise elicited by CBD was very modest, rapid, and not concentration-responsive. In addition, the CBD-induced $[Ca^{2+}]_i$ rise occurred in two distinct phases – a rapid first phase and a slower second phase. Biphasic $[Ca^{2+}]_i$ elevation has previously been established in lymphocytes to be a characteristic of SOCE (Parekh, 2003). To investigate the possibility that CBD was eliciting a release of stored Ca^{2+}, cells were treated with CBD either in the presence or absence of $[Ca^{2+}]_e$. The results showed that although the first phase of the CBD-induced $[Ca^{2+}]_i$ rise was maintained in the absence of $[Ca^{2+}]_e$, the second phase was completely abolished (figure 36). The insensitivity of the first phase to lack of $[Ca^{2+}]_e$ indicated that CBD elicits a release of stored Ca^{2+}, followed by $[Ca^{2+}]_e$ influx. Finally, to ensure that CBD was not elevating $[Ca^{2+}]_i$ by acting upon the CB2 receptor, cells were pretreated with SR2 (5 μM) for 300 s prior to CBD addition. Pretreatment with SR2 did not attenuate the CBD-mediated elevation of $[Ca^{2+}]_i$ (figure 37).

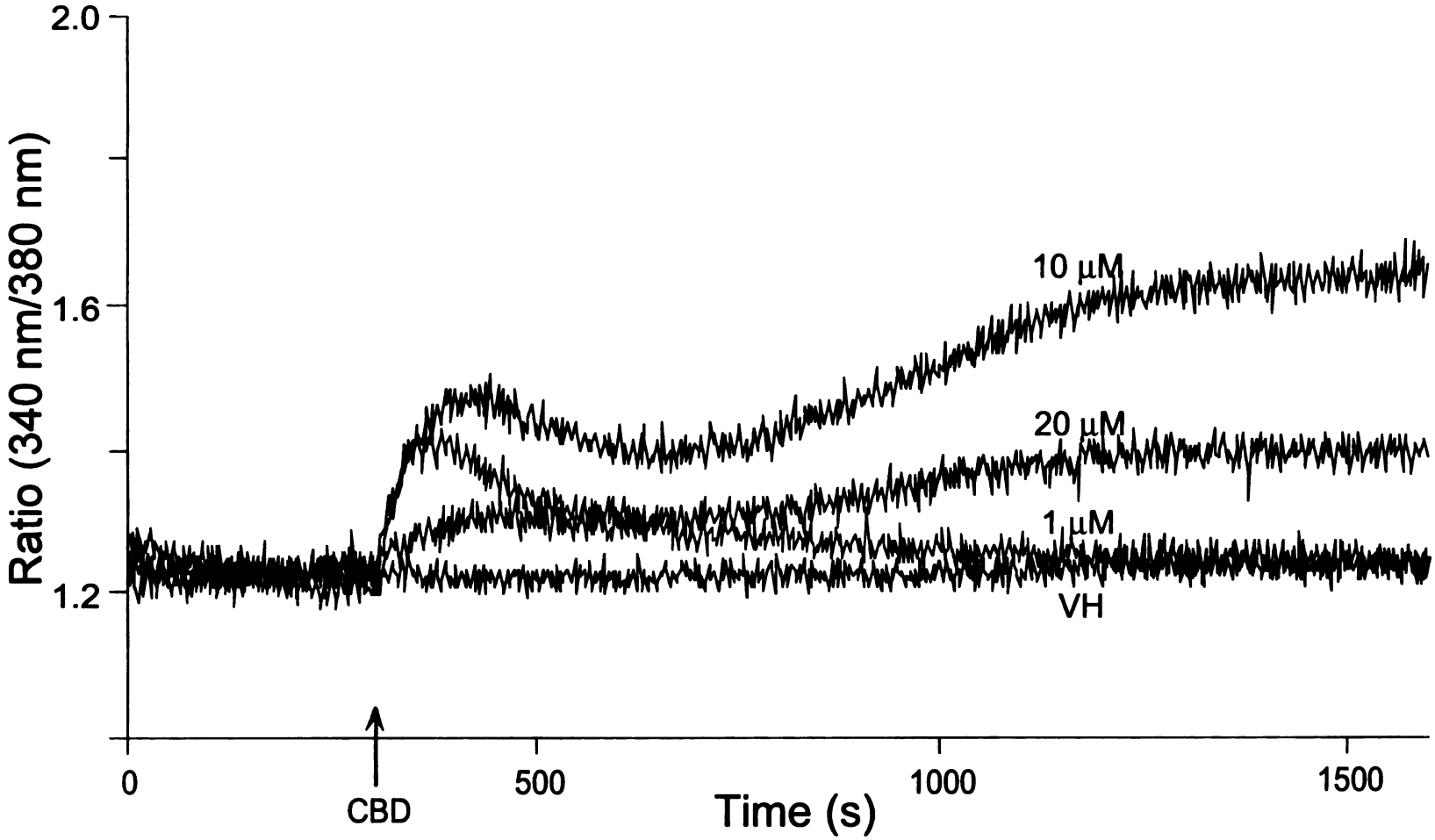

Figure 35. CBD elevates $[Ca^{2+}]_i$ in HPB-ALL cells. A 3 ml aliquot of fura-2 loaded HPB-ALL cells was placed into a cuvette with constant stirring. At 300 s, various concentrations of CBD (1-20 µM) or VH (0.1% EtOH) was injected into the cuvette and the increase in $[Ca^{2+}]_i$ was measured for a total of 1600 s. $[Ca^{2+}]_i$ changes are presented as changes in the ratio of bound to free Ca^{2+} (340 nm/380 nm). The Ca^{2+} traces represent three independent experiments.

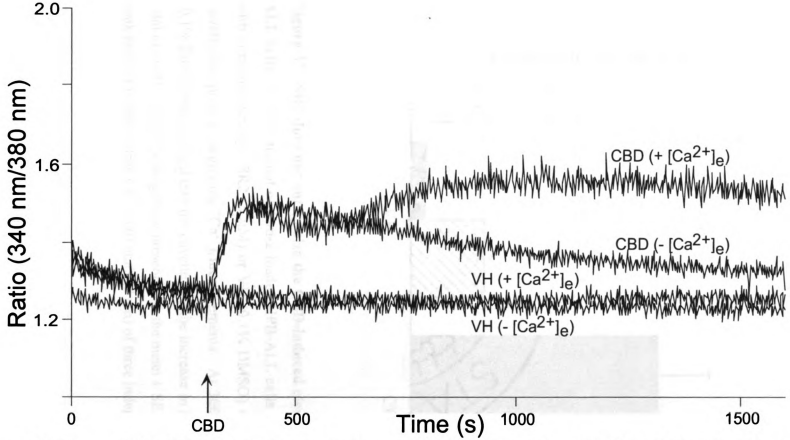

Figure 36. Removal of $[Ca^{2+}]_e$ abrogates the second phase of CBD-induced elevation of $[Ca^{2+}]_i$ in HPB-ALL cells. A 3 ml aliquot of fura-2 loaded HPB-ALL cells was resuspended in either Ca^{2+}-KREB or Ca^{2+}-free KREB buffer just prior to beginning $[Ca^{2+}]_i$ measurements. At 300 s, CBD (10 μM) or VH (0.1% EtOH) was injected into the cuvette and the increase in $[Ca^{2+}]_i$ was measured for a total of 1600 s. $[Ca^{2+}]_i$ changes are presented as changes in the ratio of bound to free Ca^{2+} (340 nm/380 nm). The Ca^{2+} traces represent three independent experiments.

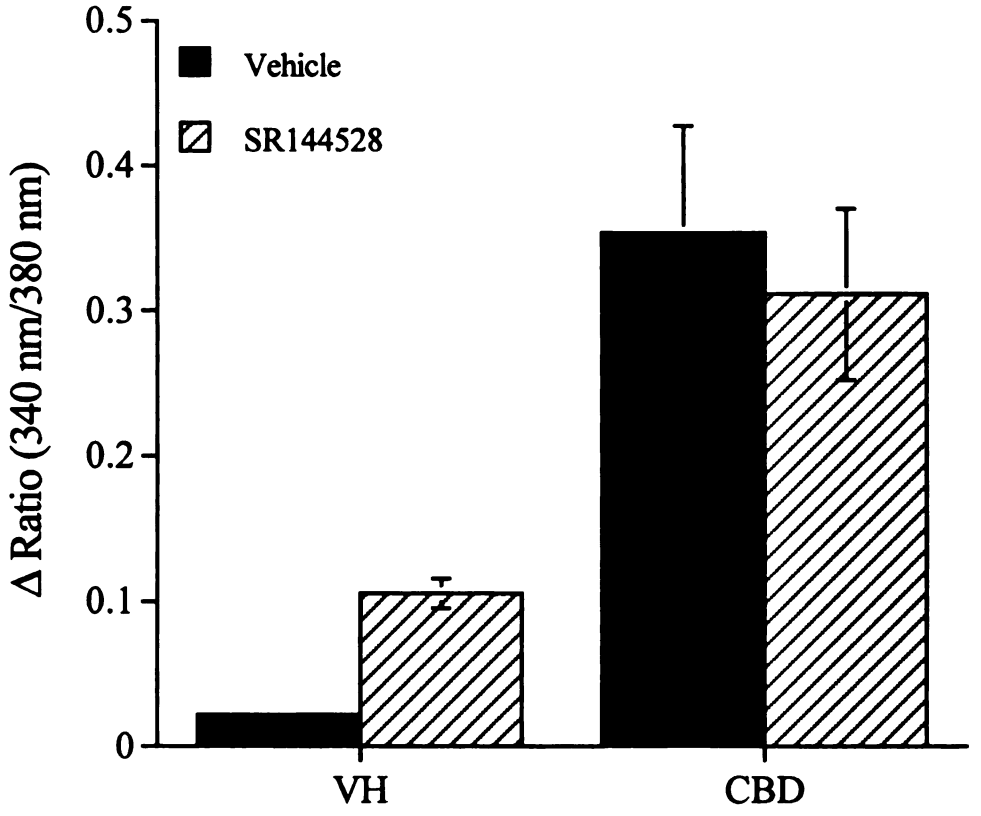

Figure 37. SR2 does not antagonize the CBD-induced elevation in $[Ca^{2+}]_i$ in HPB-ALL cells. A 3 ml aliquot of fura-2 loaded HPB-ALL cells was placed into a cuvette with constant stirring. SR2 (5 μM) or VH (0.1% DMSO) was added directly to the cuvette just prior to beginning $[Ca^{2+}]_i$ measurements. At 300 s, CBD (10 μM) or VH (0.1% EtOH) was injected into the cuvette and the increase in $[Ca^{2+}]_i$ was measured for a total of 1600 s. $[Ca^{2+}]_i$ changes are presented as the mean ± SEM of the change in base to peak ratio of bound to free Ca^{2+} (340 nm/380 nm) of three independent experiments.

I. Effect of other cannabinoids on $[Ca^{2+}]_i$

Apart from CBN, HU-210 and CBD, WIN-2 and the high-affinity CB2-selective agonist, JWH-133, were also tested for their ability to induce an influx in $[Ca^{2+}]_i$. The effect of WIN-2 on $[Ca^{2+}]_i$ elevation could not be assessed since this compound interfered with fura-2 $[Ca^{2+}]_i$ measurements. On the other hand, JWH-133 did not interfere with $[Ca^{2+}]_i$ measurements, but interestingly did not induce an elevation of $[Ca^{2+}]_i$ over a range of concentrations (0.1-20 μM) in the HPB-ALL cells (data not shown). In addition, AEA and 2-AG along with the precursor compound, arachidonic acid (AA), were also tested for their effect on $[Ca^{2+}]_i$ elevation. Surprisingly, neither the endocannabinoids (1-20 μM) nor AA (1-50 μM) elevated $[Ca^{2+}]_i$ in the HPB-ALL cells (data not shown).

III. Mechanism of Δ^9-THC-induced $[Ca^{2+}]_i$ elevation

A. Effect of Ca^{2+} channel inhibitors on the rise in $[Ca^{2+}]_i$ elicited by Δ^9-THC and TG

In order to elucidate the identity of Ca^{2+} channels involved in $[Ca^{2+}]_i$ elevation by Δ^9-THC, $[Ca^{2+}]_i$ measurements were performed in HPB-ALL cells pretreated with Ca^{2+} channel inhibitors, SKF or 2-APB, followed by Δ^9-THC treatment. In addition, $[Ca^{2+}]_i$ experiments were also carried out to examine the effects of the Ca^{2+} channel inhibitors on the $[Ca^{2+}]_i$ elevation elicited by TG (1 μM), a widely described activator of SOC current by way of Ca^{2+} store-depletion (Prakriya and Lewis, 2003; Putney, 2003). Pretreatment of HPB-ALL cells with SKF for 300 s resulted in a concentration-dependent inhibition of the Δ^9-THC-mediated elevation in $[Ca^{2+}]_i$, with substantial inhibition at 50 μM SKF (figure 38A). On the other hand, SKF only modestly attenuated the TG-induced $[Ca^{2+}]_i$

Figure 38. Effect of SKF on the elevation of $[Ca^{2+}]_i$ induced by Δ^9-THC and TG. A 3 ml aliquot of fura-2 loaded HPB-ALL cells was placed into a cuvette with constant stirring. SKF (10-50 μM) or VH (ddH_2O) was added directly to the cuvette just prior to beginning $[Ca^{2+}]_i$ measurements. At 300 s, Δ^9-THC (12.5 μM; **A**), TG (1 μM; **B**) or VH (0.1% EtOH) was injected into the cuvette and the increase in $[Ca^{2+}]_i$ was measured for a total of 1600 s. $[Ca^{2+}]_i$ changes are presented as the mean ± SEM of the change in base to peak ratio of bound to free Ca^{2+} (340 nm/380 nm) of three independent experiments. * $p < 0.05$ as compared to VH/Δ^9-THC (**A**) or VH/TG (**B**) group.

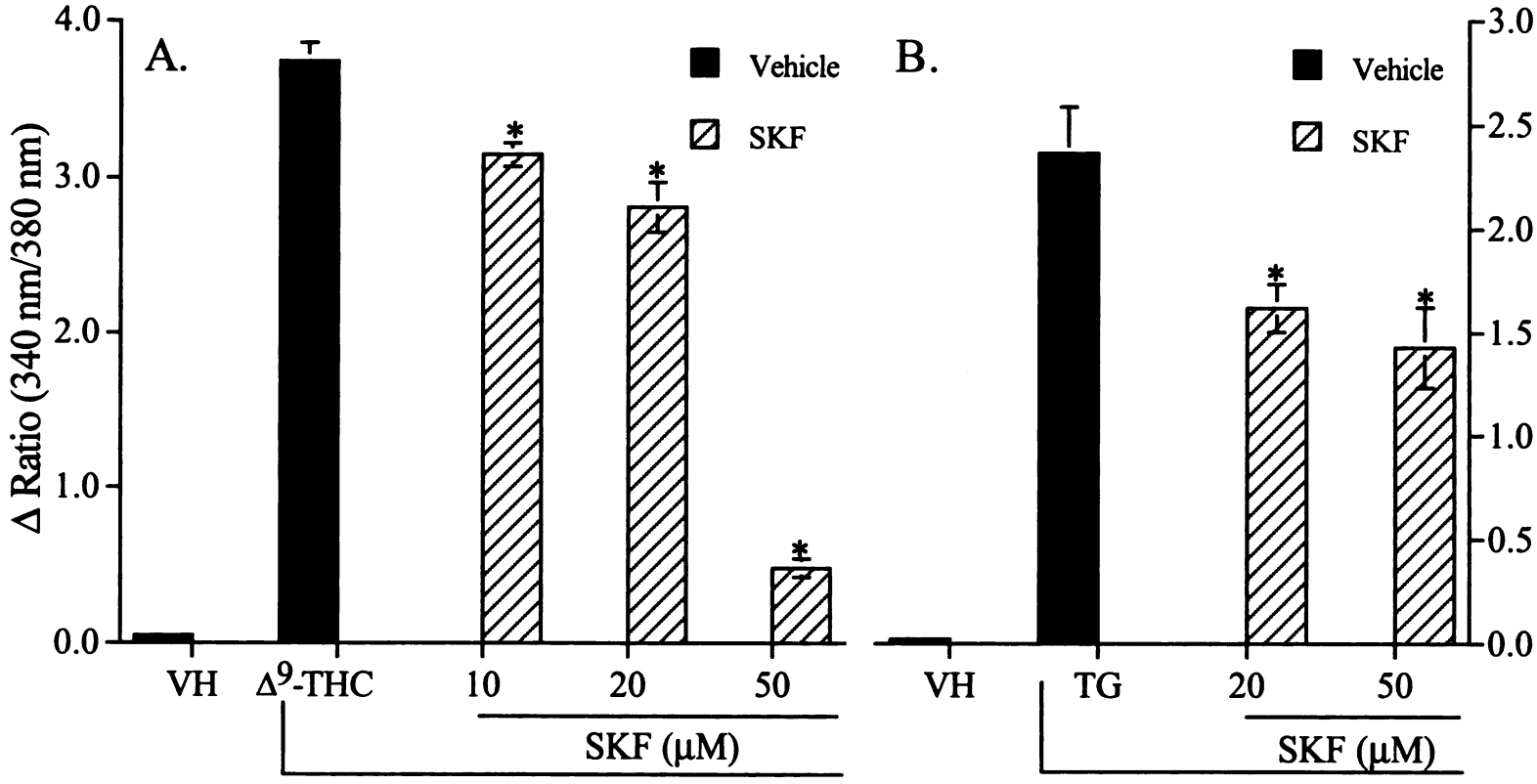

Figure 38. Effect of SKF on the elevation of $[Ca^{2+}]_i$ induced by Δ^9-THC and TG.

rise at a concentration of 50 μM (figure 38B). Conversely, 2-APB potently inhibited TG-induced $[Ca^{2+}]_i$ elevation (figure 39B) at a concentration of 25 μM, but was a weak inhibitor of the Δ^9-THC-mediated elevation in $[Ca^{2+}]_i$ even at a concentration of 100 μM (figure 39A). The contrasting effects of SKF and 2-APB on the Δ^9-THC and TG-induced rise in $[Ca^{2+}]_i$ may be explained by the prior reports demonstrating that 2-APB is an SOCC inhibitor (Vazquez et al., 2003), while SKF is an ROCC inhibitor (Merritt et al., 1990). Additionally, 2-APB may also act non-specifically to inhibit Ca^{2+} channel signaling intermediates such as PLC in lymphocytic cells (Ma et al., 2003).

To address the discrepancy of the contrasting effects of SKF and 2-APB on the Δ^9-THC- and TG-induced elevation in $[Ca^{2+}]_i$, additional studies were conducted with $LaCl_3$. La^{3+} cation is a potent inhibitor of SOCCs at submicromolar levels, and is effective at inhibiting a TG-induced $[Ca^{2+}]_i$ rise (Aussel et al., 1996). In addition, lanthanide compounds have also been reported to inhibit TRPC channels, but at concentrations in the micromolar range (Beech et al., 2003; Trebak et al., 2003b). Presently, the effect of $LaCl_3$ (20-250 μM) was examined on the Δ^9-THC- and TG-induced $[Ca^{2+}]_i$ rise. Pretreatment of cells with $LaCl_3$ markedly inhibited the Δ^9-THC-mediated elevation of $[Ca^{2+}]_i$, but only at concentrations greater than or equal to 100 μM (figure 40A). By contrast, $LaCl_3$ was potent at attenuating the TG-induced rise in $[Ca^{2+}]_i$ at a lower concentration of 20 μM (figure 40B).

In light of the above observation that the ROCC inhibitor, SKF, but not the SOCC inhibitors, 2-APB or $LaCl_3$, potently inhibited the $[Ca^{2+}]_i$ rise induced by Δ^9-THC a further set of studies were performed to investigate the putative involvement of ROCCs in the $[Ca^{2+}]_i$ rise induced by HU-210 and CBN. Cells were treated with 20-50 μM SKF

Figure 39. Effect of 2-APB on the elevation of $[Ca^{2+}]_i$ induced by Δ^9-THC and TG. A 3 ml aliquot of fura-2 loaded HPB-ALL cells was placed into a cuvette with constant stirring. 2-APB (25-100 μM) or VH (0.1% EtOH) was added directly to the cuvette just prior to beginning $[Ca^{2+}]_i$ measurements. At 300 s, Δ^9-THC (12.5 μM; **A**), TG (1 μM; **B**) or VH (0.1% EtOH) was injected into the cuvette and the increase in $[Ca^{2+}]_i$ was measured for a total of 1600 s. $[Ca^{2+}]_i$ changes are presented as the mean ± SEM of the change in base to peak ratio of bound to free Ca^{2+} (340 nm/380 nm) of three independent experiments. * $p < 0.05$ as compared to VH/Δ^9-THC (**A**) or VH/TG (**B**) group.

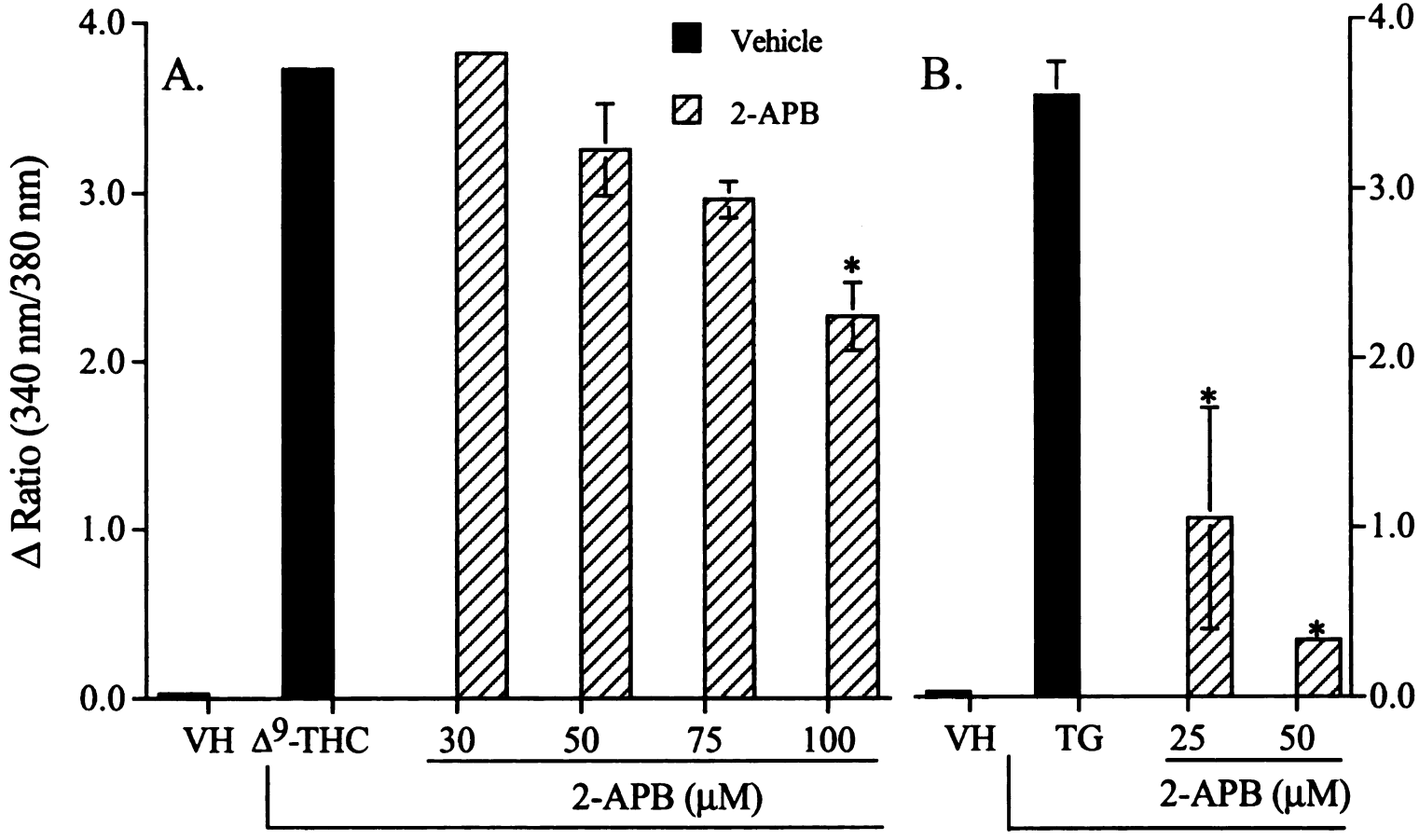

Figure 39. Effect of 2-APB on the elevation of $[Ca^{2+}]_i$ induced by Δ^9-THC and TG.

Figure 40. Effect of $LaCl_3$ on the elevation of $[Ca^{2+}]_i$ induced by Δ^9-THC and TG. A 3 ml aliquot of fura-2 loaded HPB-ALL cells in HPSS buffer was placed into a cuvette with constant stirring. $LaCl_3$ (20-250 μM) or VH (ddH_2O) was added directly to the cuvette just prior to beginning $[Ca^{2+}]_i$ measurements. At 300 s, Δ^9-THC (12.5 μM; **A**), TG (1 μM; **B**) or VH (0.1% EtOH) was injected into the cuvette and the increase in $[Ca^{2+}]_i$ was measured for a total of 1600 s. $[Ca^{2+}]_i$ changes are presented as the mean ± SEM of the change in base to peak ratio of bound to free Ca^{2+} (340 nm/380 nm) of three independent experiments. * $p < 0.05$ as compared to VH/Δ^9-THC (**A**) or VH/TG (**B**) group.

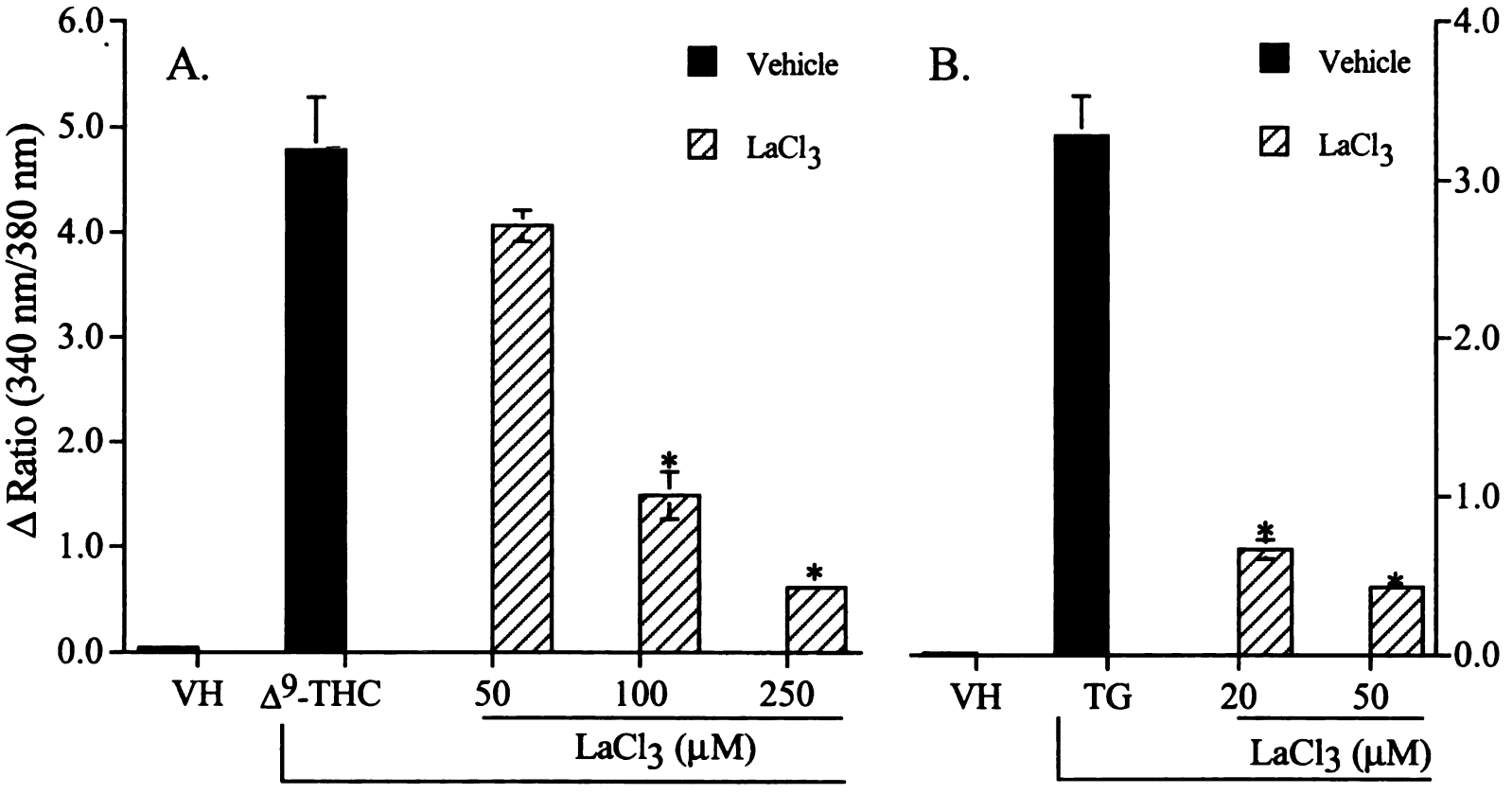

Figure 40. Effect of $LaCl_3$ on the elevation of $[Ca^{2+}]_i$ induced by Δ^9-THC and TG.

for 300 s before treatment with cannabinoids. The results showed SKF did indeed inhibit the rise in $[Ca^{2+}]_i$ elicited by both HU-210 and CBN (figure 41A, B). In accord with the antagonist studies with HU-210 and CBN, SKF too had differential effects on the HU-210- and CBN-induced rise in $[Ca^{2+}]_i$. At a concentration of 50 μM, SKF potently inhibited the CBN-induced elevation in $[Ca^{2+}]_i$ by 96.7 ± 1.2 % (n=3). At the same concentration, SKF was not as efficacious and inhibited the HU-210-mediated rise in $[Ca^{2+}]_i$ by only 47.5 ± 13.6 % (n=3). Another rather unusual effect of SKF pretreatment was that it reduced the time delay to onset of the HU-210-induced $[Ca^{2+}]_i$ elevation. Compared to VH control, the time delay to onset of $[Ca^{2+}]_i$ elevation for HU-210 (15 μM) in the presence of SKF (50 μM) was reduced by 165.3 ± 1.2 s (n=3; data not shown).

B. Δ^9-THC-mediated elevation in $[Ca^{2+}]_i$ is not abolished upon TG or 8-Br-cADPR pretreatment

The experiments outlined above suggested that the Δ^9-THC-mediated elevation in $[Ca^{2+}]_i$ was dependent on SKF-sensitive ROCCs, but was independent of SOCCs. To eliminate the possibility that Δ^9-THC was releasing stored Ca^{2+} pools and to examine the effect of Ca^{2+} store-depletion on the Δ^9-THC-mediated $[Ca^{2+}]_i$ rise, $[Ca^{2+}]_i$ measurements were performed with sequential addition of TG, followed by Δ^9-THC. In these studies, cells were first treated with TG (1 μM) at 300 s, and followed by addition of either TG (1 μM), or Δ^9-THC (12.5 μM) at 1200 s. As seen in figure 42, an initial addition of TG to the cells led to a rapid and robust increase in $[Ca^{2+}]_i$, indicating an influx of $[Ca^{2+}]_e$ following depletion of stored intracellular Ca^{2+}, and the subsequent addition of TG did

Figure 41. Effect of SKF on the elevation of $[Ca^{2+}]_i$ induced by HU-210 and CBN. A 3 ml aliquot of fura-2 loaded HPB-ALL cells was placed into a cuvette with constant stirring. SKF (20-50 μM) or VH (ddH_2O) was added directly to the cuvette just prior to beginning $[Ca^{2+}]_i$ measurements. At 300 s, HU-210 (20 μM; **A**), CBN (20 μM; **B**) or VH (0.1% EtOH) was injected into the cuvette and the increase in $[Ca^{2+}]_i$ was measured for a total of 1600 s. $[Ca^{2+}]_i$ changes are presented as the mean ± SEM of the change in base to peak ratio of bound to free Ca^{2+} (340 nm/380 nm) of three independent experiments. * $p < 0.05$ as compared to VH/HU-210 (**A**) or VH/CBN (**B**) group.

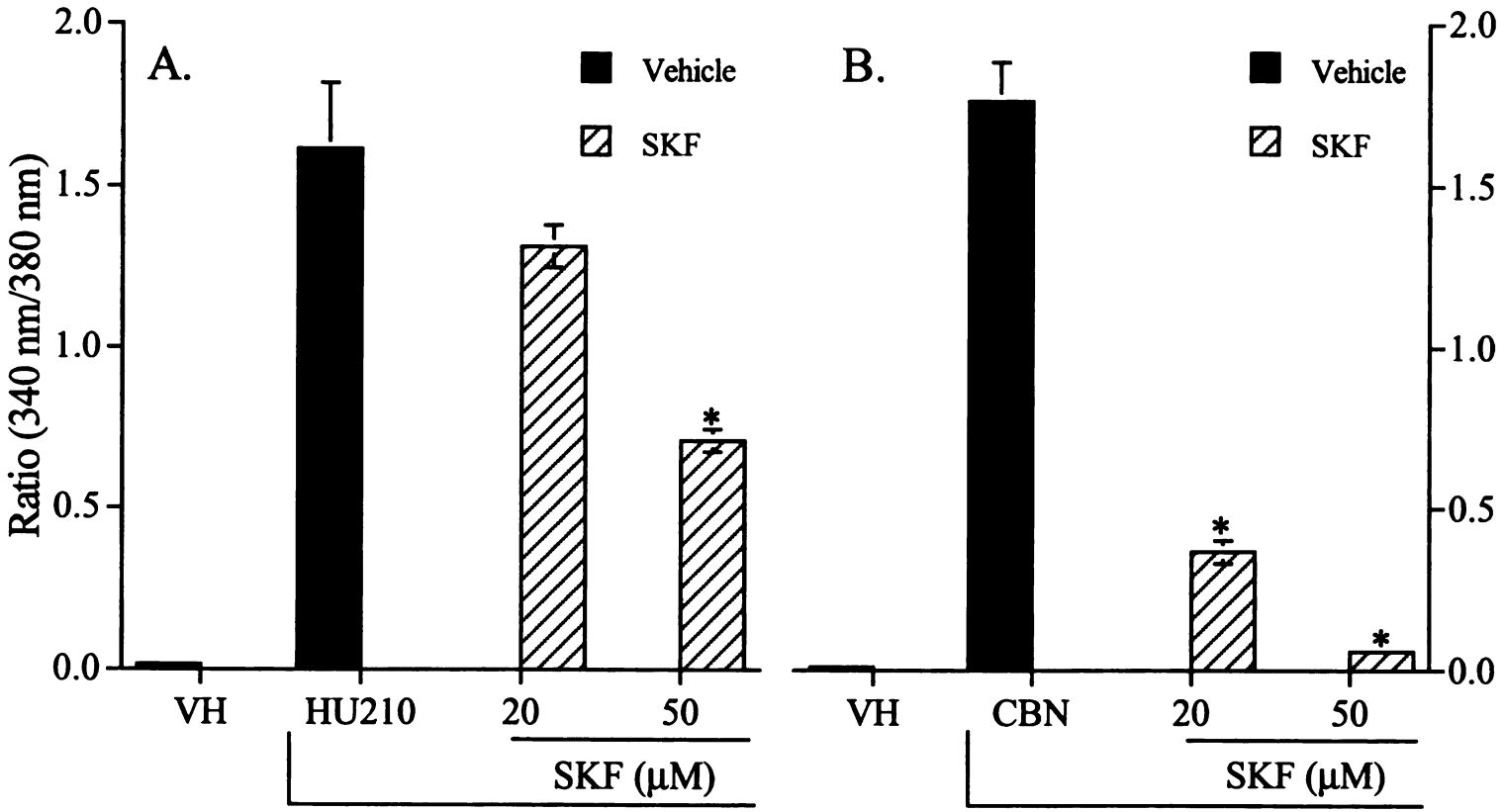

Figure 41. Effect of SKF on the elevation of $[Ca^{2+}]_i$ induced by HU-210 and CBN.

not lead to a further increase in $[Ca^{2+}]_i$. In contrast, if cells were initially treated with TG to deplete stored Ca^{2+} and then treated with Δ^9-THC, the addition of Δ^9-THC led to a further elevation of $[Ca^{2+}]_i$ over the TG-induced $[Ca^{2+}]_i$ rise (figure 42).

It has previously been reported that there are two intracellular Ca^{2+} stores: the IP_3-sensitive and -insensitive Ca^{2+} pools, which are depleted by TG; and a TG-insensitive RyR-gated Ca^{2+} pool depleted by cADPR (Guse et al., 1995). To ascertain that Δ^9-THC did not elicit the increase in $[Ca^{2+}]_i$ following depletion of cADPR-sensitive Ca^{2+} pools, HPB-ALL cells were pretreated with 8-Br-cADPR (20-75 μM), a cell-permeant antagonist of the RyR, for 300 s followed by Δ^9-THC. The resulting Δ^9-THC-mediated $[Ca^{2+}]_i$ increase was not attenuated by 8-Br-cADPR treatment even at concentrations as high as 75 μM (figure 43).

C. OAG elevates $[Ca^{2+}]_i$ in HPB-ALL cells independently of PKC

In light of the observation that Δ^9-THC-mediated elevation in $[Ca^{2+}]_i$ was independent of store-depletion and was sensitive to high concentrations of $LaCl_3$, the hypothesis that Δ^9-THC-induced elevation in $[Ca^{2+}]_i$ was mediated through ROCCs in the TRPC subfamily was tested. Recently, various groups have concluded that TRPC channels may operate either as ROCCs or SOCCs (Beech et al., 2003; Philipp et al., 2003; Singh et al., 2000; Trebak et al., 2003b; Vazquez et al., 2003). Moreover, analogs of DAG have been found to activate TRPC1, 3, 6 and 7 (Beech et al., 2003; Gamberucci et al., 2002; Hofmann et al., 1999; Lintschinger et al., 2000; Trebak et al., 2003b). In the present investigation, presence of DAG-gated channels in HPB-ALL cells was confirmed by treatment with OAG. Treatment of HPB-ALL cells with increasing concentrations of

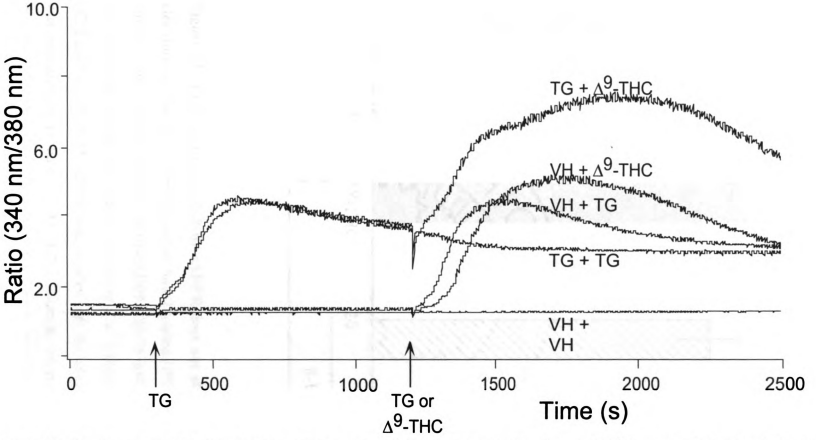

Figure 42. Pretreatment with TG does not abrogate the Δ^9-THC induced elevation in $[Ca^{2+}]_i$. A 3 ml aliquot of fura-2 loaded HPB-ALL cells was placed into a cuvette with constant stirring. At 300 s, TG (1 μM) or VH (0.1% EtOH) was injected into the cuvette, followed by a second injection with TG (1 μM) or Δ^9-THC (12.5 μM) at 1200 s. The increase in $[Ca^{2+}]_i$ was measured for a total of 2500 s. $[Ca^{2+}]_i$ changes are presented as changes in the ratio of bound to free Ca^{2+} (340 nm/380 nm). The Ca^{2+} traces represent three independent experiments.

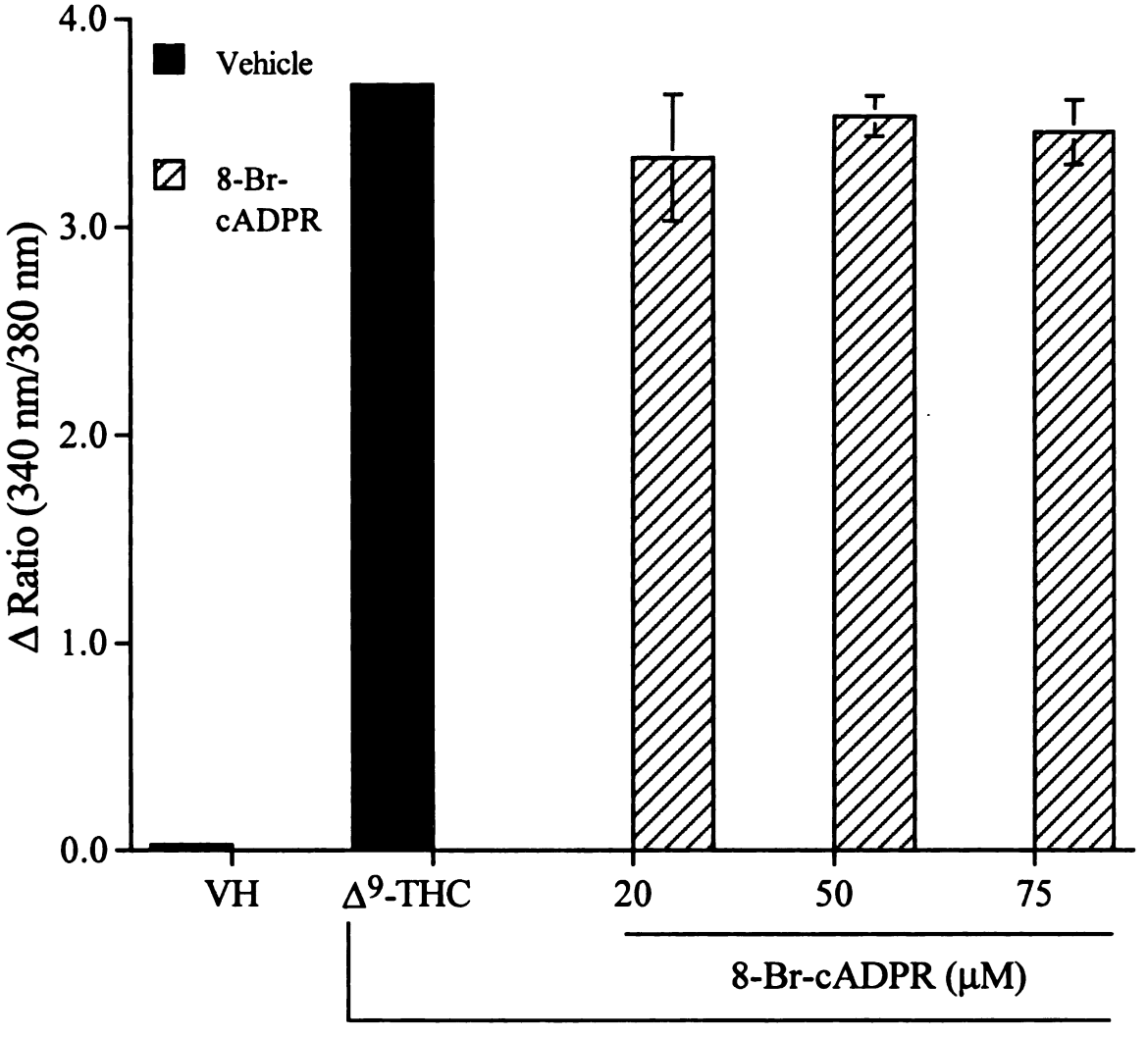

Figure 43. Pretreatment with 8-Br-cADPR does not abrogate the Δ^9-THC induced elevation in $[Ca^{2+}]_i$. A 3 ml aliquot of fura-2 loaded HPB-ALL cells was placed into a cuvette with constant stirring. 8-Br-cADPR (20-75 μM) or VH (ddH_2O) was added directly to the cuvette just prior to beginning $[Ca^{2+}]_i$ measurements. At 300 s, Δ^9-THC (12.5 μM) or VH (0.1% EtOH) was injected into the cuvette and the increase in $[Ca^{2+}]_i$ was measured for a total of 1600 s. $[Ca^{2+}]_i$ changes are presented as the mean ± SEM of the change in base to peak ratio of bound to free Ca^{2+} (340 nm/380 nm) of two independent experiments.

OAG (50-300 μM) resulted in a rapid elevation of $[Ca^{2+}]_i$ (figure 44), which was, however, smaller in magnitude when compared to the Δ^9-THC-mediated rise of $[Ca^{2+}]_i$. Next, the hypothesis that Δ^9-THC and OAG both putatively induced $[Ca^{2+}]_i$ elevations through the same TRPC channel was examined in HPB-ALL cells. Cells were sequentially treated with OAG (300 μM) for 600 s, followed by either a second addition of OAG (300 μM) or Δ^9-THC (12.5 μM) at 1200 s. As expected, treatment of cells initially with OAG rapidly elevated $[Ca^{2+}]_i$. However, as can be gleaned from figure 45, the subsequent addition of OAG did not further elevate $[Ca^{2+}]_i$. Interestingly, in cells initially treated with OAG, a subsequent addition of Δ^9-THC also failed to elicit a further elevation in $[Ca^{2+}]_i$.

Apart from gating several members of the TRPC channel subfamily, OAG is a well-known activator of PKC. To eliminate the possibility that OAG inhibits a subsequent Δ^9-THC-mediated elevation in $[Ca^{2+}]_i$ by activating PKC, cells were preincubated with VH or PMA (500 nM) for 20 h. Treatment of cells with high concentrations of PMA for extended periods of time has been demonstrated to downregulate PKC (Bordin et al., 2003; Driessens et al., 1997). However, downregulation of PKC did not affect the ability of OAG pretreatment to block the subsequent elevation in $[Ca^{2+}]_i$ elicited by Δ^9-THC (figure 46A, B), suggesting that OAG prevents the elevation of $[Ca^{2+}]_i$ by Δ^9-THC independently of PKC. Nevertheless, PKC may still be involved in the negative regulation of the TRPC channels activated Δ^9-THC. HPB-ALL cells treated with PMA (20-80 nM) for 300 s, followed by Δ^9-THC showed a modest, yet significant and concentration-responsive, attenuation of the resulting elevation in $[Ca^{2+}]_i$ (figure 47). The observation that PKC may negatively regulate TRPC

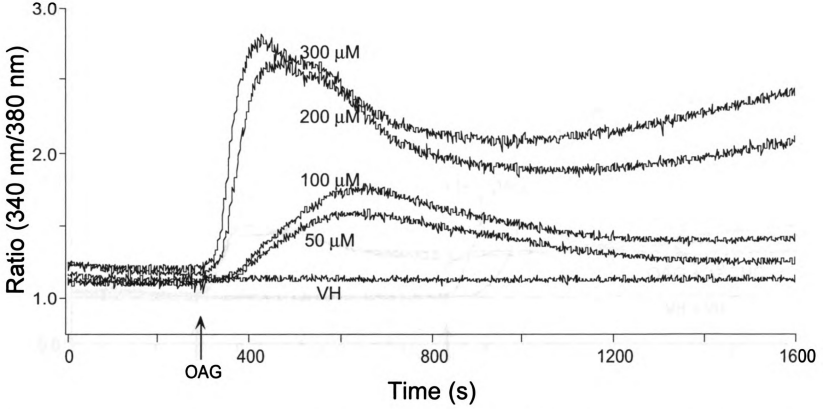

Figure 44. Treatment of HPB-ALL cells with OAG induces an elevation in $[Ca^{2+}]_i$. A 3 ml aliquot of fura-2 loaded HPB-ALL cells was placed into a cuvette with constant stirring. At 300 s, various concentrations of OAG (50-300 µM) or VH (0.1-0.3% EtOH) was injected into the cuvette without dilution in buffer and the increase in $[Ca^{2+}]_i$ was measured for a total of 1600 s. $[Ca^{2+}]_i$ changes are presented as changes in the ratio of bound to free Ca^{2+} (340 nm/380 nm). The Ca^{2+} traces represent three independent experiments.

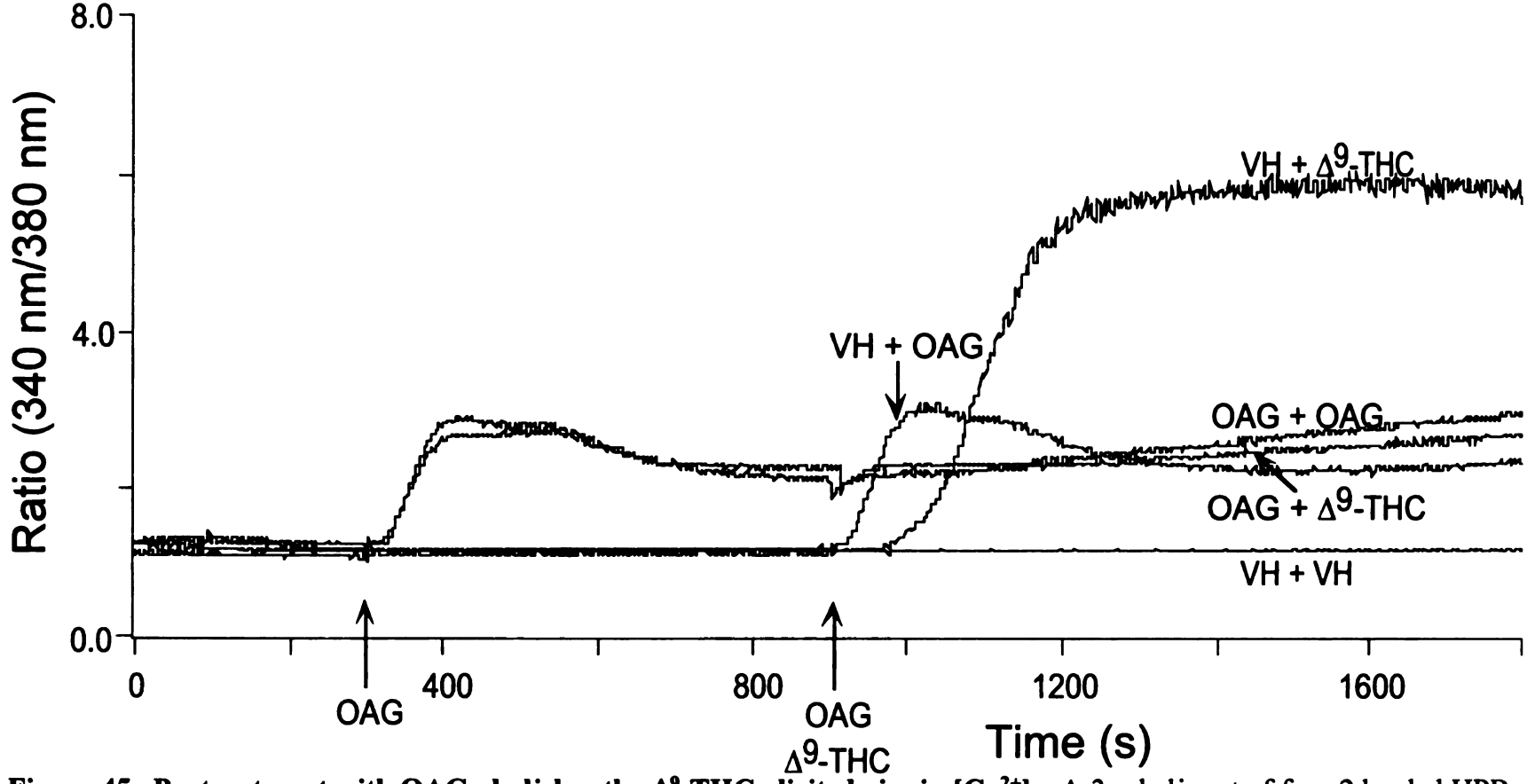

Figure 45. Pretreatment with OAG abolishes the Δ^9-THC-elicited rise in $[Ca^{2+}]_i$. A 3 ml aliquot of fura-2 loaded HPB-ALL cells was placed into a cuvette with constant stirring. At 300 s, OAG (300 μM) or VH (0.3% EtOH) was injected into the cuvette without dilution, followed by a second addition of OAG (300 μM), Δ^9-THC (12.5 μM) or VH (0.3% EtOH for OAG; 0.1% EtOH for Δ^9-THC) at 1200 s. The increase in $[Ca^{2+}]_i$ was measured for a total of 1800 s. $[Ca^{2+}]_i$ changes are presented as changes in the ratio of bound to free Ca^{2+} (340 nm/380 nm). The Ca^{2+} traces represent three independent experiments.

Figure 46. Downregulation of PKC does not affect the abrogation the Δ^9-THC-elicited rise in $[Ca^{2+}]_i$ by OAG. HPB-ALL cells were preincubated with VH (0.05% DMSO; **A**) or PMA (500 nM; **B**) for 20 h to downregulate PKC. The cells were then loaded with fura-2 and used for $[Ca^{2+}]_i$ measurements. At 300 s, OAG (300 μM) or VH (0.3% EtOH) was injected into the cuvette without dilution, followed by a second addition of OAG (300 μM), Δ^9-THC (12.5 μM) or VH (0.3% EtOH for OAG; 0.1% EtOH for Δ^9-THC) at 1200 s. The increase in $[Ca^{2+}]_i$ was measured for a total of 1800 s. $[Ca^{2+}]_i$ changes are presented as changes in the ratio of bound to free Ca^{2+} (340 nm/380 nm). The Ca^{2+} traces represent two independent experiments.

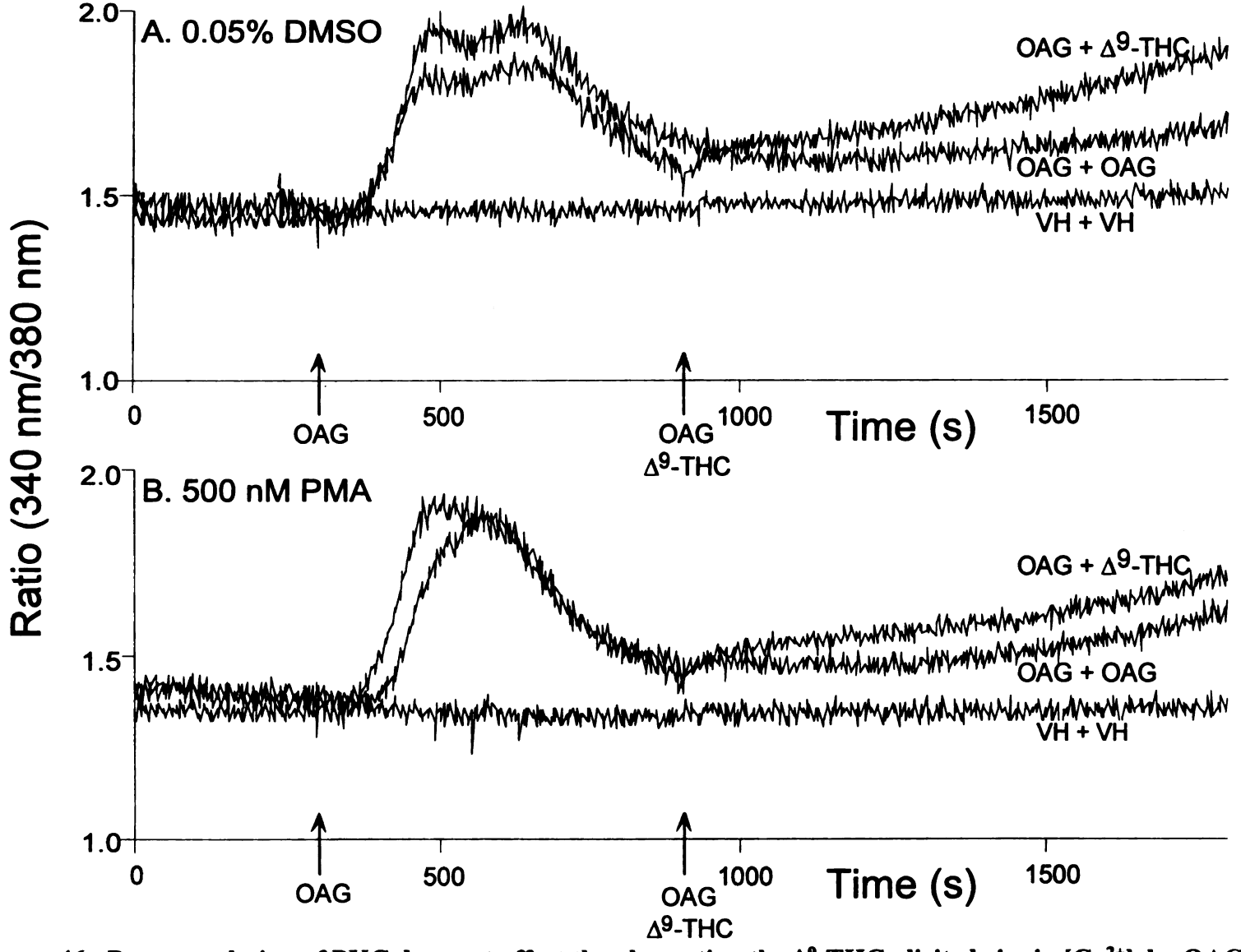

Figure 46. Downregulation of PKC does not affect the abrogation the Δ^9-THC-elicited rise in $[Ca^{2+}]_i$ by OAG.

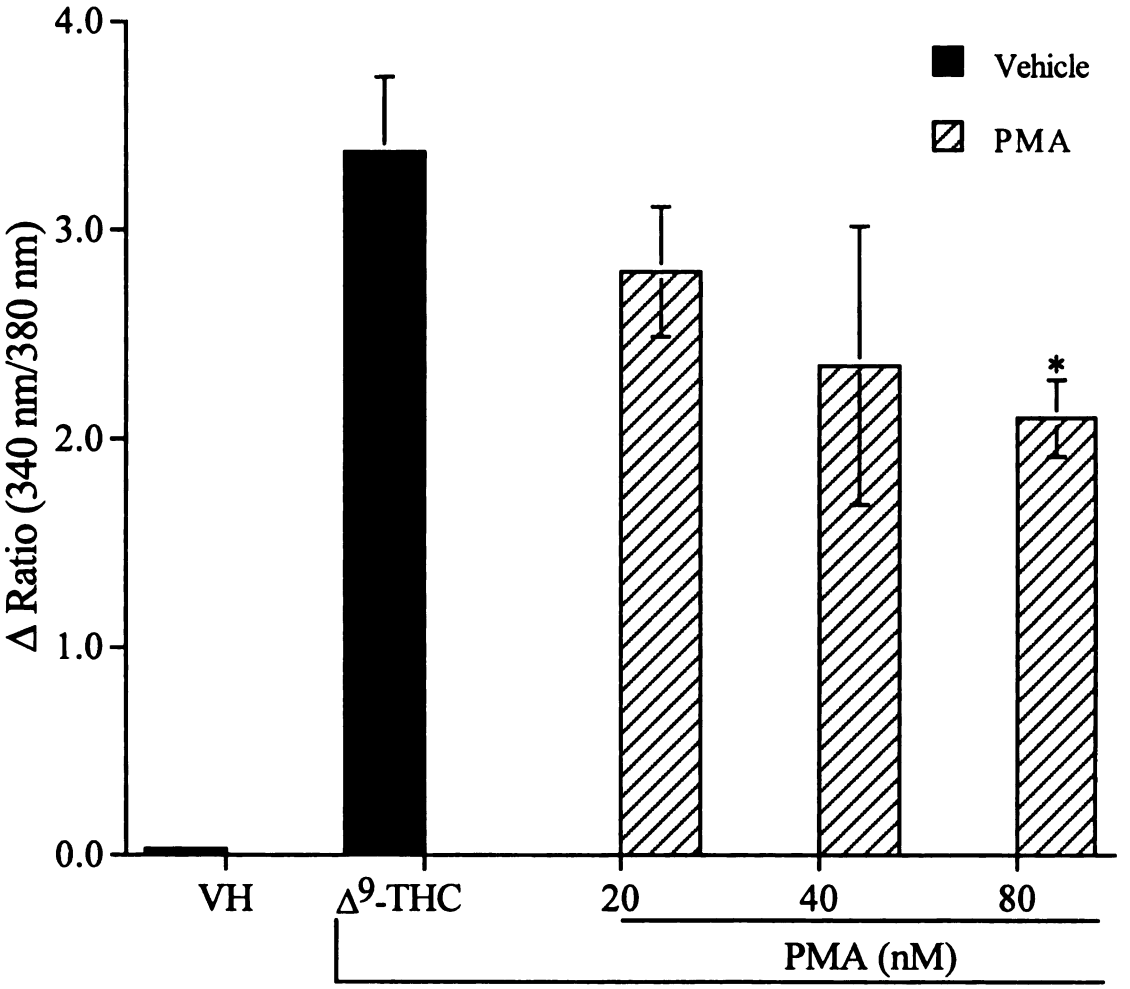

Figure 47. Pretreatment with PMA modestly attenuates the Δ^9-THC induced elevation in $[Ca^{2+}]_i$. A 3 ml aliquot of fura-2 loaded HPB-ALL cells was placed into a cuvette with constant stirring. PMA (20-80 nM) or VH (0.1% DMSO) was added directly to the cuvette just prior to beginning $[Ca^{2+}]_i$ measurements. At 300 s, Δ^9-THC (12.5 μM) or VH (0.1% EtOH) was injected into the cuvette and the increase in $[Ca^{2+}]_i$ was measured for a total of 1600 s. $[Ca^{2+}]_i$ changes are presented as the mean ± SEM of the change in base to peak ratio of bound to free Ca^{2+} (340 nm/380 nm) of three independent experiments. * $p < 0.05$ as compared to VH/Δ^9-THC group.

channels activated by Δ^9-THC is consistent with previous reports which have shown that PKC inhibits several TRPC channels (Trebak et al., 2003a; Venkatachalam et al., 2004).

Finally, the effect of Δ^9-THC on PKC activation was also assessed. It has been previously determined that several cannabinoids, including Δ^9-THC, independently activate Ca^{2+}-dependent isoforms of PKC in a murine brain preparation (Hillard and Auchampach, 1994). Here, the effect of Δ^9-THC on PKC activity was measured using a PKC substrate activity assay. HPB-ALL cells were treated with varying concentrations of Δ^9-THC (1-15 μM), VH, or PMA (80 nM) as a positive control, for 15 min. Cells were then harvested, lysed and assayed for PKC activity in the whole cell fraction. The results clearly showed that whereas the PMA treatment increased the activity of PKC, Δ^9-THC treatment over a wide concentration range did not result in an increase in PKC activity over VH (figure 48).

D. Δ^9-THC-induced elevation of $[Ca^{2+}]_i$ is independent of CaMKII

To examine whether the elevation in $[Ca^{2+}]_i$ by Δ^9-THC was dependent on CaMKII, $[Ca^{2+}]_i$ measurements were performed with the CaMKII inhibitor, KN-93, or the negative control analog, KN-92. Cells were pretreated with KN-93 or KN-92 (1-10 μM) for 300 s, followed by Δ^9-THC (figure 49). Interestingly, the elevation of $[Ca^{2+}]_i$ by Δ^9-THC was inhibited by both compounds in a concentration-dependent manner. KN-93 was slightly more potent at inhibiting the Δ^9-THC-mediated rise of $[Ca^{2+}]_i$ than was KN-92, suggesting putatively that Δ^9-THC treatment resulted in CaMKII activation. Therefore, the effect of Δ^9-THC on CaMKII activity was measured using a CaMKII substrate activity assay. HPB-ALL cells were treated with Δ^9-THC (12.5 μM) or VH and

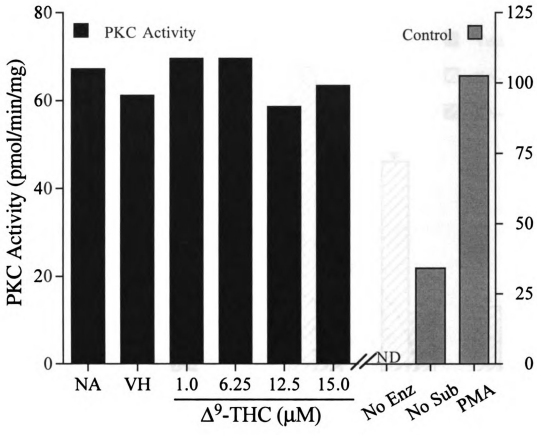

Figure 48. Δ^9-THC treatment does not result in the activation of PKC. HPB-ALL cells were left untreated (NA) or treated with VH (0.1% EtOH) or various concentrations of Δ^9-THC (1-15 μM), or PMA (80 nM) as a positive control for 15 min. Cells were then harvested, lysed and PKC phosphotransferase activity was determined in the whole cell fraction. Assay reactions were performed with 10 μCi [γ-^{32}P]-ATP for 10 min at 30°C. The assay included two negative controls performed in the absence of protein sample (no enz) or in the absence of substrate (no sub). Reactions were spotted on phosphocellulose filter papers and assayed for ^{32}P using a scintillation counter. The results are presented as pmol of [γ-^{32}P]-ATP incorporated per min per mg of protein added. The results are representative of two independent experiments. ND indicates none detected.

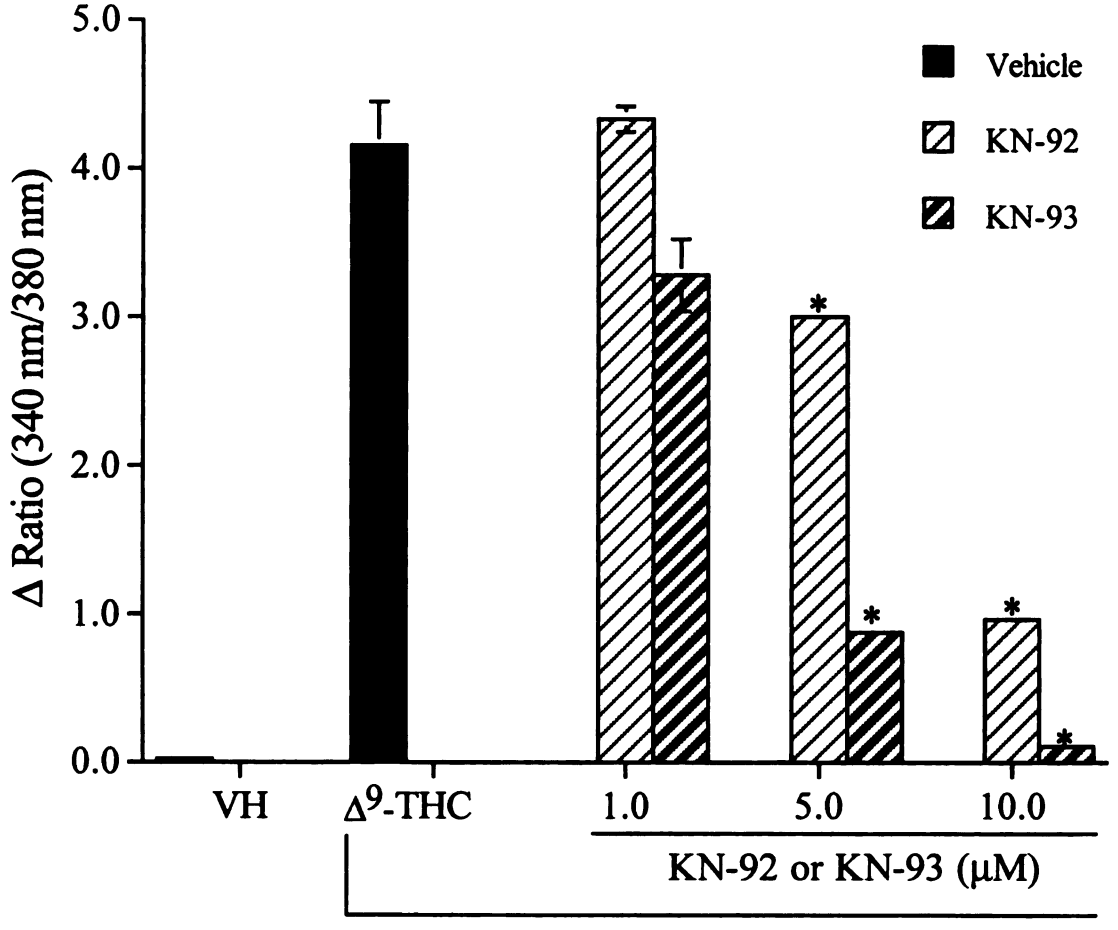

Figure 49. Pretreatment with KN-93 and KN-92 attenuates the Δ^9-THC-induced elevation in $[Ca^{2+}]_i$. A 3 ml aliquot of fura-2 loaded HPB-ALL cells was placed into a cuvette with constant stirring. KN-93 (1-10 μM), KN-92 (1-10 μM) or VH (0.1% DMSO) was added directly to the cuvette just prior to beginning $[Ca^{2+}]_i$ measurements. At 300 s, Δ^9-THC (12.5 μM) or VH (0.1% EtOH) was injected into the cuvette and the increase in $[Ca^{2+}]_i$ was measured for a total of 1600 s. $[Ca^{2+}]_i$ changes are presented as the mean ± SEM of the change in base to peak ratio of bound to free Ca^{2+} (340 nm/380 nm) of three independent experiments. * $p < 0.05$ as compared to VH/ Δ^9-THC group.

harvested at a variety of time points (0.5-30 min). The cells were lysed and assayed for CaMKII activity in the soluble fraction. The assay included a positive control, in which an aliquot of the naïve protein sample was preincubated with Ca^{2+}/CaM (1 mM/50 μg/ml). The results clearly showed that whereas the Ca^{2+}/CaM treatment strongly increased the activity of CaMKII, Δ^9-THC treatment did not result in an increase in CaMKII activity over a period of 30 min (figure 50).

The activation of CaMKII by Δ^9-THC was also examined by Western analysis. The CaMKII family of enzymes is unique in that upon Ca^{2+}/CaM binding, a high level of autonomous kinase activity is induced as a result of autophosphorylation on threonine 286 (Bui et al., 2000). Presently, HPB-ALL cells were treated with VH or Δ^9-THC (10 μM) for varying periods of time (1-60 min). Cells were harvested, lysed, and CaMKII activation was determined in the soluble fraction using Western analysis. CaMKII activation was detected using an anti-CaMKIIpT^{286} antibody. To account for loading discrepancies, the blot was further incubated with an anti-β-actin antibody. The results showed that treatment with Δ^9-THC did not lead to an increase in the autophosphorylation of CaMKII, as compared to the corresponding VH control and as normalized with a β-actin loading control (figure 51).

E. Δ^9-THC-induced elevation of $[Ca^{2+}]_i$ is independent of PLC, PI3K and soluble tyrosine kinases

The activation of TRPC channels has been reported previously to be dependent on the activation of several different enzymes including PLC, PI3K and src family tyrosine kinases (Trebak et al., 2003b). To examine whether the Δ^9-THC-induced $[Ca^{2+}]_i$ rise

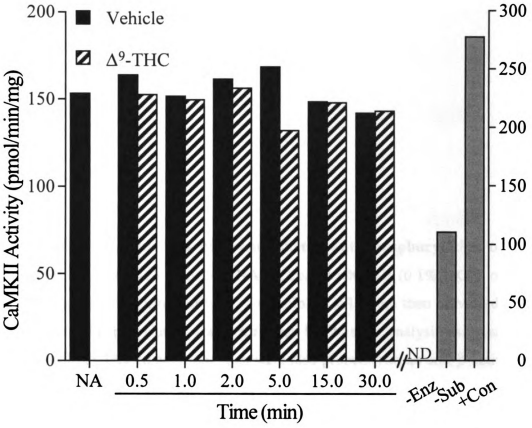

Figure 50. Δ^9-THC treatment does not result in the activation of CaMKII. HPB-ALL cells were left untreated (NA) or treated with VH (0.1% EtOH) or Δ^9-THC (12.5 μM) for various periods of time (0.5-30 min). Cells were then harvested, lysed and CaMKII phosphotransferase activity was determined in the soluble fraction. The assay reactions were performed with 10 μCi [γ-^{32}P]-ATP for 10 min at 30°C. The assay included two negative controls performed in the absence of protein sample (-enz) or in the absence of substrate (-sub); and a positive control in the presence of Ca^{2+}/CaM (1 mM/50 μg/ml). Reactions were spotted on phosphocellulose filter papers and assayed for ^{32}P using a scintillation counter. The results are presented as pmol of [γ-^{32}P]-ATP incorporated per min per mg of protein added. The results are representative of three independent experiments. ND indicates none detected.

Figure 51. Δ^9-THC treatment does not result in the autophosphorylation of CaMKII. HPB-ALL cells were left untreated (NA) or treated with VH (0.1% EtOH) or Δ^9-THC (12.5 μM) for various periods of time (5-60 min). Cells were then harvested, lysed and CaMKII autophosphorylation was determined by Western analysis using an anti-CaMKIIpT^{286} antibody (**A**). In addition, blots were also probed with an anti-β-actin antibody as a loading control (**B**). The optical density of the resulting bands was quantified using a densitometer and graphed as the optical density of CaMKIIpT^{286} normalized by β-actin (**C**). The results are representative of three independent experiments.

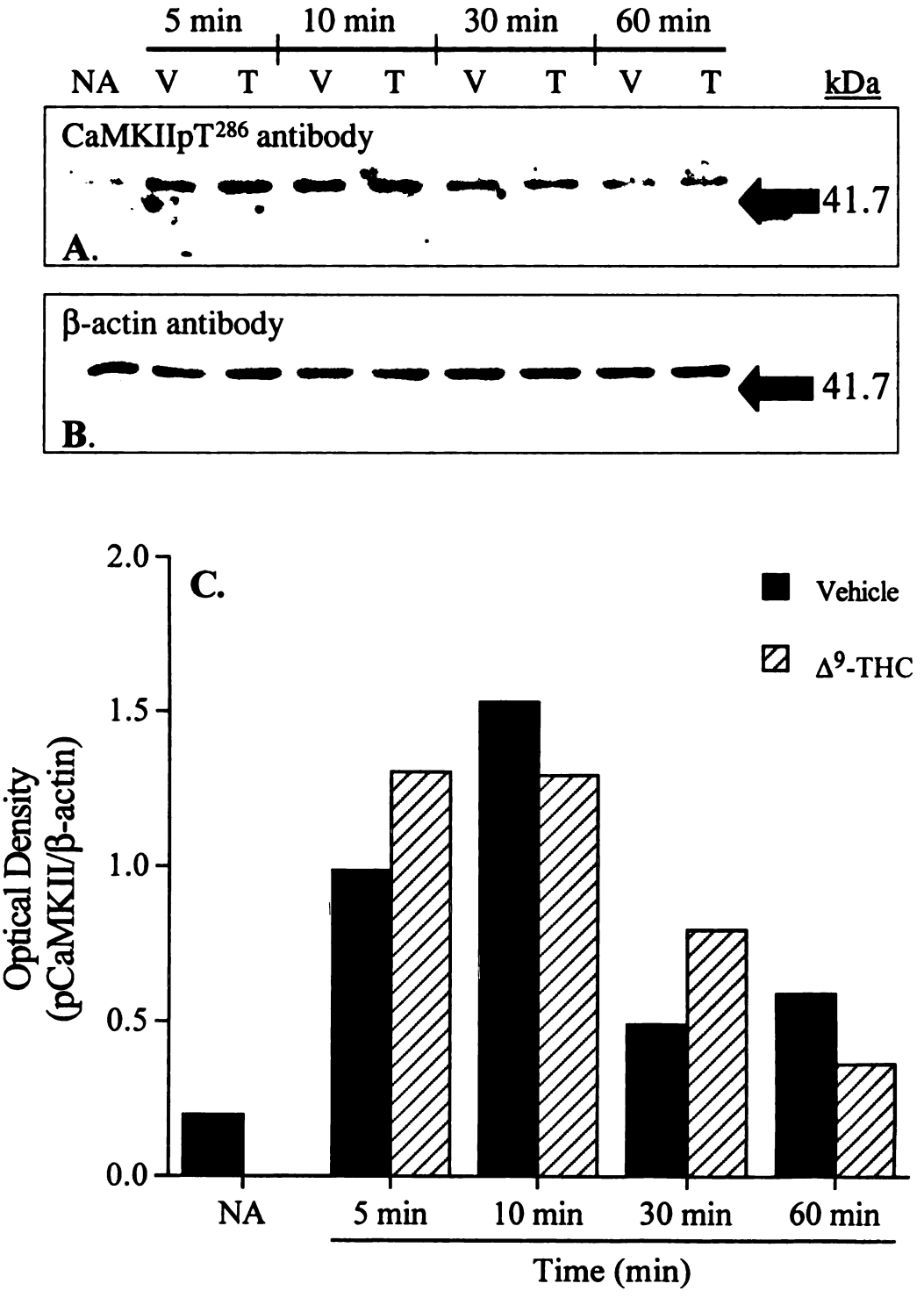

Figure 51. Δ^9-THC treatment does not result in the autophosphorylation of CaMKII.

was dependent on the activation of PLC, PI3K or src family tyrosine kinases, inhibitors of each were used in $[Ca^{2+}]_i$ measurements. HPB-ALL cells were pretreated with Et-18-OCH_3, LY294002, PP2 (1-20 μM) and/or VH for 300 s, to inhibit PLC, PI3K or src family tyrosine kinases respectively, followed by Δ^9-THC addition. It was found that the Δ^9-THC-induced $[Ca^{2+}]_i$ was not inhibited upon pretreatment with either Et-18-OCH_3, LY294002 or PP2 suggesting that Δ^9-THC elevated $[Ca^{2+}]_i$ independently of the aforementioned kinases (figure 52A, B).

F. HPB-ALL cells express transcripts for TRPC1

Results from studies of the effect of OAG on $[Ca^{2+}]_i$ suggested that both OAG and Δ^9-THC functioned through a common mechanism putatively involving TRPC channels. In order to elucidate the putative channel involved in the Δ^9-THC-mediated $[Ca^{2+}]_i$ elevation, RT-PCR was performed for TRPC1-7 in the HPB-ALL cells and the Jurkat E6-1 cells, as a comparison control. RT-PCR results demonstrated that whereas Jurkat E6-1 cells expressed transcripts for TRPC1, 3 and 6, the HPB-ALL cells expressed transcripts only for TRPC1 (figure 53). Interestingly, in addition to the 686 bp predicted TRPC1 amplicon, RT-PCR results demonstrated the presence of a second smaller amplicon in both the HPB-ALL and Jurkat E6-1 cells. The smaller TRPC1 amplicon was sequenced from both HPB-ALL and Jurkat E6-1 cells using TRPC1 forward and reverse primers. Sequencing confirmed that the smaller 532 bp product was an alternative splice variant of TRPC1, which is spliced between nucleotides 309-463 within the TRPC1 coding sequence (data not shown). However, splicing of the 154 bp from within the TRPC1 coding sequence shifts the open reading frame of TRPC1 resulting in a premature stop

Figure 52. Pretreatment with Et-18-OCH_3, LY294002 and PP2 does not attenuate the Δ^9-THC-induced elevation in $[Ca^{2+}]_i$. A 3 ml aliquot of fura-2 loaded HPB-ALL cells was placed into a cuvette with constant stirring. (**A**) Et-18-OCH_3 (1-20 μM) or VH (0.1% EtOH); or (**B**) LY294002 (1-20 μM), PP2 (1-20 μM) or VH (0.1% DMSO) was added directly to the cuvette just prior to beginning $[Ca^{2+}]_i$ measurements. At 300 s, Δ^9-THC (12.5 μM) or VH (0.1% EtOH) was injected into the cuvette and the increase in $[Ca^{2+}]_i$ was measured for a total of 1600 s. $[Ca^{2+}]_i$ changes are presented as the mean ± SEM of the change in base to peak ratio of bound to free Ca^{2+} (340 nm/380 nm) of two (**B**) or three (**A**) independent experiments.

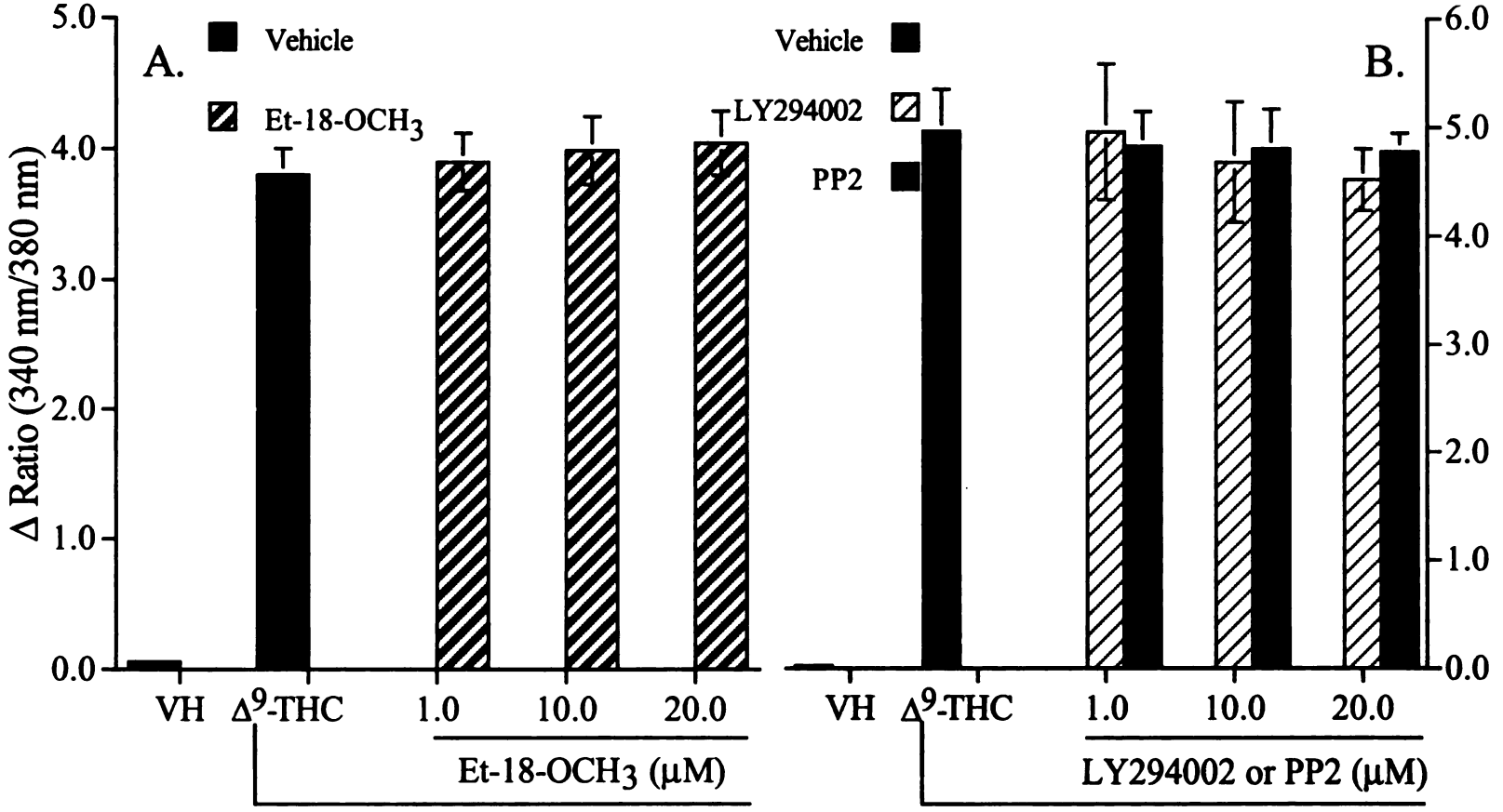

Figure 52. Pretreatment with Et-18-OCH_3, LY294002 and PP2 does not attenuate the Δ^9-THC-induced elevation in $[Ca^{2+}]_i$.

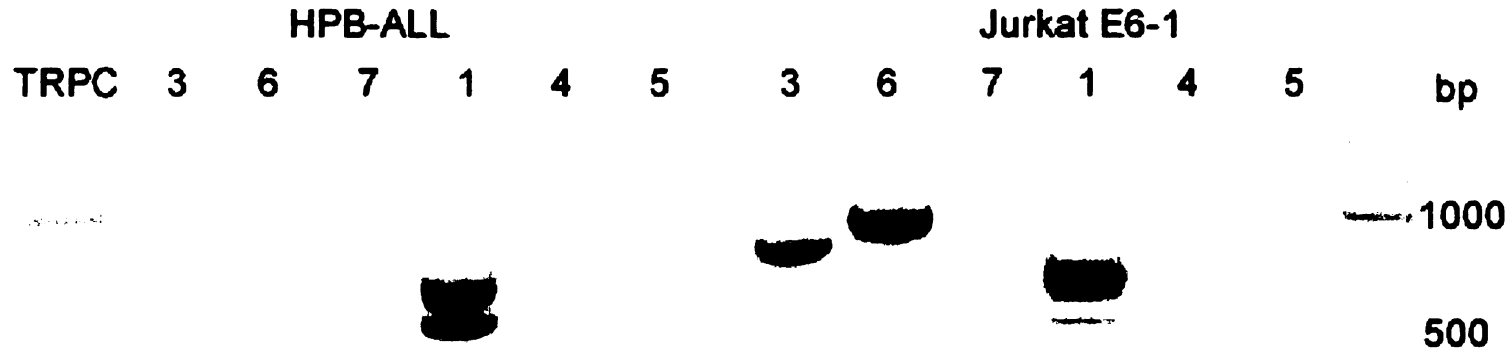

Figure 53. RT-PCR analysis of TRPC1-7 in HPB-ALL and Jurkat E6-1 cells. Total RNA was isolated from HPB-ALL and Jurkat E6-1 cells. Isolated RNA samples were reverse transcribed and assayed for expression of TRPC1-7 mRNA transcripts by PCR. The RNA samples were confirmed to be free of DNA contamination by the absence of product after PCR amplification in the absence of reverse transcriptase. The PCR reaction was performed with 40 amplification cycles using specific primers for TRPC1-7, and resolved on a 1.2% agarose gel. The results are representative of three independent experiments.

codon at nucleotides 491-493.

G. Knockdown of TRPC1 in HPB-ALL cells attenuates the Δ^9-THC-mediated rise in $[Ca^{2+}]_i$

Given that HPB-ALL cells expressed steady-state mRNA for only TRPC1, the involvement of TRPC1 in the Δ^9-THC-mediated rise in $[Ca^{2+}]_i$ was examined using siRNA-mediated gene knockdown. HPB-ALL cells were transiently transfected with siRNA (20 nM) directed against TRPC1 or a non-silencing control sequence. After a 48 h transfection, the cells were harvested, total RNA isolated and real time PCR was performed for TRPC1 and β-actin, as a loading control. Compared to VH (transfection reagent) treatment, the siRNA targeting TRPC1 yielded approximately 50% knockdown in a TRPC1 mRNA level, whereas the non-silencing control siRNA produced no significant change (figure 54A). $[Ca^{2+}]_i$ determination studies were performed in the siRNA transfected cells to determine whether knockdown of TRPC1 affected the elevation in $[Ca^{2+}]_i$ by Δ^9-THC. In accord with the real time PCR results, knockdown of TRPC1 attenuated the Δ^9-THC-induced elevation of $[Ca^{2+}]_i$, whereas the non-silencing control siRNA did not (figure 54B). siRNA directed against TRPC1 typically yielded between 30-50% attenuation of the Δ^9-THC-induced elevation of $[Ca^{2+}]_i$ as compared to VH control. Western blotting analysis to confirm TRPC1 knockdown at the protein level was attempted, but could not be verified due to cross reactivity of the TRPC1 antibody with multiple proteins bands (data not shown).

H. Δ^9-THC elevates $[Ca^{2+}]_i$ in the TRPC1$^{-/-}$ SPLC

Figure 54. siRNA against TRPC1 knocks down the mRNA expression of TRPC1 and the $[Ca^{2+}]_i$ elevation elicited by Δ^9-THC. HPB-ALL cells were transiently transfected with siRNA (20 nM) directed against TRPC1 or a non-silencing control sequence, or treated with transfection medium only (VH) for 48 h. (**A**) Total RNA was isolated, reverse transcribed, and assayed for expression of TRPC1 and β-actin by real time PCR. The relative level of TRPC1 mRNA was standardized to the housekeeping gene, β-actin, and presented as mean ± standard error of the percent knockdown of TRPC1 of VH control. (**B**) A 3 ml aliquot of fura-2 loaded HPB-ALL cells that had undergone a 48 h transient transfection with TRPC1 siRNA, control siRNA, or VH was placed into a cuvette with constant stirring. At 300 s, Δ^9-THC (12.5 μM) or VH (0.1% EtOH) was injected into the cuvette and the increase in $[Ca^{2+}]_i$ was measured for 1600 s. $[Ca^{2+}]_i$ changes are presented as changes in the ratio of bound to free Ca^{2+} (340 nm/380 nm). * $p < 0.05$ as compared to control (**A**) or control/Δ^9-THC (**B**) group. The graphs represent three (**A**) or four (**B**) independent experiments.

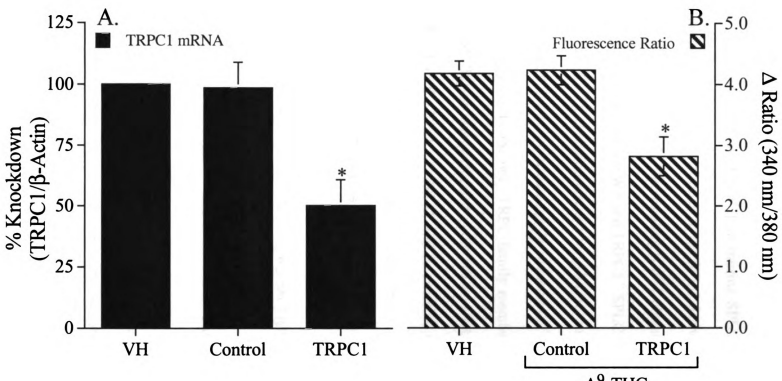

Figure 54. siRNA against TRPC1 knocks down the mRNA expression of TRPC1 and the $[Ca^{2+}]_i$ elevation elicited by Δ^9-THC.

Studies of Δ^9-THC in HPB-ALL cells strongly suggested that the mechanism by which Δ^9-THC elevates $[Ca^{2+}]_i$ involves the TRPC1 channels. In order to investigate whether Δ^9-THC-mediated elevation of $[Ca^{2+}]_i$ in murine SPLC is also dependent on TRPC1, $[Ca^{2+}]_i$ measurements were performed in the SPLC derived from C57BL/6J WT and from TRPC1$^{-/-}$ mice. Interestingly, the resulting $[Ca^{2+}]_i$ elevation elicited by Δ^9-THC (12.5 μM) was not different between the WT and TRPC1$^{-/-}$ SPLC (figure 55). The lack of difference between the $[Ca^{2+}]_i$ elevation elicited by Δ^9-THC in the WT and TRPC1$^{-/-}$ SPLC suggested that TRPC1 was not critical for the induction of $[Ca^{2+}]_i$ elevation by Δ^9-THC, or that TRPC1 may not be the only TRPC family member modulated by by Δ^9-THC. Presently, RT-PCR was also performed in the WT and TRPC1$^{-/-}$ SPLC to confirm the absence of TRPC1 in the TRPC1$^{-/-}$ SPLC, and to examine the expression of other TRPC isoforms. mRNA isolated from WT and TRPC1$^{-/-}$ SPLC was reverse transcribed and amplified for TRPC1-7 and GAPDH, as a comparison control. The results showed that WT SPLC expressed transcripts for TRPC1, 2, 3, 4, and 6 (figure 56). Curiously, however, TRPC1$^{-/-}$ SPLC expressed TRPC2, 3 and 6, but not TRPC4 (figure 56).

IV. Effects of tricyclic cannabinoids and cannabinoid antagonists in the CB1$^{-/-}$/CB2$^{-/-}$ SPLC

A. Δ^9-THC, HU-210 and CBN elevate $[Ca^{2+}]_i$ in the CB1$^{-/-}$/CB2$^{-/-}$ SPLC

Studies of the effects of Δ^9-THC and other tricyclic cannabinoids in the HPB-ALL cells provided the insight that attenuation of cannabinoid-mediated rise in $[Ca^{2+}]_i$ by SR1 or SR2 need not signify dependence on CB1 or CB2. To corroborate the above-mentioned observation that tricyclic cannabinoids, Δ^9-THC, HU-210 and CBN, elevated

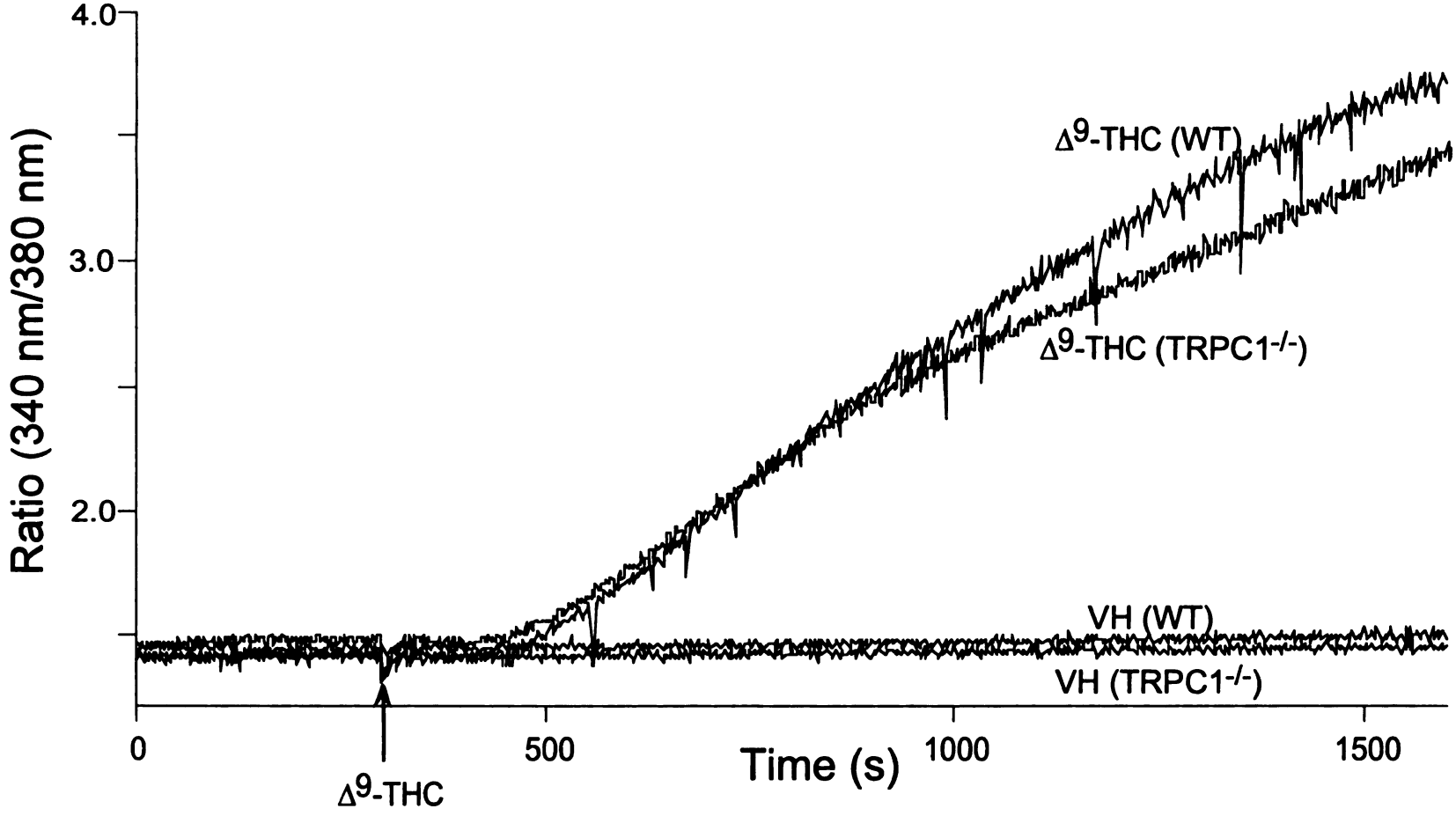

Figure 55. The elevation in $[Ca^{2+}]_i$ by Δ^9-THC is maintained in the TRPC1$^{-/-}$ SPLC. A 3 ml aliquot of fura-2 loaded SPLC from TRPC1$^{-/-}$ or WT C57BL/6J mice was placed into a cuvette with constant stirring. At 300 s, Δ^9-THC (12.5 μM) or VH (0.1% EtOH) was injected into the cuvette and the increase in $[Ca^{2+}]_i$ was measured for a total of 1600 s. $[Ca^{2+}]_i$ changes are presented as changes in the ratio of bound to free Ca^{2+} (340 nm/380 nm). The Ca^{2+} traces represent one experiment.

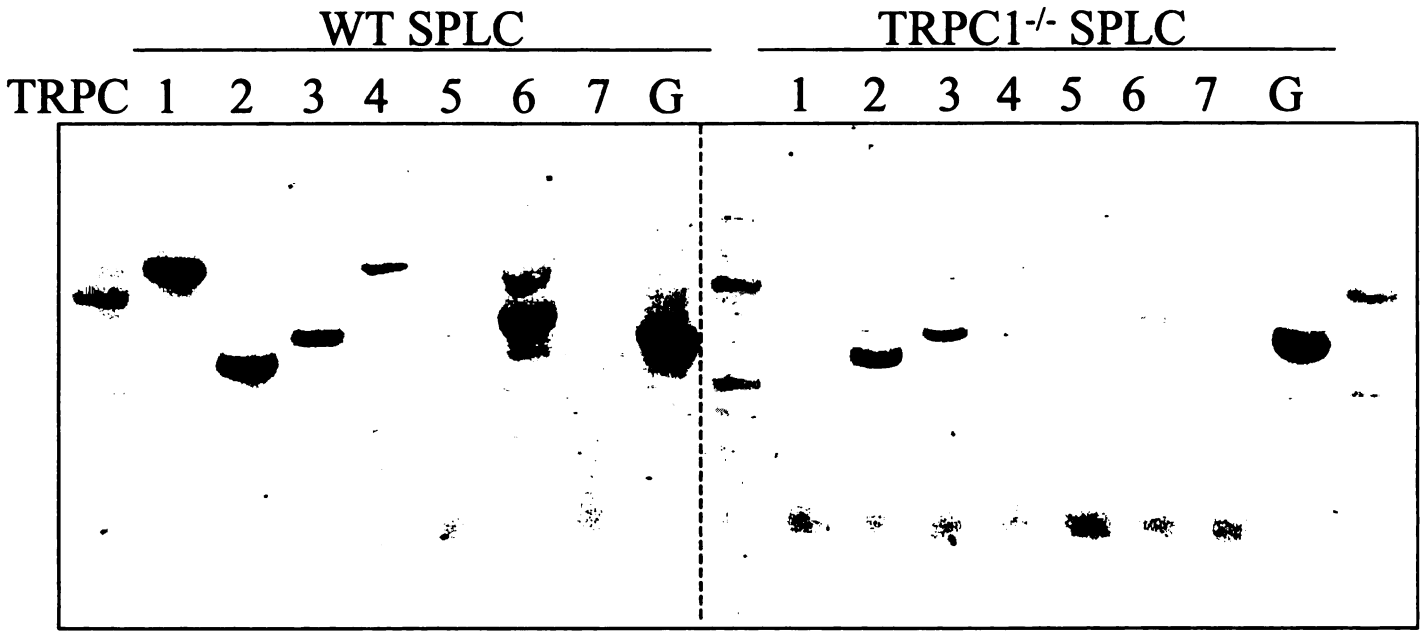

Figure 56. RT-PCR analysis for TRPC1-7 in WT and TRPC1$^{-/-}$ SPLC. Total RNA was isolated from WT (**A**) and TRPC1$^{-/-}$ (**B**) SPLC. Isolated RNA samples were reverse transcribed and assayed for expression of TRPC1-7 or GAPDH (G) mRNA transcripts by PCR. The RNA samples were confirmed to be free of DNA contamination by the absence of product after PCR amplification in the absence of reverse transcriptase. The PCR reaction was performed with 40 amplification cycles using specific primers for TRPC1-7, and resolved on a 1.2% agarose gel. The results are representative of two independent experiments.

$[Ca^{2+}]_i$ independently of either CB1 or CB2, $[Ca^{2+}]_i$ measurements were performed in SPLC derived from C57BL/6J WT and $CB1^{-/-}/CB2^{-/-}$ mice. While the WT SPLC express CB1 and CB2, the $CB1^{-/-}/CB2^{-/-}$ SPLC have been confirmed not to express either receptor (A.E.B. Springs, unpublished observations). Presently, all three tricyclic cannabinoids elicited a robust $[Ca^{2+}]_i$ rise in both WT and of $CB1^{-/-}/CB2^{-/-}$ SPLC (figure 57, 58, 59). At a concentration of 12.5 μM Δ^9-THC elicited $[Ca^{2+}]_i$ rise was robust in magnitude at 426.3 ± 49.4 nM in WT SPLC and 339.8 ± 94.2 nM in $CB1^{-/-}/CB2^{-/-}$ SPLC (n=5). By comparison, at a concentration of 20 μM, the $[Ca^{2+}]_i$ rise elicited HU-210 (272.8 ± 27.7 nM in WT SPLC and 233.6 ± 40.1 nM in $CB1^{-/-}/CB2^{-/-}$ SPLC), and CBN (243.2 ± 39.5 nM in WT SPLC and 323.0 ± 64.2 nM in $CB1^{-/-}/CB2^{-/-}$ SPLC) was smaller in magnitude. Nevertheless, there was no significant difference between the magnitude of $[Ca^{2+}]_i$ elevation elicited by any of the three cannabinoids in the $CB1^{-/-}/CB2^{-/-}$ SPLC and WT SPLC (figure 57, 58, 59). Also consistent with the previous structure-activity relationship studies performed in the HPB-ALL cells, the time delay to onset of $[Ca^{2+}]_i$ rise was varied depending on the cannabinoid. Somewhat surprisingly, the time delay to $[Ca^{2+}]_i$ elevation for 20 μM CBN (55.6 ± 3.2 s in WT SPLC; 50.1 ± 4.8 s in $CB1^{-/-}/CB2^{-/-}$ SPLC; n=5) was much shorter than for either 12.5 μM Δ^9-THC (149.4 ± 7.6 s in WT SPLC; 132.5 ± 14.2 s in $CB1^{-/-}/CB2^{-/-}$ SPLC; n=5) or 20μM HU-210 (140.8 ± 6.8 s in WT SPLC; 145.8 ± 6.1 s in $CB1^{-/-}/CB2^{-/-}$ SPLC; n=5). Once again, although the time delay to onset of $[Ca^{2+}]_i$ elevation varied depending on the cannabinoid, there was no significant variation in time delay between the WT and $CB1^{-/-}/CB2^{-/-}$ SPLC for any of the three compounds. Finally, consistent with the prior observation in B6C3F1 splenic T

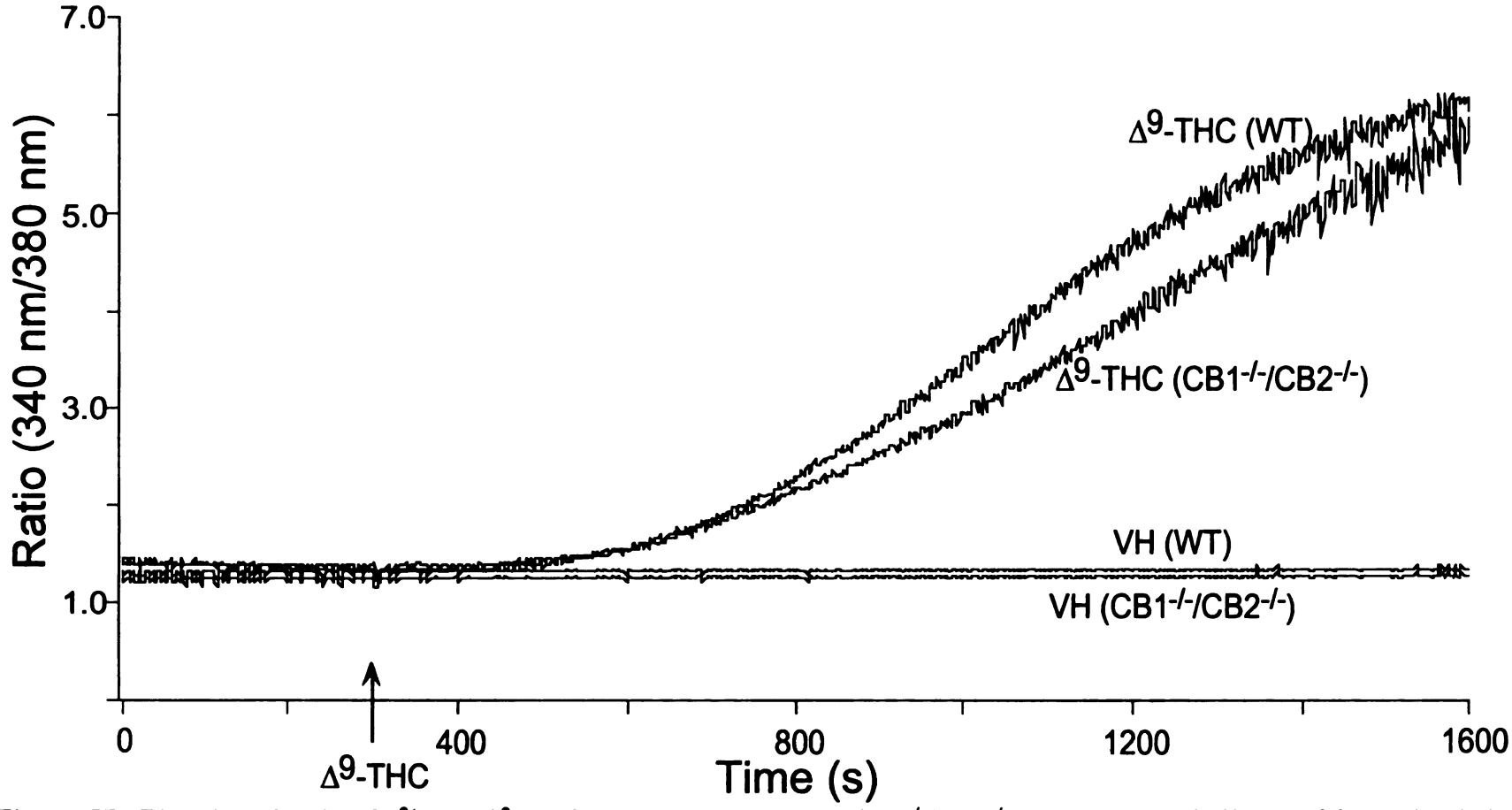

Figure 57. The elevation in $[Ca^{2+}]_i$ by Δ^9-THC is maintained in the CB1$^{-/-}$/CB2$^{-/-}$ SPLC. A 3 ml aliquot of fura-2 loaded SPLC from CB1$^{-/-}$/CB2$^{-/-}$ or WT C57BL/6J mice was placed into a cuvette with constant stirring. At 300 s, Δ^9-THC (12.5 μM) or VH (0.1% EtOH) was injected into the cuvette and the increase in $[Ca^{2+}]_i$ was measured for a total of 1600 s. $[Ca^{2+}]_i$ changes are presented as changes in the ratio of bound to free Ca^{2+} (340 nm/380 nm). The Ca^{2+} traces represent six independent experiments.

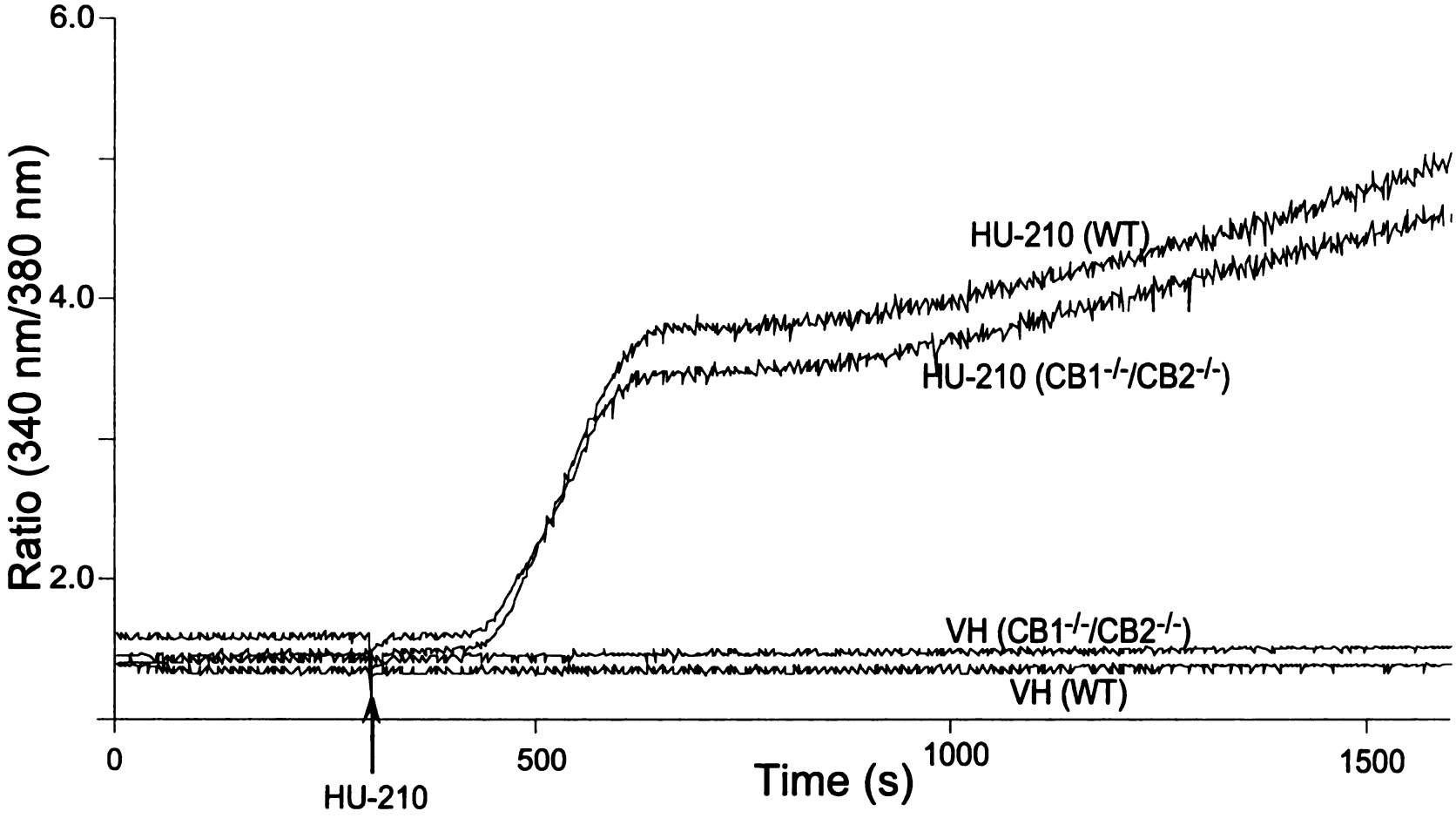

Figure 58. The elevation in $[Ca^{2+}]_i$ by HU-210 is maintained in the CB1$^{-/-}$/CB2$^{-/-}$ SPLC. A 3 ml aliquot of fura-2 loaded SPLC from CB1$^{-/-}$/CB2$^{-/-}$ or WT C57BL/6J mice was placed into a cuvette with constant stirring. At 300 s, HU-210 (20 μM) or VH (0.1% EtOH) was injected into the cuvette and the increase in $[Ca^{2+}]_i$ was measured for a total of 1600 s. $[Ca^{2+}]_i$ changes are presented as changes in the ratio of bound to free Ca^{2+} (340 nm/380 nm). Ca^{2+} traces represent five independent experiments.

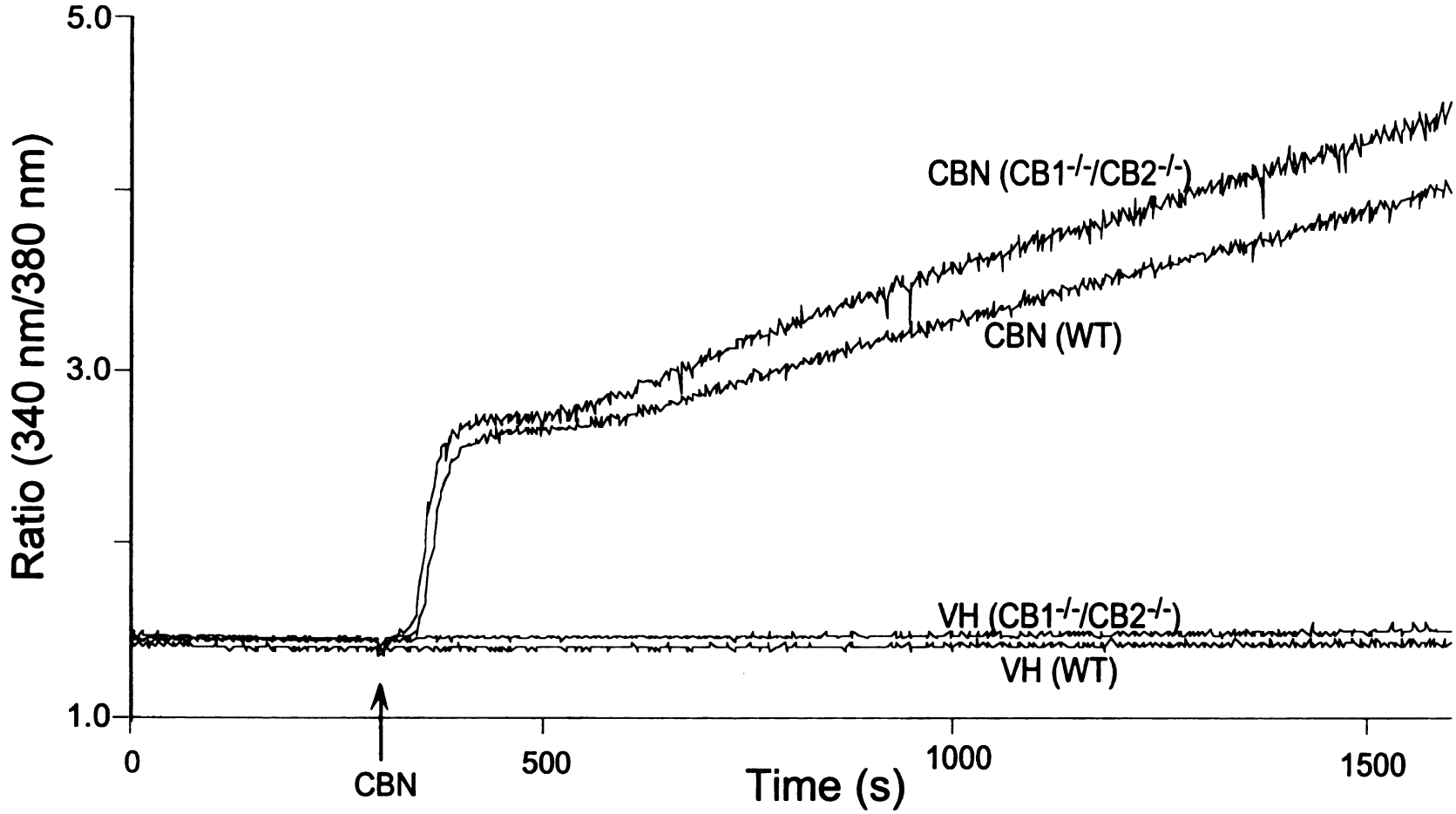

Figure 59. The elevation in $[Ca^{2+}]_i$ by CBN is maintained in the $CB1^{-/-}/CB2^{-/-}$ SPLC. A 3 ml aliquot of fura-2 loaded SPLC from $CB1^{-/-}/CB2^{-/-}$ or WT C57BL/6J mice was placed into a cuvette with constant stirring. At 300 s, CBN (20 μM) or VH (0.1% EtOH) was injected into the cuvette and the increase in $[Ca^{2+}]_i$ was measured for a total of 1600 s. $[Ca^{2+}]_i$ changes are presented as changes in the ratio of bound to free Ca^{2+} (340 nm/380 nm). The Ca^{2+} traces represent five independent experiments.

cells and HPB-ALL cells, the bicyclic cannabinoid, CP, failed to elicit an elevation in $[Ca^{2+}]_i$ in either WT or $CB1^{-/-}/CB2^{-/-}$ SPLC (data not shown).

B. SR1 and SR2 antagonize the tricyclic cannabinoid-mediated elevation of $[Ca^{2+}]_i$ in the $CB1^{-/-}/CB2^{-/-}$ SPLC

To pursue the hypothesis that SR1 and SR2 antagonize the tricyclic cannabinoid-induced $[Ca^{2+}]_i$ elevation in non-CB1 non-CB2 mediated manner, further $[Ca^{2+}]_i$ measurements were performed in WT and $CB1^{-/-}/CB2^{-/-}$ SPLC. SPLC were treated with SR1, SR2 (1-5 μM) or VH for 300 s, followed by Δ^9-THC (12.5 μM), HU-210 (20 μM), or CBN (20 μM). Similar to the prior observations in the HPB-ALL cells, the results in the WT and $CB1^{-/-}/CB2^{-/-}$ SPLC showed that SR1 and SR2 were differentially sensitive at antagonizing the $[Ca^{2+}]_i$ rise induced by different tricyclic cannabinoids. While the Δ^9-THC-mediated $[Ca^{2+}]_i$ rise was sensitive to both SR1 and SR2 (figure 60), the HU-210-induced $[Ca^{2+}]_i$ rise could be antagonized only by SR1, but not SR2, in both WT and $CB1^{-/-}/CB2^{-/-}$ SPLC (figure 61). Also, while SR1 was equally sensitive at antagonizing the HU-210-mediated $[Ca^{2+}]_i$ elevation in both models (figure 61), the Δ^9-THC-induced $[Ca^{2+}]_i$ rise was slightly more sensitive to SR1 than SR2 in the $CB1^{-/-}/CB2^{-/-}$ SPLC (figure 60). More interestingly, both SR1 and SR2 equally and significantly inhibited the CBN-induced $[Ca^{2+}]_i$ elevation only in the $CB1^{-/-}/CB2^{-/-}$ SPLC, but not the WT SPLC (figure 62).

C. Binding of $[^3H]$-SR1 to the $CB1^{-/-}/CB2^{-/-}$ SPLC

Figure 60. The elevation in $[Ca^{2+}]_i$ by Δ^9-THC in $CB1^{-/-}/CB2^{-/-}$ and WT SPLC is antagonized by SR1 and SR2. A 3 ml aliquot of fura-2 loaded SPLC from WT (**A**) or $CB1^{-/-}/CB2^{-/-}$ (**B**) C57BL/6J mice was placed into a cuvette with constant stirring. SR1 (1-5 μM), SR2 (1-5 μM) or VH (0.1% DMSO) was added directly to the cuvette just prior to beginning $[Ca^{2+}]_i$ measurements. At 300 s, Δ^9-THC (12.5 μM) or VH (0.1% EtOH) was injected into the cuvette and the increase in $[Ca^{2+}]_i$ was measured for a total of 1600 s. $[Ca^{2+}]_i$ changes are presented as the mean ± SEM of the change in base to peak ratio of bound to free Ca^{2+} (340 nm/380 nm) of three independent experiments. * $p <$ 0.05 as compared to the respective VH/Δ^9-THC group.

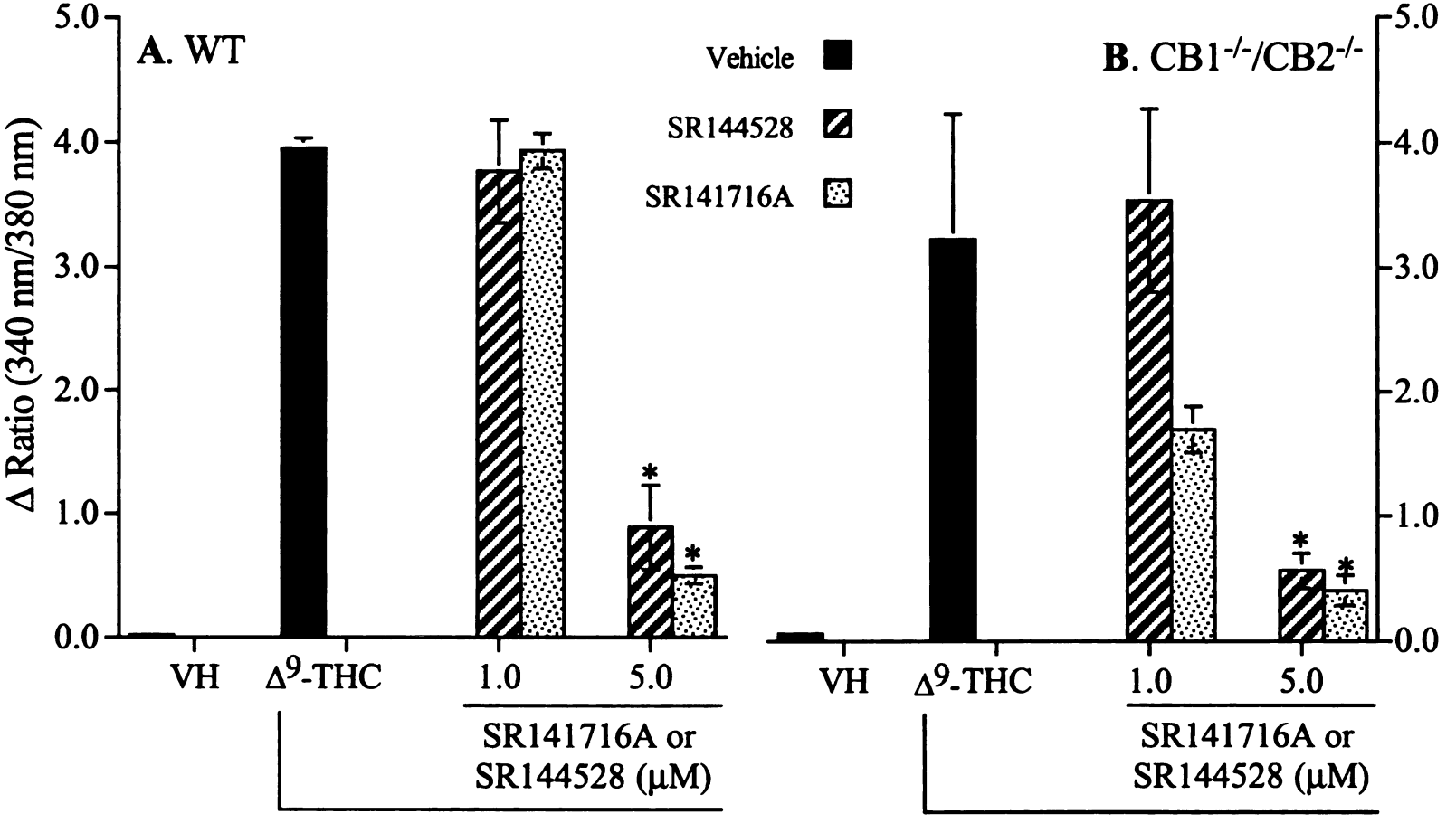

Figure 60. The elevation in $[Ca^{2+}]_i$ by Δ^9-THC in WT and CB1$^{-/-}$/CB2$^{-/-}$ SPLC is antagonized by SR1 and SR2.

Figure 61. The elevation in $[Ca^{2+}]_i$ by HU-210 in $CB1^{-/-}/CB2^{-/-}$ and WT SPLC is antagonized by SR1, but not SR2. A 3 ml aliquot of fura-2 loaded SPLC from WT (**A**) or $CB1^{-/-}/CB2^{-/-}$ (**B**) C57BL/6J mice was placed into a cuvette with constant stirring. SR1 (1-5 μM), SR2 (1-5 μM) or VH (0.1% DMSO) was added directly to the cuvette just prior to beginning $[Ca^{2+}]_i$ measurements. At 300 s, HU-210 (20 μM) or VH (0.1% DMSO) was injected into the cuvette and the increase in $[Ca^{2+}]_i$ was measured for a total of 1600 s. $[Ca^{2+}]_i$ changes are presented as the mean ± SEM of the change in base to peak ratio of bound to free Ca^{2+} (340 nm/380 nm) of three independent experiments. * $p <$ 0.05 as compared to the respective VH/HU-210 group.

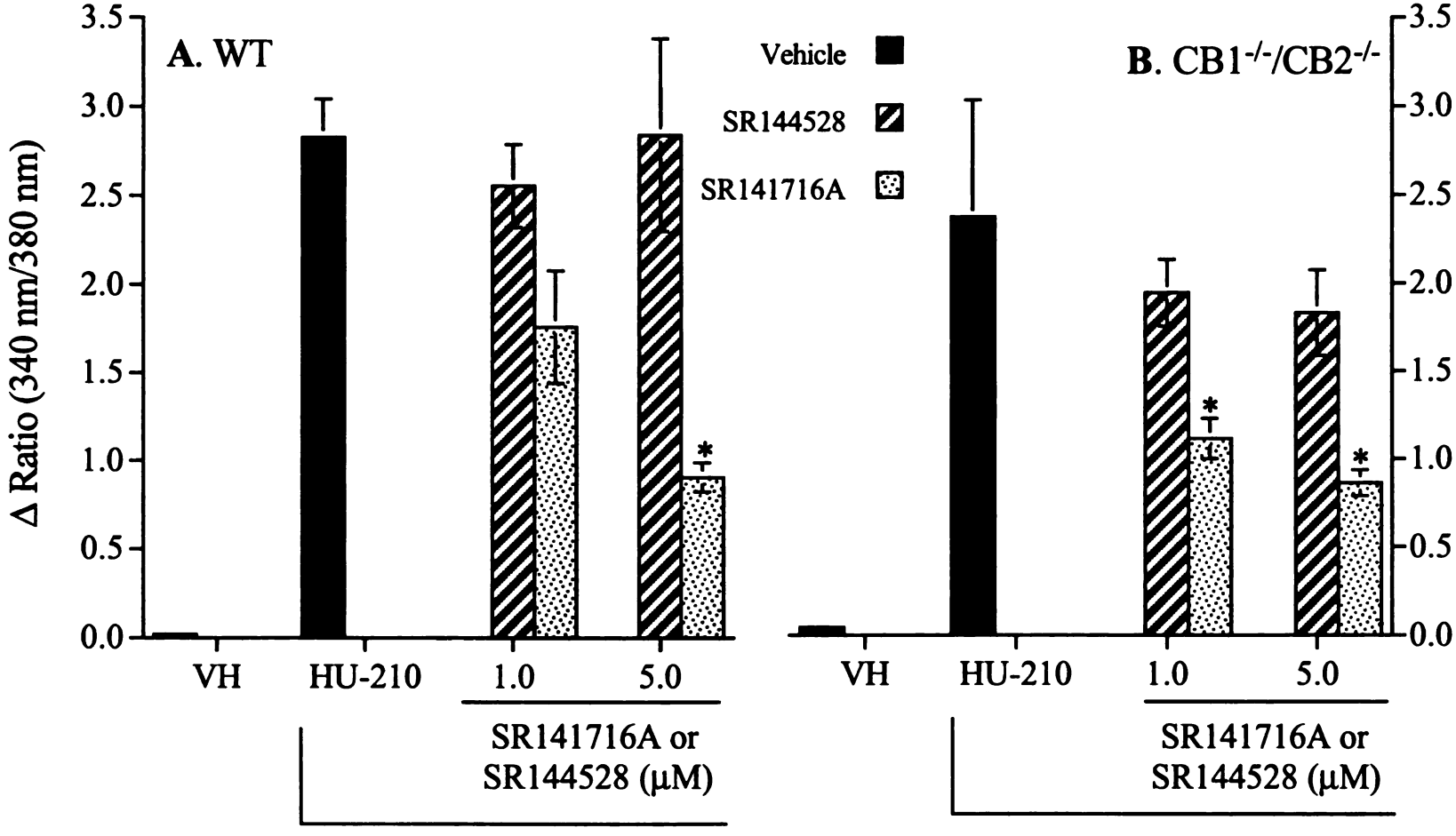

Figure 61. The elevation in $[Ca^{2+}]_i$ by HU-210 in WT and $CB1^{-/-}/CB2^{-/-}$ SPLC is antagonized by SR1, but not SR2.

Figure 62. The elevation in $[Ca^{2+}]_i$ by CBN is antagonized by SR1 and SR2 in the $CB1^{-/-}/CB2^{-/-}$ SPLC, but not WT SPLC. A 3 ml aliquot of fura-2 loaded SPLC from WT (**A**) or $CB1^{-/-}/CB2^{-/-}$ (**B**) C57BL/6J mice was placed into a cuvette with constant stirring. SR1 (1-5 μM), SR2 (1-5 μM) or VH (0.1% DMSO) was added directly to the cuvette just prior to beginning $[Ca^{2+}]_i$ measurements. At 300 s, CBN (20 μM) or VH (0.1% EtOH) was injected into the cuvette and the increase in $[Ca^{2+}]_i$ was measured for a total of 1600 s. $[Ca^{2+}]_i$ changes are presented as the mean ± SEM of the change in base to peak ratio of bound to free Ca^{2+} (340 nm/380 nm) of three independent experiments. * $p < 0.05$ as compared to the respective VH/CBN group.

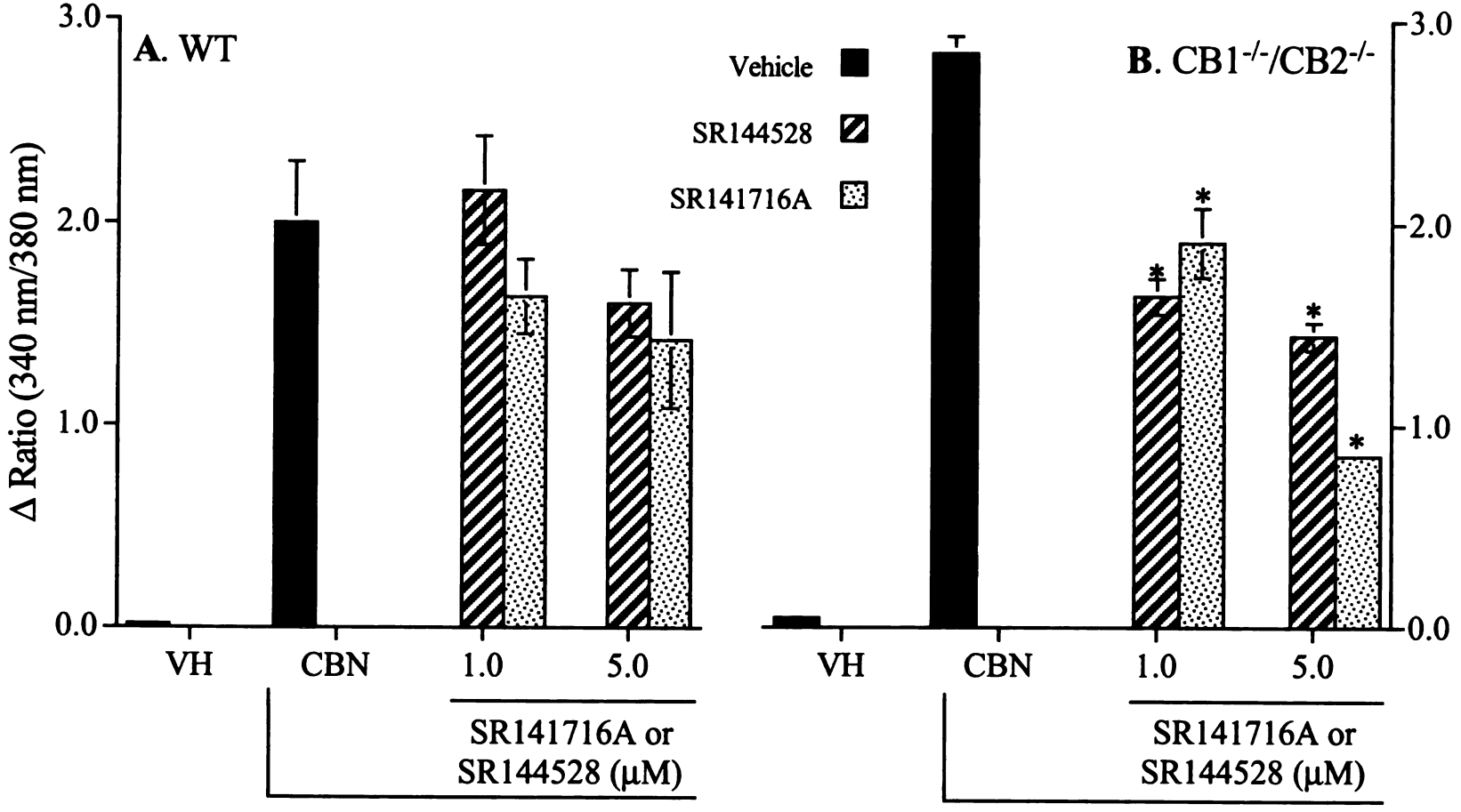

Figure 62. The elevation in $[Ca^{2+}]_i$ by CBN is antagonized by SR1 and SR2 in the $CB1^{-/-}/CB2^{-/-}$ SPLC, but not WT SPLC.

The observation that both SR1 and SR2 attenuate the tricyclic cannabinoid-induced $[Ca^{2+}]_i$ elevation, albeit with differential sensitivities, suggested that the tricyclic cannabinoids and the cannabinoid receptor antagonists may exert their effects on $[Ca^{2+}]_i$ by binding to a novel cannabinoid receptor. To test the above hypothesis, radioligand binding assays were performed using [^{3}H]-SR1 in WT and CB1$^{-/-}$/CB2$^{-/-}$ SPLC. SPLC isolated from WT and CB1$^{-/-}$/CB2$^{-/-}$ spleens were treated with various concentrations of [^{3}H]-SR1 (0.5-80 nM) and allowed to bind for 60 min at 30°C either in the presence (non-specific binding) or absence (total binding) of unlabeled SR1 (10 μM) as a competitor. The resulting total and non-specific isotherms of WT and CB1$^{-/-}$/CB2$^{-/-}$ SPLC are shown in figure 63A and 63B. The amount of non-specific binding of [^{3}H]-SR1 in WT and CB1$^{-/-}$/CB2$^{-/-}$ SPLC was high and closely overlapped total binding. Therefore, the difference between total and non-specific binding, i.e. specific binding, was negligible. The specific binding isotherms of [^{3}H]-SR1 for WT and CB1$^{-/-}$/CB2$^{-/-}$ SPLC are shown in figure 64 and 65, respectively. The specific binding of [^{3}H]-SR1 to WT and CB1$^{-/-}$/CB2$^{-/-}$ SPLC was very modest, and failed to reach saturability even at a concentration of 80 nM.

Figure 63. Total and non-specific binding of [^{3}H]-SR1 to WT and CB1$^{-/-}$/CB2$^{-/-}$ SPLC. SPLC isolated from WT (**A**) and CB1$^{-/-}$/CB2$^{-/-}$ (**B**) C57BL/6J mice were treated with various concentrations of [^{3}H]-SR1 (0.5-80 nM). The SPLC were allowed to bind [^{3}H]-SR1 for 60 min at 30°C either in the presence (for non-specific binding) or absence (for total binding) of unlabeled SR1 (10 μM) as a competitor. Reactions were filtered through glass fiber filters and assayed for ^{3}H using a scintillation counter. The resulting total and non-specific binding isotherms were fitted to a linear regression and graphed as bound [^{3}H]-SR1 vs. free [^{3}H]-SR1 (unbound - bound).

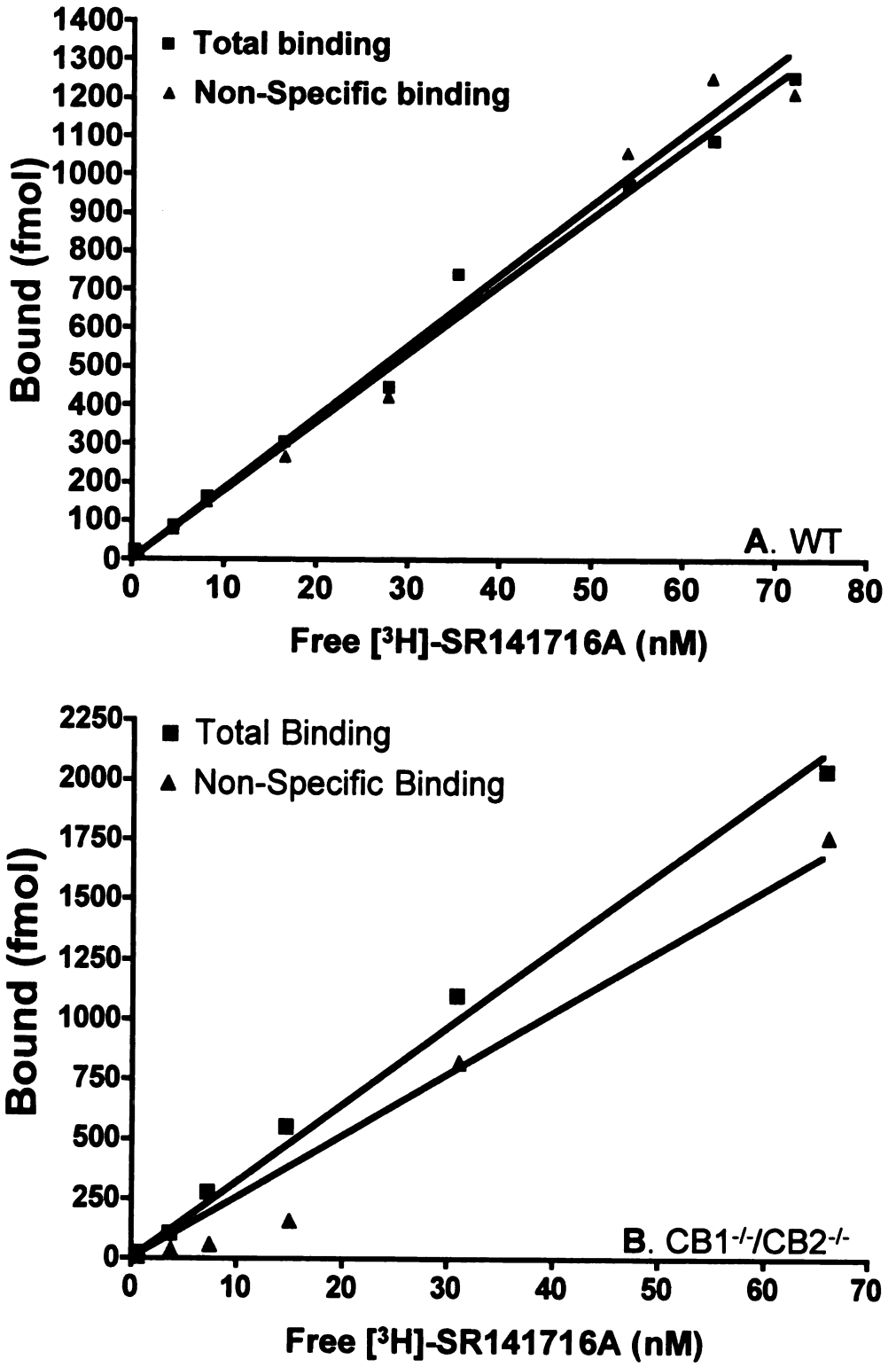

Figure 63. Total and non-specific binding of [^{3}H]-SR1 to WT and CB1$^{-/-}$ /CB2$^{-/-}$ SPLC.

Figure 64. Specific binding of [^{3}H]-SR1 to WT SPLC. The non-specific binding of [^{3}H]-SR1 (in the presence of 10 μM unlabeled SR1) was subtracted from the total binding of [^{3}H]-SR1 to yield the specific binding in WT SPLC. The resulting specific binding isotherm was fitted to a non-linear regression and graphed as specific binding of [^{3}H]-SR1 vs. free [^{3}H]-SR1 (unbound - bound). To estimate the B_{max} (total number of binding sites) and K_d (binding affinity), Scatchard analysis was performed. The resulting Scatchard plot is also shown embedded within the specific binding isotherm.

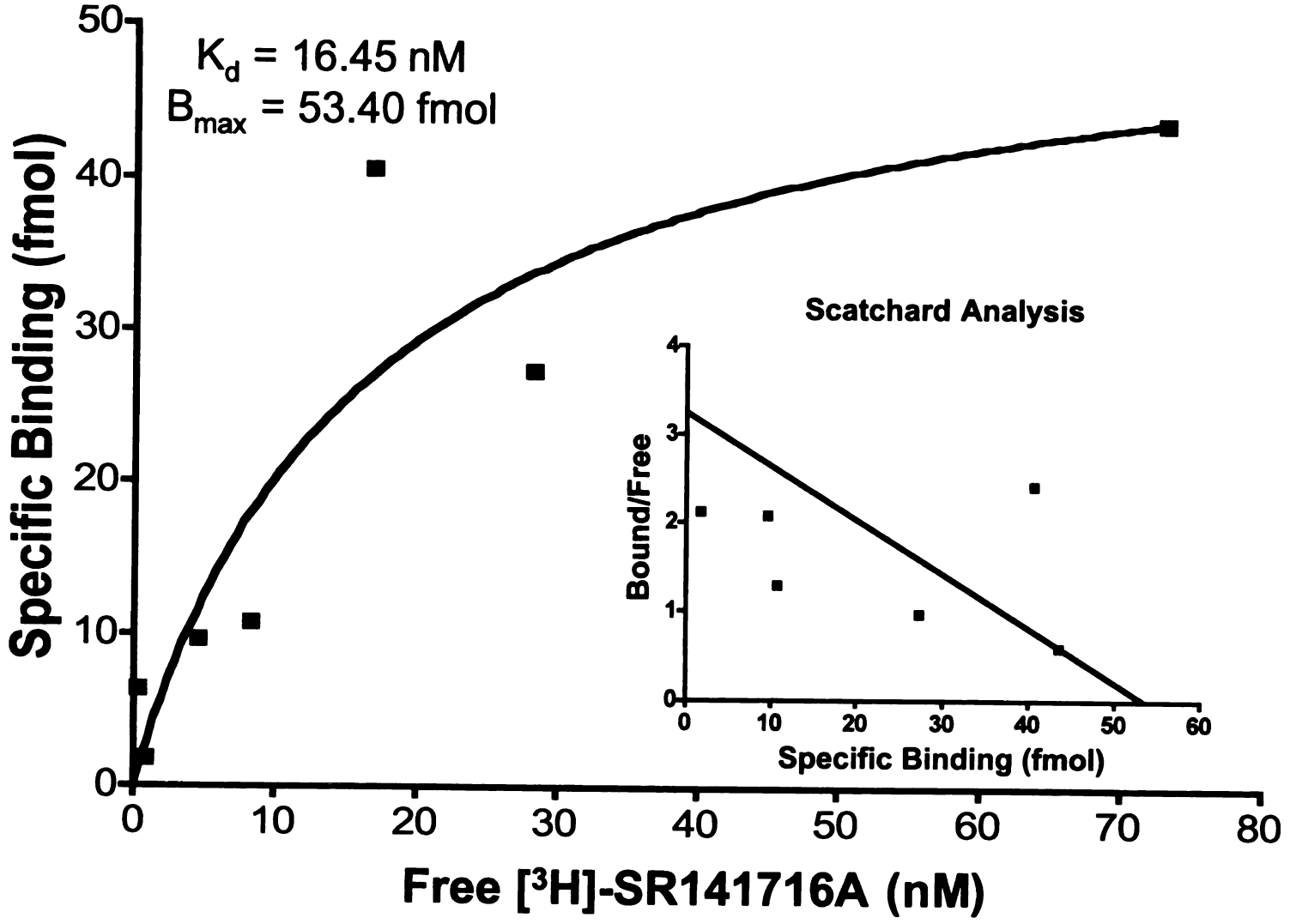

Figure 64. Specific binding of [^{3}H]-SR1 to WT SPLC.

Figure 65. Specific binding of [^{3}H]-SR1 to CB1$^{-/-}$/CB2$^{-/-}$ SPLC. The non-specific binding of [^{3}H]-SR1 (in the presence of 10 μM unlabeled SR1) was subtracted from the total binding of [^{3}H]-SR1 to yield the specific binding in CB1$^{-/-}$/CB2$^{-/-}$ SPLC. The resulting binding isotherm was fitted to a non-linear regression and graphed as specific binding of [^{3}H]-SR1 vs. free [^{3}H]-SR1 (unbound - bound). To estimate the B_{max} (total number of binding sites) and K_d (binding affinity), Scatchard analysis was performed. The resulting Scatchard plot is also shown embedded within the specific binding isotherm.

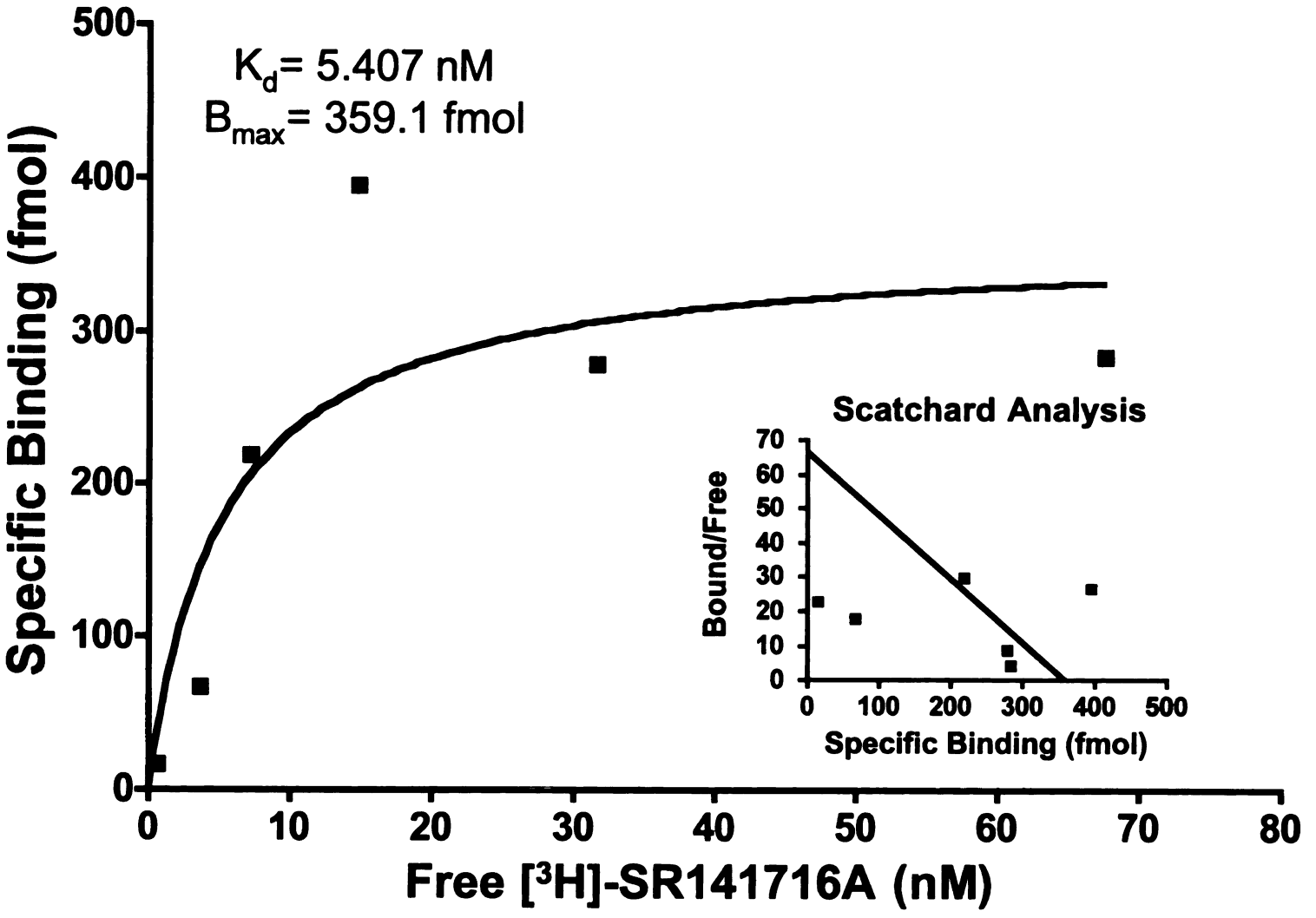

Figure 65. Specific binding of [^{3}H]-SR1 to CB1$^{-/-}$/CB2$^{-/-}$ SPLC.

DISCUSSION

The immunomodulatory effects of cannabinoids have been widely established (Berdyshev, 2000; Condie et al., 1996; Klein et al., 1998; Newton et al., 1998; Schatz et al., 1993). Δ^9-THC, the most extensively characterized cannabinoid, exhibits a broad range of immunomodulatory activity including direct effects on T cell function as evidenced by altered mitogen-induced cell proliferation, suppressed accessory cell function in T cell-dependent antibody responses, and altered production of several T cell-derived cytokines (Condie et al., 1996; Klein et al., 2000a; Newton et al., 1998; Schatz et al., 1993). Although widely studied, the specific mechanism responsible for altered T cell function by cannabinoids remains poorly understood. Therefore, the overall objective of the present dissertation project was to examine the role of the cannabinoid receptors and $[Ca^{2+}]_i$ in the mechanism of altered T cell function by cannabinoid compounds.

I. Effect of Δ^9-THC and CP on IL-2 expression

Work from several laboratories has demonstrated previously that treatment of activated T cells with cannabinoids results in the suppression of IL-2 production and secretion (Berdyshev, 2000; Condie et al., 1996; Klein et al., 2000a; Ouyang and Kaminski, 1999). Based on previous reports showing that HPB-ALL cells express normal sized CB2 transcripts, whereas the Jurkat E6-1 cells express aberrantly sized and putatively non-functional CB2 transcripts, the present set of studies aimed to elucidate the effect of cannabinoids on IL-2 secretion in both HPB-ALL and Jurkat E6-1 cells. In

particular, it was hypothesized that due to putative non-functionality of the CB2 receptor in the Jurkat E6-1 cells, cannabinoids would differentially modulate IL-2 expression in the two cell lines. In accord with the aforementioned hypothesis, Δ^9-THC suppressed IL-2 secretion only in the HPB-ALL cells and had no effect on IL-2 secretion in the Jurkat E6-1 cells. By contrast, the observation that CP, a high-affinity ligand at the CB2 receptor, did not differentially modulate IL-2 secretion suggested that the mechanism of IL-2 suppression by Δ^9-THC was likely independent of any differences in the CB2 receptor between the two cell lines. In fact, sequencing data confirmed that there was 100% homology in the CB2 coding sequence between the HPB-ALL and Jurkat E6-1 cells. Perfect homology of the CB2 coding region in the two cell lines essentially eliminated the possibility that the functional difference between HPB-ALL and Jurkat E6-1 cells in their sensitivity to Δ^9-THC could arise as a result of mutations or alternative splicing of CB2.

Despite the early indications that the suppression of IL-2 by Δ^9-THC and CP was likely independent of the CB2 receptor, IL-2 studies were performed to assess the effects of cannabinoid receptor antagonists. It was found that neither SR1 nor SR2 antagonized the decrease in IL-2 secretion by Δ^9-THC or CP. The lack of sensitivity of Δ^9-THC- and CP-mediated suppression of IL-2 secretion to either cannabinoid receptor antagonist again indicated that both cannabinoids function via non-CB1 non-CB2 mediated mechanisms. The failure of PTx to attenuate the suppression of IL-2 secretion by Δ^9-THC further supported the non-involvement of the CB1 and CB2 receptors in the suppression of IL-2 by cannabinoids.

Altogether several important insights can be gleaned from the studies of the effect of cannabinoids on IL-2 expression in HPB-ALL and Jurkat E6-1 cells. First of all, it is apparent that there is some functional difference between the HPB-ALL and Jurkat E6-1 cells in their sensitivity to Δ^9-THC, but not CP. The present observation that the Jurkat E6-1 cells are insensitive to Δ^9-THC is not unique, and is consistent with a previous report showing that Δ^9-THC failed to inhibit the forskolin-induced cAMP production (Schatz et al., 1997). More importantly, it is also clear that the differential effects of Δ^9-THC on IL-2 secretion in HPB-ALL and Jurkat E6-1 cells cannot be attributed to variations in the CB2 receptor or the associated G proteins. Finally, the observation that Δ^9-THC, but not CP, had differential effects on IL-2 secretion in HPB-ALL and Jurkat E6-1 cells indicates that the two cannabinoids exert their effect on T cells via divergent mechanisms of action, neither of which involve the CB2 receptor.

II. Effect of Δ^9-THC and CP on $[Ca^{2+}]_i$ in T cells

Recent studies investigating the effects of cannabinoids on T cell activation and IL-2 gene expression have identified alterations in NFAT DNA binding and transcriptional activity (Jan et al., 2002; Ouyang et al., 1998; Yea et al., 2000). The regulation of NFAT in T cells is critically dependent on a sustained elevation in $[Ca^{2+}]_i$ induced upon T cell activation (Rao et al., 1997). The critical role for $[Ca^{2+}]_i$ in T cell activation coupled with previous findings that cannabinoid treatment results in disrupted activation of NFAT prompted a comprehensive investigation of the effects of Δ^9-THC and CP on $[Ca^{2+}]_i$ in resting T cells. An initial characterization showed that Δ^9-THC produced a robust and concentration-responsive rise in $[Ca^{2+}]_i$ in purified murine splenic

T cells and HPB-ALL cells, but only a modest rise in $[Ca^{2+}]_i$ in Jurkat E6-1 cells. Moreover, the high affinity cannabinoid agonist, CP, failed to elicit a rise in $[Ca^{2+}]_i$ in all three cell models utilized. It was interesting to note that CP also failed to act as a neutral antagonist on the $[Ca^{2+}]_i$ rise elicited by Δ^9-THC. Together, the failure of CP both to induce an independent $[Ca^{2+}]_i$ elevation and to act as a neutral antagonist on the Δ^9-THC-induced $[Ca^{2+}]_i$ elevation indicated that the mechanism by which Δ^9-THC elevates $[Ca^{2+}]_i$ was likely independent of the CB2 receptor.

Nevertheless, $[Ca^{2+}]_i$ measurements were performed with Δ^9-THC in the presence or absence of SR1 and SR2 in the splenic T cells, HPB-ALL cells and Jurkat E6-1 cells. The ability of SR1 and SR2 to antagonize the elevation of $[Ca^{2+}]_i$ elicited by Δ^9-THC in the splenic T cells and the HPB-ALL cells was surprising given the high affinity cannabinoid ligand, CP, did not elicit a $[Ca^{2+}]_i$ rise in either model. Even more surprising was the finding that SR1 and SR2 did not significantly attenuate the small $[Ca^{2+}]_i$ rise elicited by Δ^9-THC in the Jurkat E6-1 cells. At first glance the inability of SR1 and SR2 to antagonize the $[Ca^{2+}]_i$ rise elicited by Δ^9-THC in the Jurkat E6-1 cells appears to implicate the involvement of the cannabinoid receptors in the Δ^9-THC-mediated $[Ca^{2+}]_i$ rise. However, it must also be noted that antagonism by SR1 and SR2 does not necessarily imply the involvement of CB1 or CB2. Both SR1 and SR2 at concentrations greater than 1 μM may have effects on receptors other than CB1 and CB2 (Pertwee, 1999b, 2005). Moreover, it was observed that both SR1 and SR2 inhibited the rise in $[Ca^{2+}]_i$ by Δ^9-THC in the HPB-ALL cells, despite the fact that the CB1 receptor is not expressed by HPB-ALL cells. Lastly, the elevation of $[Ca^{2+}]_i$ elicited by Δ^9-THC could not be attenuated upon the inactivation of G proteins known to couple the cannabinoid

receptors. Together, the aforementioned studies indicate that the effect of Δ^9-THC on $[Ca^{2+}]_i$ is very likely independent of both CB1 and CB2 receptors.

A salient point that arises out of the studies of $[Ca^{2+}]_i$ elevation by Δ^9-THC and CP is that there may be no functional link between the rise in $[Ca^{2+}]_i$ by cannabinoids and the suppression of IL-2, as initially conjectured. Evidence for the lack of functional link between the two aforementioned effects comes from the observation that while only Δ^9-THC elevated $[Ca^{2+}]_i$, both Δ^9-THC and CP suppressed IL-2 secretion in the HPB-ALL cells (table 3, 4). If $[Ca^{2+}]_i$ elevation was critical to the mechanism of IL-2 suppression, CP would not suppress IL-2 secretion. Moreover, the sensitivity of the Δ^9-THC-mediated $[Ca^{2+}]_i$ rise to both SR1 and SR2 further severs any possible connection between the elevation of $[Ca^{2+}]_i$ and the suppression of IL-2, as the decrease in IL-2 by both Δ^9-THC and CP was insensitive to either SR1 or SR2 (table 3, 4). The present data argue, therefore, that there are at least two modes of action for cannabinoids in T cells: one leading to the suppression of IL-2 and another leading to the elevation of $[Ca^{2+}]_i$ (figure 66). Additionally, it is apparent that only certain cannabinoids are able to function through the latter mode. All successive studies with Δ^9-THC and other cannabinoids were performed in an attempt to characterize the second mode of action, i.e. the mechanism of $[Ca^{2+}]_i$ elevation.

III. Effect of $[Ca^{2+}]_e$ removal and BAPTA-AM on the Δ^9-THC induced $[Ca^{2+}]_i$ elevation

In an effort to elucidate the manner in which Δ^9-THC robustly elevates $[Ca^{2+}]_i$ in the splenic T cells and HPB-ALL cells, $[Ca^{2+}]_i$ measurements were performed either in

Table 3. Summary of the effects of cannabinoid agonists on IL-2 secretion and $[Ca^{2+}]_i$ in various cell models used

Agonist	Response Measured	Cell Model	Effect
Δ^9-THC	PMA/Io-stimulated IL-2 secretion	HPB-ALL cells	Suppression
		Jurkat E6-1 cells	No effect
	$[Ca^{2+}]_i$	Splenic T cells	Elevation
		HPB-ALL cells	Elevation
		Jurkat E6-1 cells	Elevation
		WT SPLC	Elevation
		$CB1^{-/-}/CB2^{-/-}$ SPLC	Elevation
CP	PMA/Io-stimulated IL-2 secretion	HPB-ALL cells	Suppression
		Jurkat E6-1 cells	Suppression
	$[Ca^{2+}]_i$	Splenic T cells	No effect
		HPB-ALL cells	No effect
		Jurkat E6-1cells	No effect
		WT SPLC	No effect
		$CB1^{-/-}/CB2^{-/-}$ SPLC	No effect
CBN	$[Ca^{2+}]_i$	HPB-ALL cells	Elevation
		WT SPLC	Elevation
		$CB1^{-/-}/CB2^{-/-}$ SPLC	Elevation
HU-210	$[Ca^{2+}]_i$	HPB-ALL cells	Elevation
		WT SPLC	Elevation
		$CB1^{-/-}/CB2^{-/-}$ SPLC	Elevation
AEA	$[Ca^{2+}]_i$	HPB-ALL cells	No effect
2-AG	$[Ca^{2+}]_i$	HPB-ALL cells	No effect
JWH-133	$[Ca^{2+}]_i$	HPB-ALL cells	No effect
CBD	$[Ca^{2+}]_i$	HPB-ALL cells	Small elevation

Table 4. Summary of the effects of antagonists on cannabinoid-induced suppression of IL-2 secretion and $[Ca^{2+}]_i$ elevation in various cell models used

Antagonist	Response Measured	Cell Model	Effect
SR144528	Δ^9-THC-induced IL-2 suppression	HPB-ALL cells	No effect
	CP-induced IL-2 suppression	HPB-ALL cells	No effect
		Jurkat E6-1 cells	No effect
	Δ^9-THC-induced $[Ca^{2+}]_i$ elevation	Splenic T cells	Inhibition
		HPB-ALL cells	Inhibition
		Jurkat E6-1 cells	No effect
		WT SPLC	Inhibition
		$CB1^{-/-}/CB2^{-/-}$ SPLC	Inhibition
	HU-210-induced $[Ca^{2+}]_i$ elevation	HPB-ALL cells	Inhibition
		WT SPLC	Inhibition
		$CB1^{-/-}/CB2^{-/-}$ SPLC	Inhibition
	CBN-induced $[Ca^{2+}]_i$ elevation	HPB-ALL cells	Inhibition
		WT SPLC	Inhibition
		$CB1^{-/-}/CB2^{-/-}$ SPLC	Inhibition
	CBD-induced $[Ca^{2+}]_i$ elevation	HPB-ALL cells	No effect
SR141716A	Δ^9-THC-induced IL-2 suppression	HPB-ALL cells	No effect
	CP-induced IL-2 suppression	HPB-ALL cells	No effect
		Jurkat E6-1 cells	No effect
	Δ^9-THC-induced $[Ca^{2+}]_i$ elevation	Splenic T cells	Inhibition
		HPB-ALL cells	Inhibition
		Jurkat E6-1 cells	No effect
		WT SPLC	Inhibition
		$CB1^{-/-}/CB2^{-/-}$ SPLC	Inhibition
	HU-210-induced $[Ca^{2+}]_i$ elevation	HPB-ALL cells	Inhibition
		WT SPLC	Inhibition
		$CB1^{-/-}/CB2^{-/-}$ SPLC	Inhibition
	CBN-induced $[Ca^{2+}]_i$ elevation	HPB-ALL cells	Inhibition
		WT SPLC	Inhibition
		$CB1^{-/-}/CB2^{-/-}$ SPLC	Inhibition

Figure 66. Putative model of cannabinoid-mediated $[Ca^{2+}]_i$ regulation and suppression of IL-2 expression. Based on the findings in the present dissertation, a model by which tricyclic cannabinoids regulate $[Ca^{2+}]_i$ is proposed. CB_x represents a novel cannabinoid receptor at which tricyclic cannabinoids are agonists and SR1 and SR2 are neutral antagonists. Prot X represents a putative protein that may form a functional link between CB_x and TRPC1. Some of the possible effects that may result due to a premature elevation in $[Ca^{2+}]_i$ in T cells are also listed. In addition, the model also depicts the severing of any direct link between elevation of $[Ca^{2+}]_i$ and suppression of IL-2 expression. The current model does not illustrate a mechanism by which cannabinoids suppress IL-2 expression, as both the receptor and the precise downstream pathways involved remain elusive.

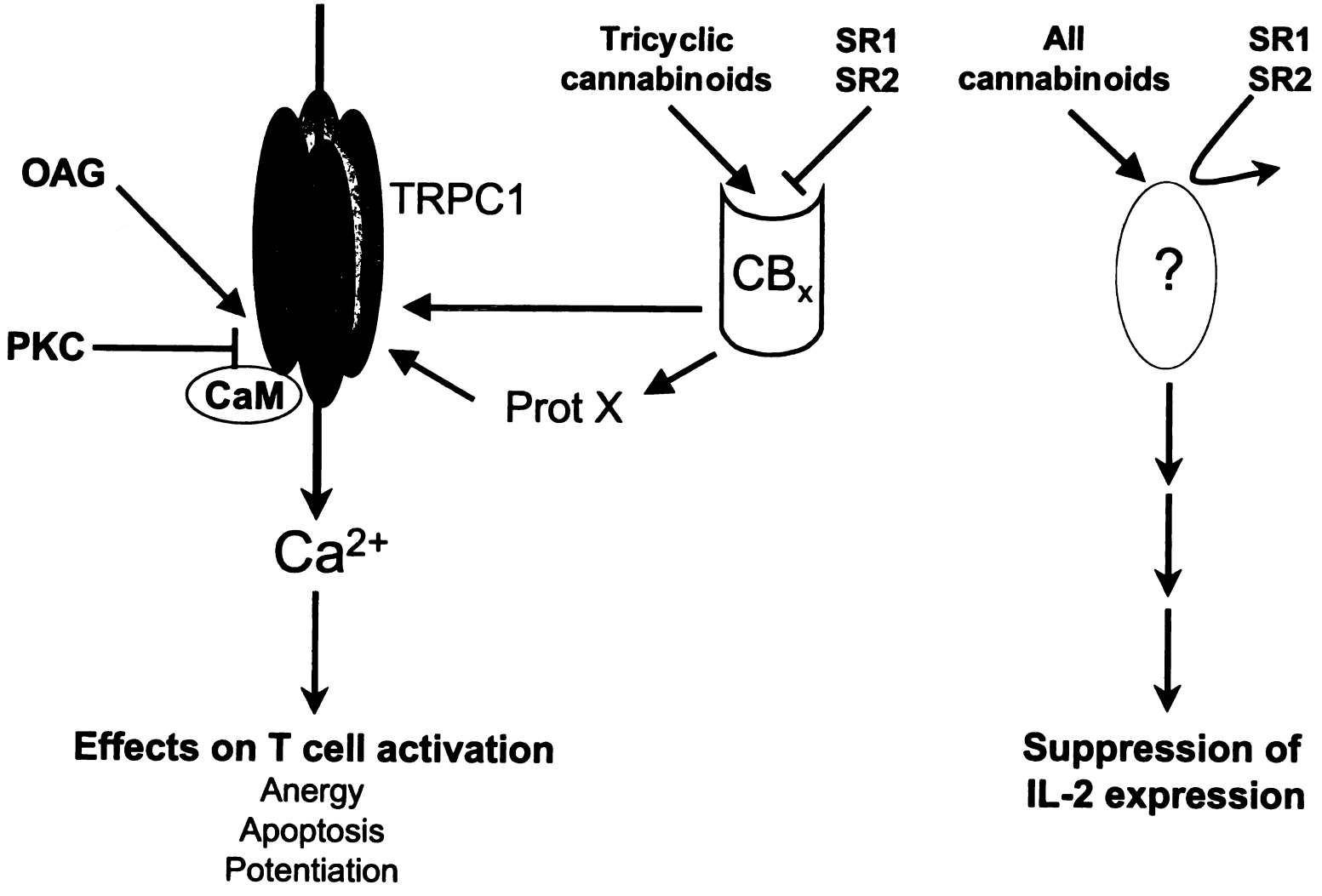

Figure 66. Model of cannabinoid-mediated $[Ca^{2+}]_i$ regulation and suppression of IL-2 production in the HPB-ALL cells.

the absence of $[Ca^{2+}]_e$ or in the presence of BAPTA-AM. In both splenic T cells and the HPB-ALL cells, the removal of $[Ca^{2+}]_e$ potently abrogated the Δ^9-THC-mediated $[Ca^{2+}]_i$ rise, leaving behind a small and delayed $[Ca^{2+}]_i$ rise. Interestingly, SR2 completely attenuated the small $[Ca^{2+}]_i$ rise elicited by Δ^9-THC in the absence of $[Ca^{2+}]_e$, suggesting the rise in $[Ca^{2+}]_i$ was an influx of residual $[Ca^{2+}]_e$. Furthermore, the characteristics of the delayed $[Ca^{2+}]_i$ rise elicited by Δ^9-THC in the absence of $[Ca^{2+}]_e$ were incongruous with Ca^{2+}-store release-mediated Ca^{2+} entry in lymphocytes (Lewis, 2001). In addition, the observation that Δ^9-THC-induced a $[Ca^{2+}]_i$ rise in BAPTA-AM loaded cells also suggested that the mechanism of Δ^9-THC-mediated $[Ca^{2+}]_i$ elevation was independent of Ca^{2+} stores. The significantly smaller elevation in $[Ca^{2+}]_i$ elicited by Δ^9-THC in BAPTA-AM loaded cells signifies Ca^{2+} entry from the extracellular space, which is buffered upon entry into the cytosol by free BAPTA-AM. Together, the studies of Δ^9-THC in the absence of $[Ca^{2+}]_e$ and the presence of BAPTA-AM strongly allude to the understanding that the Δ^9-THC-mediated elevation of $[Ca^{2+}]_i$ occurs entirely through $[Ca^{2+}]_e$ influx, and is independent of Ca^{2+}-store release.

IV. Effect of other cannabinoids on $[Ca^{2+}]_i$

Given the above observation that the tricyclic cannabinoid, Δ^9-THC, but not the bicyclic cannabinoid, CP, elevated $[Ca^{2+}]_i$, additional studies were performed to test the hypothesis that only tricyclic cannabinoids elicit an $[Ca^{2+}]_i$ elevation in T cells. It was found that treatment of HPB-ALL cells with HU-210 and CBN, classical tricyclic cannabinoids with structural similarity to Δ^9-THC, resulted in a $[Ca^{2+}]_i$ elevation. There were several similarities between the $[Ca^{2+}]_i$ elevations elicited by Δ^9-THC, HU-210 and

CBN. First, the elevation of $[Ca^{2+}]_i$ by all three cannabinoids was concentration-responsive. Second, the removal of $[Ca^{2+}]_e$ strongly abrogated the $[Ca^{2+}]_i$ rise elicited by HU-210 and CBN to a similar degree to that observed with Δ^9-THC. Next, the $[Ca^{2+}]_i$ elevation elicited by Δ^9-THC, HU-210 and CBN occurred after a significant time delay to onset. Finally, the $[Ca^{2+}]_i$ rise elicited by the three cannabinoids was sensitive to antagonism by SR1 and SR2. It is intriguing that Δ^9-THC, HU-210 and CBN all elevate $[Ca^{2+}]_i$ in an SR1- and SR2-sensitive manner in the HPB-ALL cells, especially since the HPB-ALL cells do not express the CB1 receptor. The ability of SR1 to attenuate $[Ca^{2+}]_i$ elevation indicates that both SR1 and SR2 antagonize some yet unknown cannabinoid receptor in T cells. The inability of CP, AEA, 2-AG and the CB2-selective agonist, JWH-133, to elevate $[Ca^{2+}]_i$ in the HPB-ALL cells further implies that the rise in $[Ca^{2+}]_i$ elicited by tricyclic cannabinoids is mediated by a novel cannabinoid receptor.

Despite the apparent similarities between the profile of $[Ca^{2+}]_i$ elevation of Δ^9-THC, HU-210 and CBN, many differences also exist. First and foremost, the time delay to onset of $[Ca^{2+}]_i$ elevation for HU-210 was significantly longer than for either CBN or Δ^9-THC at all concentrations used. The significance of the varying time delays to onset of $[Ca^{2+}]_i$ rise is presently unclear, but it is speculated that the time to onset may represent a signaling delay needed for gating a cell-surface Ca^{2+} channel. The significantly longer delay to onset for HU-210 in comparison with CBN or Δ^9-THC may also suggest that HU-210 is less efficacious at coupling with an effector critical for the induction of a $[Ca^{2+}]_i$ rise. It is interesting and important to note, however, that HU-210 has not previously been reported to be less efficacious at either CB1 or CB2 as compared with any other cannabinoid. Another factor differentiating the $[Ca^{2+}]_i$ responses of HU-210

and CBN from that elicited by Δ^9-THC was the differential sensitivity to SR1 and SR2. While the Δ^9-THC and CBN-induced $[Ca^{2+}]_i$ elevation was attenuated by both antagonists with similar sensitivities, the HU-210-mediated $[Ca^{2+}]_i$ elevation was more sensitive to SR1 than to SR2. It is currently not known why the SR1 and SR2 are differentially sensitive in antagonizing the $[Ca^{2+}]_i$ elevation elicited by the aforementioned cannabinoids.

It is tempting to speculate, given the $[Ca^{2+}]_i$ responses of Δ^9-THC, CBN and HU-210, that only cannabinoid compounds possessing tricyclic structures with a central pyran ring can elicit a rise in $[Ca^{2+}]_i$ in T cells. The inability of CP, AEA and 2-AG to elevate $[Ca^{2+}]_i$ in HPB-ALL cells support the aforementioned hypothesis. However, it must also be noted that existence of a tricyclic structure and a pyran ring are, by themselves, insufficient to induce a $[Ca^{2+}]_i$ elevation, as established with the tricyclic cannabinoid, JWH-133. Currently, it is postulated that only cannabinoids that possess Δ^9-THC-like three ring structures are able to robustly increase $[Ca^{2+}]_i$. Clearly, the modifications to the aliphatic chain and the additional functional groups on the mono-unsaturated cyclohexyl ring present on HU-210 did not produce an increased efficacy to elevate $[Ca^{2+}]_i$, over Δ^9-THC. Moreover, it is also apparent that there are other non-SR1/SR2-sensitive mechanisms of $[Ca^{2+}]_i$ elevation in T cells. CBD, which is neither an agonist for the cannabinoid receptors nor a tricyclic cannabinoid, modestly elevated $[Ca^{2+}]_i$, but through a mechanism distinct from the tricyclic cannabinoids. Compared to the tricyclic cannabinoids, the magnitude of the CBD-induced elevation of $[Ca^{2+}]_i$ was very modest. In addition, the CBD-induced $[Ca^{2+}]_i$ rise was not concentration-responsive, rapid and biphasic, involving both Ca^{2+} store-release and $[Ca^{2+}]_e$ influx phases. Evidently, further

in-depth studies are necessary to understand the complex structure-activity of cannabinoid compounds on $[Ca^{2+}]_i$ elevation in T cells.

V. Effect of Ca^{2+} channel inhibitors and store-depletion on the Δ^9-THC-induced $[Ca^{2+}]_i$ elevation

The primary mechanism of Ca^{2+} influx in T cells is by SOCE and is mediated by the CRAC channels (Lewis, 2001). However, preliminary studies with cannabinoids found that the mechanism of $[Ca^{2+}]_i$ entry was independent of Ca^{2+} store-depletion. Therefore, additional studies were performed to investigate the mechanism of $[Ca^{2+}]_i$ elevation by Δ^9-THC in the HPB-ALL cells. The first set of studies aimed at elucidating the class of Ca^{2+} channels involved in the elevation by Δ^9-THC. To gain additional insight and as a comparison, studies utilizing Ca^{2+} channel inhibitors were performed side-by-side with TG and Δ^9-THC. Interestingly, while SKF proved to be a potent inhibitor of the Δ^9-THC-mediated elevation in $[Ca^{2+}]_i$, SKF only modestly inhibited the TG-induced $[Ca^{2+}]_i$ rise. Conversely, 2-APB potently inhibited the TG-induced $[Ca^{2+}]_i$ elevation, but was rather weak at inhibiting the Δ^9-THC-mediated $[Ca^{2+}]_i$ elevation. Together, the results from the Ca^{2+} channel inhibitor studies suggested that whereas TG elicits an $[Ca^{2+}]_i$ rise through the SOCCs, Δ^9-THC likely utilizes the ROCCs.

To address further the contrasting effects of SKF and 2-APB on the Δ^9-THC- and TG-induced $[Ca^{2+}]_i$ elevation, studies were performed with $LaCl_3$. While generally, lanthanide cations are considered to be SOCC inhibitors, they are also known to inhibit TRPC channels at high concentrations (Aussel et al., 1996; Beech et al., 2003; Trebak et al., 2003b). Presently, the finding that $LaCl_3$ markedly inhibited the TG-induced rise in

$[Ca^{2+}]_i$ at low concentrations, and the Δ^9-THC-mediated elevation of $[Ca^{2+}]_i$ at higher concentrations, confirmed that TG functions through SOCCs and that Δ^9-THC utilizes the ROCCs, putatively from within the TRPC subfamily.

Having observed that the Δ^9-THC-mediated $[Ca^{2+}]_i$ elevation was sensitive to SKF, the effect of SKF on HU-210- and CBN-induced $[Ca^{2+}]_i$ elevation was also assessed. SKF significantly inhibited the HU-210- and CBN-mediated elevation in $[Ca^{2+}]_i$ suggesting again that all three tricyclic cannabinoids activate ROCCs. Once again, the HU-210-induced rise in $[Ca^{2+}]_i$ was differentially sensitive to SKF than that induced by Δ^9-THC or CBN. While SKF potently inhibited Δ^9-THC- and CBN-mediated $[Ca^{2+}]_i$ rise, SKF was only partially inhibitory on the HU-210-mediated rise in $[Ca^{2+}]_i$ even at high concentrations. It is unclear why the HU-210-induced $[Ca^{2+}]_i$ rise was less sensitive to treatment with SKF, but the reason may be related to the previous observation that HU-210 is less efficacious at eliciting a $[Ca^{2+}]_i$ rise then either Δ^9-THC or CBN. Nevertheless, experiments with SKF illustrate that the tricyclic cannabinoids elicit a rise in $[Ca^{2+}]_i$, at least partially, through ROC channels in T cells.

Apart from the effect of Ca^{2+} channel inhibitors, the effect Ca^{2+} store-depletion was also assessed on the Δ^9-THC-mediated $[Ca^{2+}]_i$ rise. Store-depletion was induced with TG and followed by Δ^9-THC treatment. The results showed that Δ^9-THC elicited a $[Ca^{2+}]_i$ rise that was additive with the store-depletion induced $[Ca^{2+}]_e$ influx. The additive nature of the Δ^9-THC- and TG-induced $[Ca^{2+}]_i$ rise strongly argues that the effects of Δ^9-THC and TG on $[Ca^{2+}]_i$ were mutually exclusive and unrelated. A corollary of the aforementioned result is that Δ^9-THC treatment does not lead to releases of TG-sensitive intracellular Ca^{2+} pools. Moreover, the lack of inhibition of the Δ^9-THC-

induced increase in $[Ca^{2+}]_i$ upon pretreatment with 8-Br-cADPR also argues against the release of any non-TG-sensitive intracellular Ca^{2+} pools by Δ^9-THC.

Recent studies investigating the store-dependent and -independent mechanisms of Ca^{2+} entry in non-excitable cells have focused on the TRP channel superfamily, and specifically on the TRPC channel subfamily. Various groups have conjectured that TRPC channels may operate either as ROCCs or SOCCs (Beech et al., 2003; Mori et al., 2002; Philipp et al., 2003; Singh et al., 2000; Sydorenko et al., 2003; Trebak et al., 2003b; Vazquez et al., 2003). Consistent with the results from the present studies, several reports have demonstrated that TRPC channels are sensitive to high concentrations of both lanthanide compounds, as well as 2-APB (Beech et al., 2003; Trebak et al., 2002; Trebak et al., 2003b). Along with the aforementioned reports, the results from the current investigation demonstrating the partial sensitivity of Δ^9-THC- and TG-induced $[Ca^{2+}]_i$ elevation to SOC and ROC inhibitors, respectively, may suggest that the signaling mechanisms regulating SOC and ROC entry may indeed converge onto the same channel. Nevertheless, it remains to be fully resolved whether the SOCCs and ROCCs are distinct proteins, or the same channels regulated by alternate signaling mechanisms.

VI. Effect of TRPC channel activators and inhibitors on the Δ^9-THC-induced $[Ca^{2+}]_i$ elevation

In light of the finding that Δ^9-THC-mediated elevation in $[Ca^{2+}]_i$ was independent of store-depletion and sensitive to SKF and high concentrations of $LaCl_3$, the involvement of TRPC channels therein was examined. Recently, analogs of DAG have

been demonstrated to activate four members of the TRPC subfamily, namely TRPC1, 3, 6 and 7 independently of PKC (Beech et al., 2003; Gamberucci et al., 2002; Hofmann et al., 1999; Lintschinger et al., 2000; Trebak et al., 2003b). Presently, the rapid and robust elevation in $[Ca^{2+}]_i$ produced by OAG confirmed the presence of DAG-gated channels in HPB-ALL cells. In addition, the non-additivity of OAG and Δ^9-THC upon sequential addition implied that both compounds function through a common TRPC channel. Furthermore, the possibility that OAG inhibited a subsequent Δ^9-THC-mediated $[Ca^{2+}]_i$ rise by activating PKC was eliminated by the lack of abrogation of the non-additivity of OAG and Δ^9-THC under conditions PKC downregulation. The non-involvement of PKC in the OAG-induced $[Ca^{2+}]_i$ rise is consistent with a prior report demonstrating that the activation of TRPC3 by OAG was independent of PKC (Trebak et al., 2003a). Nonetheless, the TRPC channel activated by Δ^9-THC is clearly sensitive to PKC activation, as short-term activation of PKC with PMA modestly attenuated the Δ^9-THC-induced $[Ca^{2+}]_i$ elevation. In sum, it is evident that non-additivity of OAG and Δ^9-THC does not result due to the activation of PKC, but very likely implies that both compounds function through the same TRPC channel (figure 66).

Utilizing enzyme inhibitors, the involvement of various enzymes in the elevation of $[Ca^{2+}]_i$ by Δ^9-THC was examined. $[Ca^{2+}]_i$ measurements performed with Et-18-OCH_3, PP2, LY294002, KN-93 and KN-92 showed that only the CaMKII inhibitors, KN-93 and KN-92, were effective at attenuating the Δ^9-THC-induced $[Ca^{2+}]_i$ increase. These results implied that while PLC, PI3K and src family tyrosine kinases were not involved in the regulation of the TRPC channels by Δ^9-THC, CaMKII was putatively involved. Although intriguing, CaMKII has not previously been implicated in the activation or

inhibition of TRPC channels. Upon examination of CaMKII activity utilizing both an activation assay as well as Western analysis, it was found that Δ^9-THC treatment does not result in CaMKII autophosphorylation or activation. It is proposed that the sensitivity of the Δ^9-THC-induced $[Ca^{2+}]_i$ increase to both KN-93 and KN-92 implies that CaM, and not CaMKII, is involved in the regulation of TRPC channels activated by Δ^9-THC. The KN compounds were originally developed to inhibit CaMKII by way of competing for the CaM binding domain on the enzyme (Sumi et al., 1991). While CaMKII is not implicated in TRPC channel function, CaM has been reported to bind and negatively regulate all members of the TRPC subfamily (Vennekens et al., 2002). Therefore, it is proposed that KN-93 and KN-92 competitively associate with the CaM binding domains within the TRPC channels and thereby inhibit the Δ^9-THC-induced $[Ca^{2+}]_i$ increase.

Collectively, studies of TRPC channel activators and inhibitors provide pharmacological evidence that the HPB-ALL cells express ROCCs in the TRPC subfamily. The TRPC channels activated by Δ^9-THC are gated by OAG in a manner independent of PKC. PLC, PI3K and src family tyrosine kinases, enzymes previously implicated in the regulation of TRPC channels, are clearly uninvolved in the mechanism of Δ^9-THC-induced $[Ca^{2+}]_i$ elevation. Nevertheless, the non-additivity of OAG- and Δ^9-THC-induced $[Ca^{2+}]_i$ elevations, coupled with the inhibitory effects upon PKC activation or treatment with KN-93 and KN-92 strongly implicate the involvement of ROC channels in the TRPC subfamily in the $[Ca^{2+}]_i$ rise mediated by Δ^9-THC (figure 66).

VII. Involvement of TRPC1 channels in the Δ^9-THC-induced $[Ca^{2+}]_i$ elevation

With strong pharmacological evidence that the Δ^9-THC-induced $[Ca^{2+}]_i$ elevation was mediated by a member of the TRPC subfamily, RT-PCR was performed in the HPB-ALL and Jurkat E6-1 cells for TRPC1-7. RT-PCR analysis for TRPC subfamily genes showed that while Jurkat E6-1 cells express transcripts for TRPC1, 3 and 6; HPB-ALL cells express transcripts only for TRPC1. The endogenous expression of TRPC1 in the absence of other TRPC subfamily members was, in itself, somewhat surprising because TRPC1 is generally thought to function in tandem with other TRPC proteins (Beech et al., 2003). Further, siRNA-mediated knockdown of TRPC1 demonstrated that both the expression of TRPC1 mRNA and the Δ^9-THC-mediated rise in $[Ca^{2+}]_i$ were attenuated. These results established a clear role for TRPC1 in the Δ^9-THC-mediated rise in $[Ca^{2+}]_i$ in the HPB-ALL cells. However, the above knockdown results do not eliminate the possibility that other proteins are involved in the elevation of $[Ca^{2+}]_i$ by Δ^9-THC because transfection of siRNA against TRPC1 did not result in attenuation of mRNA expression or $[Ca^{2+}]_i$ rise by more than 50%. Regardless, the sole expression of TRPC1 in HPB-ALL cells coupled with the TRPC1 knockdown studies strongly indicate that the Δ^9-THC-induced elevation of $[Ca^{2+}]_i$ is mediated, at least in part, by TRPC1 functioning as a ROC channel.

Interestingly, whereas in the HPB-ALL cells Δ^9-THC-induced elevation of $[Ca^{2+}]_i$ was clearly dependent on the TRPC1 channels, no difference was observed in the $[Ca^{2+}]_i$ rise elicited by Δ^9-THC in the WT or TRPC1$^{-/-}$ SPLC. A lack of difference in the $[Ca^{2+}]_i$ elevation by Δ^9-THC in the WT and TRPC1$^{-/-}$ SPLC suggested that TRPC1 was critical for Δ^9-THC-induced $[Ca^{2+}]_i$ elevation only in the HPB-ALL cells, and that this finding did not hold true across different cell models. It is possible that in the absence of TRPC1,

Δ^9-THC-induces an elevation of $[Ca^{2+}]_i$ through alternative TRPC proteins. In fact, the expression of several other TRPC subfamily proteins was documented in both the WT and TRPC1$^{-/-}$ SPLC. It is proposed that other TRPC proteins may compensate for TRPC1 in the TRPC1$^{-/-}$ SPLC. Alternatively, under conditions where several TRPC proteins are expressed, Δ^9-THC may normally activate one of the other TRPC proteins instead.

Taken together, it is apparent that although TRPC1 channels are involved in the Δ^9-THC-induced increase in $[Ca^{2+}]_i$, TRPC1 does not fully account for the effects of Δ^9-THC on $[Ca^{2+}]_i$. Several observations support the above conclusion. First, because the siRNA knockdown of TRPC1 did not fully attenuate TRPC1 mRNA expression or the $[Ca^{2+}]_i$ rise by Δ^9-THC, it cannot be unequivocally stated the TRPC1 solely mediates the effects of Δ^9-THC on $[Ca^{2+}]_i$. Second, no difference was observed in the Δ^9-THC-mediated $[Ca^{2+}]_i$ rise between the WT and TRPC1$^{-/-}$ SPLC. Finally, in Jurkat E6-1 cells, which express TRPC1, 3 and 6, the magnitude of $[Ca^{2+}]_i$ elevation by Δ^9-THC was modest in comparison with the HPB-ALL cells. Therefore, the overall conclusion from the studies of the mechanism of $[Ca^{2+}]_i$ elevation by Δ^9-THC is that OAG-sensitive TRPC1 channels are at least partially responsible for the Δ^9-THC-induced $[Ca^{2+}]_i$ elevation in the HPB-ALL cells. In other cell models, however, other TRPC channels or alternative mechanisms of TRPC channel regulation may be involved.

VIII. Effect of tricyclic cannabinoids and the cannabinoid antagonists on $[Ca^{2+}]_i$ in the CB1$^{-/-}$/CB2$^{-/-}$ SPLC

Preliminary experiments in the human and murine T cells with various cannabinoids and cannabinoid receptor antagonists provided circumstantial evidence to suggest that the effects of the tricyclic cannabinoids on $[Ca^{2+}]_i$, although sensitive to SR1 and SR2, may not be mediated by either CB1 or CB2. Therefore, the present set of studies using SPLC from WT or $CB1^{-/-}/CB2^{-/-}$ mice aimed to elucidate whether the $[Ca^{2+}]_i$ elevation induced by Δ^9-THC, HU-210 and CBN occurred independently of CB1 and CB2. The finding that the Δ^9-THC-, HU-210- and CBN-induced $[Ca^{2+}]_i$ elevation was not significantly different between the WT and $CB1^{-/-}/CB2^{-/-}$ SPLC provided conclusive evidence that the classical tricyclic cannabinoids function independently of both cannabinoid receptors to elicit $[Ca^{2+}]_i$. Furthermore, studies of Δ^9-THC-, HU-210- and CBN-induced $[Ca^{2+}]_i$ elevation with either SR1 or SR2 in the WT and $CB1^{-/-}/CB2^{-/-}$ SPLC showed that the cannabinoid receptor antagonists can antagonize the $[Ca^{2+}]_i$ response, even in the absence of CB1 and CB2. The results from the $[Ca^{2+}]_i$ measurements with SR1 and SR2 provided a clear and unequivocal indication both SR1 and SR2 antagonize the cannabinoid-induced $[Ca^{2+}]_i$ elevation via action at sites distinct from CB1 and CB2.

Several broad insights can be gained from the $[Ca^{2+}]_i$ studies performed with the tricyclic cannabinoid compounds and the cannabinoid receptor antagonists in the WT and $CB1^{-/-}/CB2^{-/-}$ SPLC. First and foremost, Δ^9-THC, HU-210, CBN, SR1 and SR2 all have activity at sites distinct and unrelated to CB1 or CB2. Second, antagonism of cannabinoid responses with SR1 and SR2 does not necessarily imply dependence on CB1 or CB2 receptors. Although SR1 and SR2 have been illustrated previously to exert effects on non-cannabinoid receptors, the present dissertation work provides the first such

report in lymphocytes. Next, the parallel observations in the WT and $CB1^{-/-}/CB2^{-/-}$ SPLC as well as the HPB-ALL cells showing that the tricyclic cannabinoid-mediated $[Ca^{2+}]_i$ elevation is differentially sensitive to SR1 and SR2 may imply that the different classical tricyclic cannabinoids have varying affinities, efficacies or mechanisms of action at the novel cannabinoid receptor. Another insight gained from the WT and $CB1^{-/-}/CB2^{-/-}$ SPLC, coupled with previous investigation in the HPB-ALL cells, is that CP, AEA and 2-AG, the non-tricyclic cannabinoid agonists, likely do not have activity at the novel cannabinoid binding site in T cells. The final extrapolation from the studies of $[Ca^{2+}]_i$ in the $CB1^{-/-}/CB2^{-/-}$ SPLC is that any difference in the sensitivity to cannabinoids, or in the $[Ca^{2+}]_i$ rise elicited by Δ^9-THC in the HPB-ALL and Jurkat E6-1 cells cannot be attributed to the CB2 receptor. In short, the present results strongly suggest that Δ^9-THC and structurally-related tricyclic cannabinoids mediate their action on $[Ca^{2+}]_i$ via non-CB1 non-CB2 receptors in T cells, and that SR1 and SR2 can act as neutral antagonists at the novel cannabinoid receptors (figure 66).

With the assumption that SR1 and SR2 can act as neutral antagonists at the novel cannabinoid receptor, radioligand binding analysis was performed with $[^3H]$-SR1 in WT and $CB1^{-/-}/CB2^{-/-}$ SPLC. Unfortunately, $[^3H]$-SR1 failed to exhibit significant specific and saturable binding in either WT or $CB1^{-/-}/CB2^{-/-}$ SPLC. The low amount of specific binding of $[^3H]$-SR1 is attributed to the high degree of non-specific binding of $[^3H]$-SR1 in both WT and $CB1^{-/-}/CB2^{-/-}$ SPLC. The failure of $[^3H]$-SR1 to display the characteristics of a specific ligand for the novel cannabinoid receptor may also be attributed to the high lipophilicity of $[^3H]$-SR1, high $[^3H]$-SR1 concentrations required to elicit binding, and relatively low density of cannabinoid receptor expression in SPLC.

Collectively, the present dissertation work supports the conclusion that Δ^9-THC and related tricyclic classical cannabinoids function through a novel cannabinoid binding site, distinct from CB1 and CB2, to elicit a robust influx of $[Ca^{2+}]_e$ in T cells. However, the identity of the new cannabinoid receptor in T cells remains to be resolved.

IX. **Significance and relevance**

The significance of the work presented in the current dissertation project to the broader field of cannabinoid biology is multifold. The present project demonstrates systematically that tricyclic cannabinoids, and Δ^9-THC in particular, elicit an elevation in $[Ca^{2+}]_i$ in T cells through $[Ca^{2+}]_e$ influx in a manner independent of store-release, which is, at least partially, dependent on TRPC1. Several novel and unique findings are implicit in the above-mentioned demonstration. First, the finding that Δ^9-THC and other tricyclic cannabinoids can elevate $[Ca^{2+}]_i$ independently of Ca^{2+} stores in T cells is surprising, where the primary mechanism of $[Ca^{2+}]_i$ elevation involves SOCE (Lewis, 2001). Although non-SOCE-mediated $[Ca^{2+}]_i$ elevation has been previously reported in lymphocytes (Gamberucci et al., 2002), the present studies are the first to demonstrate that cannabinoid compounds may elevate $[Ca^{2+}]_i$ through a non-SOCE mechanism. In addition to providing evidence that tricyclic cannabinoids elevate $[Ca^{2+}]_i$ independent of SOCE, the present dissertation also offers valuable insights into one putative mechanism of receptor-operated Ca^{2+} entry in T cells.

A second significant finding in the present dissertation with regard to cannabinoid biology is the demonstration of the structure-activity relationship of cannabinoids and $[Ca^{2+}]_i$ elevation in T cells. The current studies are the first to show that tricyclic

cannabinoids have effects on $[Ca^{2+}]_i$ that cannot be reproduced with non-tricyclic cannabinoids. With consideration to cannabinoid biology, the differential effects of tricyclic and non-tricyclic cannabinoids on T cells imply that a uniform mechanism of action cannot be applied to all cannabinoid compounds. Work presented in the current project suggests that cannabinoid compounds of differing structures act via divergent mechanisms to elicit their effects on lymphocytes. The divergent mechanisms of action may converge to elicit the same end result, as seen with IL-2 suppression by Δ^9-THC and CP in HPB-ALL cells, or alternatively may be completely independent of one another, as demonstrated by the effects of Δ^9-THC and CP on $[Ca^{2+}]_i$. The implications of the finding that different cannabinoids may act via divergent mechanisms are far-reaching particularly because many of the early studies with cannabinoid compounds presupposed that all cannabinoids act via the same mode of action. The present project shows indisputably that all cannabinoids do not act alike, and that the initial assumption of a uniform mechanism of action for structurally diverse cannabinoids may have to be reexamined.

Another central finding presented in the current work is that the tricyclic cannabinoid-induced $[Ca^{2+}]_i$ increase was independent of either CB1 or CB2, the two known and widely-studied cannabinoid receptors. The existence of a structure-activity relationship of cannabinoids on $[Ca^{2+}]_i$ coupled with the ability of tricyclic cannabinoids to elicit a $[Ca^{2+}]_i$ elevation in the $CB1^{-/-}/CB2^{-/-}$ mouse SPLC strongly suggests that receptors other than CB1 and CB2 are present in lymphocytes which mediate the actions of cannabinoids. Studies in other organ systems have already suggested the existence of receptors other than CB1 and CB2 (Breivogel et al., 2001; Offertaler et al., 2003; Mo et

al., 2004; Wiley and Martin, 2002). Whereas the novel cannabinoid receptors described in the brain and peripheral vasculature were described to be PTx-sensitive and, therefore, G protein-coupled, the insensitivity of the Δ^9-THC-induced $[Ca^{2+}]_i$ elevation to PTx in the HPB-ALL cells suggests that the novel cannabinoid receptor in T cells is perhaps a non-G protein-coupled receptor. Nevertheless, the current studies support the emerging view in the field of cannabinoid biology that additional unknown cannabinoid receptors mediate cannabinoid effects.

The ability of SR1 and SR2 to antagonize the actions of the tricyclic cannabinoids on $[Ca^{2+}]_i$ presents a fourth critical finding with implications to the field of cannabinoid biology. The demonstration that both SR1 and SR2 can antagonize the elevation on $[Ca^{2+}]_i$ by Δ^9-THC, CBN and HU-210 at concentrations of 5 μM or below reveals that the cannabinoid receptor antagonists are not as selective for CB1 or CB2 as originally reported. Moreover, the finding the SR1 and SR2 were able to antagonize the effects of tricyclic cannabinoids in the $CB1^{-/-}/CB2^{-/-}$ mouse SPLC further suggests that both antagonists have activity at receptors distinct from CB1 and CB2. Since their discovery SR1 and SR2 have been widely used to demonstrate that cannabinoid compounds elicit their actions through CB1 and/or CB2. Given the present findings, some previously documented cannabinoid effects, particularly in lymphocytes, attributed to CB1 and CB2, solely on the basis of antagonism by 1 μM or higher concentrations of SR1 and SR2 respectively, may have to be reevaluated.

A final point of significance of the present studies lies in the finding that the Δ^9-THC-induced $[Ca^{2+}]_i$ rise in the HPB-ALL cells was mediated by a ROCC in the TRPC subfamily. The regulation of channels in the TRPC subfamily by cannabinoid

compounds has not been previously reported. Therefore, the finding that TRPC1 is involved in the elevation of $[Ca^{2+}]_i$ by Δ^9-THC is novel. Apart from showing that TRPC1 may be regulated by Δ^9-THC upon binding to an unknown cannabinoid receptor in T cells, the very finding that TRPC1 channels may be gated upon ligand-receptor interaction in lymphocytes is also novel. Previous work in other cell systems has shown that TRPC1 is a channel gated primarily by Ca^{2+} store-release, and that it is expressed in conjunction, and oligomerizes with other TRPC subfamily members, particularly TRPC4 and TRPC5 (Beech et al., 2003). The demonstration that the HPB-ALL cells express only TRPC1 and that the Δ^9-THC-induced $[Ca^{2+}]_i$ elevation is dependent on the TRPC1 channel also suggests that TRPC1 can putatively form a homotetramer, which has not been previously demonstrated in any cell type. Therefore, the work presented in the current dissertation has important implications not only to cannabinoid biology, but also to the field of TRPC channels.

Overall, the data and interpretations in the present dissertation project contribute significantly to the current understanding of the fields of cannabinoids, T cell activation and TRPC channels. Therefore, the work presented in the current dissertation is deemed relevant to all three fields. The finding that cannabinoid treatment results in an $[Ca^{2+}]_i$ rise independent of activation stimuli in T cells suggests that one mechanism by which cannabinoids interfere with T cell activation is by eliciting a premature $[Ca^{2+}]_i$ elevation. Premature elevations in $[Ca^{2+}]_i$ may result in apoptosis of immune cells (Howe et al., 2003). Interestingly, treatment of murine SPLC with cannabinoids, including Δ^9-THC, in the absence of activation stimuli has been previously demonstrated to induce apoptosis (McKallip et al., 2002a; McKallip et al., 2002b). Alternatively, a premature elevation of

$[Ca^{2+}]_i$ may also induce T cell anergy, a state in which T cells become unresponsive to cellular stimulation (Faubert Kaplan et al., 2003; Harding et al., 1992; Nakayama et al., 1992; Nghiem et al., 1994; Schwartz, 1992).

Another point of relevance of the studies presented in the current dissertation is that the tricyclic cannabinoid-mediated $[Ca^{2+}]_i$ elevation is a response likely mediated by a non-CB1 non-CB2 cannabinoid receptor in T cells. The above finding is relevant to the field of cannabinoids because although the existence of non-CB1 non-CB2 cannabinoid receptors has been conjectured in multiple tissues, little is known about the functional responses or endpoints that may be measured to assess the activity of cannabinoid compounds at the novel receptor. Therefore, it is suggested that one pharmacological method to assess the activity of the non-CB1 non-CB2 cannabinoid receptor in T cells is the measurement of $[Ca^{2+}]_i$. Moreover, the present studies indicate that initial characterization of the non-CB1 non-CB2 cannabinoid receptor in T cells may also be performed in the presence of SR1 and SR2, both of which putatively act as neutral antagonists at the novel receptor.

Lastly, the present studies, particularly those performed in the HPB-ALL cells, are the first to demonstrate not only that Δ^9-THC treatment can activate TRPC1 channels, but also that endogenously expressed TRPC1 proteins putatively homomultimerize to form OAG-gated ROCCs. The aforementioned finding contributes significantly to the field of TRPC channels because most studies of TRPC channel structure and function have been performed in transfected cells which overexpress TRPC proteins, and in the presence of other TRPC channels. The HPB-ALL cells, therefore, provide a unique model for studying endogenously expressed TRPC1 channels in the absence of other

TRPC subfamily members. Perhaps the most important and relevant finding from the present project that contributes to the field of TRPC channels is that Δ^9-THC regulates TRPC1 independently of both store-depletion and DAG. The implication of the above finding is far reaching and indicates that yet undiscovered mechanisms of TRPC regulation exist, especially in T lymphocytes.

LITERATURE CITED

1. Ahmmed, G.U., D. Mehta, S. Vogel, M. Holinstat, B.C. Paria, C. Tiruppathi and A.B. Malik, 2004, Protein Kinase C{alpha} Phosphorylates the TRPC1 Channel and Regulates Store-operated Ca2+ Entry in Endothelial Cells, J Biol Chem 279, 20941.

2. Arata, S., T.W. Klein, C. Newton and H. Friedman, 1991, Tetrahydrocannabinol treatment suppresses growth restriction of Legionella pneumophila in murine macrophage cultures, Life Sci 49, 473.

3. Ashton, C.H., 2001, Pharmacology and effects of cannabis: a brief review, Br J Psychiatry 178, 101.

4. Aussel, C., R. Marhaba, C. Pelassy and J.P. Breittmayer, 1996, Submicromolar La3+ concentrations block the calcium release-activated channel, and impair CD69 and CD25 expression in CD3- or thapsigargin-activated Jurkat cells, Biochem J 313 (Pt 3), 909.

5. Baker, D. and G. Pryce, 2003, The therapeutic potential of cannabis in multiple sclerosis, Expert Opin Investig Drugs 12, 561.

6. Baker, D., G. Pryce, G. Giovannoni and A.J. Thompson, 2003, The therapeutic potential of cannabis, Lancet Neurol 2, 291.

7. Bakowski, D. and A.B. Parekh, 2002, Permeation through store-operated CRAC channels in divalent-free solution: potential problems and implications for putative CRAC channel genes, Cell Calcium 32, 379.

8. Barritt, G. and G. Rychkov, 2005, TRPs as mechanosensitive channels, Nat Cell Biol 7, 105.

9. Beech, D.J., K. Muraki and R. Flemming, 2004, Non-selective cationic channels of smooth muscle and the mammalian homologues of Drosophila TRP, J Physiol 559, 685.

10. Beech, D.J., S.Z. Xu, D. McHugh and R. Flemming, 2003, TRPC1 store-operated cationic channel subunit, Cell Calcium 33, 433.

11. Begg, M., F.M. Mo, L. Offertaler, S. Batkai, P. Pacher, R.K. Razdan, D.M. Lovinger and G. Kunos, 2003, G protein-coupled endothelial receptor for atypical cannabinoid ligands modulates a Ca2+-dependent K+ current, J Biol Chem 278, 46188.

12. Berdyshev, E.V., 2000, Cannabinoid receptors and the regulation of immune response, Chem Phys Lipids 108, 169.

13. Berdyshev, E.V., E. Boichot, N. Germain, N. Allain, J.P. Anger and V. Lagente, 1997, Influence of fatty acid ethanolamides and delta9-tetrahydrocannabinol on cytokine and arachidonate release by mononuclear cells, Eur J Pharmacol 330, 231.

14. Berg, I., B.V. Potter, G.W. Mayr and A.H. Guse, 2000, Nicotinic acid adenine dinucleotide phosphate (NAADP(+)) is an essential regulator of T-lymphocyte Ca(2+)-signaling, J Cell Biol 150, 581.

15. Bisogno, T., L. Hanus, L. De Petrocellis, S. Tchilibon, D.E. Ponde, I. Brandi, A.S. Moriello, J.B. Davis, R. Mechoulam and V. Di Marzo, 2001, Molecular targets for cannabidiol and its synthetic analogues: effect on vanilloid VR1 receptors and on the cellular uptake and enzymatic hydrolysis of anandamide, Br J Pharmacol 134, 845.

16. Bordin, L., G. Priante, E. Musacchio, S. Giunco, E. Tibaldi, G. Clari and B. Baggio, 2003, Arachidonic acid-induced IL-6 expression is mediated by PKC alpha activation in osteoblastic cells, Biochemistry 42, 4485.

17. Bouaboula, M., N. Desnoyer, P. Carayon, T. Combes and P. Casellas, 1999, Gi protein modulation induced by a selective inverse agonist for the peripheral cannabinoid receptor CB2: implication for intracellular signalization cross-regulation, Mol Pharmacol 55, 473.

18. Bouaboula, M., M. Rinaldi, P. Carayon, C. Carillon, B. Delpech, D. Shire, G. Le Fur and P. Casellas, 1993, Cannabinoid-receptor expression in human leukocytes, Eur. J. Biochem. 214, 173.

19. Boulay, G., 2002, Ca(2+)-calmodulin regulates receptor-operated Ca(2+) entry activity of TRPC6 in HEK-293 cells, Cell Calcium 32, 201.

20. Braun, F.J., O. Aziz and J.W. Putney, Jr., 2003, 2-aminoethoxydiphenyl borane activates a novel calcium-permeable cation channel, Mol Pharmacol 63, 1304.

21. Breivogel, C.S., G. Griffin, V. Di Marzo and B.R. Martin, 2001, Evidence for a new G protein-coupled cannabinoid receptor in mouse brain, Mol Pharmacol 60, 155.

22. Buckley, N.E., K.L. McCoy, E. Mezey, T. Bonner, A. Zimmer, C.C. Felder and M. Glass, 2000, Immunomodulation by cannabinoids is absent in mice deficient for the cannabinoid CB(2) receptor, Eur J Pharmacol 396, 141.

23. Bui, J.D., S. Calbo, K. Hayden-Martinez, L.P. Kane, P. Gardner and S.M. Hedrick, 2000, A role for CaMKII in T cell memory, Cell 100, 457.

24. Bukoski, R.D., S. Batkai, Z. Jarai, Y. Wang, L. Offertaler, W.F. Jackson and G. Kunos, 2002, CB(1) receptor antagonist SR141716A inhibits Ca(2+)-induced relaxation in CB(1) receptor-deficient mice, Hypertension 39, 251.

25. Cabral, G.A. and K. Fischer-Stenger, 1994, Inhibition of macrophage inducible protein expression by delta-9-tetrahydrocannabinol, Life Sci 54, 1831.

26. Cabral, G.A., E.M. Mishkin, F. Marciano-Cabral, P. Coleman, L.S. Harris and A.E. Munson, 1986, Effect of delta-9-tetrahydrocannabinol on herpes simplex virus type 2 vaginal infection in the guinea pig, Proc. Soc. Exp. Biol. Med. 182, 181.

27. Carayon, P., J. Marchand, D. Dussossoy, J.M. Derocq, O. Jbilo, A. Bord, M. Bouaboula, S. Galiegue, P. Mondiere, G. Penarier, G.L. Fur, T. Defrance and P. Casellas, 1998, Modulation and functional involvement of CB2 peripheral cannabinoid receptors during B-cell differentiation, Blood 92, 3605.

28. Chou, K.J., L.L. Tseng, J.S. Cheng, J.L. Wang, H.C. Fang, K.C. Lee, W. Su, Y.P. Law and C.R. Jan, 2001, CP55,940 increases intracellular Ca2+ levels in Madin-Darby canine kidney cells, Life Sci 69, 1541.

29. Condie, R., A. Herring, W.S. Koh, M. Lee and N.E. Kaminski, 1996, Cannabinoid inhibition of adenylate cyclase-mediated signal transduction and interleukin 2 (IL-2) expression in the murine T-cell line, EL4.IL-2, J Biol Chem 271, 13175.

30. Cortright, D.N. and A. Szallasi, 2004, Biochemical pharmacology of the vanilloid receptor TRPV1. An update, Eur J Biochem 271, 1814.

31. Cui, J., J.S. Bian, A. Kagan and T.V. McDonald, 2002, CaT1 contributes to the stores-operated calcium current in Jurkat T-lymphocytes, J Biol Chem 277, 47175.

32. Dalterio, S., A. Bartke and D. Mayfield, 1985, Effects of delta 9-tetrahydrocannabinol on testosterone production in vitro: influence of Ca++, Mg++ or glucose, Life Sci 37, 1425.

33. Dalterio, S., R. Steger, J. Peluso and L. de Paolo, 1987a, Acute delta 9-tetrahydrocannabinol exposure: effects on hypothalamic-pituitary-testicular activity in mice, Pharmacol Biochem Behav 26, 533.

34. Dalterio, S.L., S.A. Bernard and C.R. Esquivel, 1987b, Acute delta 9-tetrahydrocannabinol exposure alters Ca2+ ATPase activity in neuroendocrine and gonadal tissues in mice, Eur J Pharmacol 137, 91.

35. De Petrocellis, L., T. Bisogno, M. Maccarrone, J.B. Davis, A. Finazzi-Agro and V. Di Marzo, 2001, The activity of anandamide at vanilloid VR1 receptors requires facilitated transport across the cell membrane and is limited by intracellular metabolism, J Biol Chem 276, 12856.

36. Derocq, J.M., M. Segui, J. Marchand, G. Le Fur and P. Casellas, 1995, Cannabinoids enhance human B-cell growth at low nanomolar concentrations, FEBS Lett 369, 177.

37. Devane, W.A., F.A. Dysarz, M.R. Johnson, L.S. Melvin and A.C. Howlett, 1988, Determination and characterization of a cannabinoid receptor in rat brain, Mol. Pharmacol. 34, 605.

38. Devane, W.A., L. Hanus, A. Breuer, R.G. Pertwee, L.A. Stevenson, G. Griffin, D. Gibson, A. Mandelbaum, A. Etinger and R. Mechoulam, 1992, Isolation and structure of a brain constituent that binds to the cannabinoid receptor, Science 258, 1946.

39. Diana, M., M. Melis, A.L. Muntoni and G.L. Gessa, 1998, Mesolimbic dopaminergic decline after cannabinoid withdrawal, Proc Natl Acad Sci U S A 95, 10269.

40. Dietrich, A., M. Mederos y Schnitzler, J. Emmel, H. Kalwa, T. Hofmann and T. Gudermann, 2003, N-linked protein glycosylation is a major determinant for basal TRPC3 and TRPC6 channel activity, J Biol Chem 278, 47842.

41. Do, Y., R.J. McKallip, M. Nagarkatti and P.S. Nagarkatti, 2004, Activation through cannabinoid receptors 1 and 2 on dendritic cells triggers NF-kappaB-dependent apoptosis: novel role for endogenous and exogenous cannabinoids in immunoregulation, J Immunol 173, 2373.

42. Dohke, Y., Y.S. Oh, I.S. Ambudkar and R.J. Turner, 2004, Biogenesis and topology of the transient receptor potential Ca2+ channel TRPC1, J Biol Chem 279, 12242.

43. Driessens, M.H., P.E. van Hulten, E.A. van Rijthoven, R.D. Soede and E. Roos, 1997, Activation of G-proteins with AIF-4 induces LFA-1-mediated adhesion of T-cell hybridoma cells to ICAM-1 by signal pathways that differ from phorbol ester- and manganese-induced adhesion, Exp Cell Res 231, 242.

44. Faubert, B.L. and N.E. Kaminski, 2001, AP-1 activity is negatively regulated by cannabinol through inhibition of its protein components, c-fos and c-jun, J Leukoc Biol 67, 259.

45. Faubert Kaplan, B.L., C.E. Rockwell and N.E. Kaminski, 2003, Evidence for cannabinoid receptor-dependent and -independent mechanisms of action in leukocytes, J. Pharmacol. Exp. Ther. 306, 1077.

46. Felder, C.C., E.M. Briley, J. Axelrod, J.T. Simpson, K. Mackie and W.A. Devane, 1993, Anandamide, an endogenous cannabinmimetic eicosinoid, binds to the cloned human cannabinoid receptor and stimulates receptor-mediated signal transduction., Proc. Natl. Acad. Sci. USA 90, 7656.

47. Felder, C.C. and M. Glass, 1998, Cannabinoid receptors and their endogenous agonists, Annu Rev Pharmacol Toxicol 38, 179.

48. Felder, C.C., K.E. Joyce, E.M. Briley, J. Mansouri, K. Mackie, O. Blond, Y. Lai, A.L. Ma and R.L. Mitchell, 1995, Comparison of the pharmacology and signal transduction of the human cannabinoid CB1 and CB2 receptors, Mol Pharmacol 48, 443.

49. Feske, S., J. Giltnane, R. Dolmetsch, L.M. Staudt and A. Rao, 2001, Gene regulation mediated by calcium signals in T lymphocytes, Nat Immunol 2, 316.

50. Filipeanu, C.M., D. de Zeeuw and S.A. Nelemans, 1997, Delta9-tetrahydrocannabinol activates [Ca2+]i increases partly sensitive to capacitative store refilling, Eur J Pharmacol 336, R1.

51. Fischer-Stenger, K., A.W. Updegrove and G.A. Cabral, 1992, Delta-9-tetrahydrocannabinol decreases cytotoxic T lymphocyte activity to herpes simplex virus type 1-infected cells, Proc. Soc. Exp. Biol. Med. 200, 422.

52. Flemming, R., S.Z. Xu and D.J. Beech, 2003, Pharmacological profile of store-operated channels in cerebral arteriolar smooth muscle cells, Br J Pharmacol 139, 955.

53. Freichel, M., S.H. Suh, A. Pfeifer, U. Schweig, C. Trost, P. Weissgerber, M. Biel, S. Philipp, D. Freise, G. Droogmans, F. Hofmann, V. Flockerzi and B. Nilius, 2001, Lack of an endothelial store-operated Ca2+ current impairs agonist-dependent vasorelaxation in TRP4-/- mice, Nat Cell Biol 3, 121.

54. Freichel, M., R. Vennekens, J. Olausson, M. Hoffmann, C. Muller, S. Stolz, J. Scheunemann, P. Weissgerber and V. Flockerzi, 2004, Functional role of TRPC proteins in vivo: lessons from TRPC-deficient mouse models, Biochem Biophys Res Commun 322, 1352.

55. Gamberucci, A., E. Giurisato, P. Pizzo, M. Tassi, R. Giunti, D.P. McIntosh and A. Benedetti, 2002, Diacylglycerol activates the influx of extracellular cations in T-lymphocytes independently of intracellular calcium-store depletion and possibly involving endogenous TRP6 gene products, Biochem J 364, 245.

56. Gebremedhin, D., A.R. Lange, W.B. Campbell, C.J. Hillard and D.R. Harder, 1999, Cannabinoid CB1 receptor of cat cerebral arterial muscle functions to inhibit L-type Ca2+ channel current, Am J Physiol 276, H2085.

57. Glass, M. and J.K. Northup, 1999, Agonist selective regulation of G proteins by cannabinoid CB(1) and CB(2) receptors, Mol Pharmacol 56, 1362.

58. Guse, A.H., 2002, Cyclic ADP-ribose (cADPR) and nicotinic acid adenine dinucleotide phosphate (NAADP): novel regulators of Ca2+-signaling and cell function, Curr Mol Med 2, 273.

59. Guse, A.H., 2004, Regulation of calcium signaling by the second messenger cyclic adenosine diphosphoribose (cADPR), Curr Mol Med 4, 239.

60. Guse, A.H., C.P. da Silva, F. Emmrich, G.A. Ashamu, B.V. Potter and G.W. Mayr, 1995, Characterization of cyclic adenosine diphosphate-ribose-induced Ca2+ release in T lymphocyte cell lines, J Immunol 155, 3353.

61. Harding, F.A., J.G. McArthur, J.A. Gross, D.H. Raulet and J.P. Allison, 1992, CD28-mediated signalling co-stimulates murine T cells and prevents induction of anergy in T-cell clones, Nature 356, 607.

62. Harris, L.S., R.A. Carchman and B.R. Martin, 1978, Evidence for the existance of specific cannabinoid binding sites, Life Sci. 22, 1131.

63. Hassock, S.R., M.X. Zhu, C. Trost, V. Flockerzi and K.S. Authi, 2002, Expression and role of TRPC proteins in human platelets: evidence that TRPC6 forms the store-independent calcium entry channel, Blood 100, 2801.

64. Hermann, H., L. De Petrocellis, T. Bisogno, A. Schiano Moriello, B. Lutz and V. Di Marzo, 2003, Dual effect of cannabinoid CB1 receptor stimulation on a vanilloid VR1 receptor-mediated response, Cell Mol Life Sci 60, 607.

65. Herring, A.C. and N.E. Kaminski, 1999, Cannabinol-mediated inhibition of nuclear factor-kappaB, cAMP response element-binding protein, and interleukin-2 secretion by activated thymocytes, J Pharmacol Exp Ther 291, 1156.

66. Herring, A.C., W.S. Koh and N.E. Kaminski, 1998, Inhibition of the cyclic AMP signaling cascade and nuclear factor binding to CRE and κB elements by cannabinol, a minimally CNS- active cannabinoid, Biochem Pharmacol 55, 1013.

67. Hillard, C.J. and J.A. Auchampach, 1994, In vitro activation of brain protein kinase C by the cannabinoids, Biochim Biophys Acta 1220, 163.

68. Hisatsune, C., Y. Kuroda, K. Nakamura, T. Inoue, T. Nakamura, T. Michikawa, A. Mizutani and K. Mikoshiba, 2004, Regulation of TRPC6 channel activity by tyrosine phosphorylation, J Biol Chem 279, 18887.

69. Hofmann, T., A.G. Obukhov, M. Schaefer, C. Harteneck, T. Gudermann and G. Schultz, 1999, Direct activation of human TRPC6 and TRPC3 channels by diacylglycerol, Nature 397, 259.

70. Hofmann, T., M. Schaefer, G. Schultz and T. Gudermann, 2002, Subunit composition of mammalian transient receptor potential channels in living cells, Proc Natl Acad Sci U S A 99, 7461.

71. Hoth, M., C.M. Fanger and R.S. Lewis, 1997, Mitochondrial regulation of store-operated calcium signaling in T lymphocytes, J Cell Biol 137, 633.

72. Howe, C.J., M.M. LaHair, P.J. Robinson, O. Rodriguez-Mora, J.A. McCubrey and R.A. Franklin, 2003, Models of anergy in the human Jurkat T cell line, Assay Drug Dev Technol 1, 537.

73. Howlett, A.C., 1985, Cannabinoid inhibition of adenylate cyclase. Biochemistry of the response in neuroblastoma cell membranes, Mol. Pharmacol. 27, 429.

74. Howlett, A.C., C.S. Breivogel, S.R. Childers, S.A. Deadwyler, R.E. Hampson and L.J. Porrino, 2004, Cannabinoid physiology and pharmacology: 30 years of progress, Neuropharmacology 47 Suppl 1, 345.

75. Iversen, L., 2003, Cannabis and the brain, Brain 126, 1252.

76. Jan, T.R., A.K. Farraj, J.R. Harkema and N.E. Kaminski, 2003, Attenuation of the ovalbumin-induced allergic airway response by cannabinoid treatment in A/J mice small star, filled, Toxicol Appl Pharmacol 188, 24.

77. Jan, T.R. and N.E. Kaminski, 2001, Role of mitogen-activated protein (MAP) kinases in the differential regulation of interleukin-2 by cannabinol, J Leuk Biol 69, 841.

78. Jan, T.R., G.K. Rao and N.E. Kaminski, 2002, Cannabinol enhancement of interleukin-2 (IL-2) expression by T cells is associated with an increase in IL-2 distal nuclear factor of activated T cell activity, Mol Pharmacol 61, 446.

79. Jarai, Z., J.A. Wagner, K. Varga, K.D. Lake, D.R. Compton, B.R. Martin, A.M. Zimmer, T.I. Bonner, N.E. Buckley, E. Mezey, R.K. Razdan, A. Zimmer and G.

Kunos, 1999, Cannabinoid-induced mesenteric vasodilation through an endothelial site distinct from CB1 or CB2 receptors, Proc Natl Acad Sci U S A 96, 14136.

80. Jeon, Y.J., K.-H. Yang, J.T. Pulaski and N.E. Kaminski, 1996, Attenuation of iNOS gene expression by Δ9-THC is mediated through the inhibition of NF-kB/Rel activation, Mol. Pharmacol. 50, 334.

81. Jordt, S.E., D.M. Bautista, H.H. Chuang, D.D. McKemy, P.M. Zygmunt, E.D. Hogestatt, I.D. Meng and D. Julius, 2004, Mustard oils and cannabinoids excite sensory nerve fibres through the TRP channel ANKTM1, Nature 427, 260.

82. Joy, J.E., S.J. Watson, J.A. Benson and Institute of Medicine (U.S.). Division of Neuroscience and Behavioral Health., 1999, Marijuana and medicine: assessing the science base (National Academy Press, Washington, D.C.) p. xvi.

83. Kalman, L., M.L. Lindegren, L. Kobrynski, R. Vogt, H. Hannon, J.T. Howard and R. Buckley, 2004, Mutations in genes required for T-cell development: IL7R, CD45, IL2RG, JAK3, RAG1, RAG2, ARTEMIS, and ADA and severe combined immunodeficiency: HuGE review, Genet Med 6, 16.

84. Kaminski, N.E., M.E. Abood, F.K. Kessler, B.R. Martin and A.R. Schatz, 1992, Identification of a functionally relevant cannabinoid receptor on mouse spleen cells involved in cannabinoid-mediated immune modulation, Mol. Pharmacol. 42, 736.

85. Kaplan, B.L., C.E. Rockwell and N.E. Kaminski, 2003, Evidence for cannabinoid receptor-dependent and -independent mechanisms of action in leukocytes, J Pharmacol Exp Ther 306, 1077.

86. Kerschbaum, H.H. and M.D. Cahalan, 1999, Single-channel recording of a store-operated Ca2+ channel in Jurkat T lymphocytes, Science 283, 836.

87. Klein, T., Y. Kawakami, C. Newton and H. Friedman, 1991, Marijuana components suppress induction and cytolytic function of murine cytotoxic T cells in vitro and in vivo, Journal of Toxicology and Environmental Health 32, 465.

88. Klein, T.W., B. Lane, C.A. Newton and H. Friedman, 2000a, The cannabinoid system and cytokine network, Proc Soc Exp Biol Med 225, 1.

89. Klein, T.W., C. Newton and H. Friedman, 1987, Inhibition of natural killer cell function by marijuana components, J Toxicol Environ Health 20, 321.

90. Klein, T.W., C. Newton and H. Friedman, 1998, Cannabinoid receptors and immunity, Immunol Today 19, 373.

91. Klein, T.W., C. Newton, K. Larsen, J. Chou, I. Perkins, L. Lu, L. Nong and H. Friedman, 2004, Cannabinoid receptors and T helper cells, J Neuroimmunol 147, 91.

92. Klein, T.W., C. Newton, K. Larsen, L. Lu, I. Perkins, L. Nong and H. Friedman, 2003, The cannabinoid system and immune modulation, J Leukoc Biol 74, 486.

93. Klein, T.W., C. Newton, R. Widen and H. Friedman, 1993, Delta 9-tetrahydrocannabinol injection induces cytokine-mediated mortality of mice infected with Legionella pneumophila, J Pharmacol Exp Ther 267, 635.

94. Klein, T.W., C.A. Newton, N. Nakachi and H. Friedman, 2000b, Delta 9-tetrahydrocannabinol treatment suppresses immunity and early IFN-gamma, IL-12, and IL-12 receptor beta 2 responses to Legionella pneumophila infection, J Immunol 164, 6461.

95. Klein, T.W., C.A. Newton, R. Widen and H. Friedman, 1985, The effect of delta-9-tetrahydrocannabinol and 11-hydroxy-delta-9-tetrahydrocannabinol on T-lymphocyte and B-lymphocyte mitogen responses, J. Immunopharmacol 7, 451.

96. Koh, W.S., R.B. Crawford and N.E. Kaminski, 1997, Inhibition of protein kinase A and cyclic AMP response element(CRE)-specific transcription factor binding by Δ9-tetrahydrocannabiol (Δ9-THC), Biochem. Pharmacol. 53, 1477.

97. Kraft, B., W. Wintersberger and H.G. Kress, 2004, Cannabinoid receptor-independent suppression of the superoxide generation of human neutrophils (PMN) by CP55 940, but not by anandamide, Life Sci 75, 969.

98. Lee, M., K.H. Yang and N.E. Kaminski, 1995, Effects of putative cannabinoid receptor ligands, anandamide and 2-arachidonyl-glycerol, on immune function in B6C3F1 mouse splenocytes, J. Pharmacol. Exp. Ther. 275, 529.

99. Lewis, R.S., 2001, Calcium signaling mechanisms in T lymphocytes, Annu Rev Immunol 19, 497.

100. Lievremont, J.P., G.S. Bird and J.W. Putney, Jr., 2004, Canonical transient receptor potential TRPC7 can function as both a receptor- and store-operated channel in HEK-293 cells, Am J Physiol Cell Physiol 287, C1709.

101. Lintschinger, B., M. Balzer-Geldsetzer, T. Baskaran, W.F. Graier, C. Romanin, M.X. Zhu and K. Groschner, 2000, Coassembly of Trp1 and Trp3 proteins generates diacylglycerol- and Ca2+-sensitive cation channels, J Biol Chem 275, 27799.

102. Liu, X., B.B. Singh and I.S. Ambudkar, 2003, TRPC1 is required for functional store-operated Ca2+ channels. Role of acidic amino acid residues in the S5-S6 region, J Biol Chem 278, 11337.

103. Lutz, B., 2002, Molecular biology of cannabinoid receptors, Prostaglandins Leukot Essent Fatty Acids 66, 123.

104. Ma, H.T., K. Venkatachalam, K.E. Rys-Sikora, L.P. He, F. Zheng and D.L. Gill, 2003, Modification of phospholipase C-gamma-induced Ca2+ signal generation by 2-aminoethoxydiphenyl borate, Biochem J 376, 667.

105. Mackie, K., W.A. Devane and B. Hille, 1993, Anandamide, an endogenous cannabinoid, inhibits calcium currents as a partial agonist in N18 neuroblastoma cells., Mol. Pharmacol. 44, 498.

106. Mackie, K. and B. Hille, 1992, Cannabinoids inhibit N-type calcium channels in neuroblastoma-glioma cells, Proc. Natl. Acad. Sci. USA 89, 3825.

107. Mackie, K., Y. Lai, R. Westenbroek and R. Mitchell, 1995, Cannabinoids activate an inwardly rectifying potassium conductance and inhibit Q-type calcium currents in AtT20 cells transfected with rat brain cannabinoid receptor, J Neurosci 15, 6552.

108. Massi, P., D. Fuzio, D. Vigano, P. Sacerdote and D. Parolaro, 2000, Relative involvement of cannabinoid CB(1) and CB(2) receptors in the Delta(9)-tetrahydrocannabinol-induced inhibition of natural killer activity, Eur J Pharmacol 387, 343.

109. Massi, P., P. Sacerdote, W. Ponti, D. Fuzio, B. Manfredi, D. Vigano, T. Rubino, M. Bardotti and D. Parolaro, 1998, Immune function alterations in mice tolerant to delta9- tetrahydrocannabinol: functional and biochemical parameters, J Neuroimmunol 92, 60.

110. Matias, I., P. Pochard, P. Orlando, M. Salzet, J. Pestel and V. Di Marzo, 2002, Presence and regulation of the endocannabinoid system in human dendritic cells, Eur J Biochem 269, 3771.

111. Matsuda, L.A., S.J. Lolait, M.J. Brownstein, A.C. Young and T.I. Bonner, 1990, Structure of a cannabinoid receptor and functional expression of the cloned cDNA, Nature 346, 561.

112. McCoy, K.L., D. Gainey and G.A. Cabral, 1995, delta 9-Tetrahydrocannabinol modulates antigen processing by macrophages, J Pharmacol Exp Ther 273, 1216.

113. McCoy, K.L., M. Matveyeva, S.J. Carlisle and G.A. Cabral, 1999, Cannabinoid inhibition of the processing of intact lysozyme by macrophages: evidence for CB2 receptor participation, J Pharmacol Exp Ther 289, 1620.

114. McKallip, R.J., C. Lombard, M. Fisher, B.R. Martin, S. Ryu, S. Grant, P.S. Nagarkatti and M. Nagarkatti, 2002a, Targeting CB2 cannabinoid receptors as a novel therapy to treat malignant lymphoblastic disease, Blood 100, 627.

115. McKallip, R.J., C. Lombard, B.R. Martin, M. Nagarkatti and P.S. Nagarkatti, 2002b, Delta(9)-tetrahydrocannabinol-induced apoptosis in the thymus and spleen as a mechanism of immunosuppression in vitro and in vivo, J Pharmacol Exp Ther 302, 451.

116. Mechoulam, R., S. Ben-Shabat, L. Hanus, M. Ligumsky, N.E. Kaminski, A.R. Schatz, A. Gopher, S. Almog, B.R. Martin, D.R. Compton and et al., 1995, Identification of an endogenous 2-monoglyceride, present in canine gut, that binds to cannabinoid receptors, Biochem Pharmacol 50, 83.

117. Merritt, J.E., W.P. Armstrong, C.D. Benham, T.J. Hallam, R. Jacob, A. Jaxa-Chamiec, B.K. Leigh, S.A. McCarthy, K.E. Moores and T.J. Rink, 1990, SK&F 96365, a novel inhibitor of receptor-mediated calcium entry, Biochem J 271, 515.

118. Millns, P.J., V. Chapman and D.A. Kendall, 2001, Cannabinoid inhibition of the capsaicin-induced calcium response in rat dorsal root ganglion neurones, Br J Pharmacol 132, 969.

119. Mishkin, E.M. and G.A. Cabral, 1985, delta-9-Tetrahydrocannabinol decreases host resistance to herpes simplex virus type 2 vaginal infection in the B6C3F1 mouse, J Gen Virol 66 (Pt 12), 2539.

120. Mo, F.M., L. Offertaler and G. Kunos, 2004, Atypical cannabinoid stimulates endothelial cell migration via a Gi/Go-coupled receptor distinct from CB1, CB2 or EDG-1, Eur J Pharmacol 489, 21.

121. Mombouli, J.V., G. Schaeffer, S. Holzmann, G.M. Kostner and W.F. Graier, 1999, Anandamide-induced mobilization of cytosolic Ca2+ in endothelial cells, Br J Pharmacol 126, 1593.

122. Montell, C., 2001, Physiology, phylogeny, and functions of the TRP superfamily of cation channels, Sci STKE 2001, RE1.

123. Montell, C., 2005, The TRP superfamily of cation channels, Sci STKE 2005, re3.

124. Morahan, P.S., P.C. Klykken, S.H. Smith, L.S. Harris and A.E. Munson, 1979, Effects of cannabinoids on host resistance to listeria monocytogenes and herpes simplex virus, Infec. Immun. 23, 670.

125. Moran, M.M., H. Xu and D.E. Clapham, 2004, TRP ion channels in the nervous system, Curr Opin Neurobiol 14, 362.

126. Morato, R., A. Raso, T. Wood, A. Kurosky, B. Martinac and O. Hamill, 2005, TRPC1 forms the stretch-activatd cation channel in verterbrate cells, Nat Cell Biol 7, 179.

127. Moreau, B., S. Straube, R.J. Fisher, J.W. Putney, Jr. and A.B. Parekh, 2005, Ca2+-calmodulin-dependent facilitation and Ca2+ inactivation of Ca2+ release-activated Ca2+ channels, J Biol Chem 280, 8776.

128. Mori, Y., M. Wakamori, T. Miyakawa, M. Hermosura, Y. Hara, M. Nishida, K. Hirose, A. Mizushima, M. Kurosaki, E. Mori, K. Gotoh, T. Okada, A. Fleig, R. Penner, M. Iino and T. Kurosaki, 2002, Transient receptor potential 1 regulates capacitative Ca(2+) entry and Ca(2+) release from endoplasmic reticulum in B lymphocytes, J Exp Med 195, 673.

129. Mukhopadhyay, S., J.Y. Shim, A.A. Assi, D. Norford and A.C. Howlett, 2002, CB(1) cannabinoid receptor-G protein association: a possible mechanism for differential signaling, Chem Phys Lipids 121, 91.

130. Munro, S., K.L. Thomas and M. Abu-Shaar, 1993, Molecular characterization of peripheral receptor for cannabinoids, Nature 365, 61.

131. Nahas, G.G., 1972, Marihuana--deceptive weed (Raven Press, New York) p. xviii.

132. Nakano, Y., S. Pross, T. Klein and H. Friedman, 1993, Increase in cytoplasmic free calcium in murine splenocytes following stimulation with anti-CD3 antibody in the presence of delta-9- tetrahydrocannabinol, Int J Immunopharmacol 15, 423.

133. Nakano, Y., S.H. Pross and H. Friedman, 1992, Modulation of interleukin 2 activity by delta 9-tetrahydrocannabinol after stimulation with concanavalin A, phytohemagglutinin, or anti-CD3 antibody, Proc Soc Exp Biol Med 201, 165.

134. Nakayama, T., Y. Ueda, H. Yamada, E.W. Shores, A. Singer and C.H. June, 1992, In vivo calcium elevations in thymocytes with T cell receptors that are specific for self ligands, Science 257, 96.

135. Netzeband, J.G., S.M. Conroy, K.L. Parsons and D.L. Gruol, 1999, Cannabinoids enhance NMDA-elicited Ca2+ signals in cerebellar granule neurons in culture, J Neurosci 19, 8765.

136. Newton, C., T. Klein and H. Friedman, 1998, The role of macrophages in THC-induced alteration of the cytokine network, Adv Exp Med Biol 437, 207.

137. Nghiem, P., T. Ollick, P. Gardner and H. Schulman, 1994, Interleukin-2 transcriptional block by multifunctional Ca2+/calmodulin kinase, Nature 371, 347.

138. Nowycky, M.C. and A.P. Thomas, 2002, Intracellular calcium signaling, J Cell Sci 115, 3715.

139. Offertaler, L., F.M. Mo, S. Batkai, J. Liu, M. Begg, R.K. Razdan, B.R. Martin, R.D. Bukoski and G. Kunos, 2003, Selective ligands and cellular effectors of a G protein-coupled endothelial cannabinoid receptor, Mol Pharmacol 63, 699.

140. Ouyang, Y., S.G. Hwang, S.H. Han and N.E. Kaminski, 1998, Suppression of interleukin-2 by the putative endogenous cannabinoid 2- arachidonyl-glycerol is mediated through down-regulation of the nuclear factor of activated T cells, Mol Pharmacol 53, 676.

141. Ouyang, Y. and N.E. Kaminski, 1999, Phospholipase A2 inhibitors p-bromophenacyl bromide and arachidonyl trifluoromethyl ketone suppressed interleukin-2 (IL-2) expression in primary murine splenocytes, Arch Toxicol 73, 1.

142. Parekh, A.B., 2003, Store-operated Ca2+ entry: dynamic interplay between endoplasmic reticulum, mitochondria and plasma membrane, J Physiol 547, 333.

143. Parekh, A.B. and J.W. Putney, Jr., 2005, Store-operated calcium channels, Physiol Rev 85, 757.

144. Peng, J.B., X.Z. Chen, U.V. Berger, P.M. Vassilev, H. Tsukaguchi, E.M. Brown and M.A. Hediger, 1999, Molecular cloning and characterization of a channel-like transporter mediating intestinal calcium absorption, J Biol Chem 274, 22739.

145. Pertwee, R.G., 1999a, Cannabis and cannabinoids: pharmacology and rationale for clinical use, Forsch Komplementarmed 6 Suppl 3, 12.

146. Pertwee, R.G., 1999b, Pharmacology of cannabinoid receptor ligands, Curr Med Chem 6, 635.

147. Pertwee, R.G., 2001, Cannabinoid receptors and pain, Prog Neurobiol 63, 569.

148. Pertwee, R.G., 2002, Cannabinoids and multiple sclerosis, Pharmacol Ther 95, 165.

149. Pertwee, R.G., 2005, Inverse agonism and neutral antagonism at cannabinoid CB(1) receptors, Life Sci 76, 1307.

150. Philipp, S., A. Cavalie, M. Freichel, U. Wissenbach, S. Zimmer, C. Trost, A. Marquart, M. Murakami and V. Flockerzi, 1996, A mammalian capacitative calcium entry channel homologous to Drosophila TRP and TRPL, Embo J 15, 6166.

151. Philipp, S., B. Strauss, D. Hirnet, U. Wissenbach, L. Mery, V. Flockerzi and M. Hoth, 2003, TRPC3 mediates T-cell receptor-dependent calcium entry in human T-lymphocytes, J Biol Chem 278, 26629.

152. Philipp, S., C. Trost, J. Warnat, J. Rautmann, N. Himmerkus, G. Schroth, O. Kretz, W. Nastainczyk, A. Cavalie, M. Hoth and V. Flockerzi, 2000, TRP4 (CCE1) protein is part of native calcium release-activated Ca2+-like channels in adrenal cells, J Biol Chem 275, 23965.

153. Plant, T.D. and M. Schaefer, 2003, TRPC4 and TRPC5: receptor-operated Ca2+-permeable nonselective cation channels, Cell Calcium 33, 441.

154. Ponti, W., T. Rubino, M. Bardotti, G. Poli and D. Parolaro, 2001, Cannabinoids inhibit nitric oxide production in bone marrow derived feline macrophages, Vet Immunol Immunopathol 82, 203.

155. Prakriya, M. and R.S. Lewis, 2003, CRAC channels: activation, permeation, and the search for a molecular identity, Cell Calcium 33, 311.

156. Pross, S., C. Newton, T. Klein and H. Friedman, 1987, Age-associated differences in cannabinoid-induced suppression of murine spleen, lymph node and thymus cell blastogenic responses, Immunopharmacol. 14, 159.

157. Pross, S.H., T.W. Klein, C. Newton, J. Smith, R. Widen and H. Friedman, 1990, Age-related suppression of murine lymphoid cell blastogenesis by marijuana components, Dev. Comp. Immunol. 14, 131.

158. Pross, S.H., Y. Nakano, R. Widen, S. McHugh, C.A. Newton, T.W. Klein and H. Friedman, 1992, Differing effects of delta-9-tetrahydrocannabinol (THC) on murine spleen cell populations dependent upon stimulators, Int J Immunopharmacol 14, 1019.

159. Putney, J.W., Jr., 1999, TRP, inositol 1,4,5-trisphosphate receptors, and capacitative calcium entry, Proc Natl Acad Sci U S A 96, 14669.

160. Putney, J.W., Jr., 2003, Capacitative calcium entry in the nervous system, Cell Calcium 34, 339.

161. Putney, J.W., Jr., L.M. Broad, F.J. Braun, J.P. Lievremont and G.S. Bird, 2001, Mechanisms of capacitative calcium entry, J Cell Sci 114, 2223.

162. Randall, M.D., S.P. Alexander, T. Bennett, E.A. Boyd, J.R. Fry, S.M. Gardiner, P.A. Kemp, A.I. McCulloch and D.A. Kendall, 1996, An endogenous cannabinoid as an endothelium-derived vasorelaxant, Biochem Biophys Res Commun 229, 114.

163. Randall, M.D. and D.A. Kendall, 1998, Endocannabinoids: a new class of vasoactive substances, Trends Pharmacol Sci 19, 55.

164. Rao, A., C. Luo and P.G. Hogan, 1997, Transcription factors of the NFAT family: regulation and function, Annu Rev Immunol 15, 707.

165. Rao, G.K., W. Zhang and N.E. Kaminski, 2004, Cannabinoid receptor-mediated regulation of intracellular calcium by delta(9)-tetrahydrocannabinol in resting T cells, J Leukoc Biol 75, 884.

166. Riccio, A., A.D. Medhurst, C. Mattei, R.E. Kelsell, A.R. Calver, A.D. Randall, C.D. Benham and M.N. Pangalos, 2002, mRNA distribution analysis of human TRPC family in CNS and peripheral tissues, Brain Res Mol Brain Res 109, 95.

167. Rinaldi-Carmona, M., F. Barth, M. Heaulme, D. Shire, B. Calandra, C. Congy, S. Martinez, J. Mauruani, G. Neliat, D. Caput, P. Ferrara, P. Soubrie, J.C. Breliere and G. Le Fur, 1994, SR141716A, a potent and selective antagonist of the brain cannabinoid receptor., FEBS Letters 350, 240.

168. Rinaldi-Carmona, M., F. Barth, J. Millan, J.M. Derocq, P. Casellas, C. Congy, D. Oustric, M. Sarran, M. Bouaboula, B. Calandra, M. Portier, D. Shire, J.C. Breliere and G.L. Le Fur, 1998, SR 144528, the first potent and selective antagonist of the CB2 cannabinoid receptor, J Pharmacol Exp Ther 284, 644.

169. Rockwell, C.E. and N.E. Kaminski, 2004, A cyclooxygenase metabolite of anandamide causes inhibition of interleukin-2 secretion in murine splenocytes, J Pharmacol Exp Ther 311, 683.

170. Roth, M.D., G.C. Baldwin and D.P. Tashkin, 2002, Effects of delta-9-tetrahydrocannabinol on human immune function and host defense, Chem Phys Lipids 121, 229.

171. Sagan, S., L. Venance, Y. Torrens, J. Cordier, J. Glowinski and C. Giaume, 1999, Anandamide and WIN 55212-2 inhibit cyclic AMP formation through G- protein-coupled receptors distinct from CB1 cannabinoid receptors in cultured astrocytes, Eur J Neurosci 11, 691.

172. Sarafian, T.A., J.A. Magallanes, H. Shau, D. Tashkin and M.D. Roth, 1999, Oxidative stress produced by marijuana smoke. An adverse effect enhanced by cannabinoids, Am J Respir Cell Mol Biol 20, 1286.

173. Schatz, A.R., W.S. Koh and N.E. Kaminski, 1993, Δ9-tetrahydrocanabinol selectively inhibits T-cell dependent humoral immune responses through direct inhibition of accessory T-cell function, Immunopharmacol. 26, 129.

174. Schatz, A.R., M. Lee, R.B. Condie, J.T. Pulaski and N.E. Kaminski, 1997, Cannabinoid receptors CB1 and CB2: a characterization of expression and adenylate cyclase modulation within the immune system, Toxicol Appl Pharmacol 142, 278.

175. Schindl, R., H. Kahr, I. Graz, K. Groschner and C. Romanin, 2002, Store depletion-activated CaT1 currents in rat basophilic leukemia mast cells are inhibited by 2-aminoethoxydiphenyl borate. Evidence for a regulatory component that controls activation of both CaT1 and CRAC (Ca(2+) release-activated Ca(2+) channel) channels, J Biol Chem 277, 26950.

176. Schwartz, R.H., 1992, Costimulation of T lymphocytes: the role of CD28, CTLA-4, and B7/BB1 in interleukin-2 production and immunotherapy, Cell 71, 1065.

177. Shen, M. and S.A. Thayer, 1998, The cannabinoid agonist Win55,212-2 inhibits calcium channels by receptor-mediated and direct pathways in cultured rat hippocampal neurons, Brain Res 783, 77.

178. Sheng, W.S., S. Hu, X. Min, G.A. Cabral, J.R. Lokensgard and P.K. Peterson, 2005, Synthetic cannabinoid WIN55,212-2 inhibits generation of inflammatory mediators by IL-1beta-stimulated human astrocytes, Glia 49, 211.

179. Shire, D., B. Calandra, M. Bouaboula, F. Barth, M. Rinaldi-Carmona, P. Casellas and P. Ferrara, 1999, Cannabinoid receptor interactions with the antagonists SR 141716A and SR 144528, Life Sci 65, 627.

180. Silverman, A.Y., B.J. Darnell, M.M. Montiel, C.G. Smith and R.H. Asch, 1982, Response of rhesus monkey lymphocytes to short-term administration of THC, Life Sci 30, 107.

181. Singh, B.B., X. Liu and I.S. Ambudkar, 2000, Expression of truncated transient receptor potential protein 1alpha (Trp1alpha): evidence that the Trp1 C terminus modulates store-operated Ca2+ entry, J Biol Chem 275, 36483.

182. Singh, B.B., X. Liu, J. Tang, M.X. Zhu and I.S. Ambudkar, 2002, Calmodulin regulates Ca(2+)-dependent feedback inhibition of store-operated Ca(2+) influx by interaction with a site in the C terminus of TrpC1, Mol Cell 9, 739.

183. Smart, D. and J.C. Jerman, 2000, Anandamide: an endogenous activator of the vanilloid receptor, Trends Pharmacol Sci 21, 134.

184. Smith, S.R., G. Denhardt and C. Terminelli, 2001a, The anti-inflammatory activities of cannabinoid receptor ligands in mouse peritonitis models, Eur J Pharmacol 432, 107.

185. Smith, S.R., C. Terminelli and G. Denhardt, 2000, Effects of cannabinoid receptor agonist and antagonist ligands on production of inflammatory cytokines and anti-inflammatory interleukin- 10 in endotoxemic mice, J Pharmacol Exp Ther 293, 136.

186. Smith, S.R., C. Terminelli and G. Denhardt, 2001b, Modulation of cytokine responses in Corynebacterium parvum-primed endotoxemic mice by centrally administered cannabinoid ligands, Eur J Pharmacol 425, 73.

187. Srivastava, M.D., B.I. Srivastava and B. Brouhard, 1998, Delta9 tetrahydrocannabinol and cannabidiol alter cytokine production by human immune cells, Immunopharmacology 40, 179.

188. Stella, N., 2004, Cannabinoid signaling in glial cells, Glia 48, 267.

189. Sugiura, T., T. Kodaka, S. Kondo, T. Tonegawa, S. Nakane, S. Kishimoto, A. Yamashita and K. Waku, 1996, 2-Arachidonoylglycerol, a putative endogenous cannabinoid receptor ligand, induces rapid, transient elevation of intracellular free Ca2+ in neuroblastoma x glioma hybrid NG108-15 cells, Biochem Biophys Res Commun 229, 58.

190. Sugiura, T., S. Kondo, S. Kishimoto, T. Miyashita, S. Nakane, T. Kodaka, Y. Suhara, H. Takayama and K. Waku, 2000, Evidence that 2-arachidonoylglycerol but not N-palmitoylethanolamine or anandamide is the physiological ligand for the cannabinoid CB2 receptor. Comparison of the agonistic activities of various cannabinoid receptor ligands in HL-60 cells, J Biol Chem 275, 605.

191. Sugiura, T., S. Kondo, A. Sukagawa, S. Nakane, A. Shinoda, K. Itoh, A. Yamashita and K. Waku, 1995, 2-Arachidonoylglycerol: a possible endogenous cannabinoid receptor ligand in brain, Biochem Biophys Res Commun 215, 89.

192. Sumi, M., K. Kiuchi, T. Ishikawa, A. Ishii, M. Hagiwara, T. Nagatsu and H. Hidaka, 1991, The newly synthesized selective Ca2+/calmodulin dependent protein kinase II inhibitor KN-93 reduces dopamine contents in PC12h cells, Biochem Biophys Res Commun 181, 968.

193. Sydorenko, V., Y. Shuba, S. Thebault, M. Roudbaraki, G. Lepage, N. Prevarskaya and R. Skryma, 2003, Receptor-coupled, DAG-gated Ca2+-permeable cationic channels in LNCaP human prostate cancer epithelial cells, J Physiol 548, 823.

194. Tiruppathi, C., M. Freichel, S.M. Vogel, B.C. Paria, D. Mehta, V. Flockerzi and A.B. Malik, 2002a, Impairment of store-operated Ca2+ entry in TRPC4(-/-) mice interferes with increase in lung microvascular permeability, Circ Res 91, 70.

195. Tiruppathi, C., R.D. Minshall, B.C. Paria, S.M. Vogel and A.B. Malik, 2002b, Role of Ca2+ signaling in the regulation of endothelial permeability, Vascul Pharmacol 39, 173.

196. Townsend, D.t., S.A. Thayer and D.R. Brown, 2002, Cannabinoids throw up a conundrum, Br J Pharmacol 137, 575.

197. Trebak, M., G.S. Bird, R.R. McKay and J.W. Putney, Jr., 2002, Comparison of human TRPC3 channels in receptor-activated and store-operated modes. Differential sensitivity to channel blockers suggests fundamental differences in channel composition, J Biol Chem 277, 21617.

198. Trebak, M., J.B.G. St, R.R. McKay, L. Birnbaumer and J.W. Putney, Jr., 2003a, Signaling mechanism for receptor-activated canonical transient receptor potential 3 (TRPC3) channels, J Biol Chem 278, 16244.

199. Trebak, M., G. Vazquez, G.S. Bird and J.W. Putney, Jr., 2003b, The TRPC3/6/7 subfamily of cation channels, Cell Calcium 33, 451.

200. Tseng, P.H., H.P. Lin, H. Hu, C. Wang, M.X. Zhu and C.S. Chen, 2004, The canonical transient receptor potential 6 channel as a putative phosphatidylinositol 3,4,5-trisphosphate-sensitive calcium entry system, Biochemistry 43, 11701.

201. Twitchell, W., S. Brown and K. Mackie, 1997, Cannabinoids inhibit N- and P/Q-type calcium channels in cultured rat hippocampal neurons, J Neurophysiol 78, 43.

202. Vaca, L., W.G. Sinkins, Y. Hu, D.L. Kunze and W.P. Schilling, 1994, Activation of recombinant trp by thapsigargin in Sf9 insect cells, Am J Physiol 267, C1501.

203. Vanden Abeele, F., L. Lemonnier, S. Thebault, G. Lepage, J.B. Parys, Y. Shuba, R. Skryma and N. Prevarskaya, 2004, Two types of store-operated Ca2+ channels with different activation modes and molecular origin in LNCaP human prostate cancer epithelial cells, J Biol Chem 279, 30326.

204. Vanden Abeele, F., Y. Shuba, M. Roudbaraki, L. Lemonnier, K. Vanoverberghe, P. Mariot, R. Skryma and N. Prevarskaya, 2003, Store-operated Ca2+ channels in prostate cancer epithelial cells: function, regulation, and role in carcinogenesis, Cell Calcium 33, 357.

205. Vazquez, G., B.J. Wedel, O. Aziz, M. Trebak and J.W. Putney, Jr., 2004, The mammalian TRPC cation channels, Biochim Biophys Acta 1742, 21.

206. Vazquez, G., B.J. Wedel, M. Trebak, G. St John Bird and J.W. Putney, Jr., 2003, Expression level of the canonical transient receptor potential 3 (TRPC3) channel determines its mechanism of activation, J Biol Chem 278, 21649.

207. Venance, L., S. Sagan and C. Giaume, 1997, (R)-methanandamide inhibits receptor-induced calcium responses by depleting internal calcium stores in cultured astrocytes, Pflugers Arch 434, 147.

208. Venkatachalam, K., D.B. van Rossum, R.L. Patterson, H.T. Ma and D.L. Gill, 2002, The cellular and molecular basis of store-operated calcium entry, Nat Cell Biol 4, E263.

209. Venkatachalam, K., F. Zheng and D.L. Gill, 2004, Control of TRPC and store-operated channels by protein kinase C, Novartis Found Symp 258, 172.

210. Vennekens, R., T. Voets, R.J. Bindels, G. Droogmans and B. Nilius, 2002, Current understanding of mammalian TRP homologues, Cell Calcium 31, 253.

211. Walter, L., A. Franklin, A. Witting, C. Wade, Y. Xie, G. Kunos, K. Mackie and N. Stella, 2003, Nonpsychotropic cannabinoid receptors regulate microglial cell migration, J Neurosci 23, 1398.

212. Watanabe, H., J. Vriens, J. Prenen, G. Droogmans, T. Voets and B. Nilius, 2003, Anandamide and arachidonic acid use epoxyeicosatrienoic acids to activate TRPV4 channels, Nature 424, 434.

213. Wes, P.D., J. Chevesich, A. Jeromin, C. Rosenberg, G. Stetten and C. Montell, 1995, TRPC1, a human homolog of a Drosophila store-operated channel, Proc Natl Acad Sci U S A 92, 9652.

214. White, R. and C.R. Hiley, 1998, The actions of the cannabinoid receptor antagonist, SR 141716A, in the rat isolated mesenteric artery, Br J Pharmacol 125, 689.

215. Wiley, J.L. and B.R. Martin, 2002, Cannabinoid pharmacology: implications for additional cannabinoid receptor subtypes, Chem Phys Lipids 121, 57.

216. Wilson, R.I. and R.A. Nicoll, 2002, Endocannabinoid signaling in the brain, Science 296, 678.

217. Winslow, M.M., J.R. Neilson and G.R. Crabtree, 2003, Calcium signalling in lymphocytes, Curr Opin Immunol 15, 299.

218. Wu, X., G. Babnigg, T. Zagranichnaya and M.L. Villereal, 2002, The role of endogenous human Trp4 in regulating carbachol-induced calcium oscillations in HEK-293 cells, J Biol Chem 277, 13597.

219. Yahya, M.D. and R.R. Watson, 1987, Immunomodulation by morphine and marijuana, Life Sci 41, 2503.

220. Yea, S.S., K.H. Yang and N.E. Kaminski, 2000, Role of nuclear factor of activated T-cells and activator protein-1 in the inhibition of interleukin-2 gene transcription by cannabinol in EL4 T-cells, J Pharmacol Exp Ther 292, 597.

221. Yebra, M., T.W. Klein and H. Friedman, 1992, Δ9-tetrahydrocannabinol suppresses concanavalin A induced increase in cytoplasmic free calcium in mouse thymocytes, Life Sci. 51, 151.

222. Yuan, J.P., K. Kiselyov, D.M. Shin, J. Chen, N. Shcheynikov, S.H. Kang, M.H. Dehoff, M.K. Schwarz, P.H. Seeburg, S. Muallem and P.F. Worley, 2003, Homer binds TRPC family channels and is required for gating of TRPC1 by IP3 receptors, Cell 114, 777.

223. Yuan, T., S. Tencza, T.A. Mietzner, R.C. Montelaro and H.J. Vogel, 2001, Calmodulin binding properties of peptide analogues and fragments of the calmodulin-binding domain of simian immunodeficiency virus transmembrane glycoprotein 41, Biopolymers 58, 50.

224. Yue, L., J.B. Peng, M.A. Hediger and D.E. Clapham, 2001, CaT1 manifests the pore properties of the calcium-release-activated calcium channel, Nature 410, 705.

225. Zhu, X., P.B. Chu, M. Peyton and L. Birnbaumer, 1995, Molecular cloning of a widely expressed human homologue for the Drosophila trp gene, FEBS Lett 373, 193.

226. Zhu, X., M. Jiang, M. Peyton, G. Boulay, R. Hurst, E. Stefani and L. Birnbaumer, 1996, trp, a novel mammalian gene family essential for agonist-activated capacitative Ca2+ entry, Cell 85, 661.

227. Zimmer, A., A.M. Zimmer, A.G. Hohmann, M. Herkenham and T.I. Bonner, 1999, Increased mortality, hypoactivity, and hypoalgesia in cannabinoid CB1 receptor knockout mice, Proc Natl Acad Sci U S A 96, 5780.

228. Zimmerman, S., Z. A., I. Cameron and H. Laurence, 1977, Δ^1-tetrahydrocannabinol, cannabinol and cannabinol effects on the immune response of mice, Pharmacology 15, 10.